I. Stereoselective Construction of Polycyclic Architectures: Enantioselective Catalytic Transannular Ketone-Ene Reactions and an Enantioselective Total Synthesis of (+)-Reserpine II. Synthesis of Chiral Bisthioureas for Anion-Abstraction Catalysis

I. Stereoselective Construction of Polycyclic Architectures: Enantioselective Catalytic Transannular Ketone-Ene Reactions and an Enantioselective Total Synthesis of (+)-Reserpine

II. Synthesis of Chiral Bisthioureas for Anion-Abstraction Catalysis

A thesis presented

by

Naomi Samadara Rajapaksa

to

The Department of Chemistry and Chemical Biology

in partial fulfillment of the requirements

for the degree of

Doctor of Philosophy

in the subject of

Chemistry

Harvard University

Cambridge, Massachusetts

July 2013

Dissertation Advisor: Professor Eric N. Jacobsen *Naomi Samadara Rajapaksa*

I. Stereoselective Construction of Polycyclic Architectures: Enantioselective Catalytic Transannular Ketone-Ene Reactions and an Enantioselective Total Synthesis of (+)-Reserpine

II. Synthesis of Chiral Bisthioureas for Anion-Abstraction Catalysis

Abstract

The research presented herein explores three aspects of asymmetric catalysis: (1) the development of new catalytic enantioselective reactions, (2) the application of stereoselective catalysis to natural product total synthesis, and (3) the design and synthesis of new chiral catalysts.

In Chapter 1, an asymmetric transannular ene reaction of electronically unactivated ketones is reported. The transformation is catalyzed by a new chromium(III) tridentate Schiff-base catalyst and provides access to *trans*-decalinol frameworks in high diastereo- and enantioselectivity.

A convergent total synthesis of indole alkaloid (+)-reserpine is presented in Chapter 2. The synthesis uses two key catalytic asymmetric methods: an enantioselective kinetic resolution of terminal epoxides catalyzed by an oligomeric Co(salen) complex and a catalyst-controlled diastereoselective formal aza-Diels–Alder reaction catalyzed by a primary aminothiourea. These methods enabled an enantioselective synthesis of the classic target and addressed the historically problematic C3 stereocenter of the molecule.

Through the investigation of various synthetic routes we were able to access two unnatural diastereomers of methyl reserpate: 16-*epi*-(+)-methyl reserpate and 15,16-di-*epi*-(+)-methyl reserpate.

Chapter 3 describes the syntheses of rationally designed bisthioureas for anion-abstraction catalysis. Recent mechanistic investigations have led to the identification of productive and nonproductive thiourea dimerization modes in the context of an asymmetric alkylation of α-chloroethers. Based on this work, we synthesized covalently tethered thioureas that enforce proximity of the hydrogen bond donor moieties for cooperative electrophile activation while disfavoring nonproductive self-aggregation. Significant enhancements in reactivity are obtained with the bisthioureas relative to analogous monomeric thioureas in the model reaction.

Table of Contents

Acknowledgments

I was supported by several people during my time in graduate school, and today, I am very pleased to have the opportunity to thank all of them. I would like to thank Professor Eric Jacobsen for his advice, patience, and encouragement over the past six years. Eric has a talent for providing students with an ideal balance of independence and guidance, and this environment allowed me to develop as a scientist. I truly feel lucky to have worked with Eric, and I will always be grateful for his mentorship.

I acknowledge Professors Andrew Myers and Emily Balskus for serving on my thesis committee and for providing valuable suggestions and discussions. I also thank Andy for kindly allowing me to spend much of my first year in his lab during the Jacobsen lab renovation. Emily's enthusiasm for science is inspiring, and I am grateful for all of her advice on research and presentations. I would also like to thank Professors David Evans and Ted Betley for their contributions at early stages in my graduate career.

My mentors from my undergraduate years deserve credit for providing me with an essential foundation for graduate school. Professor Zhenan Bao was generous enough to accept me into her lab at Stanford University when I was just starting to explore research, and I appreciate all the encouragement she has given me since those early days. I would also like to thank Professor Barry Trost for giving me the opportunity to work in his group, an experience that shaped decisions I made in graduate school. I was fortunate enough to be paired up with Sushant Malhotra as my graduate student mentor. Although his impressive productivity may have given me an unrealistic impression of what it means to pursue a PhD in chemistry, I am grateful for everything he taught me and for his friendship. I would also like to thank John Flygare, Richard Mackman, Oliver Saunders,

and Jeff Tom for mentoring me during internships. John is a role model of mine, and I am very grateful for his advice and support throughout graduate school.

I had the opportunity to collaborate with a number of incredibly talented chemists during my time in the Jacobsen group. Meredeth McGowan deserves special thanks. She initiated and carried out much of the reserpine synthesis and taught me so much during my early years in graduate school. Matt Rienzo joined the reserpine project at a later stage as an undergraduate and made more significant contributions towards its completion than he probably realizes. I really appreciated his determined work ethic and chill attitude, and I wish him the best in graduate school. I would also like to thank Mat Lalonde and Stephan Zuend for (rather unconventional) collaborations and for their help with the FADA and Strecker reactions. Dan Lehnherr, Masa Wasa, and I worked closely on the synthesis of thiourea dimers, and I appreciated their help and suggestions. Most recently, Mike Witten and I carried out large-scale Strecker reactions together, and it was fantastic working with him.

Charles Yeung, Adam Brown, Meredeth McGowan, Cheyenne Brindle, Andy Rötheli, Dave Ford, Dan Lehnherr, and Song Lin read and provided feedback on portions of this thesis. Their input significantly improved the quality of the final product, and I gratefully acknowledge their help. I would also like to thank Corinna Schindler, who proofread just about every other document I produced during graduate school.

I had the pleasure of overlapping with a number of other people in the lab who made graduate school enjoyable. Nicole Minotti was extremely helpful, and I thank her for her encouragement (particularly during the nerve-racking moments before committee meetings!). Matt Schiffler, Meredeth McGowan, and Chris Uyeda made my transition to

graduate school a smooth one by welcoming me to pre-renovation M202A and to lunchtime Jeopardy. I should also thank Chris for not dumping a beer on my head. Bekka Klausen, Rebecca Loy, and Stephan Zuend contributed to my graduate school experience by spearheading weekly group outings to Charlie's and introducing me to mixed drinks. My post-renovation officemates, Andy Rötheli, Corinna Schindler, and Charles Yeung, have been great friends and coworkers, and they also maintained a fairly steady supply of chocolate and other equally healthy snacks in the office. Andy has been an amazingly supportive friend, and I will miss working with him. I know that graduate school would not have been so enjoyable if we did not share an office. I also thank Corinna and Cheyenne for always being willing to chat about synthesis and for numerous coffee breaks.

Adam Brown and I joined the Jacobsen group at the same time, and I thank him for being a great friend. He is a very talented chemist and is a genuinely nice guy. I wish him the best of luck, and I am sure our paths will cross in the future.

Jim Birrell, Dave Ford, and Song Lin all joined the group a year after I did, and together they represented a very hardworking and talented class. Jim and I shared a bay for the last four years, and during that time we engaged in many chemistry and non-chemistry discussions, broadened each other's exposure to music, and only occasionally drove each other crazy. Dave and I were amazingly compatible sinkmates, and I valued his insights on acquiring NMR spectra and on navigating the intricacies of email etiquette. Song is a very creative chemist and despite the numerous jokes he told at my expense, I look forward to hanging out with him on the west coast. Although this class of graduate students joined a year after Adam and I did, we all defended within months of

each other. It was priceless being able to share the entire graduate school experience—complete with frustrations and successes—with the four of them, and I hope we will remain good friends far into the future.

I wish Amanda Turek and Mike Witten the best of luck in their new roles as senior graduate students. It was a pleasure getting to know them and the younger graduate students, and I wish Gary Zhang, YP, Steven Banik (of Banik Challenge fame), Baye Galligan, Rose Kennedy, and Ania Levina all the best. Ania has a fantastic attitude, and I thank her for occasional chats during the thesis writing process.

The postdoctoral fellows in the group are truly top-notch, and I particularly enjoyed working with Mary Watson, Rob Knowles, Noah Burns, Cheyenne Brindle, Corinna Schindler, Charles Yeung, and Sean Kedrowski. The group and I benefitted tremendously from their insights, and I know that they will accomplish great things through their academic careers.

My final thanks are for my friends and family. Luckily, three of my closest friends, Victoria Chu, Vineeta Agarwala, and Cammie Lee, were in Cambridge during my time in graduate school, and I further enjoyed the experience because of them. Although Shun Kawamura and I were apart from each other for much of the past six years, his love and support carried me through the ups and downs of graduate school, and I look forward to being together with him in California. Finally, I thank my parents, Dayananda and Ranjani, and my sisters, Sam and Amanda, for encouraging me to do my best and for their constant support.

for my parents,

Dayananda and Ranjani Rajapaksa

List of Abbreviations

Å	angstrom
Ac	acetyl
AcOH	acetic acid
Ad	1-adamantyl
AIBN	azobisisobutyronitrile
APCI	atmospheric pressure chemical ionization
Ar	aryl
atm	atmosphere
Bn	benzyl
Boc	*tert*-butoxycarbonyl
brsm	based on recovered starting material
Bu	butyl
°C	degree Celsius
CAN	ceric ammonium nitrate
CH_2Cl_2	dichloromethane
conv.	conversion
cis	on the same side
δ	chemical shift in parts per million
D	dextrarotatory
D	Deuterium
DBU	1,8-diazobicyclo[5.4.0]undec-7-ene

DDQ	2,3-dichloro-5,6-dicyano-1,4-benzoquinone
DIPEA	di-isopropylethylamine
DMAP	4-*N*,*N*-dimethylaminopyridine
DMF	dimethylformamide
DMP	Dess–Martin Periodinane
DMSO	dimethyl sulfoxide
dr	diastereomeric ratio
E	*Ger*., entgegen
EDC	(1-ethyl-3-(3-dimethylaminopropyl)carbodiimide hydrochloride)
ee	enantiomeric excess
ent-	enantiomeric
equiv	equivalents
ESI	electrospray ionization
Et	ethyl
Et_2O	ethyl ether
Et_3N	triethylamine
EtOAc	ethyl acetate
EtOH	ethanol
FADA	formal aza-Diels–Alder
g	gram
GC	gas chromatography
h	hour
H_2	hydrogen

HF	hydrogen fluoride
HOBt	hydroxybenzotriazole
HPLC	high-performance liquid chromatography
HRMS	high-resolution mass spectroscopy
Hz	Hertz
i	iso
IR	infrared
J	coupling constant
KH	potassium hydride
KHMDS	potassium hexamethyldisilazide
L	liter
L	levorotatory
LDA	lithium diisopropylamide
LHMDS	lithium hexamethyldisilazide
LRMS	low-resolution mass spectrometry
m	meta
M	molar
Me	methyl
MeCN	acetonitrile
MeOH	methanol
min	minute
mol	mole
Ms	methanesulfonyl

MS	molecular sieves
n	normal
N	normal
$NaBH_4$	sodium borohydride
NMR	nuclear magnetic resonance
nOe	nuclear Overhauser effect
NOESY	nuclear Overhauser effect spectroscopy
o	ortho
p	para
Pd/C	palladium on carbon
Ph	phenyl
PMB	*p*-methoxybenzyl
ppm	parts per million
Pr	propyl
psi	pounds per square inch
PtO_2	platinum dioxide
quant.	quantitative
pyr	pyridine
R	rectus
rac-	racemic
RSM	recovered starting material
rt	room temperature
s	second

S	sinister
SFC	supercritical fluid chromatography
t	tertiary
TBAF	tetra-*n*-butylammonium fluoride
TBME	*tert*-butyl methyl ether
TBS	*t*-butyldimethylsilyl
Tf	trifluoromethanesulfonyl
TFA	trifluoroacetic acid
TFAA	trifluoroacetic anhydride
THF	tetrahydrofuran
TLC	thin-layer chromatography
TMB	3,4,5-trimethoxylbenzoyl
TMS	trimethylsilyl
trans	on opposite sides
Ts	*p*-toluenesulfonyl
p-TsOH	*p*-toluenesulfonic acid
UV	ultra-violet
Z	*Ger*., zusammen

Chapter 1

Enantioselective Catalytic Transannular Ketone-Ene Reactions[1]

[1] Portions of this chapter have been published: Rajapaksa, N. S.; Jacobsen, E. N. *Org. Lett.* **2013**, *15*, 4238.

1.1. Introduction

Transannular chemical reactions are noteworthy for generating structurally and stereochemically rich products from relatively simple precursors in a single transformation.[2] The first applications of chiral catalysts to promote transannular reactions were recently identified, and these methods will be discussed in the following section. Motivated by the power of ene-type reactions in organic synthesis, we became interested in extending the asymmetric catalytic transannular reaction concept to this important class of C–C bond-forming reactions.[3] In this chapter, we present the development of an enantioselective catalytic transannular ketone-ene reaction.

1.2. Catalytic Enantioselective Transannular Reactions

The use of chiral catalysts to achieve absolute stereocontrol in transannular reactions is an area of chemistry that has only recently received attention. As the following examples demonstrate, this powerful strategy provides access to challenging molecular architectures. Two of the examples further illustrate the elegance of the approach through the application of an asymmetric transannular reaction to a natural product total synthesis.

---

[2] For reviews on the application of transannular reactions to the synthesis of natural products, see: a) Marsault, E.; Toró, A.; Nowak, P.; Deslongchamps, P. *Tetrahedron 57*, **2001**, 4243. b) Clarke, P. A.; Reeder, A. T.; Winn, J. *Synthesis* **2009**, *5*, 691.

[3] For a general review of asymmetric ene reactions, see: a) Mikami, K.; Shimizu, M. *Chem. Rev.* **1992**, *92*, 1021.

1.2.1. Enantioselective Desymmetrization of Meso Epoxides[4]

During their investigations of base-promoted isomerizations of epoxides derived from medium-sized cyclic *cis*-olefins, Hodgson and coworkers identified a transannular bond forming process that proceeds with good enantioselectivity and high yields with a catalytic amount of chiral amine **5** (Scheme 1.1). In these transformations, a chiral lithium base effects an enantioselective α-deprotonation of *meso* epoxides **1** and **3**, which is followed by a diastereoselective bond insertion across the ring to generate fused polycyclic products **2** and **4** in good yield and enantioselectivity. Although Hodgson only demonstrated the catalytic desymmetrization with two epoxides, it is noteworthy that similar levels of product enantioenrichment were obtained for **2** and **4** despite differences in substrate ring-size (8 vs. 9) and the bond participating in the insertion reaction (C–H vs. N–C).

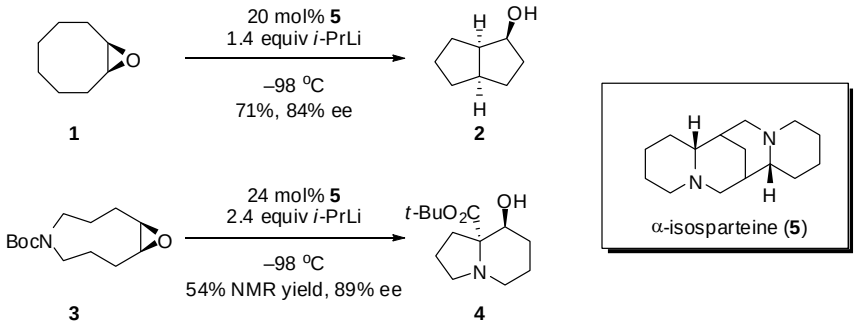

Scheme 1.1. Enantioselective Desymmetrization of *meso* Epoxides

[4] a) Hodgson, D. M.; Lee, G. P.; Marriott, R. E.; Thompson, A. J.; Wisedale, R.; Witheringon, *J. Chem. Soc. Perkin Trans. 1*, **1998**, 2151. b) Hodgson, D. M.; Robinson, L. A. *Chem Commun.* **1999**, 309. c) Hodgson, D. M.; Cameron, I. D.; Christlieb, M.; Green, R.; Lee, G. P.; Robinson, L. A. *J. Chem. Soc. Perkin Trans. 1*, **2001**, 2161.

1.2.2. Enantioselective Transannular Diels–Alder Reactions[5]

In 2007, Jacobsen and coworkers reported a highly enantioselective catalytic transannular Diels–Alder (TADA) reaction of macrocycles containing dienophiles and (*E*,*E*)-dienes. Oxazaboroldine Lewis acid **6** catalyzes this transformation and is remarkably tolerant to substrate modifications to the dienophile identity (enoate vs. enone) and ring-size (14–16) (Scheme 1.2). A range of macrocyclic substrates were found to undergo asymmetric TADA reactions to provide tricyclic products in good diastereo- and enantioselectivity.

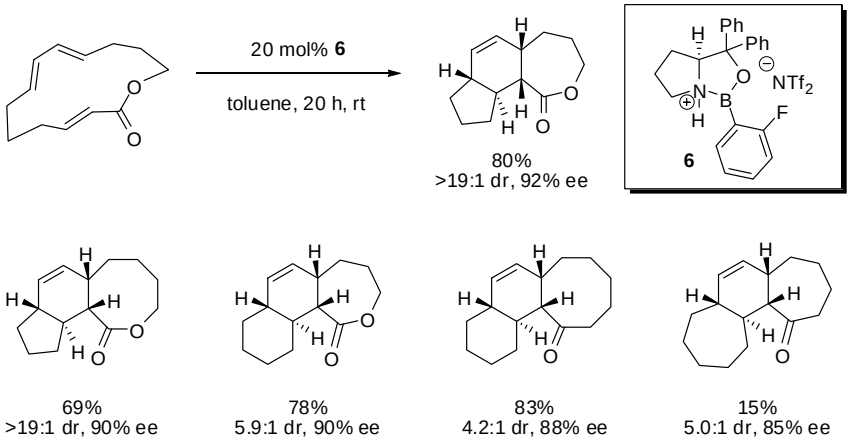

Scheme 1.2. Catalytic Asymmetric Transannular Diels–Alder (TADA) Reactions

The authors took advantage of the predictable selectivity of the oxazaborolidine-catalyzed TADA reaction in a total synthesis of bicyclic sesquiterpene natural product 11,12-diacetoxydrimane **10** (Scheme 1.3). The TADA reaction of 15-membered cyclic silyl ether **7** afforded tricycle **8** in high efficiency and selectivity, and this single operation installed all four contiguous stereocenters of natural product. Importantly, executing the Diels–Alder reaction in a transannular context was found to be essential, as an analogous acyclic substrate did not undergo the corresponding intramolecular Diels–

[5] Balskus, E. P.; Jacobsen, E. N. *Science* **2007**, *317*, 1736.

Alder with catalyst **6**, under thermal conditions, or even in the presence of a stronger Lewis acid.[6]

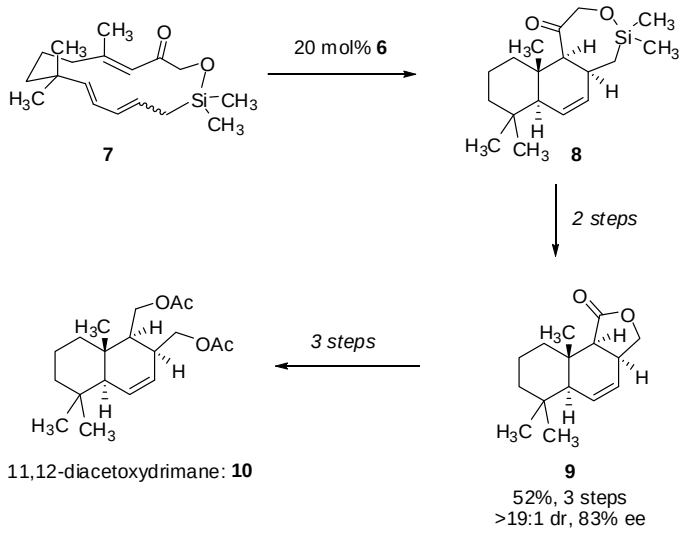

Scheme 1.3. Application of the Catalytic Asymmetric TADA to a Total Synthesis of 11,12-diacetoydrimane

1.2.3. Asymmetric Transannular Aldol Reactions[7]

List and coworkers reported an asymmetric transannular aldol reaction of medium-sized cyclic diketones that is catalyzed by 4-fluoro-proline derivative **11** (Scheme 1.4).[8] Several 1,4-cyclooctanediones were found to undergo aldol cyclizations to provide *cis*-fused bicyclic alcohols in good yields and excellent enantioselectivities (94–96% ee). The synthetic utility of the method was illustrated through an enantioselective total synthesis of (+)-hirsutene (**13**), which uses an efficient and highly selective transannular aldolization of **12** as a key step.

---

[6] Balskus, E. P. Ph.D. Dissertation, Harvard University, **2007**.

[7] Chandler, C. L.; List, B. *J. Am. Chem. Soc.* **2008**, *130*, 6737.

[8] For related examples of enantioselective transannular aldol reactions that utilize stoichiometric or super-stoichiometric chiral reagents, see: a) Inoue, M.; Sato, T.; Hirama; M. *Angew. Chem., Int. Ed.* **2006**, *45*, 4848. b) Inoue, M.; Lee, N.; Kasuya, S.; Sato, T.; Hirama; M, *J. Org. Chem.* **2007**, *72*, 3065. c) Knopff, O.; Kuhne, J.; Fehr, C. *Angew. Chem., Int. Ed.* **2007**, *46*, 1307.

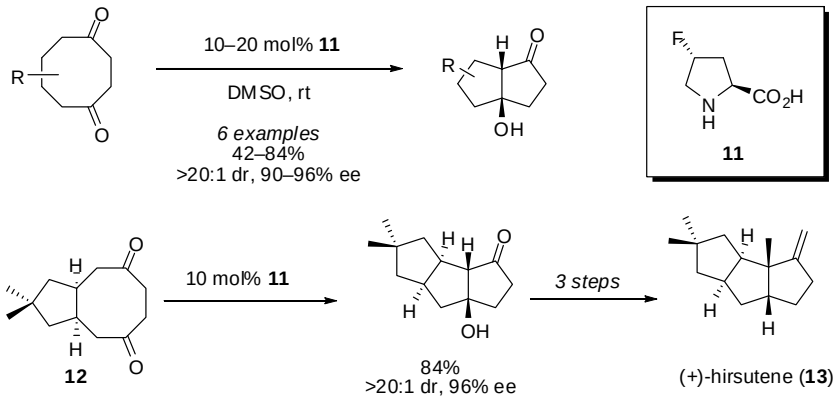

Scheme 1.4. Enantioselective Transannular Aldol Reactions

A striking feature of this chemistry is its sensitivity to deviations from the 1,4-cyclooctanedione substrate framework (Figure 1.1). For example, products **14** and **15**, which are obtained through transannular aldolizations of cyclononanediones have substantially diminished levels of enantioenrichment. Similarly, **16** and **17**, derived from 10-membered cyclic diketones are obtained in low selectivities, with **17** being formed as a racemate. Finally, 1,4-cyclononanedione and 1,4-cyclodecanedione undergo transannular aldol condensations to afford achiral products **18** and **19**.

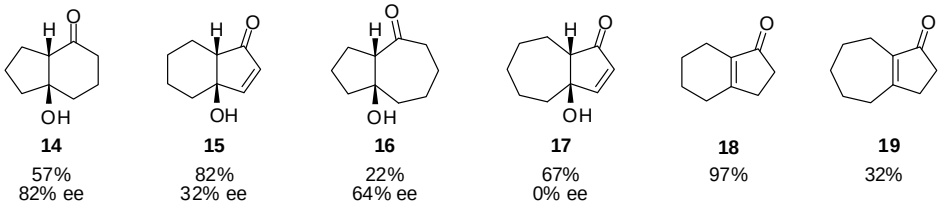

Figure 1.1. Transannular Aldolizations of 9- and 10-Membered Cyclic Diketones

1.2.4. Enantioselective Transannular Claisen Rearrangements[9]

Hiersemann and coworkers reported an asymmetric Claisen rearrangement of macrocyclic *O*-allyl-α-ketoesters (**21a**–**c**) that is catalyzed by chiral copper salt **20** (Scheme 1.5). Unlike the previous examples, this transformation does not afford

[9] Jaschinski, T.; Hiersemann, M. *Org. Lett.* **2012**, *14*, 4114.

polycyclic products but results in the synthesis of medium-sized cycloalkanes with vinyl and α-ketoester substituents. The highly Lewis acidic copper bis(oxazoline) complex **20** promotes the arrangement of a series of (*E*,*E*)-macrocyclic allyl vinyl ethers to afford *trans*-substituted cycloalkanes in excellent enantioselectivity but with low to moderate diastereoselectivity.

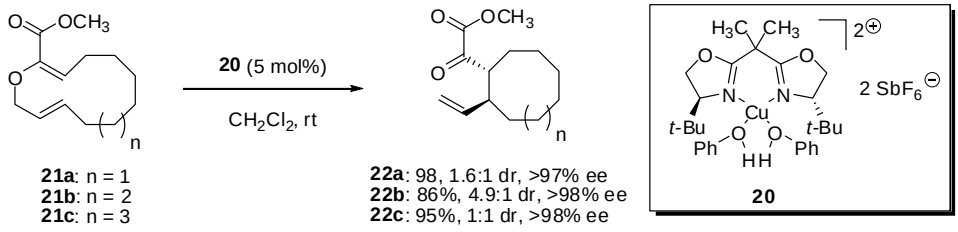

Scheme 1.5. Hiersemann's Transannular Claisen-Rearrangement

1.3. The Ketone-Ene Reaction

These four examples demonstrate the efficiency of catalytic enantioselective transannular reactions in accessing challenging scaffolds. Inspired by this precedent, we became interested in developing a chiral catalyst for enantioselective transannular ketone-ene reactions. The carbonyl-ene reaction is a valuable C–C bond forming process that occurs between an enophile (a carbonyl) and an ene component (an olefin possessing an allylic hydrogen) to afford homoallylic alcohols and generate up to two new stereocenters (Scheme 1.6).[10,11]

[10] For reviews on the carbonyl-ene reaction, see: a) Oppolzer, W.; Snieckus, V. *Angew. Chem., Int. Ed.* **1978**, *17*, 476. b) Snider, B. B. *Acc. Chem. Res.* **1980**, *13*, 426.

[11] For reviews on enantioselective, catalytic carbonyl-ene reactions, see: a) Ref. 3. b) Mikami, K.; Terada, M. in *Comprehensive Asymmetric Catalysis*, Vol. 3 (Eds. Jacobsen, E. N.; Pfaltz, A.; Yamamoto, H.) Springer, Berlin, **1999**, 1143. c) Clarke, M. L.; France, M. B., *Tetrahedron* **2008**, *64*, 9003.

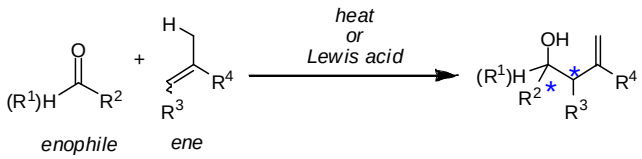

Scheme 1.6. The Carbonyl-Ene Reaction

This pericyclic reaction can be promoted under thermal or Lewis acidic conditions. Although a number of Lewis acid-catalyzed aldehyde-ene reactions have been reported,[11] ketones are generally very poor reacting partners in Lewis acid-catalyzed processes. To date, enantioselective catalytic ketone-ene reactions have only been achieved with highly electrophilic ketones bearing strongly electron-withdrawing substituents. [12, 13] In 2000, Evans and coworkers reported the first catalytic enantioselective ketone-ene reaction. They demonstrated that C2-symmetric copper bis(oxazoline) complex **23** catalyzes ketone-ene reactions between 1,1-disubstituted olefins (used in 5–10-fold excess) and methyl pyruvate (**24**) in high yield and enantioselectivity (Scheme 1.7).[12a]

[12] For selected examples of metal-catalyzed enantioselective carbonyl-ene reactions of α-ketoester and diketones, see: a) Evans, D. A.; Tregay, S. W.; Burgey, C. S.; Paras, N. A.; Vojkovsky, T. *J. Am. Chem. Soc.* **2000**, *122*, 7936. b) Yang, D.; Yang, M.; Zhu, N.–Y. *Org. Lett.* **2003**, *5*, 3749. c) Mikami, K.; Aikawa, K.; Kainuma, S.; Kawakami, Y.; Saito, T.; Sayo, N.; Kumobayashi, H. *Tetrahedron: Asymmetr.* **2004**, *15*, 3885. d) Doherty, S.; Knight, J. G.; Smyth, C. H.; Harrington, R. W.; Clegg, W. *J. Org. Chem.* **2006**, *71*, 9751. e) Mikami, K.; Kawakami, Y.; Akiyama, K.; Aikawa, K. *J. Am. Chem. Soc.* **2007**, *129*, 12950. f) Zhao, J.–F.; Tsui, H. –Y.; Wu, P. –J.; Lu, J.; Loh, T. –P. *J. Am. Chem. Soc.* **2008**, *130*, 16492. g) Luo, H.–K.; Woo, Y. –L.; Schumann, H.; Jacob, C.; van Meurs, M.; Yang, H.–Y.; Tan, Y.–T. *Adv. Synth. Catal.* **2010**, *352*, 1356. h) Zheng, K.; Yang, Y.; Zhao, J.; Yin, C.; Lin, L.; Liu, X.; Feng, X. *Chem. Eur. J.* **2010**, *16*, 9969. i) Zhao, Y.–J.; Li, B.; Tan, L.–J. S.; Shen, Z.–L.; Loh, T.–P. *J. Am. Chem. Soc.* **2010**, *132*, 10242.

[13] Examples of Brønsted acid catalyzed ketone-ene reaction of α,α,α-trifluoropyruvates: a) Clarke, M. L.; Jones, C. E. S.; France, M. B. *Beilstein J. Org. Chem.* **2007**, *3*, 24. b) Rueping, M.; Thiessmann, T.; Kuenkel, A.; Koenigs, R. M. *Angew. Chem., Int. Ed.* **2008**, *47*, 6798.

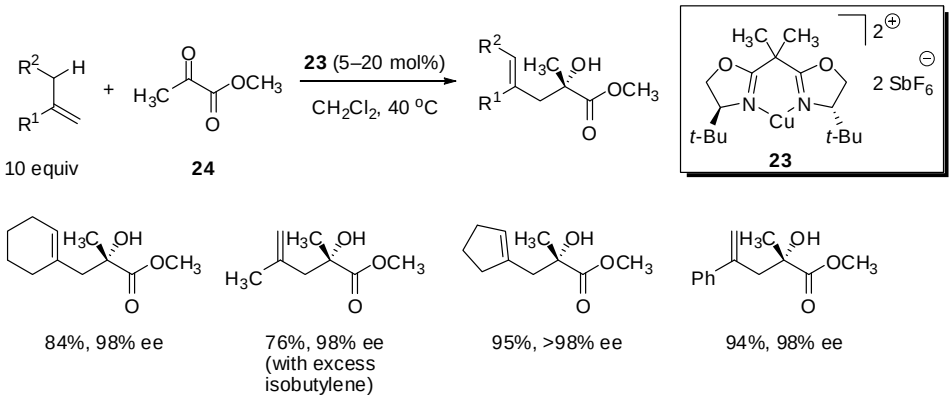

Scheme 1.7. Evans's Enantioselective Copper Bis(oxazoline)-Catalyzed Ene Reactions of Methyl Pyruvate

Since this pioneering report, all subsequently reported enantioselective ketone-ene reactions have also employed α-keto-carbonyl compounds, either due to the necessity for two-point binding of the substrate to the catalyst, or because of the enhanced electrophilicity of the ketone. Yang demonstrated that intramolecular ene reactions of α-keto-esters with internal olefins were catalyzed in high yield and selectivity by a related copper bis(oxazoline) complex (Scheme 1.8A).[12b] Strategies to expand the scope of either the ene or enophile component in asymmetric intermolecular ketone-ene reactions have centered on electronic activation. Mikami showed that a dicationic palladium complex prepared through an *in situ* counterion exchange of **26** catalyzes the intermolecular ene reaction of α-ketoesters.[12c] With the introduction of the highly electron-withdrawing trifluoromethyl group, pyruvate **27** undergoes selective ene reactions with typically unreactive monosubstituted olefins (Scheme 1.8B). In a subsequent report, the same group demonstrated that the use of silyl enol ethers allowed the enophile scope to be expanded to α-diketones.[12e] In a particularly impressive example,

unsymmetrical diketone **28** is converted to **29** as a single regioisomer and in excellent enantioselectivity (Scheme 1.8C).

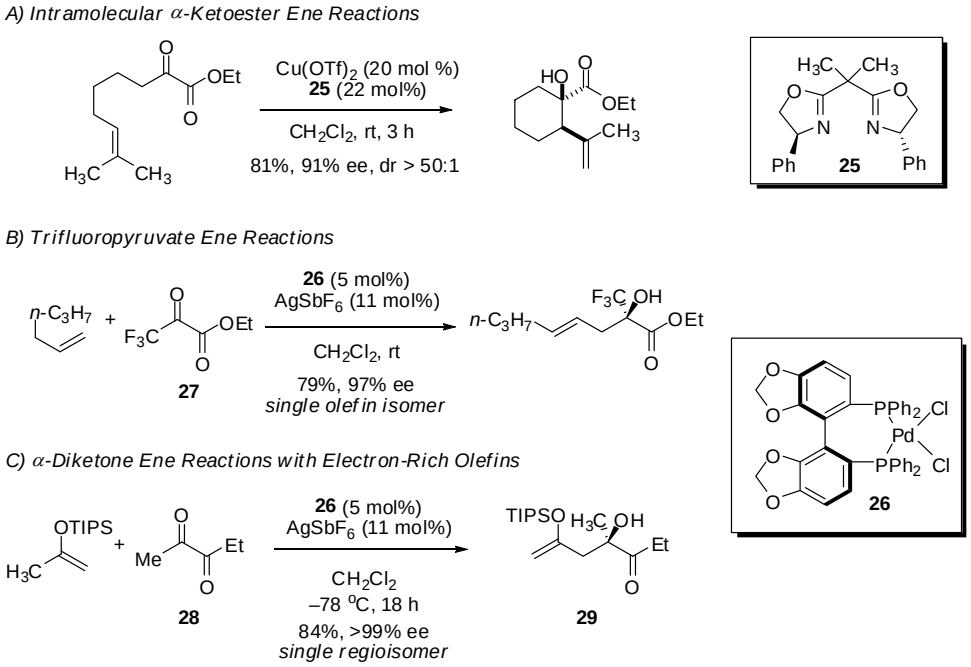

Scheme 1.8. Lewis Acid-Catalyzed Enantioselective Ketone-Ene Reactions

Recently, Brønsted acid catalysts **30** and **31** have also been shown to catalyze enantioselective ketone-ene reactions (Scheme 1.9). However, both of these methods are limited to the highly reactive trifluoromethyl pyruvate **27**.[13]

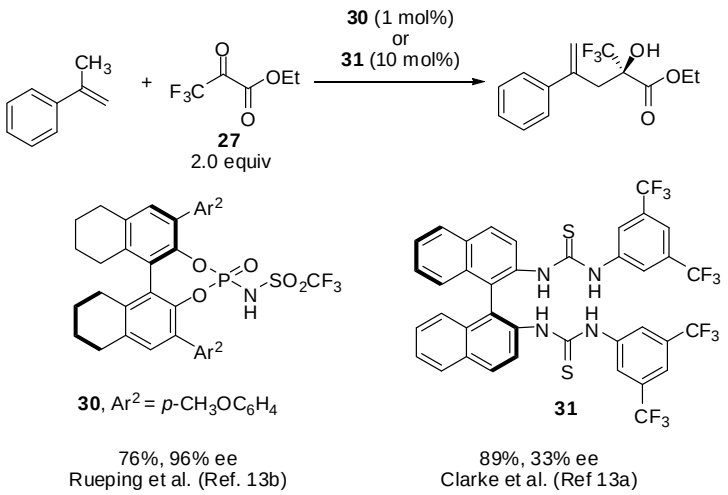

Scheme 1.9. Brønsted Acid Catalyzed Ketone-Ene Reactions

The Jacobsen group's work in the area of enantioselective hetero-ene reactions has involved the development of chiral Cr(III) tridentate Schiff-base complexes for inter- and intramolecular aldehyde-ene reactions (Scheme 1.10).[14,15] The Cr(III)-catalyzed intermolecular aldehyde-ene reaction occurs only with electron-rich olefins, and the intramolecular variant readily takes place with unactivated olefins. However, attempted extension of the developed aldehyde-ene methodologies to asymmetric inter- or intramolecular ketone-ene reactions of even highly activated trifluoromethyl ketones yielded unsatisfactory results (Scheme 1.11).[14c,15b]

[14] a) Ruck, R.; Jacobsen, E. N. *J. Am. Chem. Soc.* **2002**, *124*, 2882. b) Ruck, R. T.; Jacobsen, E. N. *Angew. Chem., Int. Ed.* **2003**, *39*, 4771. c) Ruck, R. T. Ph.D. Dissertation, Harvard University, **2003**.

[15] a) Grachan, M. L.; Tudge, M. T.; Jacobsen, E. N. *Angew. Chem., Int. Ed.* **2008**, *47*, 1469. b) Grachan, M. L. Ph.D. Dissertation, Harvard University, **2008**.

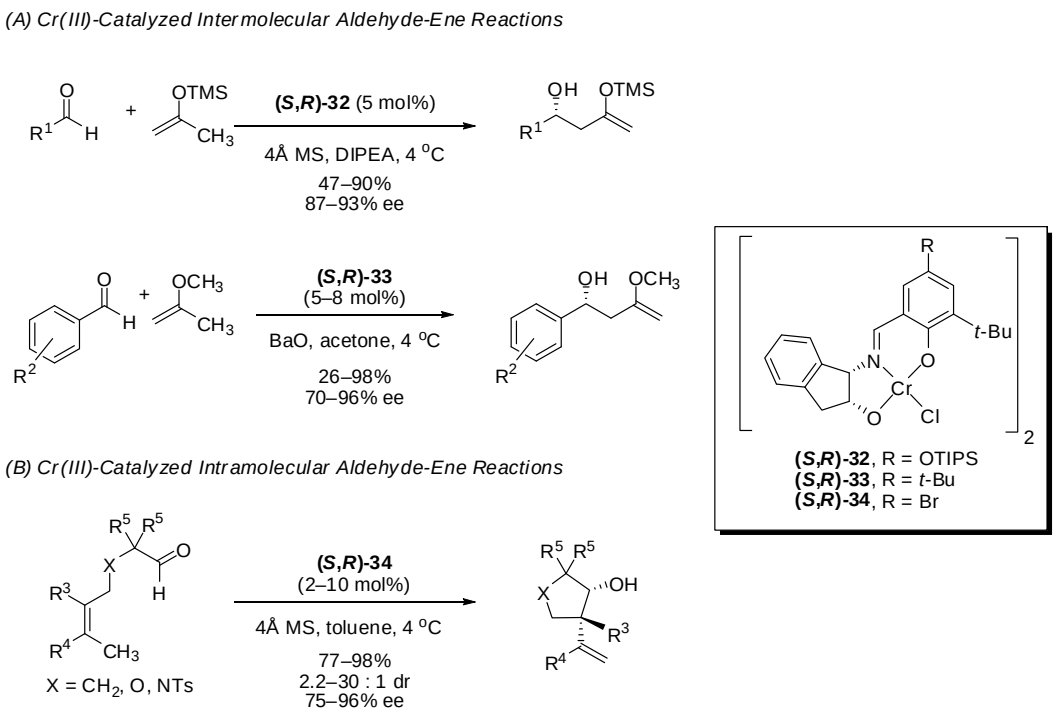

Scheme 1.10. Cr(III)-Catalyzed Aldehyde-Ene Reactions

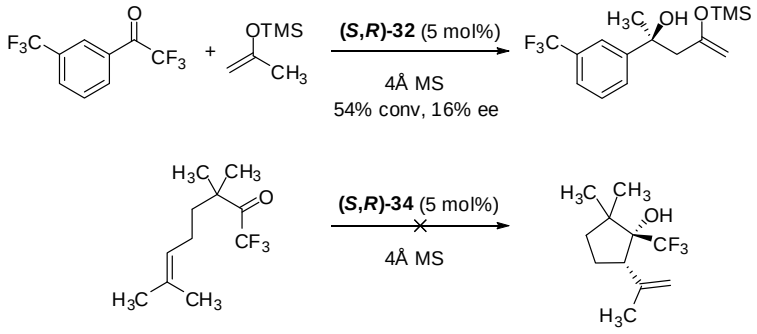

Scheme 1.11. Ketone-Ene Reactions with Cr(III) Tridentate Schiff-Base Catalysts

Although the scope of reported ketone-ene methodologies remains limited by the apparent necessity for an activated α-dicarbonyl functionality, we envisioned that a transannular ketone-ene reaction may not require this feature. Given that the transannular disposition of reacting partners can confer a significant entropic advantage and corresponding reactivity enhancements, we considered the possibility of effecting

enantioselective transannular ene reactions of electronically unactivated ketones using chiral Schiff-base chromium(III) catalysts.

1.4. Substrate Choice

We were particularly interested in studying the transannular ketone-ene reaction of (*E*)-cyclodecenones, as the resulting products contain a decalinol framework that is prevalent in terpene natural products (Scheme 1.12).[16] Furthermore, diastereoselective ketone-ene reactions of this substrate framework have been demonstrated. Yamamura reported thermal and Lewis acid-promoted transannular ketone-ene reactions of natural product preisocalamendiol **35** to afford dienol **36** in good yield (Scheme 1.13).[17] The successful cyclization in the presence of $AlCl_3$ under mild conditions suggested that chiral Lewis acid catalysts may be able to induce enantioselective transannular ketone-ene reactions of cyclodecenone substrates. Additionally, the use of elevated temperatures (180 ^{o}C) to effect the thermal ketone-ene reaction of preisocalamendiol is an indication that background cyclization of related substrates would likely not compete with a Lewis acid-catalyzed pathway.

[16] For a recent review of natural sesquiterpenoids, see: Fraga, B. M. *Nat. Prod. Rep.*, **2011**, *28*, 1580.

[17] Niwa, M.; Iguchi, M.; Yamamura, S. *Bull. Chem. Soc. Jpn.* **1976**, *49*, 3148.

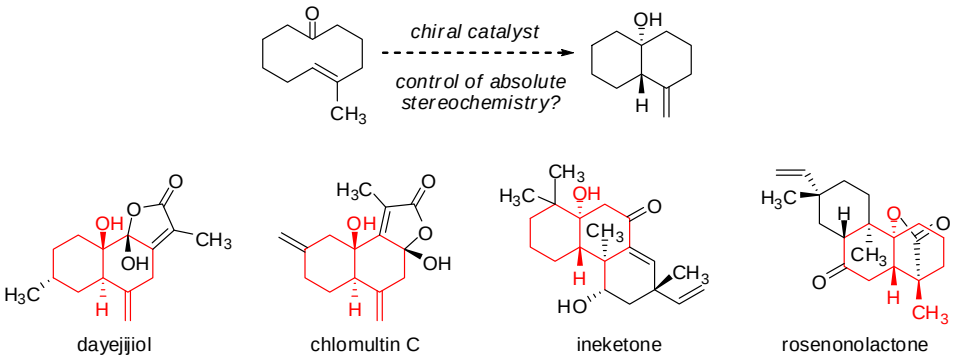

Scheme 1.12. Proposed Enantioselective Transannular Ketone-Ene Reaction and Selected Examples of Natural Products Featuring *trans*-Decalinol Frameworks

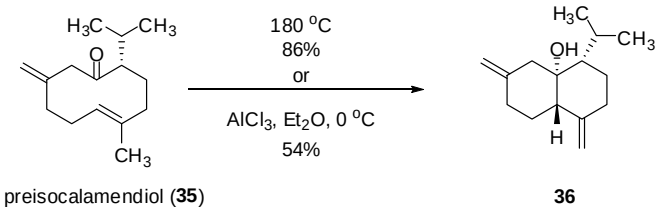

Scheme 1.13. Thermal and Lewis Acid-Promoted Transannular Ketone-Ene Reactions of Preisocalamendiol

We recognized that our efforts would need take into consideration the known temperature-dependent planar chirality of medium-sized cyclic (*E*)-olefin substrates.[18] For efficient, enantioselective transannular ene reactions to be possible, the reaction must necessarily occur under conditions where interconversion of the enantiomeric conformers of the substrate takes place. In that context, Barriault has studied diastereoselective ene reactions of (*E*)-cyclodecenones in cascade oxy-Cope-ene transformations and has shown that those cyclic structures are configurationally flexible under the elevated temperatures of the thermal reaction (140–220 °C) (Scheme 1.14).[19] Additionally, the configurational

[18] Nakazaki, M.; Yamamoto, K.; Naemura, K. in Stereochemistry, Topics in Current Chemistry, vol. 125 (Eds. Vogtle, F.; Weber, E.) Springer, Berlin, **1984**, 1.

[19] a) Warrington, J. M.; Yap, G. P. A.; Barriault, L. *Org. Lett.* **2000**, *2*, 663. Sauer, E. L. O.; Hooper, J.; Woo, T.; Barriault, L. *J. Am. Chem. Soc.* **2007**, *129*, 2112. b) Sauer, E. L. O.; Barriault, L. *J. Am. Chem. Soc.* **2004**, *126*, 8670.

instability of some cyclic (*E*)-olefins, determined through racemization half-life measurements, suggests that elevated temperatures will not be required for conformer interconversion of cyclodecenones containing trisubstituted olefins (Figure 1.2).[20]

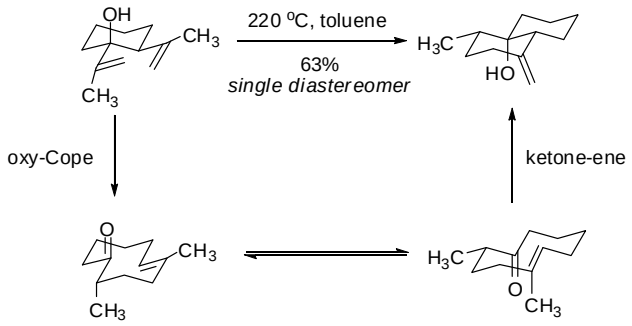

Scheme 1.14. Barriault's Tandem Oxy-Cope-Ene Reaction

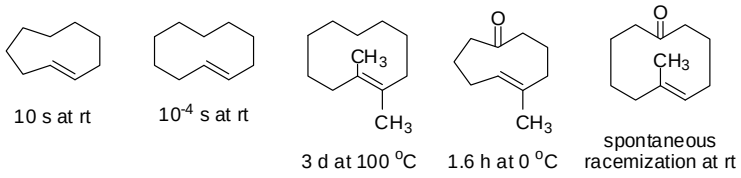

Figure 1.2. The Half-Life of Racemization for Medium-Sized Cyclic (*E*)-Olefins

1.5. Results and Discussion

1.5.1. Substrate Synthesis

Based on the prior studies on this substrate framework, we chose to study the transannular ketone-ene reaction of (*E*)-5-methyl-cyclodec-5-enone **39a**, which was readily synthesized from cyclohexene oxide in four steps (Scheme 1.15).[19a] A copper-catalyzed epoxide opening with isopropenyl magnesium bromide provided secondary alcohol **37** in quantitative yield. Under Swern oxidation conditions, the alcohol was converted to a β,γ-unsaturated ketone, which was reacted with vinylmagnsium bromide to

[20] a) Cope, A. C.; Banholzer, K.; Keller, H.; Pawson, B. A.; Whang, J. J.; Winkler, H. J. S. *J. Am. Chem. Soc.* **1965**, *87*, 3644. b) Westen, H. H. Helv. Chim. Acta **1964**, *47*, 575. c) Binsch, G.; Roberts, J. D. *J. Am. Chem. Soc.* **1965**, *87*, 5158. d) Tomooka, K.; Ezawa, T.; Inoue, H.; Uehara, K.; Igawa, K. *J. Am. Chem. Soc.* **2011**, *133*, 1754.

provide divinyl alcohol **38** in good yield and in >19:1 diastereomeric ratio. Treatment of **38** with potassium hydride and 18-crown-6 ether effected an anionic oxy-Cope rearrangement to provide **39a** as a single olefin isomer.[21] Cyclodecenone **39a** can be stored neat at –30 °C for at least three months without decomposition or isomerization.[22]

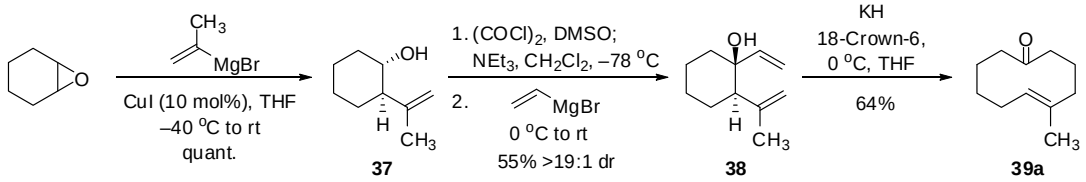

Scheme 1.15. Synthesis of Model Substrate (*E*)-5-methyl-cyclodec-5-enone **39a**

1.5.2. Catalyst Screen

With the model substrate in hand, an evaluation of chiral metal(salen) and metal tridentate Schiff-base complexes, was conducted under conditions that afforded no observable background conversion of cyclodecenone **39a** (Scheme 1.16). Of the Lewis acids evaluated, the chromium(III) tridentate Schiff-base complex **33**,[14b, 23] was uniquely effective in promoting the desired transformation. The ketone-ene reaction catalyzed by **33** provided *trans*-decalinol **40a** as a single regioisomer in 62% yield, >19:1 dr, and 79% ee. The high substrate conversion along with high product enantioenrichment confirmed that cyclodecenone **39a** is configurationally dynamic under the reaction conditions.

[21] Evans, D. A.; Golob, A. M. *J. Am. Chem. Soc.* **1975**, *97*, 4765.

[22] Many of the cyclodecenones studied, including **39a**, undergo ene reactions in the presence of acid. As such, NMR samples were only taken in $CDCl_3$ that was pre-treated with K_2CO_3, and cyclodecenones were purified on Davisil™ or neutral alumina instead of silica gel.

[23] The (*R*,*S*)- or (*S*,*R*)- designation preceding catalyst numbers refers to the stereochemistry of the *cis*-1,2-aminoindanol portion of the ligand.

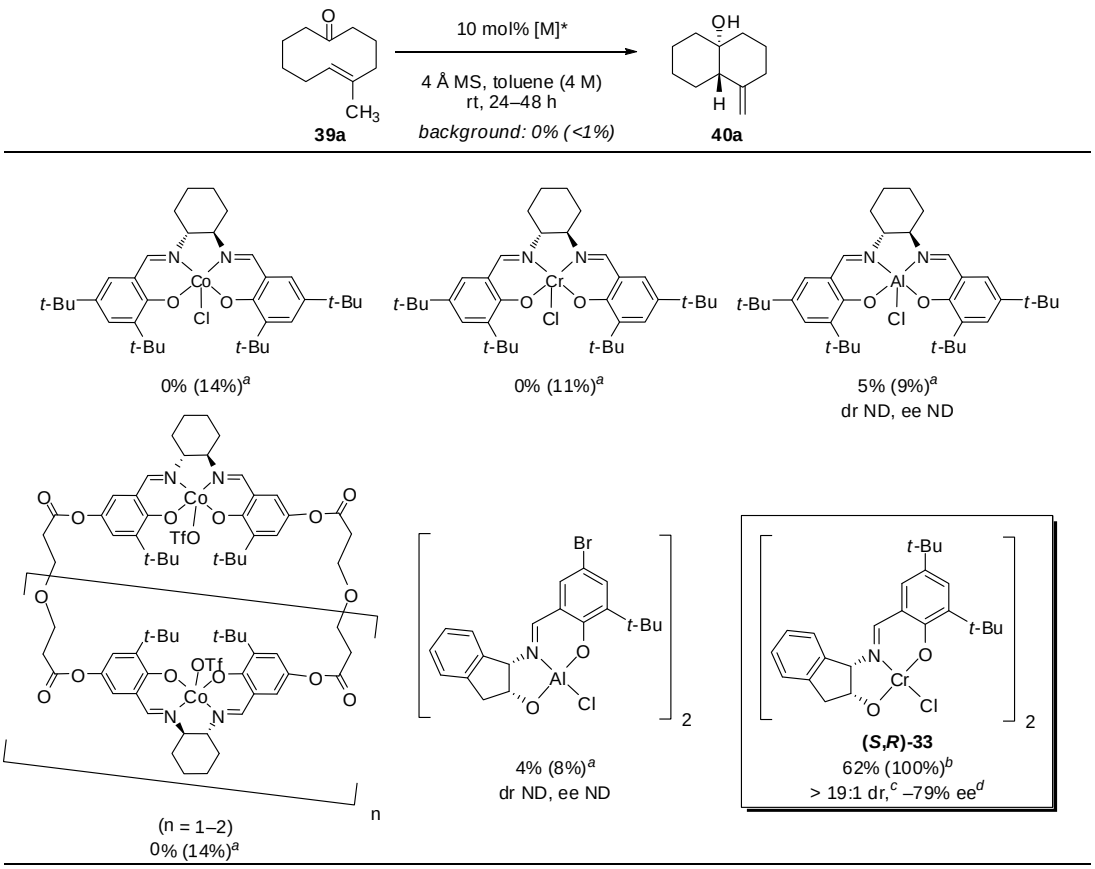

[a]Yields and conversions (in parantheses) were deteremined by ^{1}H NMR analysis of crude reaction mixtures using 1,3,5-trimethoxybenzene as an internal standard. [b] **39a** was completely consumed, and afforded **40** as a single regioisomer and diastereomer, as deteremined by ^{1}H NMR analysis of the crude reaction mixture. Yield was determined by isolation. [d]Determined by GC analysis using commercial chiral columns.

Scheme 1.16. Initial Screen of Chiral Lewis Acids

1.5.3. Chromium(III) Tridentate Schiff-Base Catalysts

Chromium(III) tridentate Schiff-base complexes were first developed for enantioselective hetero-Diels–Alder (HDA) reactions of aldehydes and monooxygenated dienes (Scheme 1.17A).[24] Related complexes were subsequently shown to be effective for a number of other asymmetric pericyclic transformations involving aldehyde and

[24] a) Dossetter, A. G.; Jamison, T. F.; Jacobsen, E. N. *Angew. Chem., Int. Ed.* **1999**, *38*, 2398. b) Gademann, K.; Chavez, D. E.; Jacobsen, E. N. *Angew. Chem., Int. Ed.* **2002**, *41*, 3059. c) Chavez, D. E.; Jacobsen, E. N. *Org. Synth.* **2005**, 82, 34.

quinone substrates, including variants of the HDA reaction,[25] aldehyde-ene reactions (Scheme 1.10), and quinone-Diels-Alder (QDA) cycloadditions (Scheme 1.17B).[26] Mechanistic investigations have indicated that the catalysts activate carbonyl groups through single-point binding.[14c]

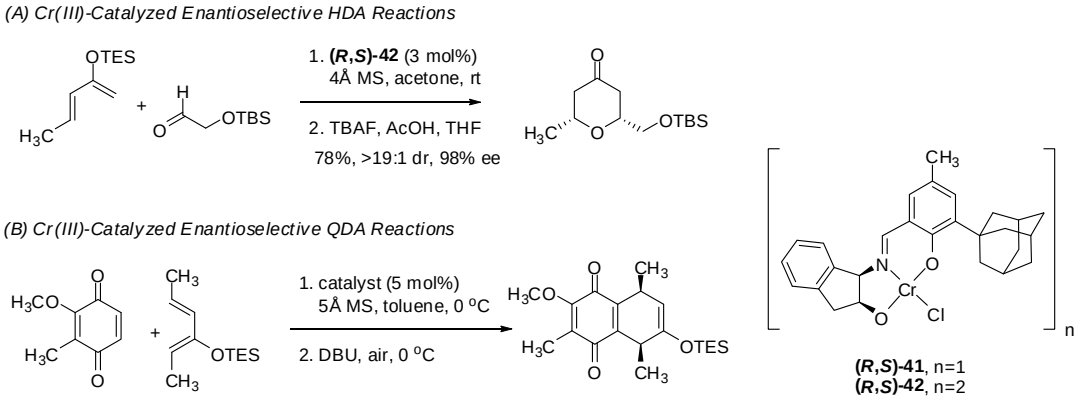

entry	catalyst	time	yield	ee	regioselectivity
1	**(*R*,*S*)-41**	10 min	86	96	12:1
2	**(*R*,*S*)-42**	26 h	82	39	3.3:1

Scheme 1.17. Enantioselective Cr(III)-Catalyzed HDA and QDA Reactions

The depictions of complexes **32**–**34** and **41**–**42** used in Schemes 1.10 and 1.17 summarize key structural data that has been gained about these catalysts (Scheme 1.18). X-ray crystallography data indicate that complex **34**, derived from *ortho*-*t*-Bu-substituted salicylaldimine **43**, is a dimer in the solid state with the two Cr(III) centers bridged by oxygen atoms of the aminoindanol ligand. This class of dimeric catalysts will be referred to as Type II dimers for the remainder of the chapter.[27] The optimal HDA catalyst (**42**)

[25] a) Joly, G. D.; Jacobsen, E. N. *Org. Lett.* **2002**, *4*, 1795. b) Chavez, D. E.; Jacobsen, E. N. *Org. Lett.* **2003**, *5*, 2563.

[26] Jarvo, E. R.; Lawrence. B. M.; Jacobsen, E. N. *Angew. Chem., Int. Ed.* **2005**, *44*, 6043

[27] This notation was used by Rebecca Ruck (Ref. 14c).

displays an alternate dimerization mode (Type I), wherein a water molecule bridges the two Cr(III) centers. This complex is derived from *ortho*-(1-adamantyl)-substituted Schiff-base ligand **44**. The bulky adamantyl group is thought to preclude formation of an aminoindanol bridged Type II dimer. Mechanistic studies carried out by former graduate student, Rebecca Ruck, provided evidence that the dimeric structures of **34** and **42** are maintained in solution and are relevant for catalysis of the aldehyde-ene and HDA reactions.[28] Complex **41**, which is also derived from tridentate Schiff base **44**, is prepared under identical conditions to complex **42** except for an acidic workup. This catalyst was found to crystallize as a monomer. Evidence that solid structure data for **41** and **42** have reactivity implications is shown in Scheme 1.17B. Monomer **41** affords faster and more selective QDA reactions than dimeric catalyst **42** (entries 1–2). The Cr(III) centers of all three of these complexes have octahedral geometry with water molecules occupying available coordination sites. A feature common to all methods that employ Cr(III) tridentate Schiff-base complexes is the requirement for desiccant (molecular sieves or BaO). It is proposed that this additive sequesters a coordinated water molecule from the highly Lewis acidic Cr(III) center to provide a free coordination site for carbonyl activation.

[28] A lack of a nonlinear effect (NLE) upon varying the ee of catalyst **34** in the aldehyde-ene reaction, in combination with a positive NLE upon varying the ee of ligand **43**, provide strong evidence that the catalyst is dimeric in solution and does not undergo ligand exchange. Molecular weight osmometry studies and a first order kinetic dependence on the catalyst indicate that catalyst **42** is dimeric in the solution state.

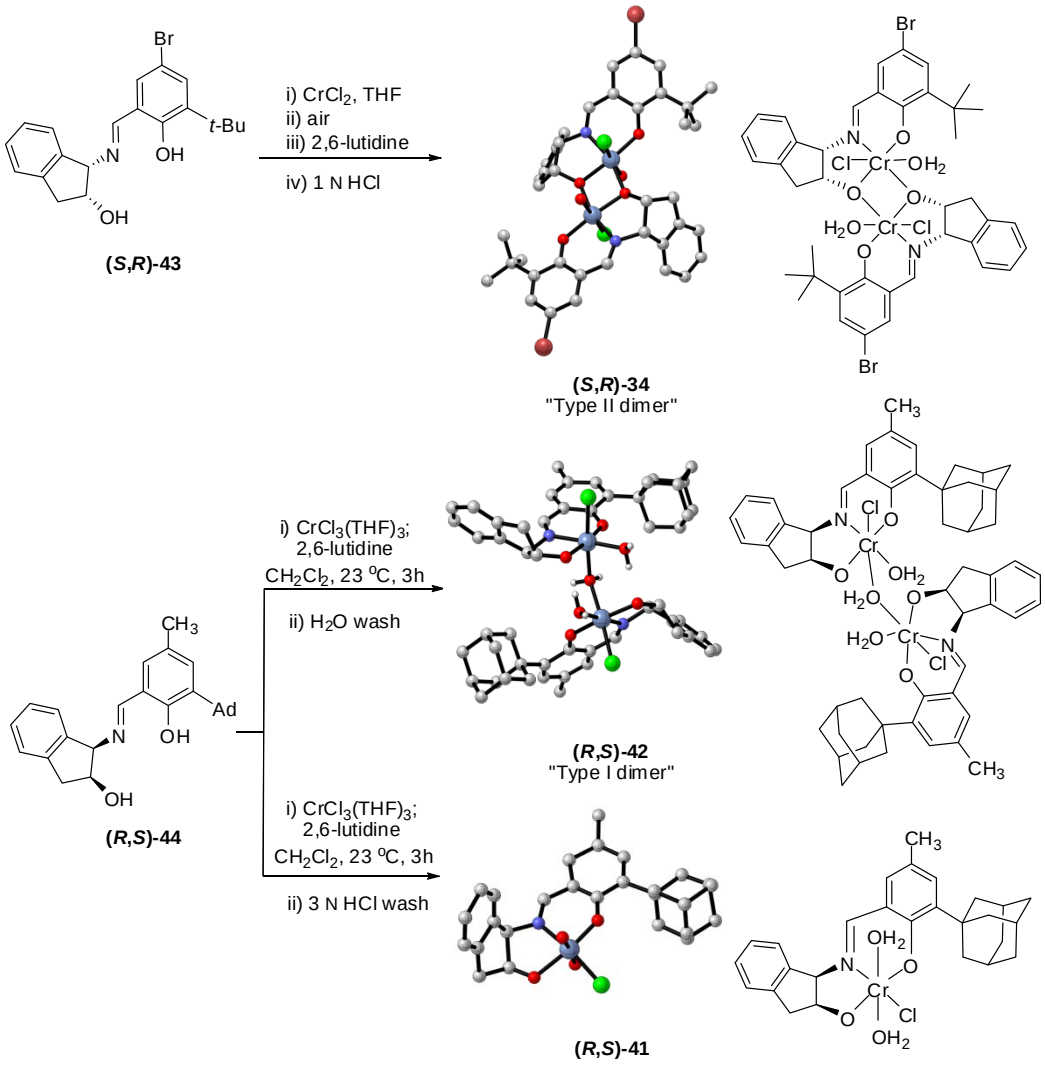

Scheme 1.18. Different Classes of Cr(III) Tridentate Schiff-Base Complexes

1.5.4. Catalyst Optimization Studies

Based on the results of our initial catalyst screen, we evaluated complexes **34**, **41**, and **42** as representative members of each Cr(III) tridentate Schiff-base crystal-type (Type II dimer, monomer, and Type I dimer, respectively) for the transannular ketone-ene reaction of **39a** (Table 1.1). In the presence of activated 4Å molecular sieves, all three catalyzed the desired reaction providing nearly complete conversion after 48 h. These catalysts afforded *trans*-decalinol **40a** in moderate to good enantioselectivity and

all provided the same sense of enantioinduction. Unlike the QDA reaction, the transannular ketone-ene reaction does not show a pronounced selectivity difference with monomeric and dimeric catalysts **41** and **42** (entries 2 and 3).[29]

Table 1.1. Evaluation of Structurally Different Cr(III) Tridentate Schiff-Base Complexes

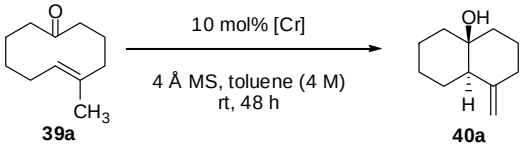

39a **40a**

entry	catalyst	conversion[a]	ee[b]
1	**(*S*,*R*)-34**	100	–83
2	**(*S*,*R*)-41**	96	–60
3	**(*S*,*R*)-42**	98	–60

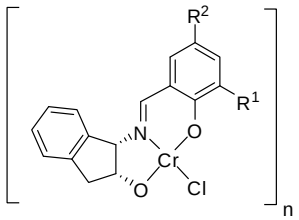

(*S*,*R*)-34, R^1=*t*-Bu, R^2=Br, n=2
(*S*,*R*)-41, R^1=Ad, R^2=CH_3, n=1
(*S*,*R*)-42, R^1=Ad, R^2=CH_3, n=2

[a] Conversion was approximated as 100*(**40a**–**39a**)/(**40a**+**39a**), based on ^{1}H NMR integration of the crude reaction mixture. Product diastereomeric ratio was determined to be >19:1 based on ^{1}H NMR analysis of the crude reaction mixture. [b]Determined by GC analysis using commercial chiral columns.

Further optimization studies were carried out on the two dimeric catalyst scaffolds.[30] A series of catalysts containing variation at the *para*-position of the salicylaldehyde portion of the Schiff-base ligands was evaluated (Table 1.2). However, the effect of modifying this substituent on product enantioselectivity was minimal for both types of dimers.

[29] In general, the Cr(III)-catalyzed ketone-ene reactions of **39a** afforded **40a** as a single regioisomer and in >19:1 dr; exceptions will be noted. The volatility of product **40a** caused significant errors in isolated yield measurements during early optimization studies. For this reason, conversion data will be presented.

[30] These designations are based on the assumption that chloride complexes containing an *ortho*-Ad group and prepared with a neutral aqueous work up are Type I dimers and catalysts containing an *ortho*-*t*-Bu are Type II dimers.

Table 1.2 Variation of the Schiff-base *para*-Substituent

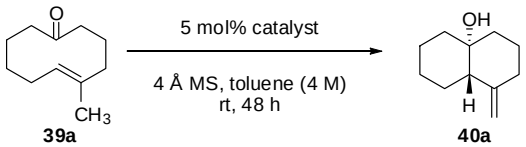

39a **40a**

entry	catalyst	R^1	R^2	conversion[a]	ee[b]
1	**(*S*,*R*)-45**	Ad	Br	100	–67
2	**(*S*,*R*)-42**	Ad	CH_3	96	–60
3	**(*S*,*R*)-46**	Ad	OAc	100	–46
4	**(*S*,*R*)-34**	*t*-Bu	Br	100	–83
5	**(*S*,*R*)-47**	*t*-Bu	CH_3	100	–87
6	**(*S*,*R*)-48**	*t*-Bu	OAc	100	–83

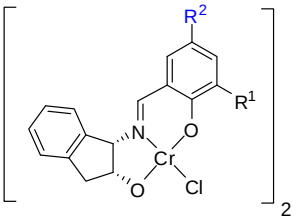

[a] Conversion was approximated as 100*(**40a**–**39a**)/(**40a**+**39a**), based on ^{1}H NMR integration of the crude reaction mixture. Product diastereomeric ratio was determined to be >19:1 based on ^{1}H NMR analysis of the crude reaction mixture.[b]Determined by GC analysis using commercial chiral columns.

The HDA reaction shows reactivity and selectivity dependence on the identity of the catalyst counterion.[24a,c] A counterion exchange on complex **42** from chloride to the noncoordinating SbF_6^- counterion induced rate accelerations and selectivity enhancements for some substrates. Hence, we broadly investigated the impact of modifying the counterion associated with catalyst **42** on the ketone-ene reaction. Pronounced effects were observed, with reactivity increasing steadily as the coordinating ability of the counterion decreased (Table 1.3). Catalysts **52** and **53**, bearing PF_6^- and SbF_6^- counterions, respectively, promoted complete conversion within 24 h, albeit with diminished enantioselectivities as compared to the chloride complex (entries 6–7 vs. entry 1).[31] Complexes bearing sulfonate counterions were somewhat less reactive, but induced significantly improved enantioselectivities (entries 3 and 4), with triflate complex **50** identified as the optimal catalyst of the series.

[31] The transannular ketone-ene reaction conducted with complex **53** afforded minor olefin byproducts (<10%), an indication of diminished regioselectivity with this more Lewis acidic catalyst.

Table 1.3. Counterion Effects on Reactivity and Selectivity

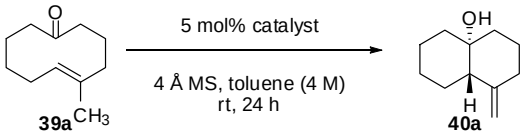

entry	catalyst	conv. (%)[a]	dr[b]	ee (%)[c]
1	**(*R*,*S*)-42** (X = Cl)	50	>19:1	60
2	**(*S*,*R*)-49** (X = OTs)	67	>19:1	–84
3	**(*R*,*S*)-50** (X = OTf)	76	>19:1	93
4	**(*R*,*S*)-51** (X = NTf_2)	98	>19:1	46
5	**(*R*,*S*)-52** (X = PF_6)	100	>19:1	50
6	**(*R*,*S*)-53** (X = SbF_6)	100	>19:1	56

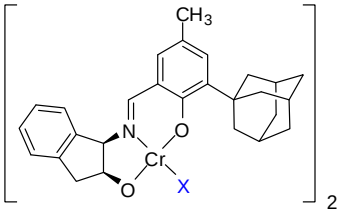

(*R*,*S*)-catalyst

[a]Determined by GC analysis of the crude reaction mixtures using dodecane as an internal standard. [b]Determined by 1H NMR analysis of the crude reaction mixtures. [c]Determined by GC analysis using commercial chiral columns.

Analogous counterion exchanges were carried out on the optimal Type I and II chloride complexes **45** and **47** (identified from the experiments in Table 1.2) and monomer **41**. Triflate **54** catalyzed a more selective ketone-ene reaction than the corresponding chloride complex, providing decalinol **40a** in 87% ee. This enhancement in selectivity is in accord with the counterion effect observed between Type I chloride complex **42** and triflate **50**. Enantioselectivity induced by triflate **55** was fairly similar to that of the corresponding Type II chloride complex (85% vs. 87% ee). In contrast, the triflate complex **56** provided the ketone-ene product with significantly lower enantioenrichment than the corresponding monomeric chloride complex (1% ee vs. 60% ee). Although these data are not conclusive about the structure of optimal catalyst **50**, they empirically indicate that the catalyst preparation procedure is important.[32]

[32] CD spectroscopy, which has previously been used to characterize all three structural types of Cr(III) complexes, could not distinguish triflate catalysts **50** and **56**.

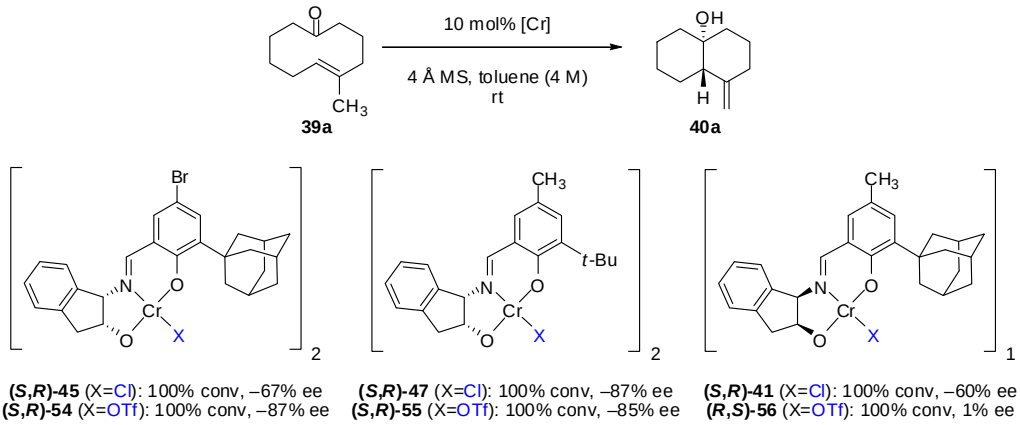

Scheme 1.19. Counterion Effects Based on the Chloride Complex Structure Type

1.55. Substrate Scope[33]

With complex **50** identified as the optimal catalyst, the substrate scope of the enantioselective transannular ketone-ene reaction was evaluated (Table 1.4). Full conversion of cyclodecenone **39a** was achieved by extending the reaction time to 48 h, and product **40a** was obtained in 81% yield and 93% ee (entry 1). The absolute stereochemistry of **40a** was determined by X-ray crystallographic analysis of the corresponding *para*-Br-benzoate, and the assignments for the other products were made by analogy (Figure 1.3).

[33] Cyclodecenones were synthesized via anionic or palladium-catalyzed oxy-Cope rearrangements of divinyl alcohols: a) Ref 21. b) Bluthe, N.; Malacria, M.; Gore, J. *Tetrahedron Lett.* **1983**, *24*, 1157.

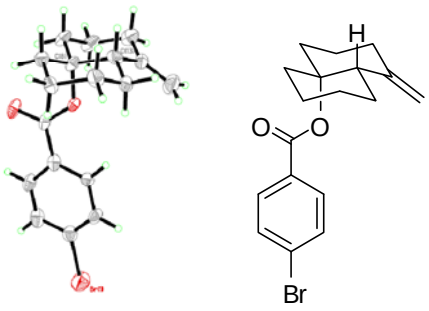

Figure 1.3. ORTEP Diagram of the *para*-Br-benzoate of **40a** Showing 50% Probability Displacement

Gem-dimethyl-substituted *trans*-decalinols **40b** and **40c**, were accessed in high yield and enantioselectivity (entries 2 and 3), but the closely analogous product **40d** was obtained in low yield and as a racemate (entry 4). Analysis of the chair-chair conformations of these substrates provides a plausible explanation (Figure 1.4).[34] Only cyclodecenone **40d** possesses a *syn*-pentane relationship between its methyl substituents, and the pseudo-axial methyl substituent at C3 is also likely to interfere with complexation of the Lewis acidic catalyst. With these substitution effects in mind, we probed more highly functionalized substrates (Table 1.4, entries 5 and 6). The acid-sensitive acetal **40e** and unconjugated diene **40f** both proved to be effective substrates, affording the corresponding ene products in high enantioselectivities and good yields. Additionally, ether **57** and cyclononenone **59** underwent enantioselective ketone-ene reactions to afford the corresponding bicyclic alcohol products, although in diminished yields and enantioselectivities.

[34] Chair-like transition structures that are consistent with reaction outcomes have been determined computationally for diastereoselective thermal ketone-ene reactions of (*E*)-cyclodecenones: Terada, Y.; Yamamura, S. *Tetrahedron Lett.* **1979**, *20*, 1623.

Table 1.4. Substrate Scope of the Cr(III)-Catalyzed Ketone-Ene

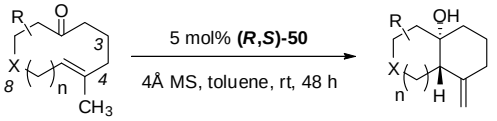

entry	substrate	product	yield (%)[a,b]	dr[c]	ee (%)[d]
1	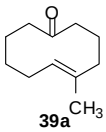 **39a**	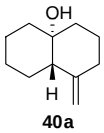 **40a**	81	>19:1	93
2	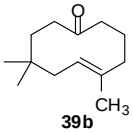 **39b**	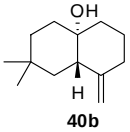 **40b**	96	>19:1	94
3	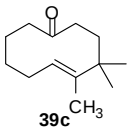 **39c**	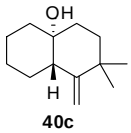 **40c**	84	>19:1	94
4	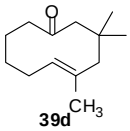 **39d**	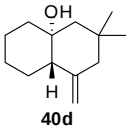 **40d**	32[e]	>19:1	0
5	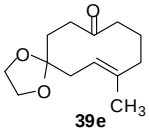 **39e**	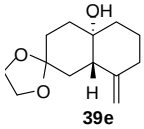 **39e**	87	>19:1	96
6	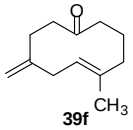 **39f**	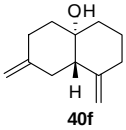 **40f**	62	>19:1	94
7[f]	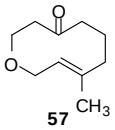 **57**	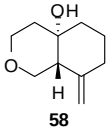 **58**	13	>19:1	49
8[f]	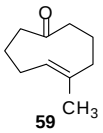 **59**	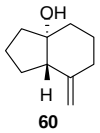 **60**	18	>19:1	68

[a]Reactions were performed on a 0.2 mmol scale with 5 mol% catalyst **50** (10 mol% based on Cr) and in the presence of powdered 4 Å molecular sieves at rt in anhydrous toluene ([**substrate**] = 4 M). Unless otherwise noted, reactions showed complete conversion after 48 h and the bicyclic alcohol product was obtained as a single regioisomer. [b]Isolated yield of the ketone-ene products following purification by flash chromatography. [c]Determined by ^{1}H NMR analysis of the crude reaction mixtures. [d]Determined by GC analysis using commercial chiral columns. [e]Combined yield of **40d** and an inseparable regioisomeric product. [f]Reaction time was 24 h.

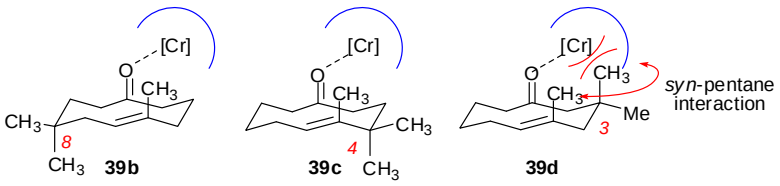

Figure 1.4. Rationale for the Low Observed Reactivity of **39d** Relative to **39b** and **39c**

Tetrasubstituted alkene **61** proved much less reactive than trisubstituted olefins **39a-f** under the catalytic conditions, undergoing only 19% conversion after 24 h at 50 °C. The transannular ketone-ene reaction afforded *trans*-decalinol **62**, bearing a quaternary stereocenter, in 12% yield and 73% ee (Scheme 1.20). Cyclodecenone **(+)-61** was recovered in 69% yield and in 10% ee, confirming that this substrate undergoes racemization slowly under the catalytic conditions, and that complex **50** induced a measurable kinetic resolution.[35]

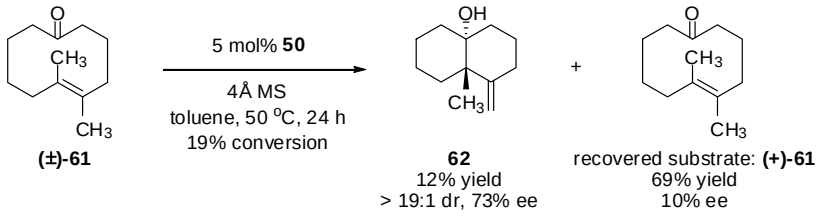

Scheme 1.20. Kinetic Resolution of Planar Chiral Cyclodecenone **61**

1.56. Limitations

Acyclic ketones **63** and **64** did not undergo intramolecular ene reactions under the optimized conditions or at 50 °C (Scheme 1.21). These results may be an indication that the reactivity enhancements conferred to transannular substrates are essential for Cr(III)-catalyzed ketone-ene reaction. However, attempted ketone-ene reactions of a number of

[35] A kinetic resolution of planar chiral cyclic ethers has been achieved through an enantioselective transannular [2,3]-Wittig rearrangement: Tomooka, K.; Komine, N.; Fujiki, D.; Nakai, T.; Yanagitsuru, S. *J. Am. Chem. Soc.* **2005**, *127*, 12182.

other cyclic substrates were unsuccessful as well. For example, (*Z*)-5-methyl-cyclodecenone (**65**), the olefin isomer of model substrate **39a** did not afford any of the predicted *cis*-fused decalinol. (*E*)-Cyclodecenones **66** and **67**, which differ from **39a** in the relative positions of the ene and enophile components in the ring, and were predicted to afford [3.5.0]-bicyclic alcohols, were also unreactive. Finally, 11-membered cyclic keto-olefin **68** did not afford the corresponding ketone-ene product. The sensitivity of the reaction to perturbations in ring-size is similar to that of List's transannular aldol reaction.[7] These data suggest that the transannular strategy, which properly aligned the two reactive components of model substrate **39a** for the ene reaction, might have the opposite effect with many of these other medium-sized cyclic substrates, prohibiting the desired reaction from taking place.

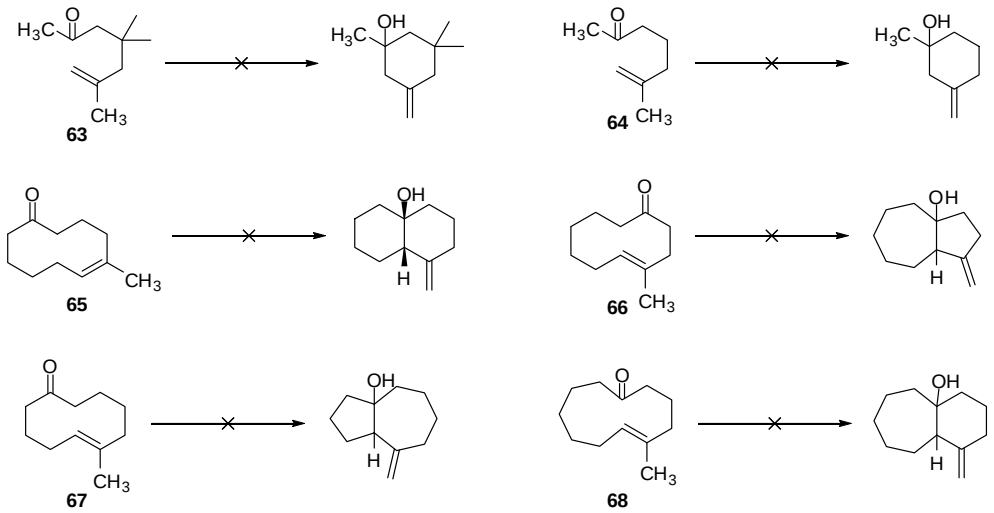

Scheme 1.21. Unsuccessful Substrates

1.6. Conclusions

In conclusion, we have demonstrated that chiral chromium(III) tridentate Schiff-base complex **50** catalyzes transannular ketone-ene reactions of (*E*)-cyclodecenones in

high diastereo- and enantioselectivity to access *trans*-decalinols. The dramatic counterion effects observed in the ketone-ene reaction are intriguing and are not well understood at this time. Structural elucidation of complex **50** may provide an understanding of the role the triflate counterion has in defining the chiral environment of the catalyst.

Significantly, the transannular strategy provides entropic activation for the ketone-ene reaction and allows electronically unactivated ketones to be engaged as substrates in a chiral Lewis acid-catalyzed process. This finding is in line with previous observations regarding the Cr(III)-catalyzed aldehyde-ene reactions: intermolecular reactions occurs only with activated electron-rich olefins whereas the entropically activated intramolecular variant tolerates unactivated olefins. This trend suggests that other typically inert functional groups may undergo transannular reactions with appropriate electronic tuning of the reaction partner.

1.7. Experimental Section

A. General Information

Unless otherwise noted, all reactions were performed under a positive pressure of anhydrous nitrogen or argon in flame- or oven-dried glassware. Moisture- and air-sensitive reagents were dispensed using oven-dried stainless steel syringes or cannulae and were introduced to reaction flasks through rubber septa. Reactions conducted below ambient temperature were cooled by external baths (dry ice/acetone for –78 ^{o}C and ice/water for 0 ^{o}C). Reactions conducted above ambient temperature were heated by an oil bath.

Analytical thin layer chromatography (TLC) was performed on glass plates pre-coated with silica 60 F_{254} (0.25 mm) or on aluminum sheets pre-coated with neutral aluminum oxide 60 F_{254} (0.2 mm). Visualization was carried out by exposure to a UV-lamp (short wave 254 nm, long wave 365 nm), and by heating after staining the plate with a ceric ammonium molybdate, potassium permanganate, or phosphomolybdic acid solution. Extraction and chromatography solvents were reagent or HPLC grade and were used without further purification. Flash column chromatography was carried out over silica gel (60 Å, 230–400 mesh) from EM Science, Davisil^{TM} (Grade 643, 150 Å, 200–425 mesh) from Aldrich, or activated neutral aluminum oxide (Brockman I standard grade, 58 Å, 150 mesh) from Aldrich. Flash column chromatography was conducted on a Biotage Isolera automated chromatography system.

Materials. Commercial reagents and solvents were used with the following exceptions: tetrahydrofuran, diethyl ether, toluene, and dichloromethane employed as reaction solvents were dried by passage through columns of activated alumina. Triethylamine was distilled from calcium hydride at 760 torr prior to use. Chloroform-d was treated with and stored over anhydrous potassium carbonate prior to use. Powdered 4Å MS were purchased from Sigma-Aldrich, activated by heating in a commercial microwave oven, and stored in a vial sealed with parafilm in a desiccator. 4,4-dimethyl-cyclohexanone was prepared according to the reported procedure.[36] Intermediates **S10**, **S11** and **S12** were prepared according to reported procedures.[37,38,39]

Instrumentation. Proton nuclear magnetic resonance (^{1}H NMR) spectra and carbon nuclear magnetic resonance (^{13}C NMR) spectra were recorded on a Varian Mercury-400 (400MHz), Inova-500 (500MHz), or an Inova-600 (600MHz) spectrometer at 23 ^{o}C, unless otherwise noted. Chemical shifts for protons are reported in parts per million (ppm, δ scale) downfield from tetramethylsilane and are referenced to residual protium in the NMR solvent ($CHCl_3$: 7.26 ppm). Chemical shifts for carbons are reported in parts per million (ppm, δ scale) downfield from tetramethylsilane and are referenced to the NMR solvent ($CDCl_3$: 77.16 ppm). Data are represented as follows: chemical shift, multiplicity (s = singlet, d = doublet, t = triplet, q = quartet, m = multiplet, br = broad), integration, and coupling constant (*J*) in Hertz (Hz). Infrared (IR) spectroscopy was performed on the neat compounds on a Brucker Tensor 27 FT-IR

[36] Meyer, W. L.; Brannon, M. J.; Burgos, C. d. G.; Goodwin, T. E.; Howard, R. W. *J. Org. Chem.* **1985**, *50*, 438.

[37] Reetz, M. T.; Kindler, A. *J. Organomet. Chem.* **1995**, *502*, C5.

[38] Grisé, C. M.; Rodrigue, E. M.; Barriault, L. *Tetrahedron* **2008**, *64*, 797.

[39] Clément, R.; Grisé, C. M.; Barriault, L. *Chem. Commun.* **2008**, 3004.

Spectrometer using OPUS software. Data are represented as follows: frequency of absorption (cm^{-1}), intensity of absorption (s = strong, m = medium, w = weak). Mass spectra were obtained on an Agilent 1200 series 6120 Quadrupole LC/MS. Optical rotation data were collected using a 1-mL cell using a 0.5 dm path length on a Jasco P-2000 polarimeter and are reported as $[\alpha]_D^{23}$ (concentration in grams/100 mL solvent). Reported rotations are the average of 3–5 measurements per sample.

B. Catalyst Preparation and Characterization

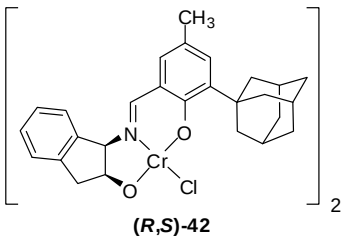

(*R*,*S*)-42

Chromium(III) Chloride Complex **(*R*,*S*)-42**

Catalyst (***R***,***S***)-**42** was prepared according to the published procedure.[24c]

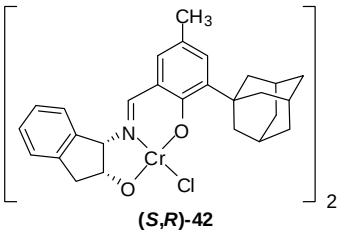

(*S*,*R*)-42

Chromium(III) Chloride Complex **(*S*,*R*)-42**

Catalyst **(*S*,*R*)-42** was prepared according to the published procedure.[24c]

General Procedure A – Counteranion Exchange

A flame-dried 50 mL round-bottom flask equipped with a stir bar and septum was wrapped with aluminum foil and charged with a silver salt bearing the desired counterion (0.0924 mmol, 0.95 equiv). To this flask was added complex **42** (50 mg, 0.097 mmol, 1 equiv). To the flask, under an atmosphere of argon, was added TBME (16.2 mL). The reaction mixture was stirred at room temperature for 3 h, after which the contents were filtered through Celite®. The pad of Celite® was rinsed with an additional portion of

TBME (16.2 mL). The filtrate was concentrated to afford the desired complex, which was used without further purification.

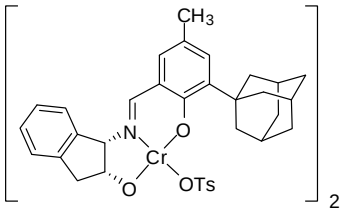

(*S*,*R*)-49

Chromium(III) Tosylate Complex **(*S*,*R*)-49**

Following General procedure A, the counterion exchange was performed with **(*S*,*R*)-42** (100 mg, 0.19 mmol, 1 equiv) and AgOTs (50.5 mg, 0.18 mmol, 0.95 equiv) to provide catalyst **(*S*,*R*)-49** as a brown powder (84%). FTIR (neat, cm^{-1}) 3198 (br m) 2902 (m) 1616 (s) 1538 (m) 1434 (m) 1307 (w) 1229 (s) 1169 (m) 1078 (m) 1010 (m) 945 (w) 812 (m) 744 (s).

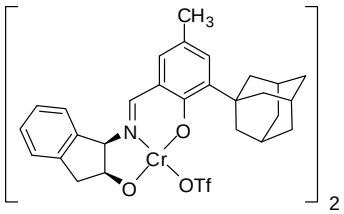

(*R*,*S*)-50

Chromium(III) Triflate Complex **(*R*,*S*)-50**

Following General Procedure A, the counterion exchange was performed with **(*R*,*S*)-42** (200 mg, 0.39 mmol, 1 equiv) and AgOTf (95 mg, 0.37 mmol, 0.95 equiv) to provide catalyst **(*R*,*S*)-50** as a brown powder (244 mg, 98%). FTIR (neat, cm^{-1}) 3271 (br w) 2902 (m) 2845 (w) 1614 (m) 1538 (m) 1453 (w) 1294 (m) 1227 (s) 1170 (s) 1026 (s) 980 (w) 811 (w) 746 (s).

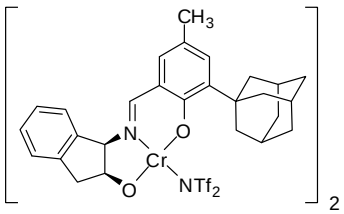

(*R*,*S*)-51

Chromium(III) Triflimide Complex **(*R*,*S*)-51**

Following General Procedure A, the counterion exchange was performed with **(*R*,*S*)-42** (50 mg, 0.097 mmol, 1 equiv) and $AgNTf_2$ (35.9 mg, 0.0924 mmol, 0.95 equiv) to provide

catalyst **(*R*,*S*)-51** as a brown powder (62.3 mg, 83%). FTIR (neat, cm^{-1}) 3538 (br w) 2905 (w) 2850 (w) 1614 (m) 1541 (m) 1431 (w) 1349 (m) 1298 (m) 1227 (m) 1188 (s) 1135 (m) 1057 (s) 981 (m) 748 (m).

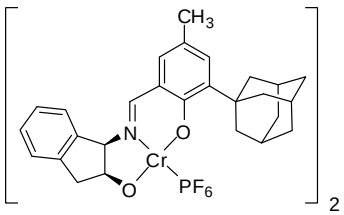

(*R*,*S*)-52

Chromium(III) Hexafluorophosphate Complex **(*R*,*S*)-52**

Following General Procedure A, the counterion exchange was performed with **(*R*,*S*)-42** (50 mg, 0.097 mmol, 1 equiv) and $AgPF_6$ (23.4 mg, 0.0924 mmol, 0.95 equiv) to provide catalyst **(R,S)-52** as a brown powder (50.3 mg, 82%). FTIR (neat, cm^{-1}) 3532 (br w) 2901 (m) 2848 (w) 1614 (m) 1538 (m) 1431 (w) 1300 (w) 1228 (m) 1151 (m) 1054 (m) 839 (s) 749 (m).

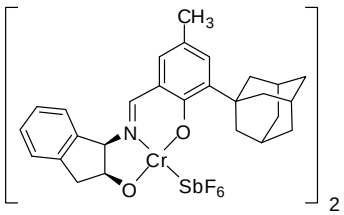

(*R*,*S*)-53

Chromium(III) Hexafluoroantimonate Complex **(*R*,*S*)-53**

Following General Procedure A, the counterion exchange was performed with **(*R*,*S*)-42** (50 mg, 0.097 mmol, 1 equiv) and AgSbF6 (31.8 mg, 0.0924 mmol, 0.95 equiv) to provide catalyst **53** as a brown powder (67.4 mg, 96%). This complex has previously been characterized.[24c]

C. Substrate Syntheses

General Synthetic Scheme for Transannular Ketone-Ene Substrates **39a**, **39c**, 3**9d**, and **59**

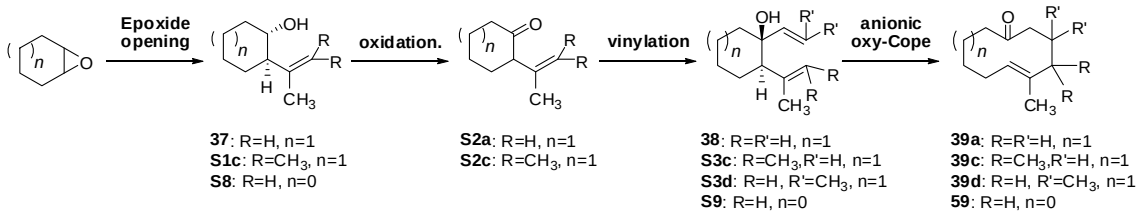

General Procedure B – Cu-catalyzed addition of Grignard reagents to meso epoxides[40]

A flame-dried 3 L round-bottom flask under N_2 was charged with CuI (2.9g, 15.3 mmol, 0.15 equiv) and THF (1 L) and cooled to –30 ^oC (dry ice/acetone). To this suspension was added a solution of Grignard in THF (150 mmol, 1.5 equiv) over a period of 30 m. After another 10 m at –30 ^oC, meso epoxide (100 mmol, 1 equiv) was added dropwise, neat, over 10 m, and the reaction mixture was allowed to gradually warm to room temperature overnight. The dark reaction mixture was cooled to 0 ^oC and quenched by slow addition of saturated aqueous NH_4Cl (200 mL). The contents were diluted with DI H_2O (200 mL) and extracted with Et_2O (3 x 500 mL). The combined organics were dried over Na_2SO_4, filtered, and concentrated *in vacuo*. The residue was re-dissolved in CH_2Cl_2, dried over Na_2SO_4, filtered, and concentrated to afford crude alcohol that, unless otherwise noted, was carried on to the next reaction without further purification.

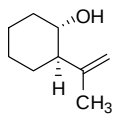

37

(±)-(1S,2R)-2-(prop-1-en-2-yl)cyclohexanol (**37**)[41]

[40] This procedure is adapted from Huynh, C.; Derguini-Boumechal, F.; Linstrumelle, G. *Tetrahedron Lett.* **1979**, *17*, 1503.

[41] Warrington, J. M.; Yap, G. P. A.; Barriault, L. *Org. Lett.* **2000**, *2*, 663.

This compound was prepared according to General Procedure B, with cyclohexene oxide (9.8 g, 100 mmol, 1 equiv) and isopropenylmagnesium bromide (0.5 M in THF, 300mL, 150 mmol, 1.5 equiv). The known alcohol **37** was obtained as a yellow oil (12.7 g) that was carried forward to the following reactions without further purification.

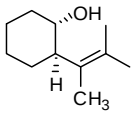

S1c

(±)-(1S,2R)-2-(3-methylbut-2-en-2-yl)cyclohexanol (**S1c**)

This compound was synthesized according to General Procedure B, with cyclohexene oxide (600 mg, 6.11 mmol, 1 equiv) and (3-methylbut-2-en-2-yl)magnesium bromide (0.25 M, 30mL, 1.5 equiv). The crude product was purified by flash column chromatography (SiO_2, Biotage, 0 to 50% Et_2O/hexanes) to afford **S1c** (698mg, 4.15 mmol, 68%) as a clear oil. R*f*=0.2 (50% Et_2O/hexanes); ^1H NMR (500 MHz, $CDCl_3$) δ ppm 3.43 (td, *J*=9.84, 4.58 Hz, 1 H) 2.45 (ddd, *J*=11.79, 9.96, 3.89 Hz, 1 H) 2.02 - 2.09 (m, 1 H) 1.75 - 1.82 (m, 1 H) 1.73 (s, 3 H) 1.71 (s, 3 H) 1.64 - 1.70 (m, 2 H) 1.58 (s, 3 H) 1.44 - 1.52 (m, 1 H) 1.18 - 1.39 (m, 4 H); ^{13}C NMR (126 MHz, $CDCl_3$) δ ppm 128.7, 127.6, 71.2, 49.1, 34.3, 29.3, 26.0, 25.1, 21.4, 20.4, 13.1; FTIR (neat, cm^{-1}) 3417 (br m) 2929 (s) 2857 (m) 1449 (m) 1375 (w) 1272 (w) 1162 (w) 1146 (w) 1060 (s) 1010 (m) 962 (m) 852 (m). MS (APCI) *m/z* calc'd for $C_{11}H_{19}$ $[M–H_2O+H]^+$: 151.1; found: 151.1.

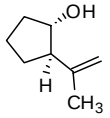

S8

(±)-(1S,2R)-2-(prop-1-en-2-yl)cyclopentanol (**S8**)

This compound was prepared according to General Procedure B with cyclopentene oxide (8.4 g, 100 mmol, 1 equiv) and isopropenylmagnesium bromide (0.5M in THF, 300 mL, 1.5 equiv). The crude product was obtained as a yellow oil (8.6 g) and was carried forward to the following reaction without further purification.

General Procedure C – Swern oxidation to generate β-γ unsaturated ketone intermediates

An oven-dried 250 mL round-bottom flask under argon was charged with a stir bar, CH_2Cl_2 (39 mL), and oxalyl chloride (3.5 mL, 40.9 mmol, 1.2 equiv) and cooled to –78 ^oC. To this solution was added dropwise a solution of DMSO (6.0 mL, 85.2 mmol, 2.5 equiv) in CH_2Cl_2 (39 mL). After the mixture was stirred for 5 m, a solution of alcohol (34.1 mmol, 1.0 equiv) in CH_2Cl_2 (30 + 2 x 5 mL rinses) was added dropwise. The reaction mixture was stirred 1 h at –78 ^oC, at which point it was quenched by addition of NEt_3 (23.8 mL, 170 mmol, 5.0 equiv) and immediately warmed to room temperature. The contents were diluted with DI H_2O (50 mL) and extracted with CH_2Cl_2 (3 x 50 mL). The combined organics were dried over Na_2SO_4, filtered, and concentrated. To remove amine salts, the crude residue was twice suspended in 5% Et_2O/hexanes, filtered, and concentrated to isolate the β-γ unsaturated ketone. This product was carried forward without further purification.[42]

General Procedure D – Grignard addition to β-γ enone intermediates

A flame-dried 500 mL round-bottom flask was charged with a stir bar, β-γ unsaturated ketone (14.5 mmol, 1 equiv) and THF (145 mL) and cooled to 0 ^oC. A solution of Grignard reagent in THF (17.4 mmol, 1.2 equiv) was added dropwise under argon. The reaction was allowed to warm to room temperature overnight and was then quenched by slow addition of saturated aqueous NH_4Cl (50 mL). The crude mixture was diluted with

[42] Attempted purification of some β-γ unsaturated ketone intermediates resulted in partial isomerization to the conjugated enone.

DI H_2O (50 mL) and extracted with Et_2O (3 x 100 mL). The combined organics were diluted with CH_2Cl_2, dried over Na_2SO_4, filtered, and concentrated. The crude residue was purified by flash column chromatography to afford the divinyl alcohol.

General Procedure E – Cerium trichloride mediated Grignard addition to β-γ enones[43]

A flame-dried 100 mL round-bottom flask was charged with anhydrous cerium trichloride (2.1 g, 8.5 mmol, 2.5 equiv) and THF (17 mL), and the resultant suspension was stirred for 2 h at room temperature. The flask was cooled to –78 ^oC, and *t*-butyllithium (1.7 M in pentane) was added dropwise until the suspension took on a persistent faint pink color (~5 drops). The flask was brought to room temperature, and β-γ unsaturated ketone (3.4 mmol, 1.0 equiv) was added as a solution in THF (10 mL + 2 x 3.5 mL rinses). The suspension was stirred under N_2 at room temperature for an additional 2 h. The flask was cooled to –78 ^oC and the reaction mixture was stirred at this temperature for 8 h, at which point saturated aqueous NH_4Cl was added (20 mL) and the flask was brought to room temperature. The resultant emulsion was treated with 1 N HCl (10 mL) and was extracted with Et_2O (3 x 20 mL). The combined organics were diluted with CH_2Cl_2, dried over Na_2SO_4, filtered, and concentrated to afford the crude product which was purified by flash column chromatography to afford the desired divinyl alcohol.

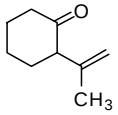

S2a

2-(prop-1-en-2-yl)cyclohexanone (**S2a**)[41]

Alcohol **37** (4.78g, 34.1 mmol, 1 equiv) was oxidized according to General

[43] Martin, C. L.; Overman, L. E.; Rohde, J. M. *J. Am. Chem. Soc.* **2008**, *130*, 7568.

Procedure C to afford known ketone **2a** as a dark orange oil (4.2 g). This product was carried forward without further purification.

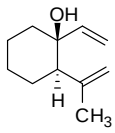

38

(±)-(1*S*,2*R*)-2-(prop-1-en-2-yl)-1-vinylcyclohexanol (**38**)[19]

According to General Procedure D, crude ketone **S2a** (2.0 g, 14.5 mmol) was reacted with vinylmagnesium bromide (1.0 M in THF, 17.4 mL, 17.4 mmol, 1.2 equiv) to afford the crude addition product in 20:1 dr in favor of the title compound. The crude residue was purified by flash column chromatography (SiO_2, Biotage, 0 to 6% Et_2O/hexanes) to afford the divinyl alcohol **38** (1.32 g, 7.9 mmol, 55% yield) as a pale yellow oil. R*f*=0.34 (10% Et_2O/hexanes, $KMnO_4$); ^1H NMR (500 MHz, $CDCl_3$) δ ppm 5.87 (ddd, *J*=17.17, 10.76, 1.37 Hz, 1 H) 5.11 - 5.23 (m, 1 H) 4.92 - 5.02 (m, 1 H) 4.81 - 4.89 (m, 1 H) 4.73 (d, *J*=0.92 Hz, 1 H) 2.04 (dd, *J*=12.59, 3.43 Hz, 1 H) 1.74 (s, 3 H) 1.71 - 1.80 (m, 2 H) 1.58 - 1.71 (m, 2 H) 1.49 - 1.57 (m, 1 H) 1.39 - 1.49 (m, 2 H) 1.21 - 1.30 (m, 1 H); ^{13}C NMR (126 MHz, $CDCl_3$) δ ppm 148.4, 146.5, 111.8, 110.7, 72.8, 52.5, 38.1, 27.4, 26.2, 25.7, 21.3; FTIR (neat, cm^{-1}) 3551 (m), 3482 (br m), 3082 (w), 2933 (s), 2856 (m), 2671 (w), 1638 (m), 1447 (m), 1373 (m), 1285 (m), 1197 (w), 1077 (m), 997 (m), 971 (s), 916 (s), 856 (m), 838 (m), 666 (m), 611 (m). MS (APCI) *m/z* calc'd for $C_{11}H_{17}$ $[M–H_2O+H]^+$: 149.1; found: 149.1.

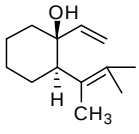

S3c

(±)-(1*S*,2*R*)-2-(3-methylbut-2-en-2-yl)-1-vinylcyclohexanol (**S3c**)

Alcohol **S1c** (650 mg, 3.9 mmol, 1 equiv) was oxidized according to General Procedure C to afford ketone **S2c**, which was carried forward without purification. According to General Procedure E, ketone **S2c** was reacted with

vinylmagnesium bromide (1.0 M in THF, 9.6 mL, 9.6 mmol, 2.5 equiv) to afford the crude addition product in >19:1 dr in favor of the title compound. The crude residue was purified by flash column chromatography (SiO_2, Biotage, 0 to 25% Et_2O/hexanes) to afford **S3c** as a clear oil (518 mg, 2.7 mmol, 68% yield over 2 steps). R*f* = 0.37 (10% Et_2O/hexanes) ^{1}H NMR (500 MHz, $CDCl_3$) δ ppm 5.86 (dd, *J*=17.40, 10.99 Hz, 1 H) 5.12 (dd, *J*=16.94, 1.37 Hz, 1 H) 4.91 (dd, *J*=10.99, 1.37 Hz, 1 H) 2.55 (dd, *J*=12.59, 2.98 Hz, 1 H) 1.84 - 1.97 (m, 1 H) 1.75 - 1.83 (m, 1 H) 1.66 - 1.74 (m, 1 H) 1.64 (br. s., 3 H) 1.62 (s, 6 H) 1.51 - 1.61 (m, 3 H) 1.18 - 1.39 (m, 3 H); ^{13}C NMR (126 MHz, $CDCl_3$) δ ppm 148.4, 146.5, 111.8, 110.7, 72.8, 52.5, 38.1, 27.4, 26.2, 25.7, 21.3; FTIR (neat, cm^{-1}) 3491 (br m) 3084 (w) 2929 (s) 2959 (m) 1640 (w) 1447 (s) 1413 (m) (1375 (m) 1268 (m) 1244 (m) 1164 (m) 1150 (m) 1056 (w) 992 (m) 963 (s) 916 (s) 859 (w) 816 (m) 668 (m). MS (APCI) *m/z* calc'd for $C_{13}H_{21}$ $[M–H_2O+H]^+$: 177.2; found: 177.2.

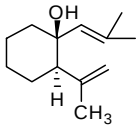

S3d

(±)-(1S,2R)-1-(2-methylprop-1-enyl)-2-(prop-1-en-2-yl)cyclohexanol (**S3d**)

According to General Procedure D, crude ketone **S2a** (1.0 g, 7.2 mmol, 1 equiv) was reacted with 2-methyl-1-propenylmagnesium bromide (0.5 M in THF, 17.4 mL, 17.4 mmol, 1.2 equiv) to afford the crude addition product in 6:1 dr in favor of the title compound. The crude product was purified by flash column chromatography (Davisil®, Biotage, 0 to 25% Et_2O/hexanes) to afford **S3d** (452 mg, 2.3 mmol, 32% yield) as a pale yellow oil. R*f*=0.75 (10% Et_2O/hexanes, $KMnO_4$); ^{1}H NMR (500 MHz, $CDCl_3$) δ ppm 5.19 (s, 1 H) 4.88 (s, 1 H) 4.78 (s, 1 H) 2.06 (dd, *J*=12.36, 2.75 Hz, 1 H) 1.88 (d, *J*=14.19 Hz, 1 H) 1.83 (s, 3 H) 1.81 (s, 3 H) 1.69 - 1.78 (m, 3 H) 1.67 (s, 3 H) 1.35 - 1.63 (m, 4 H) 1.23 (qt, *J*=13.58, 3.20 Hz, 1 H); ^{13}C NMR (126 MHz, $CDCl_3$)

δ ppm 149.2, 132.49, 132.46, 112.2, 73.5, 53.5, 38.5, 27.8 (2 C) 26.3, 25.7, 21.6, 18.8; FTIR (neat, cm^{-1}) 3559 (m) 3502 (br m) 2078 (w) 2930 (s) 2855 (s) 1667 (m) 1637 (m) 1447 (s) 1375 (m) 1323 (w) 1286 (m) 1212 (w) 1179 (w) 1069 (m) 978 (s) 949 (m) 895 (s) 863 (m) 734 (m). MS (ESI) *m/z* calc'd for $C_{13}H_{21}$ $[M–H_2O+H]^+$: 177.1638; found: 177.1637.

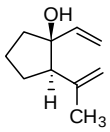

S9

(±)-(1S,2R)-2-(prop-1-en-2-yl)-1-vinylcyclopentanol (**S9**)

Alcohol **S8** (1.0g, 7.9 mmol, 1 equiv) was dissolved in CH_2Cl_2 (80 mL) in a 200 mL round-bottom flask. Dess–Martin periodinane (4.0 g, 9.4 mmol, 1.2 equiv) was added as a solid in one portion. The reaction was stirred at room temperature under N_2 for 1 h, at which point the contents of the flask were poured into a 1 L Erlenmeyer flask containing a large stir bar and Et_2O (80 mL). A 10% aqueous sodium thiosulfate solution (80 mL) and saturated aqueous $NaHCO_3$ (80 mL) were added to the flask, and the contents were vigorously stirred for 1 h. The organic layer was separated and the aqueous layer was extracted with CH_2Cl_2 (3 x 50 mL). The combined organics were dried over Na_2SO_4, filtered, and concentrated. The crude ketone was taken forward without purification.

According to General Procedure D, the intermediate ketone was reacted with vinylmagnesium bromide (1.0 M in THF, 9.5 mL, 9.5 mmol, 1.2 equiv) to afford the crude addition product in 9:1 dr in favor of the title compound. The crude product was purified by flash column chromatography (SiO_2, Biotage, 0 to 25% Et_2O/hexanes) to afford divinyl alcohol **S9** as a yellow oil (497 mg, 3.2 mmol, 41% over 2 steps). Characterization data match reported values.[20d]

General Procedure F – Anionic oxy-Cope rearrangement

A flame-dried 250 mL round-bottom flask was charged with KH (866 mg, 21.7 mmol, 2.4 equiv), 18-crown-6 (6.8 g, 25.7 mmol, 2.8 equiv), and THF (150 mL) and cooled to 0 ^{o}C under an atmosphere of argon. A solution of divinyl alcohol (9.0 mmol, 1 equiv) in THF (30 mL + 10 mL rinse) was added dropwise via cannula. The reaction was stirred at 0 ^{o}C for 30 m, after which it was warmed to room temperature. Once the reaction was determined to be complete by TLC analysis, the flask was cooled to 0 ^{o}C and quenched by slow addition of saturated aqueous NH_4Cl (10 mL). The reaction was further diluted with 100 mL DI H_2O and extracted with Et_2O (3 x 100 mL). The combined organics were diluted with CH_2Cl_2, dried over Na_2SO_4, filtered, and concentrated. The crude residue was purified by flash column chromatography to afford the keto-olefin.

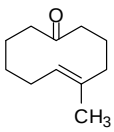

39a

(*E*)-5-methylcyclodec-5-enone (**39a**)[33b]

According to General Procedure F, divinyl alcohol **38** (1.5g, 9.0 mmol, 1 equiv) underwent an anionic oxy-Cope rearrangement. The crude product was purified by flash column chromatography (neutral Al_2O_3, Biotage, 0 to 10% Et_2O/hexanes) to afford cyclodecenone **39a** (978 mg, 5.9 mmol, 65% yield). The product is a clear oil at room temperature and freezes to a white solid upon storage at 5 ^{o}C. R*f*=0.26 (10% Et_2O/hexanes, CAM); ^{1}H NMR (500 MHz, 23 ^{o}C,$CDCl_3$) δ ppm 5.17 (t, *J*=7.10 Hz, 1 H) 1.47 (s, 3 H) 1.12 - 2.81 (m, 14 H); ^{1}H NMR (500 MHz, –20 ^{o}C, $CDCl_3$) δ ppm 5.18 (dd, *J*=10.07, 3.20 Hz, 1 H) 2.64 (dd, *J*=16.25, 9.84 Hz, 1 H) 2.25 - 2.47 (m, 3 H) 2.17 (dd, *J*=12.36, 5.95 Hz, 1 H) 1.97 - 2.12 (m, 3 H) 1.52 - 1.89 (m, 5 H) 1.46 (s, 3 H) 1.20 - 1.40 (m, 1 H); ^{13}C NMR (126 MHz, $CDCl_3$) δ ppm 209.6, 137.9, 126.8, 45.3, 43.4, 41.4, 29.0, 28.6, 26.0, 22.5, 16.0; FTIR (neat, cm^{-1}) 3392 (w), 2922 (s), 2852 (m),

2678 (w), 1703 (s), 1443 (s), 1425 (s), 1359 (m), 1181 (w), 1096 (s), 1017 (w), 924 (m), 859 (m), 809 (m), 774 (m), 733 (w). MS (ESI) *m/z* calc'd for $C_{11}H_{19}O$ $[M+H]^+$: 167.1430; found: 167.1425.

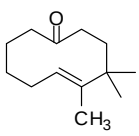

39c

(E)-4,4,5-trimethylcyclodec-5-enone (**39c**)

According to General Procedure F, divinyl alcohol **S3c** (388 mg, 2.0 mmol, 1 equiv) underwent an anionic oxy-Cope rearrangement. The crude product was purified by flash column chromatography (neutral Al_2O_3, Biotage, 0 to 50% Et_2O/hexanes and SiO_2, Biotage, 0 to 10% Et_2O/hexanes) to afford cyclodecenone **39c** (294 mg, 0.1.5 mmol, 76% yield) as a pale yellow oil. ^{1}H NMR (500 MHz, 23^{o}C, $CDCl_3$) δ ppm 5.24 (td, *J*=7.33, 0.92 Hz, 1 H) 2.18 - 2.81 (m, 4 H) 2.09 (br. s., 3 H) 1.48 - 1.97 (m, 5 H) 1.45 (s, 3 H) 1.07 (s, 6 H); ^{1}H NMR (500 MHz, –40 ^{o}C, $CDCl_3$) δ ppm 5.19 (d, *J*=10.74 Hz, 1 H) 2.57 (dd, *J*=16.36, 10.01 Hz, 1 H) 2.49 (t, *J*=13.70 Hz, 1 H) 2.26 - 2.38 (m, 2 H) 2.06 - 2.17 (m, 1 H) 1.95 - 2.05 (m, 1 H) 1.90 (dd, *J*=14.89, 4.64 Hz, 1 H) 1.66 - 1.82 (m, 2 H) 1.51 - 1.63 (m, 1 H) 1.39 (s, 3 H) 1.23 - 1.35 (m, 2 H) 1.06 (s, 3 H) 0.97 (s, 3 H); ^{13}C NMR (126 MHz, –40 ^{o}C, $CDCl_3$) δ ppm 210.2, 143.0, 124.4, 45.8, 39.3, 39.1, 39.0, 29.3, 28.6, 28.0, 24.8, 22.1, 13.6; FTIR (neat, cm^{-1}) 2921 (m) 1705 (s) 1446 (m) 1370 (m) 1355 (m) 1179 (w) 1132 (s) 1080 (w) 1064 (w) 1040 (m) 1000 (w) 910 (m) 853 (m) 807 (m) 733 (m); MS (ESI) *m/z* calc'd for $C_{13}H_{21}$ $[M–H_2O+H]^+$: 177.1638; found: 177.1642.

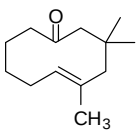

39d

(*E*)-3,3,5-trimethylcyclodec-5-enone (**39d**)

According to General Procedure F, divinyl alcohol **S3d** (200 mg, 1.03 mmol, 1 equiv) underwent an anionic oxy-Cope rearrangement. The crude product was purified by flash column chromatography (neutral Al_2O_3, Biotage, 0 to 5%

Et_2O/hexanes) to afford cyclodecenone **39d** (120 mg, 0.61 mmol, 61% yield) as a white crystalline solid. R*f*=0.4 (10% Et_2O/hexanes); ^1H NMR (500 MHz, –40 ^oC, $CDCl_3$) δ ppm 5.20 (t, *J*=6.80 Hz, 1 H) 2.60 (dd, *J*=16.36, 10.50 Hz, 1 H) 2.40 (d, *J*=14.65 Hz, 1 H) 2.27 (dd, *J*=16.36, 9.03 Hz, 1 H) 1.95 - 2.03 (m, 3 H) 1.92 (d, *J*=14.65 Hz, 1 H) 1.85 (d, *J*=12.21 Hz, 1 H) 1.68 - 1.78 (m, 2 H) 1.55 (s, 3 H) 1.45 - 1.57 (m, 1 H) 1.36 (s, 3 H) 1.24 - 1.33 (m, 1 H) 0.91 (s, 3 H); ^{13}C NMR (126 MHz, $CDCl_3$) δ ppm 209.9, 138.6, 129.0, 54.1, 53.0, 46.4, 43.3, 34.8, 28.5 (2C), 27.1, 22.2, 18.8; FTIR (neat, cm^{-1}) 2952 (s) 2925 (m) 1703 (s) 1447 (m) 1365 (m) 1286 (w) 1152 (m) 1109 (m) 1057 (m) 979 (m) 890 (w) 793 (m) 735 (m). MS (APCI) *m/z* calc'd for $C_{13}H_{23}O$ $[M+H]^+$: 195.2; found: 195.2.

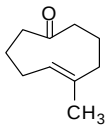
59

(*E*)-5-methylcyclonon-5-enone (**59**)

According to General Procedure F, divinyl alcohol **S9** (200 mg, 1.32 mmol, 1 equiv) underwent an anionic oxy-Cope rearrangement. The crude product was purified by flash column chromatography (neutral Al_2O_3, Biotage, 0 to 5% Et_2O/hexanes) to afford cyclononenone **59** (83 mg, 0.54 mmol, 42% yield) as a pale yellow solid. Characterization data match reported values.[20d]

Scheme for the Synthesis of Transannular Ketone-Ene Substrate 39b

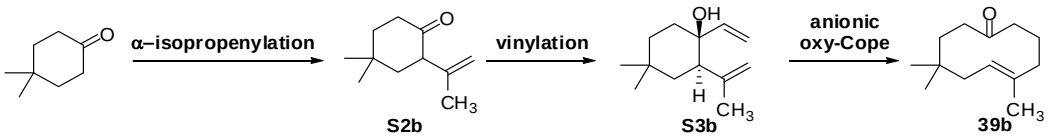

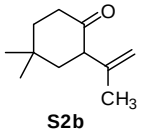
S2b

4,4-dimethyl-2-(prop-1-en-2-yl)cyclohexanone (**S2b**)[44]

[44] This procedure was adapted from: Huang, J.; Bunel, E. Faul, M. M. *Org. Lett.* **2007**, *9*, 4343.

A thick-walled vial was charged with a stir bar, 4,4-dimethyl cyclohexanone (252 mg, 2.0 mmol, 1 equiv), and [(*t*-Bu_3P)$PdBr]_2$ (19 mg, 0.025 mmol, 1.25 mol%) and sealed with a pressure septum cap. Under a positive pressure of N_2, toluene (4 mL) was added followed by a solution of LHMDS (1.0 M in toluene, 5 mL, 5 mmol, 2.5 equiv). The resultant suspension was stirred for 5 m at room temperature, after which 2-bromopropene (262 μL, 3.0 mmol, 1.5 equiv) was added in a single portion. The N_2 inlet was removed, and the vial was immersed in a 80 ^oC oil bath and stirred at this temperature for 24 h. The vial was cooled to room temperature and the contents were poured into Et_2O (10 mL) and washed with saturated aqueous NH_4Cl (5 mL) and DI water (5mL). The organic layer was diluted with CH_2Cl_2, dried over Na_2SO_4, filtered, and concentrated. The crude residue was purified by flash column chromatography (SiO_2, Biotage, 0 to 40% Et_2O/hexanes) to afford **S2b** (146 mg, 0.88 mmol, 44% yield) as a clear oil. R*f*=0.45 (20% Et_2O/hexanes); ^1H NMR (600 MHz, $CDCl_3$) δ ppm 4.90 - 4.97 (m, 1 H) 4.72 (dt, *J*=1.76, 0.88 Hz, 1 H) 3.15 (dd, *J*=13.33, 5.42 Hz, 1 H) 2.44 - 2.55 (m, 1 H) 2.29 (ddd, *J*=14.64, 4.69, 2.90 Hz, 1 H) 1.79 (t, *J*=13.47, 1H) 1.61 - 1.76 (m, 3 H) 1.72 (s, 3 H) 1.23 (s, 3 H) 1.05 (s, 3 H); ^{13}C NMR (126 MHz, $CDCl_3$) δ ppm 211.3, 143.5, 113.1, 54.1, 44.8, 39.7, 38.5, 31.6, 30.7, 24.4, 21.2; FTIR (neat, cm^{-1}) 2955 (m), 2925 (m), 2865 (m), 1712 (s), 1649 (w), 1462 (m), 1446 (m), 1308 (w), 1153 (m), 1099 (m), 1009 (w), 890 (s), 828 (w), 732 (w); MS (ESI) *m/z* calc'd for $C_{11}H_{19}O$ $[M+H]^+$: 167.1430; found: 167.1422.

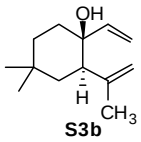

S3b

(±)-(1S,2R)-4,4-dimethyl-2-(prop-1-en-2-yl)-1-vinylcyclohexanol (**S3b**)

According to General Procedure E, ketone **S2b** (267.3 mg, 1.6 mmol, 1.0 equiv) was reacted with vinylmagnesium bromide (1.0 M in THF, 4.0 mL, 4.0 mmol, 2.5 equiv) to afford the crude addition product in 4.6:1 dr in favor of the title compound. The

crude residue was purified by flash column chromatography (SiO_2, Biotage, 0 to 5% Et_2O/hexanes) to afford **S3b** (114 mg, 0.58 mmol, 36% yield) as a pale yellow oil. R*f*=0.59 (5% Et_2O/hexanes, $KMnO_4$); ^1H NMR (500 MHz, $CDCl_3$) δ ppm 5.90 (dd, *J*=17.09, 10.74 Hz, 1 H) 5.19 (dd, *J*=17.09, 0.98 Hz, 1 H) 4.99 (dd, *J*=10.74, 0.98 Hz, 1 H) 4.90 (t, *J*=1.47 Hz, 1 H) 4.75 (s, 1 H) 2.23 (dd, *J*=13.67, 3.42 Hz, 1 H) 1.75 (s, 3 H) 1.58 - 1.72 (m, 4 H) 1.48 (dt, *J*=12.94, 3.05 Hz, 1 H) 1.19 (ddd, *J*=12.21, 5.37, 2.44 Hz, 1 H) 1.12 (dt, *J*=13.18, 2.93 Hz, 1 H) 0.96 (s, 3 H) 0.94 (s, 3 H); ^{13}C NMR (100 MHz, $CDCl_3$) δ ppm 147.9, 146.2, 111.8, 110.9, 72.3, 47.8, 40.0, 34.1, 33.7, 33.0, 30.2, 25.7, 23.9; FTIR (neat, cm^{-1}) 3553 (m), 3482 (br m), 3083 (m), 2951 (s), 2865 (m), 1638 (m), 1449 (m), 1365 (m), 1283 (m), 1099 (m), 992 (m), 962 (s), 917 (s), 897 (s), 668 (m); MS (ESI) *m/z* calc'd for $C_{13}H_{21}$ $[M–H_2O+H]^+$: 177.1638; found: 177.1639.

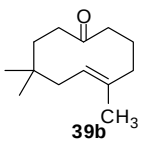

39b

(*E*)-5,8,8-trimethylcyclodec-5-enone (**39b**)

According to General Procedure F, divinyl alcohol **S3b** (110 mg, 0.57 mmol, 1 equiv) underwent an anionic oxy-Cope rearrangement. The crude product was purified by flash column chromatography (Davisil®, Biotage, 0 to 7% Et_2O/hexanes) to afford cyclodecenone **39b** (55 mg, 0.28 mmol, 50% yield) as a white crystalline solid. R*f*=0.24 (10% Et_2O/hexanes, $KMnO_4$); ^1H NMR (500 MHz, 23 ^oC,$CDCl_3$) δ ppm 5.30 (t, *J*=7.33 Hz, 1 H) 1.51 - 3.09 (m, 12 H) 1.41 (s, 3 H) 0.97 (br. s., 6 H); ^1H NMR (500 MHz, –40 ^oC, $CDCl_3$) δ ppm 5.30 (d, *J*=11.87 Hz, 1 H) 2.85 (dd, *J*=16.65, 10.20 Hz, 1 H) 2.23 - 2.35 (m, 2 H) 2.16 (dd, *J*=12.13, 6.20 Hz, 1 H) 2.03 - 2.13 (m, 2 H) 1.99 (dd, *J*=14.07, 12.26 Hz, 1 H) 1.76 - 1.90 (m, 2 H) 1.60 - 1.72 (m, 2 H) 1.41 (s, 3 H) 1.19 (t, *J*=12.39 Hz, 1 H) 1.00 (s, 3 H) 0.91 (s, 3 H); ^{13}C NMR (126 MHz, –40 ^oC, $CDCl_3$) δ ppm 210.0, 138.6, 123.4, 43.4, 41.5, 40.7, 40.0, 34.3, 34.2, 33.1, 26.4, 24.3, 16.0; FTIR (neat, cm^{-1})

2951 (m) 2928 (m) 2868 (w) 1707 (s) 1472 (w) 1443 (m) 1426 (m) 1386 (m) 1363 (m) 1173 (w) 1108 (s) 910 (w) 839 (w) 740 (w). MS (ESI) *m/z* calc'd for $C_{13}H_{23}O$ $[M+H]^+$: 195.1743; found: 195.1739.

Schemes for the Synthesis of Transannular Ketone-Ene Substrates **39e** and **39f**

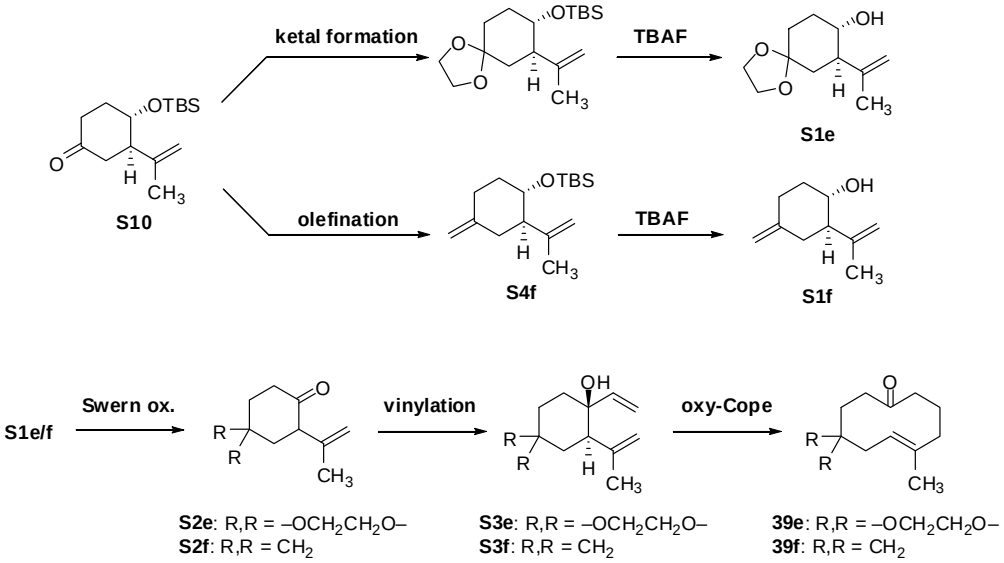

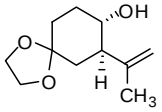
S1e

(±)(7R,8S)-7-(prop-1-en-2-yl)-1,4-dioxaspiro[4.5]decan-8-ol (**S1e**)

An oven-dried 50 mL round-bottom flask fitted with a Dean-Stark trap and reflux condenser was charged with **S10** (1.4 g, 5.2 mmol, 1 equiv), ethylene glycol (294 μL, 5.2 mmol, 1 equiv), benzene (10.4 mL) and pTsOH•H_2O (15 mg, cat.). The side arm of the Dean-Stark trap was filled with benzene (10 mL), and the flask was immersed in a 80°C oil bath under N_2 overnight. The contents of the flask were concentrated to afford the crude acetal an orange oil that was carried forward without purification.

An oven-dried 50 mL round-bottom flask was charged with the intermediate silyl ether and THF (5 mL) and cooled to 0 °C. To this was added a solution of TBAF (1.0M

in THF, 10.4 mL, 10.4 mmol, 2 equiv). The ice bath was removed and the reaction was stirred at room temperature for 48 h. The reaction was quenched with DI water and extracted with Et_2O (3 x 5 mL). The combined organics were diluted with CH_2Cl_2, dried over Na_2SO_4, filtered, and concentrated. The crude residue was purified by flash column chromatography (SiO_2, Biotage, 20 to 100% Et_2O/hexanes) to afford **S1e** (681mg, 3.44 mmol, 66% yield, 2 steps) as a pale yellow oil. R*f*=0.28 (50% Et_2O/hexanes, CAM); ^1H NMR (500 MHz, $CDCl_3$) δ ppm 4.93 (s, 1 H) 4.91 (s, 1 H) 3.90 - 4.00 (m, 4 H) 3.44 - 3.55 (m, 1 H) 2.33 (ddd, *J*=13.18, 9.77, 3.91 Hz, 1 H) 1.98 - 2.09 (m, 1 H) 1.83 (d, *J*=1.95 Hz, 1 H) 1.78 (dt, *J*=9.40, 2.87 Hz, 1 H) 1.71 (s, 3 H) 1.67 - 1.73 (m, 1 H) 1.58 - 1.67 (m, 3 H); ^{13}C NMR (126 MHz, $CDCl_3$) δ ppm 145.32, 113.97, 108.42, 69.90, 64.59, 64.55, 51.26, 37.98, 33.23, 31.03, 18.93; FTIR (neat, cm^{-1}) 3454 (br m), 3073 (w), 2946 (m), 2881 (m), 1646 (w), 1361 (m), 1142 (m), 1142 (m), 1088 (s), 1022 (s), 947 (m), 924 (s); MS (ESI) *m/z* calc'd for $C_{11}H_{19}O_3$ $[M+H]^+$: 199.1329, found: 199.1338.

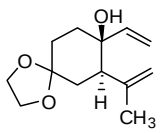

S3e

(±)-(7R,8S)-7-(prop-1-en-2-yl)-8-vinyl-1,4-dioxaspiro[4.5]decan-8-ol (**S3e**)

Alcohol **S1e** (681 mg, 3.4 mmol, 1.0 equiv) was oxidized according to General Procedure C to afford the corresponding β,γ-unsaturated ketone **S2e** that was carried forward without further purification.

According to General Procedure E, crude ketone **S2e** (267.3 mg, 1.6 mmol, 1.0 equiv) was reacted with vinylmagnesium bromide (1.0 M in THF, 8.4 mL, 8.4 mmol, 2.5 equiv) to afford the crude addition product as a yellow oil and in 9.7:1 dr in favor of the title compound. The crude residue was purified by flash column chromatography (SiO_2,

Biotage, 0 to 40% Et_2O/hexanes) to afford **S3e** (441 mg, 2.0 mmol, 57% yield over 2 steps) as a clear oil. R*f*=0.54 (50% Et2O/hexanes, CAM); ^{1}H NMR (500 MHz, $CDCl_3$) δ ppm 5.88 (dd, *J*=17.17, 10.76 Hz, 1 H) 5.20 (d, *J*=17.40 Hz, 1 H) 5.01 (d, *J*=10.53 Hz, 1 H) 4.91 (d, *J*=1.37 Hz, 1 H) 4.74 (s, 1 H) 3.80 - 4.11 (m, 4 H) 2.44 (dd, *J*=13.74, 3.66 Hz, 1 H) 2.06 (t, *J*=13.28 Hz, 1 H) 1.96 (td, *J*=13.39, 4.35 Hz, 1 H) 1.70 - 1.85 (m, 2 H) 1.74 (s, 3 H) 1.61 - 1.68 (m, 1H) 1.55 - 1.60 (m, 1 H) 1.51 (dt, *J*=12.82, 2.98 Hz, 1 H); ^{13}C NMR (126 MHz, $CDCl_3$) δ ppm 146.81, 145.41, 112.44, 111.50, 109.08, 72.03, 64.39, 49.60, 35.80, 35.60, 30.03, 25.58, 25.55; FTIR (neat, cm^{-1}) 3483 (br w), 2965 (m), 2883 (w), 1683 (w), 1438 (w), 1343 (m), 1272 (m), 1211 (w), 1180 (m), 1101 (s), 1037 (m), 992 (s), 953 (s), 917 (s), 733 (s). MS (ESI) *m/z* calc'd for $C_{13}H_{19}O_2$ $[M–H_2O+H]^+$: 207.1380, found: 207.1377; calc'd for $C_{13}H_{20}NaO_3$ $[M+Na]^+$ 247.1305, found 247.1313.

General Procedure G – Palladium-Catalyzed oxy-Cope Rearrangement

A flame-dried 50 mL round-bottom flask was charged with a stir bar, divinyl alcohol (1.79 mmol, 1 equiv), and THF (17.9 mL). To the resultant solution was added $(C_6H_5CN)_2PdCl_2$ (69 mg, 0.18 mmol, 0.1 equiv) as a solid. The flask was capped with a plastic stopper and was stirred at room temperature overnight. The reaction mixture was concentrated to afford the crude product, which was purified by flash column chromatography.

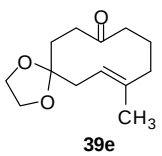

39e

(*E*)-12-methyl-1,4-dioxaspiro[4.9]tetradec-12-en-8-one (**39e**)

According to General Procedure G, divinyl alcohol **S3e** (401 mg, 1.79 mmol, 1 equiv), underwent the palladium-catalyzed oxy-Cope

rearrangement. The crude product, an orange solid, was purified by flash column chromatography (SiO_2, Biotage, 0 to 50% EtOAc/hexanes) to afford **39e** (234 mg, 1.04 mmol, 58% yield) as a white crystalline solid. R*f*=0.24 (20% EtOAc/hexanes, CAM); ^{1}H NMR (500 MHz, $CDCl_3$, 23 ^{o}C) δ ppm 5.29 (t, *J*=6.87 Hz, 2 H) 3.84 - 4.02 (m, 4 H) 3.04 (br. s., 1 H) 1.49 - 2.55 (m, 11 H) 1.44 (s, 3 H); ^{1}H NMR (500 MHz, $CDCl_3$, –40 ^{o}C) δ ppm 5.26 (d, *J*=11.23 Hz, 1 H) 3.84 - 4.05 (m, 4 H) 3.03 (dd, *J*=17.09, 10.25 Hz, 1 H) 1.97 - 2.47 (m, 8 H) 1.81 (td, *J*=12.21, 3.40 Hz, 1 H) 1.65 (d, *J*=10.25 Hz, 1 H) 1.51 - 1.61 (m, 1 H) 1.41 (s, 3 H); ^{13}C NMR (126 MHz, $CDCl_3$, 23 ^{o}C) δ ppm 208.66, 139.99, 121.42, 109.78, 64.33, 42.86, 40.97, 39.00, 37.84, 31.10, 25.17, 15.79; FTIR (neat, cm^{-1}) 2936 (M), 2904 (m) 2882 (m), 1696 (s), 1428 (m), 1363 (m), 1261 (m), 1173 (w), 1107 (s), 1033 (s), 983 (m), 915 (s), 888 (s), 673 (w). MS (ESI) *m/z* calc'd for $C_{13}H_{21}O_3$ $[M+H]^+$: 225.1485, found: 225.1499; calc'd for $C_{13}H_{20}NaO_3$ $[M+Na]^+$ 247.1305, found 247.1319.

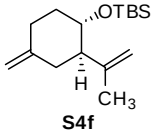

S4f

(±)-tert-butyldimethyl((1R,2S)-4-methylene-2-(prop-1-en-2-yl)cyclohexyloxy)silane (**S4f**)

To an oven-dried 25 mL round-bottom flask containing a stir bar and methyltriphenylphosphonium bromide (845 mg, 2.25 mmol, 1.5 equiv) was added Et_2O (10 mL) under nitrogen. The white suspension was cooled to 0 ºC, and after 5 m at this temperature, KO*t*-Bu (236 mg, 2.1 mmol, 1.4 equiv) was added as a solid, portion-wise (roughly thirds) over 10 m, resulting in the formation of a bright yellow suspension. After stirring the reaction mixture at 0 ^{o}C for an additional 30 m, a solution of ketone **S10** (402 mg, 1.5 mmol, 1 equiv) in Et_2O (2 mL + 2 x 1 mL rinses to complete the transfer) was

added dropwise. The reaction mixture was stirred under nitrogen allowing the temperature to gradually reach room temperature. After 16 h, the pale orange reaction mixture was quenched by addition of saturated aqueous NH_4Cl (5 mL). The reaction mixture was diluted with H_2O (15 mL) and extracted with Et_2O (3 x 10 mL). The combined organics were diluted with CH_2Cl_2, dried over Na_2SO_4, filtered, and concentrated to provide a yellow solid which was purified by flash column chromatography (silica gel, Biotage, 0 to 4% Et_2O in hexanes) to provide the desired silyl ether **S4f** as a clear oil (385 mg, 1.44 mmol, 96% yield). R*f* = 0.9 (5% Et_2O in hexanes) ^{1}H NMR (500 MHz, $CDCl_3$) δ ppm 4.78 (d, *J*=5.37 Hz, 1 H), 4.78 (d, *J*=5.37 Hz, 1 H), 4.64 (d, *J*=6.35 Hz, 1 H), 4.64 (d, *J*=6.35 Hz, 1 H), 3.63 (td, *J*=9.16, 4.15 Hz, 1 H) 2.29 (dt, *J*=14.16, 3.90 Hz, 1 H) 2.22 (dd, *J*=8.79, 1.95 Hz, 1 H) 2.00 - 2.14 (m, 3 H) 1.95 (dq, *J*=12.57, 3.95 Hz, 1 H) 1.71 (s, 3 H) 1.33 - 1.45 (m, 1 H) 0.85 (s, 9 H) 0.03 (s, 3 H) 0.01 (s, 3 H); ^{13}C NMR (126 MHz, $CDCl_3$) δ ppm 147.72, 147.22, 111.69, 108.05, 72.98, 54.23, 38.44, 36.33, 32.76, 25.96 (3 C), 20.98, 18.23, -3.85, -4.70; FTIR (neat, cm^{-1}) 2937 (m), 2857 (m), 1650 (w), 1462 (w), 1362 (w), 1255 (m), 1101 (s), 1055 (w), 1006 (w), 886 (s), 834 (s), 773 (s), 670 (m); MS (ESI) *m/z* calc'd for $C_{16}H_{31}OSi$ $[M+H]^+$: 267.2139, found: 267.2140; calc'd for $C_{16}H_{30}KO$ $[M+K]^+$ 305.1698, found 305.1699.

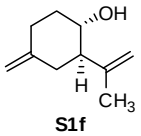

S1f

(±)-(1S,2R)-4-methylene-2-(prop-1-en-2-yl)cyclohexanol (**S1f**)

An oven-dried 25 mL round-bottom flask under nitrogen was charged with a stir bar, **S4f** (755.1 mg, 2.83 mmol, 1 equiv), and Et_2O (2.8 mL), in that order. The resultant solution was cooled to 0 ^oC, and after stirring for 5 m at this temperature, TBAF (5.7 mL, 1 M solution in THF, 5.7 mmol, 2.0 equiv) was added dropwise. The flask was

brought to room temperature and the reaction mixture was stirred for 48 h, at which point it was returned to 0 ^{o}C and quenched by the addition of DI H_2O (5 mL). The mixture was diluted with H_2O (5 mL) and extracted with Et_2O (3 x 10 mL). The combined organics were diluted with CH_2Cl_2, dried over Na_2SO_4, filtered, and concentrated to provide the crude product as an orange oil, which was purified by flash column chromatography (silica, Biotage, 0 to 40% Et_2O/hexanes) to provide **S1f** as a clear oil (412 mg, 2.7 mmol, 96% yield) R*f* = 0.12 (20% Et_2O in hexanes, $KMnO_4$); ^{1}H NMR (500 MHz, $CDCl_3$) δ ppm 4.89 (quin, *J*=1.60 Hz, 1 H) 4.84 (s, 1 H) 4.64 - 4.67 (m, 1 H) 4.63 (d, *J*=1.37 Hz, 1 H) 3.55 (td, *J*=10.07, 4.12 Hz, 1 H) 2.26 - 2.33 (m, 1 H) 2.19 - 2.24 (m, 1 H) 1.97 - 2.14 (m, 5 H) 1.70 (s, 3 H) 1.27 - 1.37 (m, 1 H); ^{13}C NMR (126 MHz, $CDCl_3$) δ ppm 146.82, 145.86, 113.40, 108.66, 70.37, 55.03, 37.93, 34.63, 32.73, 18.99; FTIR (neat, cm^{-1}) 3404 (br, m), 3073 (w), 2938 (m), 1647 (m), 1439 (m), 1253 (w), 1067 (s), 1043 (m), 1021 (m), 888 (s), 834 (w), 654 (s). MS (ESI) *m/z* calc'd for $C_{10}H_{17}O$ $[M+H]^+$: 153.1274, found: 153.1273; calc'd for $C_{10}H_{16}NaO$ $[M+Na]^+$ 175.1093, found 175.1101.

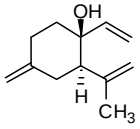

S3f

(±)-(1S,2R)-4-methylene-2-(prop-1-en-2-yl)-1-vinylcyclohexanol (**S3f**)

Alcohol **S1f** (400 mg, 2.63 mmol, 1.0 equiv) was oxidized according to General Procedure C to afford the corresponding β,γ-unsaturated ketone **S2f** that was carried forward without further purification.

According to General Procedure E, ketone **S2f** was reacted with vinylmagnesium bromide (1.0 M in THF, 6.5 mL, 6.5 mmol, 2.5 equiv) to afford the crude addition product as a yellow oil and in >19:1 dr in favor of the title compound. The crude material was purified by flash column chromatography (SiO_2, Biotage, 0 to 10% Et_2O/hexanes) to

provide **S3f** as a pale yellow oil (246 mg, 1.4 mmol, 52% yield, 2 steps). R*f* = 0.43 (10% Et_2O in hexanes, $KMnO_4$); ^1H NMR (500 MHz, $CDCl_3$) δ ppm 5.85 (dd, *J*=17.17, 10.76 Hz, 1 H) 5.20 (dd, *J*=17.40, 1.37 Hz, 1 H) 5.00 (dd, *J*=10.53, 1.37 Hz, 1 H) 4.89 - 4.94 (m, 1 H) 4.77 (s, 1 H) 4.65 - 4.68 (m, 1 H) 4.62 - 4.65 (m, 1 H) 2.54 (td, *J*=13.05, 1.37 Hz, 1 H) 2.38 - 2.50 (m, 1 H) 2.17 (dd, *J*=13.28, 3.66 Hz, 1 H) 2.13 (dquin, *J*=13.28, 1.83 Hz, 1 H) 2.05 (ddd, *J*=13.30, 3.66, 1.83 Hz, 1 H) 1.82 (d, *J*=1.83 Hz, 1 H) 1.75 (s, 3 H) 1.72 (dd, *J*=4.81, 2.52 Hz, 1 H) 1.56 (tdd, *J*=13.74, 4.58, 1.83 Hz, 1 H); ^{13}C NMR (126 MHz, $CDCl_3$) δ ppm 148.70, 147.41, 145.50, 112.07, 111.33, 107.32, 72.68, 53.60, 39.12, 36.12, 30.05, 25.54; FTIR (neat, cm^{-1}) 3547 (br, m), 3072 (m), 2981 (m), 2938 (m), 2918 (m), 2849 (w), 1843 (w), 1786 (w), 1650 (m), 1639 (m), 1438 (m), 1374 (m), 1281 (m), 1135 (m), 997 (m), 950 (s), 888 (s). MS (APCI) *m/z* calc'd for $C_{12}H_{16}$ $[M–H_2O+H]^+$: 161.1; found: 161.1.

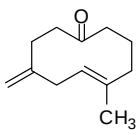

39f

(*E*)-5-methyl-8-methylenecyclodec-5-enone (**39f**)

According to General Procedure F, divinyl alcohol **S3f** (200 mg, 1.12 mmol, 1 equiv) underwent an anionic oxy-Cope rearrangement. The crude material was purified by flash column chromatography (Davisil™, Biotage, 0 to 5% Et_2O/hexanes) to provide cyclodecenone **39f** as a clear oil (95 mg, 0.53 mmol, 47 yield). R*f* = 0.31 (5% Et_2O/hexanes, $KMnO_4$); ^1H NMR (500 MHz, 23 °C, $CDCl_3$) δ ppm 5.09 (t, *J*=7.33 Hz, 1 H) 4.73 - 4.76 (m, 1 H) 4.72 (s, 1 H) 1.54 - 3.14 (m, 12 H) 1.46 (s, 3 H); ^1H NMR (399 MHz, –20 °C, $CDCl_3$) δ ppm 5.08 (d, *J*=10.53 Hz, 1 H) 4.73 (s, 1 H) 4.70 (s, 1 H) 2.71 - 2.86 (m, 1 H) 2.51 - 2.71 (m, 2 H) 2.41 (dd, *J*=14.43, 9.75 Hz, 2 H) 2.10 - 2.34 (m, 4 H) 2.04 (d, *J*=12.48 Hz, 1 H) 1.77 (td, *J*=12.48, 3.51 Hz, 1 H) 1.57 - 1.70 (m, 1 H)

1.44 (s, 3 H); ^{13}C NMR (126 MHz, $CDCl_3$) δ ppm 209.2, 149.2, 138.8, 124.9, 113.0, 45.2, 43.0, 41.0, 37.8, 30.9, 25.0, 15.8; FTIR (neat, cm^{-1}) 3071 (w), 2924 (m), 2856 (m), 1703 (s), 1638 (m), 1443 (m), 1426 (m), 1381 (w), 1351 (m), 1260 (w), 1175 (w), 1103 (s), 1081 (m), 1020 (w), 907 (s), 846 (m), 804 (m), 633 (m). MS (ESI) *m/z* calc'd for $C_{12}H_{18}ONa$ $[M+Na]^+$ 201.1250, found 201.1259.

Scheme for the Synthesis of Transannular Ketone-Ene Substrate **57**

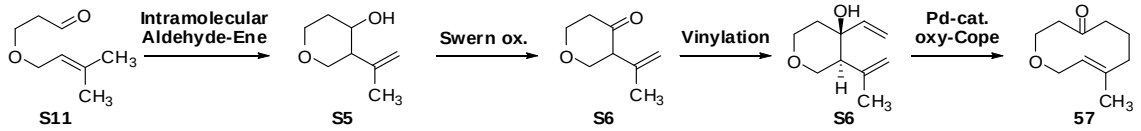

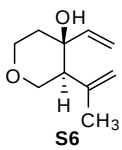

(±)-(3*S*,4*S*)-3-(prop-1-en-2-yl)-4-vinyltetrahydro-2H-pyran-4-ol (**S6**)[45]

A 200 mL round-bottom flask was charged with a stir bar and powdered 4Å MS. The sieves were activated by flame-drying under reduced pressure (1 torr) and cooled under argon. CH_2Cl_2 (86 mL) was added by syringe, followed by aldehyde **S11** (6.1 g, 43 mmol, 1 equiv). The resultant suspension was cooled to –78 °C, and $SnCl_4$ (4.4 mL, 38 mmol, 0.90 equiv) was added neat, dropwise. The flask was transferred to a –60 °C cryocool and the mixture was stirred at this temperature overnight. The flask was transferred to a 0 °C bath, and the reaction was quenched by slow addition of saturated aqueous $NaHCO_3$ (50 mL). The contents were diluted with an additional 50 mL DI H_2O, and extracted with CH_2Cl_2 (3 x 50 mL). The combined organics were dried over Na_2SO_4, filtered, and concentrated to afford the crude product as a yellow oil and a 1.8:1.0 mixture of diastereomeric alcohols (**S5**, 2.8 g). This crude product was taken on to the next step without further purification.

[45] The first two steps of this sequence are modified versions of the procedure reported in ref. 37

The crude product **S5** was oxidized according to General Procedure C to afford **S6**, which was carried forward without further purification.

According to General Procedure D, the intermediate ketone **S6** was reacted with vinylmagnesium bromide (1.0 M in THF, 23.6 mL, 23.6 mmol, 1.2 equiv) to afford the crude addition product in 3.9:1 dr in favor of the title compound. The crude product was purified by flash column chromatography (SiO_2, Biotage, 0 to 50% EtOAc/hexanes) to afford divinyl alcohol **S6** as a clear oil (1.2 g, 7.1 mmol, 17% over 3 steps). R*f*=0.32 (20% EtOAc/hexanes); ^{1}H NMR (600 MHz, $CDCl_3$) δ ppm 5.89 (dd, *J*=17.13, 10.69 Hz, 1 H) 5.25 (dd, *J*=17.13, 1.03 Hz, 1 H) 5.07 (dd, *J*=10.69, 1.03 Hz, 2 H) 4.97 (d, *J*=1.17 Hz, 1 H) 4.69 (s, 1 H) 3.74 - 3.86 (m, 2 H) 3.61 - 3.72 (m, 2 H) 2.37 (dd, *J*=11.42, 4.69 Hz, 1 H) 1.89 (d, *J*=2.34 Hz, 1 H) 1.83 (dddd, *J*=13.95, 11.31, 6.66, 2.34 Hz, 1 H) 1.77 (s, 3 H) 1.52 (d, *J*=13.77 Hz, 1 H); ^{13}C NMR (126 MHz, $CDCl_3$) δ ppm 144.8, 143.9, 113.0, 112.1, 70.6, 66.8, 63.5, 50.9, 37.0, 26.6; FTIR (neat, cm^{-1}) 3436 (br m) 3085 (w) 2954 (m) 2869 (m) 1639 (m) 1374 (m) 1289 (w) 1215 (w) 1114 (s) 968 (s) 917 (s) 867 (s) 815 (m) 734 (m); MS (APCI) *m/z* calc'd for $C_{10}H_{15}O$ $[M–H_2O+H]^+$ 151.1; found 151.2.

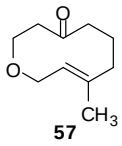

57

(*E*)-8-methyl-5,6,7,10-tetrahydro-2H-oxecin-4(3H)-one (**57**)

According to General Procedure G, divinyl alcohol **S6** (1.1 g, 6.5 mmol, 1.0 equiv) underwent the palladium-catalyzed oxy-Cope rearrangement. The crude product was purified by flash column chromatography (neutral Al_2O_3, 0 to 40% EtOAc/hexanes) to afford keto-olefin **57** (528 mg, 3.14 mmol, 48%) as a white solid. R*f*=0.56 (25% EtOAc/hexanes, Al_2O_3); ^{1}H NMR (500 MHz, $CDCl_3$) δ ppm 5.22 - 5.40 (m, 1 H) 4.13 (d, *J*=12.70 Hz, 1 H) 3.86 - 3.98 (m, 2 H) 3.59 - 3.77 (m, 1 H) 2.94 (dd, *J*=15.38, 8.55 Hz, 1

H) 2.36 - 2.50 (m, 2 H) 2.31 (dd, *J*=15.14, 7.81 Hz, 1 H) 2.16 - 2.26 (m, 1 H) 2.10 (d, *J*=11.23 Hz, 1 H) 1.83 - 1.99 (m, 1 H) 1.78 (d, *J*=11.72 Hz, 1 H) 1.51 (s, 3 H); ^{13}C NMR (126 MHz, $CDCl_3$) δ ppm 208.6, 143.1, 123.9, 68.6, 66.8, 47.4, 43.5, 41.1, 26.3, 16.3; FTIR (neat, cm^{-1}) 2931 (m) 2868 (m) 1692 (s) 1422 (w) 1354 (m) 1297 (m) 1259 (m) 1241 (m) 1103 (s) 1071 (s) 1044 (s) 859 (m) 808 (m) 791 (m); MS (ESI) *m/z* calc'd for $C_{10}H_{17}O_2$ $[M+H]^+$ 169.1223, found 169.1227; calc'd for $C_{10}H_{15}O$ $[M–H_2O+H]^+$ 151.1117, found 151.1114.

Scheme for the Synthesis of Planar Chiral Transannular Ketone-Ene Substrate **61**

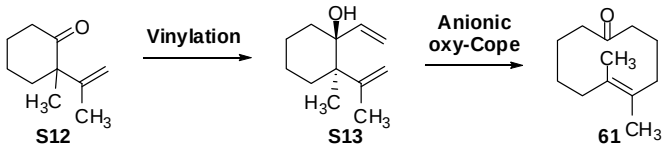

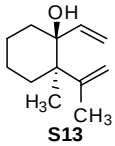

(±)-(1S,2R)-2-methyl-2-(prop-1-en-2-yl)-1-vinylcyclohexanol (**S13**)

According to General Procedure F, ketone **S12** (1.16 g, 7.62 mmol, 1 equiv) was reacted with vinylmagnesium bromide (1.0 M in THF, 18.8 mL, 18.8 mmol, 2.5 equiv) to afford the desired divinyl alcohol in >19:1 dr. The crude product was purified (neutral Al_2O_3, Biotage, 0 to 10% Et_2O/hexanes) to afford divinyl alcohol **S13** (476 mg, 2.64 mmol, 35%) as a yellow oil. Rf=0.34 (10% Et_2O/hexanes, Al_2O_3); ^{1}H NMR (500 MHz, $CDCl_3$) δ ppm 6.10 (dd, *J*=17.09, 10.74 Hz, 1 H) 5.19 (dd, *J*=17.09, 1.46 Hz, 1 H) 5.07 (t, *J*=1.50 Hz, 1 H) 5.00 (dd, *J*=10.74, 1.47 Hz, 1 H) 4.96 (s, 1 H) 2.18 (td, *J*=12.45, 5.37 Hz, 1 H) 2.07 (d, *J*=2.44 Hz, 1 H) 1.79 (s, 3 H) 1.72 - 1.78 (m, 1 H) 1.65 - 1.71 (m, 1 H) 1.53 - 1.59 (m, 2 H) 1.47 - 1.53 (m, 1 H) 1.39 - 1.46 (m, 1 H) 1.22 (s, 3 H) 1.13 - 1.20 (m, 1 H); ^{13}C NMR (126 MHz, $CDCl_3$) δ ppm 151.0, 144.4, 114.1, 112.0, 74.2, 46.4, 33.2, 32.9, 23.9, 21.5, 20.9, 19.3; FTIR (neat, cm^{-1}) 3540 (br m) 2088 (w) 2929 (s) 2966

(m) 1623 (m) 1447 (m) 1379 (m) 1315 (m) 1195 (w) 1088 (m) 1040 (m) 1000 (m) 975 (s) 917 (s) 901 (s) 888 (s) 684 (m). MS (APCI) *m/z* calc'd for $C_{12}H_{19}$ $[M–H_2O+H]^+$: 163.1; found: 163.2.

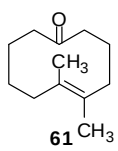

61

(±)-(*E*)-5,6-dimethylcyclodec-5-enone (**61**)

According to General Procedure F, divinyl alcohol **S13** (243 mg, 1.34 mmol, 1 equiv) underwent an anionic oxy-Cope rearrangement. The crude residue was purified by flash column chromatography (neutral Al_2O_3, 0 to 10% Et_2O/hexanes) to afford planar chiral cyclodecenone **61** (124 mg, 0.69 mmol, 51%) as a clear oil. ^{1}H NMR (500 MHz, $CDCl_3$) δ ppm 2.52 (ddt, *J*=16.03, 8.70, 0.90, 0.90 Hz, 1 H) 2.33 - 2.48 (m, 3 H) 2.22 - 2.30 (m, 2 H) 2.00 (dd, *J*=14.65, 6.41 Hz, 1 H) 1.82 (s, 3 H) 1.50 - 1.86 (m, 7 H) 1.48 (s, 3 H); ^{13}C NMR (126 MHz, $CDCl_3$) δ ppm 208.5; 132.0, 129.1, 43.1, 41.5, 34.4, 34.2, 26.5, 26.0, 22.4, 19.1, 18.8; FTIR (neat, cm^{-1}) 3382 (br m) 2958 (m) 2952 (s) 2861 (s) 1701 (s) 1445 (m) 1428 (m) 1372 (m) 1353 (m) 1199 (w) 1126 (s) 1061 (m) 893 (w) 788 (w). MS (ESI) *m/z* calc'd for $C_{12}H_{19}$ $[M–H_2O+H]^+$ 163.1481; found 163.1484; calc'd for $C_{12}H_{20}NaO$ $[M+Na]^+$ 203.1406; found 203.1418.

D. Enantioselective Transannular Ketone-Ene Reactions

General Procedure H – Enantioselective Cr(III)-Catalyzed Transannular Ketone-Ene Reaction

An oven-dried 0.5 dram screw-top vial was charged with a stir bar, activated 4Å MS (10 mg) and was sealed with a cap containing a Teflon-lined septum. The sieves were flame-dried under vacuum (1 torr) and allowed to cool to room temperature under N_2. To the cooled vial was added catalyst **50** (12.7 mg, 0.02 mmol, 5 mol%, which is 10 mol%

based on Cr). The keto-olefin substrate (either **39b**, **39d**, **39e**, **57**, and **59**) (0.2 mmol) was added as a solid to the vial, followed by toluene (50 μL) by microliter syringe. For keto-olefin substrates **39a**, **39c**, and **39f**: toluene (50 μL) was first added, followed by the substrate, which was added neat by microliter syringe. The N_2 line was removed, the cap was wrapped with parafilm, and the reaction mixture was stirred at room temperature for 48 h. At this point, an aliquot (~2 μL) was removed from the vial and diluted into an NMR tube with $CDCl_3$ to determine the product diastereomeric ratio. The NMR sample along with the remainder of the crude reaction mixture was directly loaded onto a column (SiO_2, neutral Al_2O_3, or Davisil™) and eluted to isolate the bicyclic alcohol product.

(4a*R*,8a*S*)-1-methylenedecahydronaphthalen-4a-ol (**40a**)

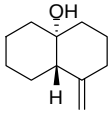

40a

Following General Procedure H, cyclodecenone **39a** (33.3 mg, 0.2 mmol, 1 equiv) underwent a transannular ketone-ene rearrangement to afford **40a** as a single diastereomer. The crude product was purified by flash column chromatography (neutral Al_2O_3, Biotage, 0 to 10% Et_2O/hexanes, followed by 10% to 50% EtOAc/hexanes) to afford **40a** (27.1 mg, 0.163 mmol, 81% yield) as a pale yellow oil. R*f*=0.16 (10% Et_2O/hexanes, SiO_2, $KMnO_4$). $[\alpha]_D^{23}$= +33.2^o (c=0.82, $CHCl_3$). ^{1}H NMR (500 MHz, $CDCl_3$) δ ppm 4.86 - 4.92 (m, 1 H) 4.63 (d, *J*=0.98 Hz, 1 H) 2.33 (dquin, *J*=12.70, 2.40, 1 H) 1.92 - 2.06 (m, 2 H) 1.80 (dquin, *J*=13.18, 3.40 Hz, 1 H) 1.66 - 1.75 (m, 2 H) 1.54 - 1.66 (m, 3 H) 1.38 - 1.54 (m, 4 H) 1.33 (td, *J*=13.31, 4.15 Hz, 1 H) 1.21 - 1.37 (m, 1 H) ^{13}C NMR (126 MHz, $CDCl_3$) δ ppm 150.4, 108.6, 72.0, 49.5, 40.0, 38.7, 36.7, 26.1, 24.0, 23.9, 21.4; FTIR (neat, cm^{-1}) 3474 (br m), 2930 (s) 2853 (m) 1643 (w) 1446 (m) 1251 (w) 1186 (w) 1089 (m) 949 (s) 893 (m) 756 (m) 700 (m). MS (APCI) *m/z* calc'd for $C_{11}H_{19}O$ $[M+H]^+$: 167.2; found: 167.1. The enantiomeric excess was

determined to be 93% by chiral GC analysis (CHIRALDEX β-PH, 100 °C, 14 psi, 20:1 split) t_R(minor) = 21.47 min, t_R(major) = 22.60 min.

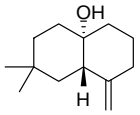

40b

(4a*S*,8a*S*)-7,7-dimethyl-1-methylenedecahydronaphthalen-4a-ol (**40b**)

Following General Procedure H, cyclodecenone **39b** (38.9 mg, 0.2 mmol, 1 equiv) underwent a transannular ketone-ene rearrangement to afford **40b** as a single diastereomer. The crude product was purified by flash column chromatography (SiO_2, Biotage, 0 to 10% Et_2O/hexanes) to afford **40b** as a clear oil (37.7 mg, 0.19 mmol, 97% yield). R*f*=0.34 (10% Et_2O/hexanes, $KMnO_4$). $[\alpha]_D^{23}$ = +17.4 (*c*=0.43, $CHCl_3$). ^{1}H NMR (500 MHz, $CDCl_3$) δ ppm 4.90 (q, *J*=1.53 Hz, 1 H) 4.65 (d, *J*=0.92 Hz, 1 H) 2.36 (ddt, *J*=12.93, 4.01, 2.06, 2.06 Hz, 1 H) 2.18 (d, *J*=14.19 Hz, 1 H) 2.04 (td, *J*=13.16, 4.81 Hz, 1 H) 1.53 - 1.78 (m, 7 H) 1.41 - 1.50 (m, 2 H) 1.15 - 1.21 (m, 2 H) 0.99 (s, 3 H) 0.94 (s, 3 H); ^{13}C NMR (126 MHz, $CDCl_3$) δ ppm 150.3, 108.5, 71.6, 45.1, 39.6, 36.83, 36.75, 34.9, 34.0, 33.4, 30.6, 24.3, 24.0; FTIR (neat, cm^{-1}) 3471 (br m), 3083 (w), 2931 (s), 1644 (m), 1441 (m), 1364 (m), 1252 (w), 1194 (w), 1093 (m), 1039 (w), 970 (m), 948 (m), 923 (m), 893 (s), 758 (w). MS (ESI) *m/z* calc'd for $C_{13}H_{23}O$ $[M+H]^+$: 195.1743; found: 195.1736; calc'd for $C_{13}H_{26}NO$ $[M+NH_4]^+$ 212.2009; found 212.2007. The enantiomeric excess was determined to be 94% by chiral GC analysis (CHIRALDEX β-PH, 100 °C, 14 psi, 20:1 split) t_R(minor) = 28.24 min, t_R(major) = 30.18 min.

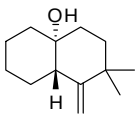

40c

(4a*R*,8a*S*)-2,2-dimethyl-1-methylenedecahydronaphthalen-4a-ol (**40c**)

Following General Procedure H, cyclodecenone **39c** (38.9 mg, 0.2 mmol, 1

equiv) underwent a transannular ketone-ene rearrangement to afford **40c** as a single diastereomer. The crude product was purified by flash column chromatography (neutral Al_2O_3, Biotage, 0 to 10% Et_2O/hexanes, followed by 10% to 50% EtOAc/hexanes) to afford **40c** (32.8 mg, 0.169 mmol, 84% yield) as a pale yellow oil. $[\alpha]_D^{24}$= +16.2° (*c*=1.0, $CHCl_3$). ^{1}H NMR (500 MHz, $CDCl_3$) δ ppm 4.91 - 4.98 (m, 1 H) 4.70 (s, 1 H) 2.19 - 2.29 (m, 1 H) 1.78 - 1.87 (m, 1 H) 1.72 (dquin, *J*=13.74, 2.30 Hz, 1 H) 1.54 - 1.69 (m, 2 H) 1.42 - 1.54 (m, 4 H) 1.33 - 1.40 (m, 2 H) 1.22 - 1.33 (m, 2 H) 1.12 (s, 3 H) 1.08 (s, 3 H); ^{13}C NMR (126 MHz, $CDCl_3$) δ ppm 156.8, 106.9, 72.1, 45.3, 38.9, 36.99, 36.93, 36.4, 29.7, 26.3, 26.0, 24.7, 21.5; FTIR (neat, cm^{-1}) 3474 (br m) 3096 (w) 2930 (s) 2854 (m) 1707 (w) 1632 (m) 1449 (m) 1364 (m) 1179 (w) 1081 (m) 990 (m) 955 (s) 915 (m) 898 (s) 857 (m); MS (ESI) *m/z* calc'd for $C_{13}H_{21}$ $[M–H_2O+H]^+$: 177.1638; found: 177.1639; calc'd for $C_{13}H_{22}NaO$ $[M+Na]^+$ 217.1563; found 217.1567. The enantiomeric excess was determined to be 94% by chiral GC analysis (CHIRALDEX β-PH, 100 °C, 14 psi, 20:1 split) t_R(minor) = 40.28 min, t_R(major) = 41.89 min.

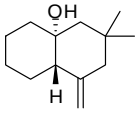

40d

(4a*R*,8a*S*)-3,3-dimethyl-1-methylenedecahydronaphthalen-4a-ol (**40d**)

Following General Procedure H, cyclodecenone **39d** (38.9 mg, 0.2 mmol, 1 equiv) underwent a transannular ketone-ene rearrangement to afford **40d**, as a single diastereomer but as a mixture of regioisomers. The crude product was purified by flash column chromatography (neutral Al_2O_3, Biotage, 0 to 10% Et_2O/hexanes, followed by 10% to 50% EtOAc/hexanes). The product was isolated as a mixture with an inseparable olefin isomer in a combined yield of 32% and was formed as a racemate. The characterization data provided here were measured on a racemic sample. ^{1}H NMR

(500 MHz, $CDCl_3$) δ ppm 4.85 (d, *J*=1.83 Hz, 1 H) 4.71 (s, 1 H) 2.04 (dd, *J*=12.82, 2.29 Hz, 1 H) 1.99 (d, *J*=12.82 Hz, 0 H) 1.90 (dd, *J*=10.99, 4.58 Hz, 1 H) 1.74 - 1.86 (m, 1 H) 1.64 - 1.72 (m, 1 H) 1.41 - 1.64 (m, 5 H) 1.36 (d, *J*=14.19 Hz, 1 H) 1.15 - 1.33 (m, 3 H) 1.01 (s, 3 H) 0.95 (s, 3 H); ^{13}C NMR (126 MHz, $CDCl_3$) δ ppm 148.4, 109.3, 73.0, 52.2, 50.4, 49.4, 39.7, 34.0, 33.4, 27.4, 26.1, 23.7, 21.1; FTIR (neat, cm^{-1}) 3491 (br m) 2081 (w) 2927 (s) 2861 (m) 1648 (m) 1450 (m) 1365 (m) 1162 (m) 1073 (m) 972 (s) 156 (m) 889 (s) 812 (m) 697 (w). MS (ESI) *m/z* calc'd for $C_{13}H_{21}$ $[M–H_2O+H]^+$: 177.2, found: 177.1.

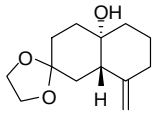

40e

(4a'*S*,8a'*S*)-8'-methyleneoctahydro-1'H-spiro[[1,3]dioxolane-2,2'-naphthalen]-4a'-ol (**40e**)

Following General Procedure H, cyclodecenone **39e** (44.9 mg, 0.2 mmol, 1 equiv) underwent a transannular ketone-ene rearrangement to afford **40e** as a single diastereomer. The crude product was purified by flash column chromatography (SiO_2, Biotage, 0 to 25% EtOAc/hexanes) to afford **40e** (38.9 mg, 0.173 mmol, 87% yield) as a clear oil.; $[\alpha]_D^{23}$= +58.3° (c=0.107, $CHCl_3$). ^1H NMR (500 MHz, $CDCl_3$) δ ppm 4.89 (d, *J*=1.37 Hz, 1 H) 4.59 (s, 1 H) 3.84 - 4.06 (m, 3 H) 2.32 (dd, *J*=13.05, 1.60 Hz, 2 H) 1.86 - 2.06 (m, 2 H) 1.81 (t, *J*=12.82 Hz, 1 H) 1.63 - 1.76 (m, 3 H) 1.50 - 1.63 (m, 3 H) 1.44 (td, *J*=13.30, 4.12 Hz, 1 H) 1.47 (br. s., 1 H); ^{13}C NMR (126 MHz, $CDCl_3$) δ ppm 149.2, 109.7, 108.8, 71.1, 64.4, 46.9, 38.9, 36.1, 36.0, 32.9, 30.2, 23.8; FTIR (neat, cm^{-1}) 3491 (br w), 2932 (s) 2879 (m) 1646 (w) 1441 (w) 1358 (m) 1296 (m) 1270 (m) 1153 (m) 1091 (s) 1031 (m) 988 (m) 965 (m) 950 (m) 932 (m) 898 (m) 836 (m) 757 (m); MS (ESI) *m/z* calc'd for $C_{13}H_{19}O_2$ $[M–H_2O+H]^+$: 207.1380; found: 207.1370; calc'd for

$C_{13}H_{20}NaO_3$ $[M+Na]^+$ 247.1305; found 247.1297. The enantiomeric excess was determined to be 96% by chiral GC analysis (CHIRALDEX β-Cyclodex, 140 °C, 14 psi, 20:1 split) t_R(minor) = 38.63 min, t_R(major) = 40.96 min.

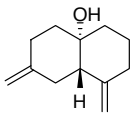

40f

(4a*S*,8a*S*)-1,7-dimethylenedecahydronaphthalen-4a-ol (**40f**)

Following General Procedure H, cyclodecenone **39f** (35.7 mg, 0.2 mmol, 1 equiv) underwent a transannular ketone-ene rearrangement to afford **40f** as a single diastereomer. The crude product was purified by flash column chromatography (SiO_2, Biotage, 0 to 5% Et_2O/hexanes) to afford **40f** (22.2 mg, 0.124 mmol, 62% yield) as a clear oil.; $[\alpha]_D^{24}$= +107.8° (c=0.66, $CHCl_3$). ^{1}H NMR (500 MHz, $CDCl_3$) δ ppm 4.93 (d, *J*=1.46 Hz, 1 H) 4.66 - 4.69 (m, 2 H) 4.64 - 4.66 (m, 1 H) 2.42 (tdd, *J*=13.70, 13.70, 4.88, 1.95 Hz, 1 H) 2.35 (dquin, *J*=13.18, 2.00 Hz, 1 H) 2.26 - 2.38 (m, 1 H) 2.04 - 2.17 (m, 3 H) 1.98 (td, *J*=13.18, 4.39 Hz, 1 H) 1.85 (ddd, *J*=13.43, 4.88, 2.20 Hz, 1 H) 1.65 - 1.78 (m, 2 H) 1.49 - 1.65 (m, 2 H) 1.43 (tdd, *J*=13.49, 13.49, 9.16, 4.39 Hz, 2 H)^{13}C NMR (126 MHz, $CDCl_3$) δ ppm 149.7, 148.9, 108.9, 107.5, 71.8, 50.6, 39.8, 39.4, 36.3, 32.9, 30.2, 23.7; FTIR (neat, cm^{-1}) 3471 (br m) 3071 (w) 2932 (s) 2850 (m) 1724 (w) 1648 (m) 1441 (m) 1270 (m) 1095 (m) 937 (s) 887 (s) 838 (w) 655 (m). MS (ESI) *m/z* calc'd for $C_{12}H_{17}$ $[M–H_2O+H]^+$: 161.1325; found: 161.1325. The enantiomeric excess was determined to be 94% by chiral GC analysis (CHIRALDEX β-Cyclodex, 100 °C, 14 psi, 20:1 split) t_R(minor) = 44.84 min, t_R(major) = 48.31 min.

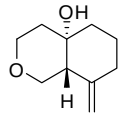
58

(4a*S*,8a*R*)-8-methyleneoctahydro-1H-isochromen-4a-ol (**58**)

Following General Procedure H, with the exception of a 24 h reaction time, ether **57** (33.6 mg, 0.2 mmol, 1 equiv) underwent a transannular ketone-ene rearrangement to afford **58** as a single diastereomer. The crude product was purified by flash column chromatography (SiO_2, Biotage, 0 to 40% EtOAc/hexanes) to afford **58** (4.4 mg, 0.026 mmol, 13% yield) as a clear oil. R*f*=0.40 (25% EtOAc/hexanes, CAM); $[\alpha]_D^{23}$= +15.3° (c=0.36, $CHCl_3$). ^{1}H NMR (500 MHz, $CDCl_3$) δ ppm 4.90 (s, 1 H) 4.40 (s, 1 H) 3.71 - 3.85 (m, 3 H) 3.66 (t, *J*=11.20 Hz, 1 H) 2.26 - 2.36 (m, 2 H) 2.06 (td, *J*=13.18, 4.88 Hz, 1 H) 1.54 - 1.80 (m, 6 H) 1.42 - 1.54 (m, 1 H); ^{13}C NMR (126 MHz, $CDCl_3$) δ ppm 146.5, 108.9, 69.9, 65.0, 64.0, 48.6, 38.9, 38.2, 36.3, 23.5; FTIR (neat, cm^{-1}) 3448 (br m) 2934 (m) 2867 (m) 1647 (m) 1439 (w) 1391 (w) 1250 (w) 1170 (m) 1120 (m) 1081 (s) 1025 (m) 967 (s) 945 (m) 888 (s) 854 (s) 832 (w). MS (APCI) *m/z* calc'd for $C_{10}H_{15}O$ $[M–H_2O+H]^+$: 151.1; found: 151.1. The enantiomeric excess was determined to be 49% by chiral GC analysis (CHIRALDEX γ-TA, 100 °C, 14 psi, 20:1 split) t_R(major) = 26.30 min, t_R(minor) = 29.25 min.

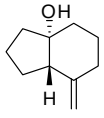
60

(3a*R*,7a*S*)-7-methyleneoctahydro-1H-inden-3a-ol (**60**)

Following General Procedure H, with the exception of a 24 h reaction time, cyclononenone **59** (30.4 mg, 0.2 mmol, 1 equiv) underwent a transannular ketone-ene rearrangement to afford **60** as a single diastereomer. The crude product was purified by flash column chromatography (SiO_2, Biotage, 0 to 10% Et_2O/hexanes) to afford **60** (5.6 mg, 0.037 mmol, 18% yield) as a clear oil. R*f*=0.42 (10%Et_2O/hexanes); $[\alpha]_D^{23}$= +6.1° (c=0.17, $CHCl_3$). ^{1}H NMR (600 MHz, $CDCl_3$) δ ppm 4.93 (q, *J*=1.76 Hz, 1 H) 4.69 (q,

J=1.76 Hz, 1 H) 2.32 (ddd, *J*=15.55, 3.81, 1.76 Hz, 1 H) 2.13 (dd, *J*=12.03, 6.16 Hz, 1 H) 1.90 - 2.01 (m, 2 H) 1.72 - 1.87 (m, 4 H) 1.63 - 1.71 (m, 2 H) 1.60 (dt, *J*=13.50, 4.40 Hz, 1 H) 1.52 - 1.57 (m, 1 H) 1.43 (td, *J*=13.21, 4.70 Hz, 1 H) 1.34 (br. s., 1 H); ^{13}C NMR (126 MHz, $CDCl_3$) δ ppm 148.5, 108.5, 80.5, 53.9, 38.0, 36.3, 35.2, 24.0, 23.7, 20.3. FTIR (neat, cm^{-1}) 3476 (br m), 2930 (s) 1650 (m) 1439 (m) 1287 (w) 1246 (m) 1188 (w) 1056 (m) 964 (s) 893 (s) 873 (s) 756 (s). MS (APCI) *m/z* calc'd for $C_{10}H_{15}$ $[M–H_2O+H]^+$: 135.1; found: 135.1. The enantiomeric excess was determined to be 68% by chiral GC analysis (CHIRALDEX β-Cyclosil, 90 °C, 14 psi, 100:1 split) t_R(minor) = 29.16 min, t_R(major) = 29.62 min.

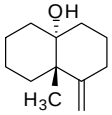

62

(4a*R*,8a*S*)-8a-methyl-1-methylenedecahydronaphthalen-4a-ol (**62**)

An oven-dried 0.5 dram screw-top vial was charged with a stir bar, activated 4 Å MS (10 mg) and was sealed with a cap containing a Teflon-lined septum. The sieves were flame-dried under vacuum (1 torr) and allowed to cool to room temperature under N_2. To the cooled vial was added catalyst **50** (12.7 mg, 0.02 mmol, 5 mol %, which is 10 mol % based on Cr). Toluene (50 μL) was first added, followed by the cyclodecenone **61** (36.0 mg, 0.2 mmol, 1 equiv), which was added neat by microliter syringe. The N_2 line was removed, the cap was wrapped with electrical tape, and the vial was immersed in an oil bath at 50 °C and stirred at this temperature for 24 h. 1,3,5-trimethoxybenzene (3.4 mg, 0.02 mmol, 0.1 equiv) was added as a solid followed by $CDCl_3$ (~1 mL). The conversion was determined to be 19%, based on integration of the ^{1}H NMR spectrum. The crude product was purified by flash column chromatography (neutral Al_2O_3, Biotage, 0 to 10% Et_2O/hexanes). Recovered **61** eluted first and was

isolated as a clear oil (24.6 mg, 0.137 mmol, 69%), and decalinol **62** was isolated as a clear oil (4.3 mg, 0.024 mmol, 12% yield). R*f*=0.3 (10% Et_2O/hexanes). ^1H NMR (600 MHz, $CDCl_3$) δ ppm 4.90 (t, *J*=1.76 Hz, 1 H) 4.72 (s, 1 H) 2.40 - 2.54 (m, 1 H) 2.10 - 2.17 (m, 1 H) 1.82 - 1.93 (m, 1 H) 1.64 - 1.80 (m, 3 H) 1.53 - 1.63 (m, 3 H) 1.44 - 1.52 (m, 1 H) 1.40 (m, *J*=13.50 Hz, 1 H) 1.23 - 1.32 (m, 3 H) 1.19 (s, 3 H); ^{13}C NMR (126 MHz, $CDCl_3$) δ ppm 154.9, 109.3, 74.1, 44.0, 34.2, 33.2, 31.8, 30.8, 29.8, 23.3, 22.7, 21.4; FTIR (neat, cm^{-1}) 3433 (br w) 2922 (s) 2852 (m) 1718 (w) 1642 (w) 1462 (m) 1377 (w) 1260 (w) 1103 (m) 803 (w). MS (APCI) *m/z* calc'd for $C_{12}H_{19}$ $[M–H_2O+H]^+$ 163.1; found 163.2. The enantiomeric excess was determined to be 73% by chiral GC analysis (CHIRALDEX γ-TA, 90 °C, 14 psi, 20:1 split) t_R(minor) = 33.28 min, t_R(major) = 34.94 min.

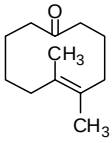
recovered **61**

Characterization for recovered **61**: $[\alpha]_D^{23}$= +2.4° (c=0.68, $CHCl_3$), The enantiomeric excess was determined to be 10% by chiral HPLC analysis (CHIRALCEL OD-H, 2% IPA/hexanes, 1 mL/min, 210 nm) t_R(major) = 5.89 min, t_R(minor) = 6.32 min.

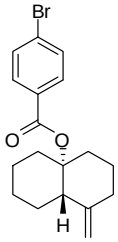
S14

E. Determination of Absolute Configuration

A solution of KHMDS in THF (1.0 M, 0.36 mL, 0.36 mmol, 5 equiv) was added dropwise to a stirred solution of enantioenriched **(+)-40a** (93% ee, 12 mg, 0.072 mmol, 1 equiv) in THF at 0 °C and under a positive pressure of N_2. The resultant solution was stirred at 0 °C for 30 m, at which point a solution of *p*-bromo-

benzoyl chloride in THF (0.86 M, 0.5 mL, 0.43 mmol, 6 equiv) was added in one portion. The reaction vial was sealed with parafilm and stirred at 4 ^{o}C for 16 h, after which it was quenched by slow addition of DI H_2O (1 mL) and extracted with Et_2O (3 x 0.5 mL). The combined organics were diluted with dichloromethane (1 mL), dried with Na_2SO_4, filtered, and concentrated to afford a white solid. The crude product was purified by column chromatography (Biotage, SiO_2, 0 to 5% Et_2O/hexanes) to afford a clear oil, which was re-evaporated from hexanes twice to afford the desired benzoate **S14** as a white solid (13.3 mg, 0.038 mmol, 53% yield). R*f*=0.53 (5% Et_2O/hexanes); ^{1}H NMR (500 MHz, $CDCl_3$) δ ppm 7.87 (d, *J*=8.30 Hz, 2 H) 7.55 (d, *J*=8.79 Hz, 2 H) 4.87 (d, *J*=1.46 Hz, 1 H) 4.76 (d, *J*=1.46 Hz, 1 H) 2.82 - 2.98 (m, 2 H) 2.33 - 2.45 (m, 1 H) 2.11 (td, *J*=12.70, 4.88 Hz, 1 H) 1.96 (t, *J*=7.81 Hz, 1 H) 1.82 (dd, *J*=12.21, 3.42 Hz, 1 H) 1.71 - 1.79 (m, 2 H) 1.62 - 1.70 (m, 1 H) 1.52 - 1.60 (m, 1 H) 1.27 - 1.51 (m, 5 H); ^{13}C NMR (126 MHz, $CDCl_3$) δ ppm 164.5, 149.4, 131.7 (2 C), 131.3 (2 C), 127.7, 107.5, 85.5, 50.1, 36.5, 34.5, 34.4, 25.8, 24.4, 23.2, 21.5; FTIR (neat, cm^{-1}) 2932 (s) 2855 (m) 1715 (s) 1590 (m) 1484 (w) 1446 (m) 1397 (w) 1279 (s) 1259 (s) 1225 (w) 1173 (m) 1070 (m) 1012 (s) 911 (m) 848 (w) 758 (s). MS (ESI) *m/z* calc'd for $C_{18}H_{21}BrO_2$ $[M+H]^+$: 349.0798; found: 349.0803. $[\alpha]_D^{25}$= –17.1^{o} (c=0.41, $CHCl_3$). Slow evaporation of a hexanes solution of **S14** at room temperature afforded single crystals (white needles) suitable for X-ray analysis.

1.8. X-Ray Crystallographic Analysis of *para*-Br-Benzoate S14

Acknowledgment

We thank Dr. Shao-Liang Zheng at the Center for Crystallographic Studies at Harvard University for X-ray data collection and structure determination.

Procedure

A crystal mounted on a diffractometer was collected data at 100 K. The intensities of the reflections were collected by means of a Bruker APEX II DUO CCD diffractometer ($Cu_{K\alpha}$ radiation, λ=1.54178 Å), and equipped with an Oxford Cryosystems nitrogen flow apparatus. The collection method involved 1.0° scans in ω at 30°, 55°, 80° and 115° in 2θ. Data integration down to 0.84 Å resolution was carried out using SAINT V8.30 A (Bruker diffractometer, 2013) with reflection spot size optimisation. Absorption corrections were made with the program SADABS (Bruker diffractometer, 2013). The structure was solved by the direct methods procedure and refined by least-squares methods again F^2 using SHELXS-2013 and SHELXL-2013 (Sheldrick, 2008). Non-hydrogen atoms were refined anisotropically, and hydrogen atoms were allowed to ride on the respective atoms. Crystal data as well as details of data collection and refinement are summarized in Table 1.5, and geometric parameters are shown in Table 1.6. The Ortep plots produced with SHELXL-2013 program, and the other drawings were produced with Accelrys DS Visualizer 2.0 (Accelrys, 2007).

Table 1.5. Experimental details

	NSR-9-086
Crystal data	
Chemical formula	$C_{72}H_{84}Br_4O_8$
M_r	1397.03
Crystal system, space group	Monoclinic, *C*2
Temperature (K)	100
a, *b*, *c* (Å)	34.7369 (6), 7.4593 (1), 30.4529 (5)
β (°)	124.346 (1)
V (Å^3)	6514.95 (19)
Z	4
Radiation type	Cu *K*α
μ (mm^{-1})	3.45
Crystal size (mm)	0.01 × 0.01 × 0.01
Data collection	
Diffractometer	Bruker D8 goniometer with CCD area detector diffractometer
Absorption correction	Multi-scan *SADABS*
T_{min}, T_{max}	0.672, 0.806
No. of measured, independent and observed [$I > 2\sigma(I)$] reflections	68346, 10935, 10256
R_{int}	0.060
$(\sin\theta/\lambda)_{max}$ (Å^{-1})	0.596
Refinement	
$R[F^2 > 2\sigma(F^2)]$, $wR(F^2)$, *S*	0.051, 0.104, 1.14
No. of reflections	10935
No. of parameters	791
No. of restraints	78
H-atom treatment	H-atom parameters constrained
$\Delta\rho_{max}$, $\Delta\rho_{min}$ (e Å^{-3})	0.59, -0.60
Absolute structure	Flack x determined using 4289 quotients [(I+)-(I-)]/[(I+)+(I-)] (Parsons and Flack (2004), Acta Cryst. A60, s61).
Flack parameter	-0.007 (10)

Computer programs: *APEX2* v2013.4.1 (Bruker-AXS, 2013), *SAINT* 8.30A (Bruker-AXS, 2012), *SHELXS2013* (Sheldrick, 2013), *SHELXL2013* (Sheldrick, 2013), Bruker *SHELXTL* (Sheldrick, 2013).

Table 1.6. Geometric parameters (Å, º)

C1—C2	1.383 (11)	C48—C49	1.519 (10)
C1—C6	1.395 (11)	C48—C57	1.527 (11)
C1—H1	0.9500	C48—C53	1.536 (11)
C2—C3	1.364 (11)	C49—C50	1.533 (11)
C2—H2	0.9500	C49—H49A	0.9900
C3—C4	1.393 (12)	C49—H49B	0.9900
C3—Br1	1.915 (8)	C50—C51	1.509 (12)
C4—C5	1.377 (12)	C50—H50A	0.9900
C4—H4	0.9500	C50—H50B	0.9900
C5—C6	1.387 (10)	C51—C52	1.497 (11)
C5—H5	0.9500	C51—H51A	0.9900
C6—C7	1.500 (11)	C51—H51B	0.9900
C7—O2	1.218 (10)	C52—C58	1.322 (11)
C7—O1	1.321 (9)	C52—C53	1.528 (10)
C8—O1	1.472 (9)	C53—C54	1.521 (10)
C8—C9	1.518 (10)	C53—H53	1.0000
C8—C17	1.519 (10)	C54—C55	1.533 (12)
C8—C13	1.549 (10)	C54—H54A	0.9900
C9—C10	1.526 (10)	C54—H54B	0.9900
C9—H9A	0.9900	C55—C56	1.534 (13)
C9—H9B	0.9900	C55—H55A	0.9900
C10—C11	1.513 (12)	C55—H55B	0.9900
C10—H10A	0.9900	C56—C57	1.522 (12)
C10—H10B	0.9900	C56—H56A	0.9900
C11—C12	1.512 (11)	C56—H56B	0.9900
C11—H11A	0.9900	C57—H57A	0.9900
C11—H11B	0.9900	C57—H57B	0.9900
C12—C18	1.321 (12)	C58—H58A	0.9500
C12—C13	1.530 (10)	C58—H58B	0.9500

Table 1.6. (Continued)

C13—C14	1.521 (10)	C61—C66	1.387 (10)
C13—H13	1.0000	C61—C62	1.395 (10)
C14—C15	1.517 (11)	C61—H61	0.9500
C14—H14A	0.9900	C62—C63	1.378 (10)
C14—H14B	0.9900	C62—H62	0.9500
C15—C16	1.519 (10)	C63—C64	1.377 (10)
C15—H15A	0.9900	C63—Br4	1.898 (7)
C15—H15B	0.9900	C64—C65	1.387 (11)
C16—C17	1.520 (10)	C64—H64	0.9500
C16—H16A	0.9900	C65—C66	1.380 (10)
C16—H16B	0.9900	C65—H65	0.9500
C17—H17A	0.9900	C66—C67	1.512 (11)
C17—H17B	0.9900	C67—O8	1.204 (11)
C18—H18A	0.9500	C67—O7	1.336 (11)
C18—H18B	0.9500	O7—C68A	1.520 (17)
C21—C26	1.391 (11)	O7—C68	1.525 (15)
C21—C22	1.391 (11)	C68—C69	1.511 (17)
C21—H21	0.9500	C68—C77	1.513 (16)
C22—C23	1.364 (12)	C68—C73	1.526 (17)
C22—H22	0.9500	C69—C70	1.518 (18)
C23—C24	1.382 (11)	C69—H69A	0.9900
C23—Br2	1.903 (8)	C69—H69B	0.9900
C24—C25	1.380 (12)	C70—C71	1.522 (17)
C24—H24	0.9500	C70—H70A	0.9900
C25—C26	1.391 (12)	C70—H70B	0.9900
C25—H25	0.9500	C71—C72	1.520 (18)
C26—C27	1.509 (11)	C71—H71A	0.9900
C27—O4	1.209 (10)	C71—H71B	0.9900
C27—O3	1.331 (10)	C72—C78	1.29 (2)
C28—O3	1.474 (9)	C72—C73	1.510 (18)
C28—C37	1.521 (12)	C73—C74	1.531 (15)

Table 1.6. (Continued)

C28—C29	1.531 (10)	C73—H73	1.0000
C28—C33	1.556 (11)	C74—C75	1.496 (19)
C29—C30	1.509 (10)	C74—H74A	0.9900
C29—H29A	0.9900	C74—H74B	0.9900
C29—H29B	0.9900	C75—C76	1.49 (2)
C30—C31	1.532 (11)	C75—H75A	0.9900
C30—H30A	0.9900	C75—H75B	0.9900
C30—H30B	0.9900	C76—C77	1.529 (17)
C31—C32	1.511 (12)	C76—H76A	0.9900
C31—H31A	0.9900	C76—H76B	0.9900
C31—H31B	0.9900	C77—H77A	0.9900
C32—C38	1.293 (11)	C77—H77B	0.9900
C32—C33	1.500 (12)	C78—H78A	0.9500
C33—C34	1.536 (12)	C78—H78B	0.9500
C33—H33	1.0000	C68A—C69A	1.509 (18)
C34—C35	1.522 (15)	C68A—C77A	1.523 (17)
C34—H34A	0.9900	C68A—C73A	1.532 (18)
C34—H34B	0.9900	C69A—C70A	1.517 (19)
C35—C36	1.517 (17)	C69A—H69C	0.9900
C35—H35A	0.9900	C69A—H69D	0.9900
C35—H35B	0.9900	C70A—C71A	1.51 (2)
C36—C37	1.525 (14)	C70A—H70C	0.9900
C36—H36A	0.9900	C70A—H70D	0.9900
C36—H36B	0.9900	C71A—C72A	1.52 (2)
C37—H37A	0.9900	C71A—H71C	0.9900
C37—H37B	0.9900	C71A—H71D	0.9900
C38—H38A	0.9500	C72A—C78A	1.33 (2)
C38—H38B	0.9500	C72A—C73A	1.499 (18)
C41—C46	1.380 (11)	C73A—C74A	1.535 (18)
C41—C42	1.382 (12)	C73A—H73A	1.0000
C41—H41	0.9500	C74A—C75A	1.50 (2)

Table 1.6. (Continued)

C42—C43	1.365 (12)	C74A—H74C	0.9900
C42—H42	0.9500	C74A—H74D	0.9900
C43—C44	1.400 (11)	C75A—C76A	1.50 (2)
C43—Br3	1.896 (8)	C75A—H75C	0.9900
C44—C45	1.389 (12)	C75A—H75D	0.9900
C44—H44	0.9500	C76A—C77A	1.523 (18)
C45—C46	1.388 (11)	C76A—H76C	0.9900
C45—H45	0.9500	C76A—H76D	0.9900
C46—C47	1.512 (11)	C77A—H77C	0.9900
C47—O6	1.213 (10)	C77A—H77D	0.9900
C47—O5	1.318 (10)	C78A—H78C	0.9500
C48—O5	1.475 (10)	C78A—H78D	0.9500
C2—C1—C6	121.0 (7)	C50—C49—H49B	109.3
C2—C1—H1	119.5	H49A—C49—H49B	108.0
C6—C1—H1	119.5	C51—C50—C49	111.0 (7)
C3—C2—C1	118.0 (7)	C51—C50—H50A	109.4
C3—C2—H2	121.0	C49—C50—H50A	109.4
C1—C2—H2	121.0	C51—C50—H50B	109.4
C2—C3—C4	122.9 (8)	C49—C50—H50B	109.4
C2—C3—Br1	119.5 (6)	H50A—C50—H50B	108.0
C4—C3—Br1	117.6 (7)	C52—C51—C50	112.3 (7)
C5—C4—C3	118.0 (8)	C52—C51—H51A	109.1
C5—C4—H4	121.0	C50—C51—H51A	109.1
C3—C4—H4	121.0	C52—C51—H51B	109.1
C4—C5—C6	120.8 (8)	C50—C51—H51B	109.1
C4—C5—H5	119.6	H51A—C51—H51B	107.9
C6—C5—H5	119.6	C58—C52—C51	122.9 (8)
C5—C6—C1	119.2 (8)	C58—C52—C53	123.1 (8)
C5—C6—C7	119.1 (7)	C51—C52—C53	113.9 (7)
C1—C6—C7	121.7 (7)	C54—C53—C52	115.1 (7)

Table 1.6. (Continued)

O2—C7—O1	126.6 (8)	C54—C53—C48	111.6 (6)
O2—C7—C6	122.5 (7)	C52—C53—C48	109.5 (6)
O1—C7—C6	110.9 (6)	C54—C53—H53	106.7
O1—C8—C9	111.6 (6)	C52—C53—H53	106.7
O1—C8—C17	109.7 (6)	C48—C53—H53	106.7
C9—C8—C17	111.5 (6)	C53—C54—C55	111.6 (7)
O1—C8—C13	101.6 (6)	C53—C54—H54A	109.3
C9—C8—C13	111.5 (7)	C55—C54—H54A	109.3
C17—C8—C13	110.5 (6)	C53—C54—H54B	109.3
C8—C9—C10	112.9 (6)	C55—C54—H54B	109.3
C8—C9—H9A	109.0	H54A—C54—H54B	108.0
C10—C9—H9A	109.0	C54—C55—C56	110.7 (7)
C8—C9—H9B	109.0	C54—C55—H55A	109.5
C10—C9—H9B	109.0	C56—C55—H55A	109.5
H9A—C9—H9B	107.8	C54—C55—H55B	109.5
C11—C10—C9	109.6 (7)	C56—C55—H55B	109.5
C11—C10—H10A	109.8	H55A—C55—H55B	108.1
C9—C10—H10A	109.8	C57—C56—C55	110.4 (8)
C11—C10—H10B	109.8	C57—C56—H56A	109.6
C9—C10—H10B	109.8	C55—C56—H56A	109.6
H10A—C10—H10B	108.2	C57—C56—H56B	109.6
C12—C11—C10	112.1 (7)	C55—C56—H56B	109.6
C12—C11—H11A	109.2	H56A—C56—H56B	108.1
C10—C11—H11A	109.2	C56—C57—C48	112.9 (7)
C12—C11—H11B	109.2	C56—C57—H57A	109.0
C10—C11—H11B	109.2	C48—C57—H57A	109.0
H11A—C11—H11B	107.9	C56—C57—H57B	109.0
C18—C12—C11	122.4 (8)	C48—C57—H57B	109.0
C18—C12—C13	123.5 (8)	H57A—C57—H57B	107.8
C11—C12—C13	114.1 (7)	C52—C58—H58A	120.0
C14—C13—C12	115.1 (7)	C52—C58—H58B	120.0

Table 1.6. (Continued)

C14—C13—C8	111.3 (6)	H58A—C58—H58B	120.0
C12—C13—C8	108.4 (6)	C47—O5—C48	123.5 (6)
C14—C13—H13	107.2	C66—C61—C62	120.2 (6)
C12—C13—H13	107.2	C66—C61—H61	119.9
C8—C13—H13	107.2	C62—C61—H61	119.9
C15—C14—C13	110.9 (6)	C63—C62—C61	117.8 (7)
C15—C14—H14A	109.5	C63—C62—H62	121.1
C13—C14—H14A	109.5	C61—C62—H62	121.1
C15—C14—H14B	109.5	C64—C63—C62	122.8 (7)
C13—C14—H14B	109.5	C64—C63—Br4	118.3 (5)
H14A—C14—H14B	108.0	C62—C63—Br4	118.8 (5)
C14—C15—C16	112.1 (6)	C63—C64—C65	118.6 (7)
C14—C15—H15A	109.2	C63—C64—H64	120.7
C16—C15—H15A	109.2	C65—C64—H64	120.7
C14—C15—H15B	109.2	C66—C65—C64	120.0 (7)
C16—C15—H15B	109.2	C66—C65—H65	120.0
H15A—C15—H15B	107.9	C64—C65—H65	120.0
C15—C16—C17	111.0 (6)	C65—C66—C61	120.5 (7)
C15—C16—H16A	109.4	C65—C66—C67	117.9 (7)
C17—C16—H16A	109.4	C61—C66—C67	121.6 (7)
C15—C16—H16B	109.4	O8—C67—O7	126.4 (8)
C17—C16—H16B	109.4	O8—C67—C66	122.9 (9)
H16A—C16—H16B	108.0	O7—C67—C66	110.7 (7)
C8—C17—C16	113.1 (6)	C67—O7—C68A	110.9 (9)
C8—C17—H17A	109.0	C67—O7—C68	130.9 (8)
C16—C17—H17A	109.0	C69—C68—C77	113.6 (12)
C8—C17—H17B	109.0	C69—C68—O7	107.5 (17)
C16—C17—H17B	109.0	C77—C68—O7	105.3 (11)
H17A—C17—H17B	107.8	C69—C68—C73	111.7 (14)
C12—C18—H18A	120.0	C77—C68—C73	111.9 (12)
C12—C18—H18B	120.0	O7—C68—C73	106.3 (11)

Table 1.6. (Continued)

H18A—C18—H18B	120.0	C68—C69—C70	113.1 (17)
C7—O1—C8	123.5 (6)	C68—C69—H69A	109.0
C26—C21—C22	119.6 (8)	C70—C69—H69A	109.0
C26—C21—H21	120.2	C68—C69—H69B	109.0
C22—C21—H21	120.2	C70—C69—H69B	109.0
C23—C22—C21	118.8 (8)	H69A—C69—H69B	107.8
C23—C22—H22	120.6	C69—C70—C71	109.9 (16)
C21—C22—H22	120.6	C69—C70—H70A	109.7
C22—C23—C24	122.7 (8)	C71—C70—H70A	109.7
C22—C23—Br2	118.6 (6)	C69—C70—H70B	109.7
C24—C23—Br2	118.7 (7)	C71—C70—H70B	109.7
C25—C24—C23	118.6 (8)	H70A—C70—H70B	108.2
C25—C24—H24	120.7	C72—C71—C70	110.9 (14)
C23—C24—H24	120.7	C72—C71—H71A	109.5
C24—C25—C26	120.0 (8)	C70—C71—H71A	109.5
C24—C25—H25	120.0	C72—C71—H71B	109.5
C26—C25—H25	120.0	C70—C71—H71B	109.5
C25—C26—C21	120.3 (8)	H71A—C71—H71B	108.1
C25—C26—C27	119.1 (7)	C78—C72—C73	122.4 (17)
C21—C26—C27	120.7 (8)	C78—C72—C71	123.0 (17)
O4—C27—O3	126.1 (8)	C73—C72—C71	114.5 (13)
O4—C27—C26	123.3 (8)	C72—C73—C68	111.4 (11)
O3—C27—C26	110.6 (7)	C72—C73—C74	116.8 (13)
O3—C28—C37	110.7 (7)	C68—C73—C74	111.2 (12)
O3—C28—C29	110.4 (6)	C72—C73—H73	105.5
C37—C28—C29	112.8 (7)	C68—C73—H73	105.5
O3—C28—C33	100.9 (6)	C74—C73—H73	105.5
C37—C28—C33	112.0 (7)	C75—C74—C73	113.3 (13)
C29—C28—C33	109.4 (7)	C75—C74—H74A	108.9
C30—C29—C28	113.3 (6)	C73—C74—H74A	108.9
C30—C29—H29A	108.9	C75—C74—H74B	108.9

Table 1.6. (Continued)

C28—C29—H29A	108.9	C73—C74—H74B	108.9
C30—C29—H29B	108.9	H74A—C74—H74B	107.7
C28—C29—H29B	108.9	C76—C75—C74	114.1 (14)
H29A—C29—H29B	107.7	C76—C75—H75A	108.7
C29—C30—C31	110.5 (6)	C74—C75—H75A	108.7
C29—C30—H30A	109.6	C76—C75—H75B	108.7
C31—C30—H30A	109.6	C74—C75—H75B	108.7
C29—C30—H30B	109.6	H75A—C75—H75B	107.6
C31—C30—H30B	109.6	C75—C76—C77	109.2 (12)
H30A—C30—H30B	108.1	C75—C76—H76A	109.8
C32—C31—C30	110.2 (7)	C77—C76—H76A	109.8
C32—C31—H31A	109.6	C75—C76—H76B	109.8
C30—C31—H31A	109.6	C77—C76—H76B	109.8
C32—C31—H31B	109.6	H76A—C76—H76B	108.3
C30—C31—H31B	109.6	C68—C77—C76	114.4 (12)
H31A—C31—H31B	108.1	C68—C77—H77A	108.7
C38—C32—C33	124.7 (10)	C76—C77—H77A	108.7
C38—C32—C31	120.7 (10)	C68—C77—H77B	108.7
C33—C32—C31	114.6 (7)	C76—C77—H77B	108.7
C32—C33—C34	116.2 (8)	H77A—C77—H77B	107.6
C32—C33—C28	110.9 (6)	C72—C78—H78A	120.0
C34—C33—C28	110.4 (7)	C72—C78—H78B	120.0
C32—C33—H33	106.2	H78A—C78—H78B	120.0
C34—C33—H33	106.2	C69A—C68A—O7	105 (2)
C28—C33—H33	106.2	C69A—C68A—C77A	113.2 (14)
C35—C34—C33	112.2 (9)	O7—C68A—C77A	119.5 (13)
C35—C34—H34A	109.2	C69A—C68A—C73A	112.5 (17)
C33—C34—H34A	109.2	O7—C68A—C73A	94.2 (12)
C35—C34—H34B	109.2	C77A—C68A—C73A	110.6 (14)
C33—C34—H34B	109.2	C68A—C69A—C70A	116.0 (19)
H34A—C34—H34B	107.9	C68A—C69A—H69C	108.3

Table 1.6. (Continued)

C36—C35—C34	112.3 (9)	C70A—C69A—H69C	108.3
C36—C35—H35A	109.1	C68A—C69A—H69D	108.3
C34—C35—H35A	109.1	C70A—C69A—H69D	108.3
C36—C35—H35B	109.1	H69C—C69A—H69D	107.4
C34—C35—H35B	109.1	C71A—C70A—C69A	111.1 (18)
H35A—C35—H35B	107.9	C71A—C70A—H70C	109.4
C35—C36—C37	109.6 (10)	C69A—C70A—H70C	109.4
C35—C36—H36A	109.8	C71A—C70A—H70D	109.4
C37—C36—H36A	109.8	C69A—C70A—H70D	109.4
C35—C36—H36B	109.8	H70C—C70A—H70D	108.0
C37—C36—H36B	109.8	C70A—C71A—C72A	114.7 (16)
H36A—C36—H36B	108.2	C70A—C71A—H71C	108.6
C28—C37—C36	112.8 (9)	C72A—C71A—H71C	108.6
C28—C37—H37A	109.0	C70A—C71A—H71D	108.6
C36—C37—H37A	109.0	C72A—C71A—H71D	108.6
C28—C37—H37B	109.0	H71C—C71A—H71D	107.6
C36—C37—H37B	109.0	C78A—C72A—C73A	121 (2)
H37A—C37—H37B	107.8	C78A—C72A—C71A	123 (2)
C32—C38—H38A	120.0	C73A—C72A—C71A	116.4 (15)
C32—C38—H38B	120.0	C72A—C73A—C68A	112.0 (15)
H38A—C38—H38B	120.0	C72A—C73A—C74A	117.8 (15)
C27—O3—C28	122.5 (6)	C68A—C73A—C74A	112.7 (14)
C46—C41—C42	120.1 (8)	C72A—C73A—H73A	104.2
C46—C41—H41	120.0	C68A—C73A—H73A	104.2
C42—C41—H41	120.0	C74A—C73A—H73A	104.2
C43—C42—C41	119.4 (7)	C75A—C74A—C73A	112.1 (14)
C43—C42—H42	120.3	C75A—C74A—H74C	109.2
C41—C42—H42	120.3	C73A—C74A—H74C	109.2
C42—C43—C44	122.4 (8)	C75A—C74A—H74D	109.2
C42—C43—Br3	119.5 (6)	C73A—C74A—H74D	109.2
C44—C43—Br3	118.1 (7)	H74C—C74A—H74D	107.9

Table 1.6. (Continued)

C45—C44—C43	117.1 (8)	C74A—C75A—C76A	112.5 (17)
C45—C44—H44	121.5	C74A—C75A—H75C	109.1
C43—C44—H44	121.5	C76A—C75A—H75C	109.1
C46—C45—C44	121.1 (9)	C74A—C75A—H75D	109.1
C46—C45—H45	119.4	C76A—C75A—H75D	109.1
C44—C45—H45	119.4	H75C—C75A—H75D	107.8
C41—C46—C45	119.9 (8)	C75A—C76A—C77A	109.0 (14)
C41—C46—C47	120.7 (8)	C75A—C76A—H76C	109.9
C45—C46—C47	119.3 (7)	C77A—C76A—H76C	109.9
O6—C47—O5	126.6 (8)	C75A—C76A—H76D	109.9
O6—C47—C46	122.5 (8)	C77A—C76A—H76D	109.9
O5—C47—C46	110.9 (7)	H76C—C76A—H76D	108.3
O5—C48—C49	111.0 (7)	C76A—C77A—C68A	113.3 (14)
O5—C48—C57	109.7 (7)	C76A—C77A—H77C	108.9
C49—C48—C57	111.0 (6)	C68A—C77A—H77C	108.9
O5—C48—C53	102.0 (6)	C76A—C77A—H77D	108.9
C49—C48—C53	112.2 (6)	C68A—C77A—H77D	108.9
C57—C48—C53	110.7 (7)	H77C—C77A—H77D	107.7
C48—C49—C50	111.6 (6)	C72A—C78A—H78C	120.0
C48—C49—H49A	109.3	C72A—C78A—H78D	120.0
C50—C49—H49A	109.3	H78C—C78A—H78D	120.0
C48—C49—H49B	109.3		
C6—C1—C2—C3	1.5 (12)	C49—C50—C51—C52	53.5 (10)
C1—C2—C3—C4	-2.2 (13)	C50—C51—C52—C58	123.5 (9)
C1—C2—C3—Br1	177.5 (6)	C50—C51—C52—C53	-54.1 (10)
C2—C3—C4—C5	1.5 (14)	C58—C52—C53—C54	1.9 (12)
Br1—C3—C4—C5	-178.3 (6)	C51—C52—C53—C54	179.5 (7)
C3—C4—C5—C6	0.0 (13)	C58—C52—C53—C48	-124.8 (9)
C4—C5—C6—C1	-0.7 (12)	C51—C52—C53—C48	52.8 (9)
C4—C5—C6—C7	179.4 (7)	O5—C48—C53—C54	-63.1 (8)
C2—C1—C6—C5	-0.1 (11)	C49—C48—C53—C54	178.1 (7)

Table 1.6. (Continued)

C2—C1—C6—C7	179.8 (7)	C57—C48—C53—C54	53.5 (9)
C5—C6—C7—O2	8.7 (11)	O5—C48—C53—C52	65.5 (7)
C1—C6—C7—O2	-171.2 (7)	C49—C48—C53—C52	-53.3 (9)
C5—C6—C7—O1	-172.5 (7)	C57—C48—C53—C52	-177.9 (7)
C1—C6—C7—O1	7.7 (10)	C52—C53—C54—C55	178.9 (7)
O1—C8—C9—C10	-56.0 (9)	C48—C53—C54—C55	-55.5 (10)
C17—C8—C9—C10	-179.1 (7)	C53—C54—C55—C56	56.6 (11)
C13—C8—C9—C10	56.8 (9)	C54—C55—C56—C57	-55.9 (11)
C8—C9—C10—C11	-55.5 (10)	C55—C56—C57—C48	55.7 (11)
C9—C10—C11—C12	53.8 (9)	O5—C48—C57—C56	57.6 (10)
C10—C11—C12—C18	125.1 (10)	C49—C48—C57—C56	-179.5 (8)
C10—C11—C12—C13	-55.6 (10)	C53—C48—C57—C56	-54.2 (10)
C18—C12—C13—C14	-1.5 (12)	O6—C47—O5—C48	8.0 (12)
C11—C12—C13—C14	179.3 (7)	C46—C47—O5—C48	-171.5 (6)
C18—C12—C13—C8	-126.9 (9)	C49—C48—O5—C47	-63.8 (9)
C11—C12—C13—C8	53.9 (9)	C57—C48—O5—C47	59.2 (9)
O1—C8—C13—C14	-62.3 (7)	C53—C48—O5—C47	176.5 (6)
C9—C8—C13—C14	178.7 (6)	C66—C61—C62—C63	0.2 (12)
C17—C8—C13—C14	54.1 (9)	C61—C62—C63—C64	-0.2 (12)
O1—C8—C13—C12	65.3 (7)	C61—C62—C63—Br4	-178.4 (6)
C9—C8—C13—C12	-53.7 (8)	C62—C63—C64—C65	1.1 (13)
C17—C8—C13—C12	-178.3 (7)	Br4—C63—C64—C65	179.4 (6)
C12—C13—C14—C15	-179.7 (6)	C63—C64—C65—C66	-2.0 (12)
C8—C13—C14—C15	-55.8 (9)	C64—C65—C66—C61	2.0 (12)
C13—C14—C15—C16	56.3 (9)	C64—C65—C66—C67	-178.9 (7)
C14—C15—C16—C17	-54.6 (9)	C62—C61—C66—C65	-1.1 (12)
O1—C8—C17—C16	57.9 (8)	C62—C61—C66—C67	179.9 (7)
C9—C8—C17—C16	-178.0 (7)	C65—C66—C67—O8	-9.5 (12)
C13—C8—C17—C16	-53.4 (9)	C61—C66—C67—O8	169.5 (8)
C15—C16—C17—C8	53.7 (9)	C65—C66—C67—O7	172.9 (7)
O2—C7—O1—C8	4.2 (12)	C61—C66—C67—O7	-8.0 (11)

Table 1.6. (Continued)

C6—C7—O1—C8	-174.7 (6)	O8—C67—O7—C68A	-2.9 (14)
C9—C8—O1—C7	-61.2 (9)	C66—C67—O7—C68A	174.6 (9)
C17—C8—O1—C7	62.9 (8)	O8—C67—O7—C68	-3.9 (16)
C13—C8—O1—C7	179.9 (6)	C66—C67—O7—C68	173.6 (10)
C26—C21—C22—C23	0.3 (12)	C67—O7—C68—C69	-50.2 (15)
C21—C22—C23—C24	0.6 (13)	C68A—O7—C68—C69	-53 (3)
C21—C22—C23—Br2	179.6 (6)	C67—O7—C68—C77	71.2 (14)
C22—C23—C24—C25	-1.6 (14)	C68A—O7—C68—C77	68 (3)
Br2—C23—C24—C25	179.4 (6)	C67—O7—C68—C73	-170.0 (9)
C23—C24—C25—C26	1.6 (13)	C68A—O7—C68—C73	-173 (4)
C24—C25—C26—C21	-0.7 (12)	C77—C68—C69—C70	-177.6 (18)
C24—C25—C26—C27	178.4 (8)	O7—C68—C69—C70	-61 (2)
C22—C21—C26—C25	-0.2 (12)	C73—C68—C69—C70	55 (3)
C22—C21—C26—C27	-179.4 (7)	C68—C69—C70—C71	-57 (3)
C25—C26—C27—O4	-1.1 (12)	C69—C70—C71—C72	55 (2)
C21—C26—C27—O4	178.0 (8)	C70—C71—C72—C78	125.0 (19)
C25—C26—C27—O3	178.8 (7)	C70—C71—C72—C73	-53 (2)
C21—C26—C27—O3	-2.1 (10)	C78—C72—C73—C68	-127.7 (16)
O3—C28—C29—C30	-54.7 (9)	C71—C72—C73—C68	50.6 (17)
C37—C28—C29—C30	-179.2 (7)	C78—C72—C73—C74	2 (2)
C33—C28—C29—C30	55.5 (8)	C71—C72—C73—C74	179.9 (13)
C28—C29—C30—C31	-57.0 (8)	C69—C68—C73—C72	-50.1 (19)
C29—C30—C31—C32	54.3 (8)	C77—C68—C73—C72	-178.7 (12)
C30—C31—C32—C38	123.3 (10)	O7—C68—C73—C72	66.9 (14)
C30—C31—C32—C33	-54.8 (9)	C69—C68—C73—C74	177.7 (16)
C38—C32—C33—C34	3.3 (14)	C77—C68—C73—C74	49.2 (16)
C31—C32—C33—C34	-178.6 (8)	O7—C68—C73—C74	-65.3 (14)
C38—C32—C33—C28	-123.8 (10)	C72—C73—C74—C75	-179.5 (13)
C31—C32—C33—C28	54.3 (9)	C68—C73—C74—C75	-50.1 (17)
O3—C28—C33—C32	63.9 (8)	C73—C74—C75—C76	54.0 (19)
C37—C28—C33—C32	-178.2 (7)	C74—C75—C76—C77	-53.7 (19)

Table 1.6. (Continued)

C29—C28—C33—C32	-52.4 (8)	C69—C68—C77—C76	179.8 (18)
O3—C28—C33—C34	-66.3 (8)	O7—C68—C77—C76	62.4 (14)
C37—C28—C33—C34	51.5 (9)	C73—C68—C77—C76	-52.7 (16)
C29—C28—C33—C34	177.3 (7)	C75—C76—C77—C68	53.6 (18)
C32—C33—C34—C35	-179.8 (8)	C67—O7—C68A—C69A	-78.2 (16)
C28—C33—C34—C35	-52.4 (11)	C68—O7—C68A—C69A	100 (3)
C33—C34—C35—C36	56.4 (13)	C67—O7—C68A—C77A	50.4 (17)
C34—C35—C36—C37	-56.6 (13)	C68—O7—C68A—C77A	-132 (4)
O3—C28—C37—C36	57.4 (10)	C67—O7—C68A—C73A	167.1 (9)
C29—C28—C37—C36	-178.3 (8)	C68—O7—C68A—C73A	-15 (3)
C33—C28—C37—C36	-54.4 (11)	O7—C68A—C69A—C70A	-50 (3)
C35—C36—C37—C28	56.0 (12)	C77A—C68A—C69A—C70A	177 (3)
O4—C27—O3—C28	-1.0 (12)	C73A—C68A—C69A—C70A	51 (4)
C26—C27—O3—C28	179.1 (6)	C68A—C69A—C70A—C71A	-49 (4)
C37—C28—O3—C27	64.6 (9)	C69A—C70A—C71A—C72A	45 (3)
C29—C28—O3—C27	-61.0 (9)	C70A—C71A—C72A—C78A	132 (2)
C33—C28—O3—C27	-176.6 (6)	C70A—C71A—C72A—C73A	-46 (3)
C46—C41—C42—C43	0.5 (11)	C78A—C72A—C73A—C68A	-131.9 (19)
C41—C42—C43—C44	0.1 (12)	C71A—C72A—C73A—C68A	46 (2)
C41—C42—C43—Br3	-179.4 (6)	C78A—C72A—C73A—C74A	1 (3)
C42—C43—C44—C45	-0.5 (12)	C71A—C72A—C73A—C74A	179.3 (17)
Br3—C43—C44—C45	179.0 (6)	C69A—C68A—C73A—C72A	-48 (2)
C43—C44—C45—C46	0.3 (12)	O7—C68A—C73A—C72A	61.0 (16)
C42—C41—C46—C45	-0.7 (11)	C77A—C68A—C73A—C72A	-175.3 (15)
C42—C41—C46—C47	177.1 (7)	C69A—C68A—C73A—C74A	177 (2)
C44—C45—C46—C41	0.3 (11)	O7—C68A—C73A—C74A	-74.6 (15)
C44—C45—C46—C47	-177.5 (7)	C77A—C68A—C73A—C74A	49.2 (19)
C41—C46—C47—O6	-170.2 (8)	C72A—C73A—C74A—C75A	176.6 (17)
C45—C46—C47—O6	7.6 (11)	C68A—C73A—C74A—C75A	-51 (2)
C41—C46—C47—O5	9.4 (10)	C73A—C74A—C75A—C76A	55 (2)
C45—C46—C47—O5	-172.8 (7)	C74A—C75A—C76A—C77A	-58 (2)

Table 1.6. (Continued)

O5—C48—C49—C50	-57.9 (9)	C75A—C76A—C77A—C68A	57 (2)
C57—C48—C49—C50	179.8 (7)	C69A—C68A—C77A—C76A	179 (2)
C53—C48—C49—C50	55.4 (9)	O7—C68A—C77A—C76A	54 (2)
C48—C49—C50—C51	-54.5 (10)	C73A—C68A—C77A—C76A	-53.5 (18)

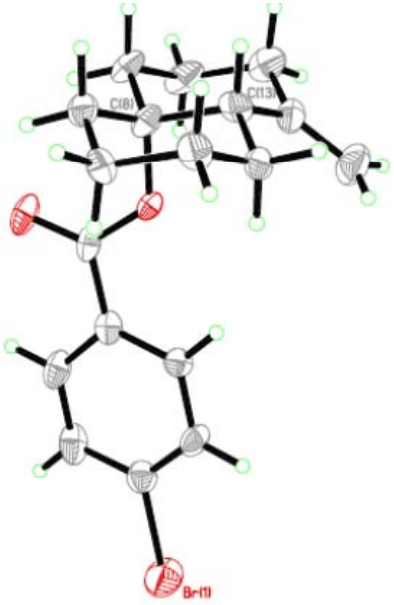

Figure 1.5. Perspective views showing 50% probability displacement.

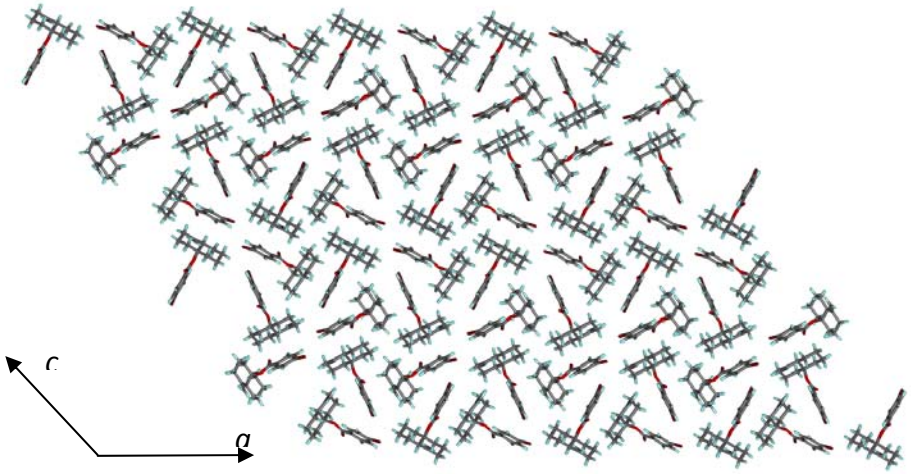

Figure 1.6. Three-dimensional supramolecular architecture viewed along the *b*-axis direction.

Chapter 2

Enantioselective Total Synthesis of (+)-Reserpine[1]

[1] Portions of this chapter have been published: Rajapaksa, N. S.; McGowan, M. A.; Rienzo, M.; Jacobsen, E. N. *Org. Lett.* **2013**, *15*, 706.

2.1. Introduction

Reserpine (**1**, Figure 2.1) is a biologically active indole alkaloid natural product that has, since its isolation six decades ago, represented an iconic target for organic synthesis.[2] Its stereochemically complex pentacyclic structure has inspired some of the most important work in the history of stereoselective synthesis, and it continues to inspire new synthetic methodologies today.[3,4] Woodward and coworkers disclosed the first total synthesis of reserpine in 1956,[5a] and since then a number of synthetic studies have been published. At the outset of this project there were ten reported total syntheses along with numerous partial synthetic studies.[5] Despite the scope of this effort, each successful approach to this molecule has relied on the same fundamental strategy, namely a late-stage generation of the C-ring and its embedded C3

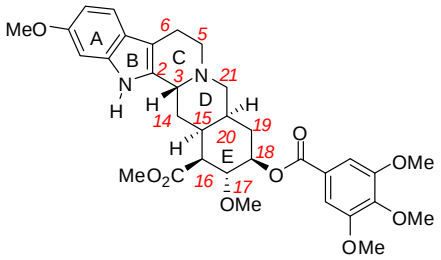

Figure 2.1. Reserpine **(–)-1**

[2] Müller, J.; Schlittler, E.; Bein, H. *Experientia* **1952**, *8*, 338.

[3] Nicolaou, K. C.; Sorensen, E. J. Classics in Total Synthesis; VCH: New York, **1996**.

[4] For reviews of synthetic efforts directed toward reserpine, see: a) McGowan, M. A. Ph.D. dissertation, Harvard University, **2010**. b) Chen, F-E.; Huang, J. *Chem. Rev.* **2005**, *105*, 4671.

[5] (a) Woodward, R. B.; Bader, F. E.; Bickel, H.; Frey, A. J.; Kierstead, R. W. *J. Am. Chem. Soc.* **1956**, *78*, 2023. (b) Woodward, R. B.; Bader, F. E.; Bickel, H.; Kierstead, R. W. *Tetrahedron* **1958**, *2*, 1. (c) Woodward, R. B.; Bader, F. E.; Bickel, H.; Frey, A. J.; Kierstead, R. W. *J. Am. Chem. Soc.* **1956**, *78*, 2657. (d) Pearlman, B. A. *J. Am. Chem. Soc.* **1979**, *101*, 6398. (e) Wender, P. A.; Schaus, J. M.; White, A. W. *J. Am. Chem. Soc.* **1980**, *102*, 6157. (f) Wender, P. A.; Schaus, J. M.; White, A. W. *Heterocycles* **1987**, *25*, 263. (g) Martin, S. F.; Grzejszczak, S.; Rueger, H.; Williamson, S. A. *J. Am. Chem. Soc.* **1985**, *107*, 4072. (h) Martin, S. F.; Rueger, H.; Williamson, S. A.; Grzejszczak, S. *J. Am. Chem. Soc.* **1987**, *109*, 6124. (i) Stork, G. *Pure & Appl. Chem.* **1989**, *61*, 439. (j) Gomez, A. M.; Lopez, J. C.; Fraser-Reid, B. *J. Org. Chem.* **1994**, *59*, 4048. (k) Gomez, A. M.; Lopez, J. C.; Fraser-Reid, B. *J. Org. Chem.* **1995**, *60*, 3859. (l) Chu, C.-S.; Liao, C.-C.; Rao, P. D. *Chem. Commun.* **1996**, 1537. (m) Hanessian, S.; Pan, J. W.; Carnell, A.; Bouchard, H.; Lesage, L. *J. Org. Chem.* **1997**, *62*, 465. (n) Mehta, G.; Reddy, D. S. *J. Chem. Soc., Perkin Trans. 1* **2000**, 1399. (o) Sparks, S. M.; Shea, K. J. *Org. Lett.* **2001**, *3*, 2265. (p) Sparks, S. M.; Gutierrez, A. J.; Shea, K. J. *J. Org. Chem.* **2003**, *68*, 5274. (q) Stork, G.; Tang, P. C.; Casey, M.; Goodman, B.; Toyota, M. *J. Am. Chem. Soc.* **2005**, *127*, 16255.

stereocenter from a 2,3-*seco*-derivative (**2**, Scheme 2.1).[6] These approaches target five of the molecule's six stereogenic centers through the formation of an appropriately functionalized E-ring or *cis*-fused D/E-ring fragment. However, the late-stage C-ring installation is generally complicated by preferential formation of the final C3 stereocenter with the undesired, thermodynamically favored relative stereochemistry.[7] As an introduction to this chapter, key strategies that have been employed to address this undesired outcome are reviewed, and a recently reported alternative approach to the reserpine framework is presented.

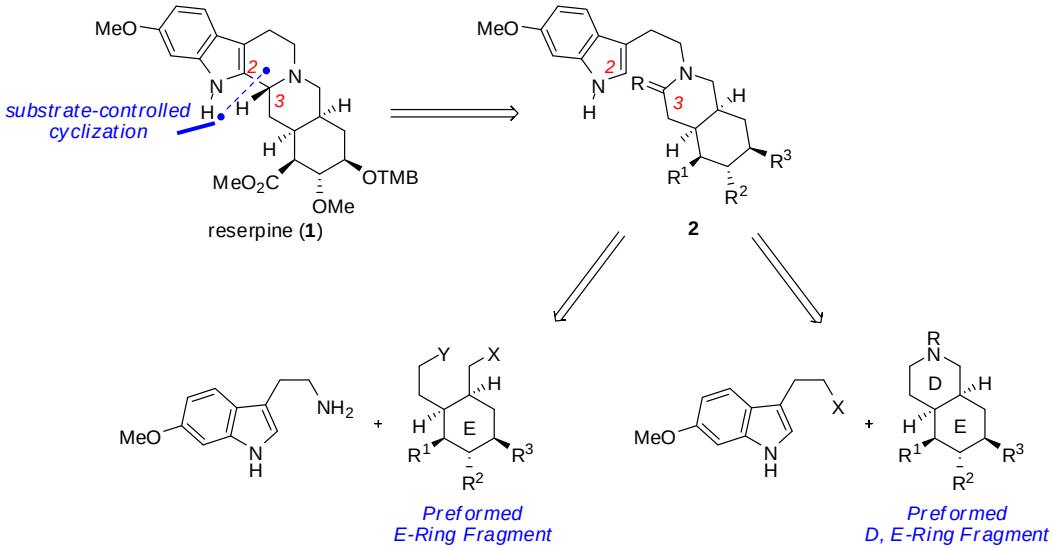

Scheme 2.1. Synthetic Strategies Common to All Previous Successful Approaches to Reserpine

2.2. Previous Strategies to Obtain the Desired C3 Configuration of Reserpine

2.2.1. The Woodward Approach: Conformational Biasing and C3 Epimerization

[6] The numbering scheme presented in Figure 2.1 is used for various intermediates throughout this chapter.

[7] Epimerization of reserpine (**1**) to 3-*epi*-reserpine (isoreserpine) occurs under acidic or basic conditions and is driven by the removal of unfavorable streic interactions between the axial C3 indole group and the D-ring. Subjecting **1** to AcOH under reflux affords an equilibrium mixture of 1.0:3.5 (reserpine:isoresrepine). For details, see: a) Gaskell, A. J.; Joule, J. A. *Tetrahedron* **1967**, *23*, 4053. b) Zhang, L.-H.; Gupta, A. K.; Cook, J. M. *J. Org. Chem.* **1989**, *54*, 4708. c) Sakai, S.; Ogawa, M. *Chem. Pharm. Bull.* **1978**, *26*, 678. d) Lounasmaa, M.; Berner, M.; Tolvanen, A. *Heterocycles* **1998**, *48*, 1275.

Woodward's landmark synthesis of reserpine involved a Bischler–Napieralski cyclization of lactam **3** and reduction of the resultant iminium ion with sodium borohydride (Scheme 2.2).[5a] However, nucleophilic addition selectively produced pentacycle **4**, which contains the undesired configuration at C3. Woodward reasoned that the C3 center could be epimerized after fixing the molecule in an unstable conformation. To this end, intermediate **4** was converted into rigid lactone **5**, and an equilibration of the C3 center under acidic conditions provided the correct relative stereochemistry of reserpine.

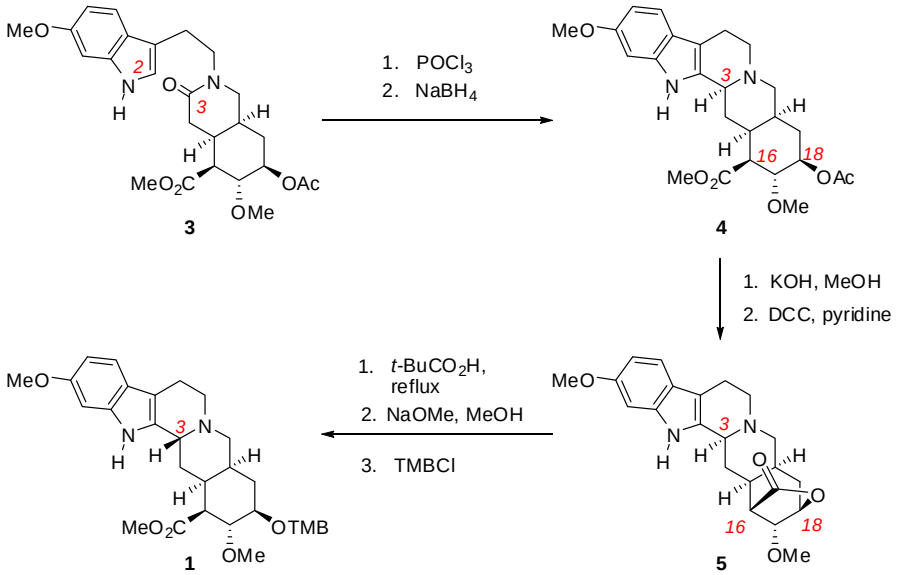

Scheme 2.2. Woodward's Synthesis of the C-ring and C3 Epimerization

2.2.2. The Stork Approach: Kinetic Cyclization of an Amino-Nitrile

The challenge posed by the C3 stereocenter of reserpine was overcome in a notable and most elegant manner by Stork and coworkers (Scheme 2.3).[5i,q] They predicted that cyclization of amino-nitrile **6** would generate a dialkyl iminium ion that could be trapped through a kinetic nucleophilic attack by the pendant indole to access methyl reserpate (**10**). However, in refluxing acetonitrile, **6** underwent a C2-C3 bond formation to furnish pentacycle **8**, which contains the undesired C3 stereochemistry. This

unexpected outcome was rationalized as occurring through a tight ion pair (**7**), in which the cyanide counterion blocks the desired trajectory of nucleophilic addition. Based on this hypothesis, amino-nitrile **6** was treated with either dilute HCl or silver tetrafluoroborate to generate a loose ion pair (**9**), which underwent a kinetically controlled cyclization to afford methyl reserpate (**10**).[8]

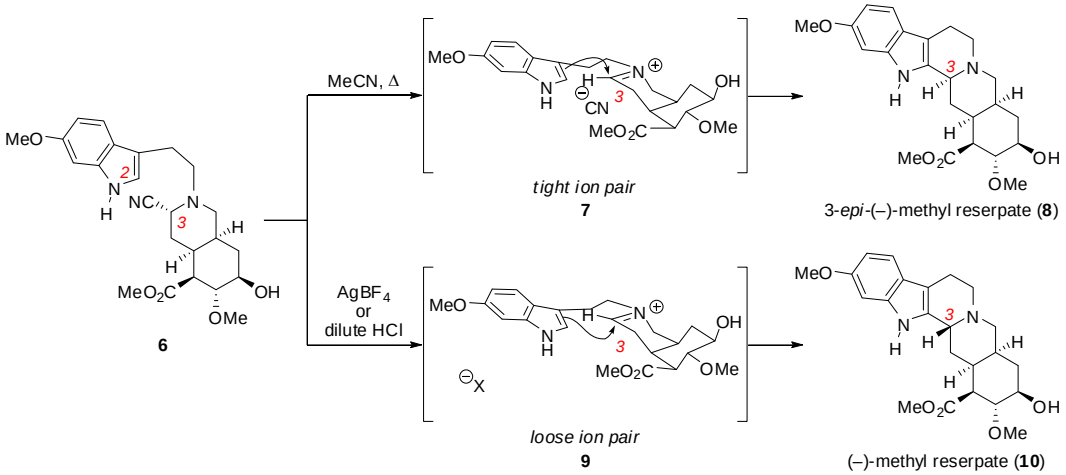

Scheme 2.3. Cyclizations of Amino-Nitrile **6** in the Stork Synthesis of Reserpine

2.2.3. The Kwon Approach: C3 Stereochemical Relay via a 6π-Electrocyclization

The complex architecture of reserpine continues to serve as a forum for exploring the frontiers of stereoselective synthesis. In 2012, Kwon and coworkers reported progress towards the synthesis of (±)-reserpine (**1**) through the application of a diastereoselective 6π-electrocyclization.[9] Kwon's strategy is relevant to the work presented in this chapter as it also represents a fundamental departure from the previous syntheses of reserpine in that the C3 stereocenter is generated at an early stage in the route. Racemic bromides **(*Z*/*E*)-12** were generated in a 1:2 ratio of olefin isomers in 11

[8] A related cyclization of amino-nitriles was recently employed in the syntheses of C3-epimeric natural products venenatine and alstovenine: Lebold, T. P.; Wood, J. L.; Deitch, J.; Lodewyk, M. W.; Tantillo, D. J.; Sarpong, R. *Nat. Chem.* **2013**, *5*, 126.

[9] a) Barcan, G. A.; Patel, A.; Houk, K. N.; Kwon, O. *Org. Lett.* **2012,** *14*, 5388. b) Patel, A.; Barcan, G. A.; Kwon, O.; Houk, K. N. *J. Am. Chem. Soc.* **2013**, *135*, 4878.

steps from methyl ester **11**. A Negishi cross-coupling of vinyl zinc species **13** with bromide **(*Z*/*E*)-12** afforded triene **14** which underwent an *in situ* 6π-electrocyclization to directly afford acetonide **15** in good yield and as a single diastereomer (Scheme 2.4). Pentacycle **15** was advanced to olefin **16** through hydrolysis of the acetonide followed by a PtO_2-catalyzed hydrogenation of the resultant α-keto-ester. Through the cascade Negishi/6π-electrocyclization, the authors demonstrated an efficient and unprecedented relay of stereochemical information from the C3 stereocenter of triene **14** to the remote C18 center of a highly functionalized pentacycle (**15**). However, the product was selectively generated with the undesired relative stereochemistry, and this outcome may present challenges for advancing **16** to reserpine (**1**).

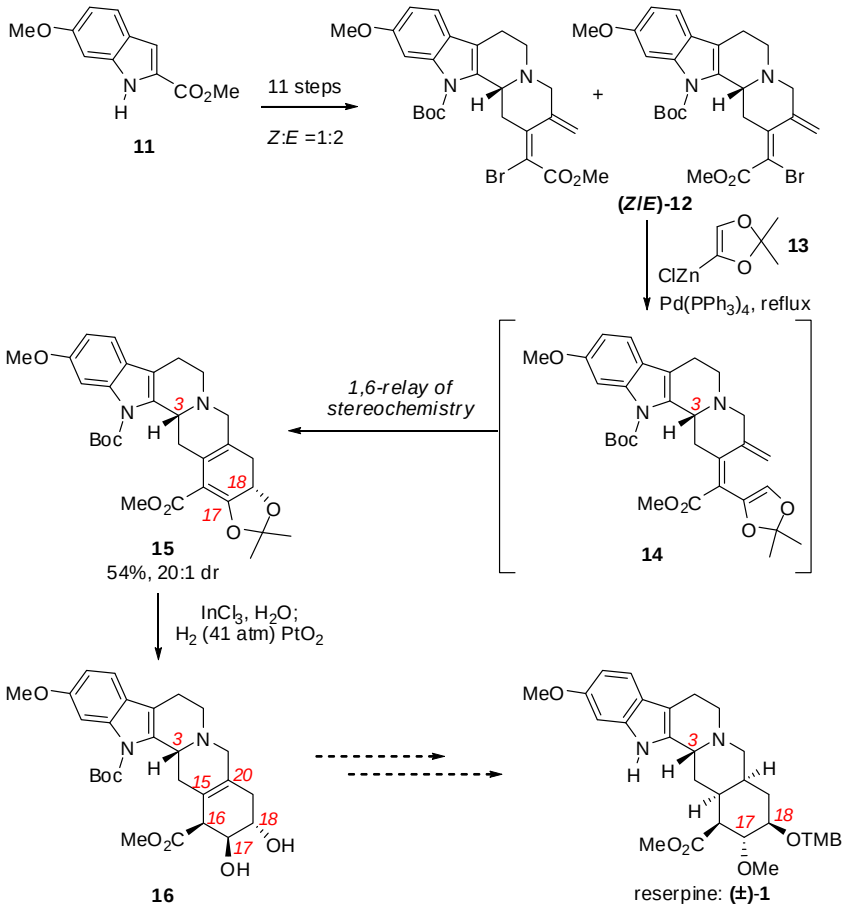

Scheme 2.4. Kwon's Diastereoselective 6π-Electrocyclization

2.3. Previous Work towards the Synthesis of (+)-Reserpine in the Jacobsen Group

Meredeth McGowan, a former graduate student in the Jacobsen group, became interested in investigating a new approach to reserpine based on a recently developed asymmetric formal aza-Diels–Alder (FADA) method. The motivations for pursuing the synthesis were to demonstrate the synthetic utility of the transformation and to address the historically problematic C3 stereocenter by using the newly developed method to install the problematic stereocenter with catalyst control. Together with Mathieu Lalonde, another former graduate student, she developed a highly diastereo- and enantioselective synthesis of chiral benzo- and indoloquinolizidine frameworks via FADA reactions of enones and cyclic imines (Scheme 2.5).[10] This transformation is catalyzed by bifunctional primary aminothiourea **17** that is proposed to activate the enone as its corresponding dienamine and simultaneously associate with the imine as a thiourea-bound iminium ion.

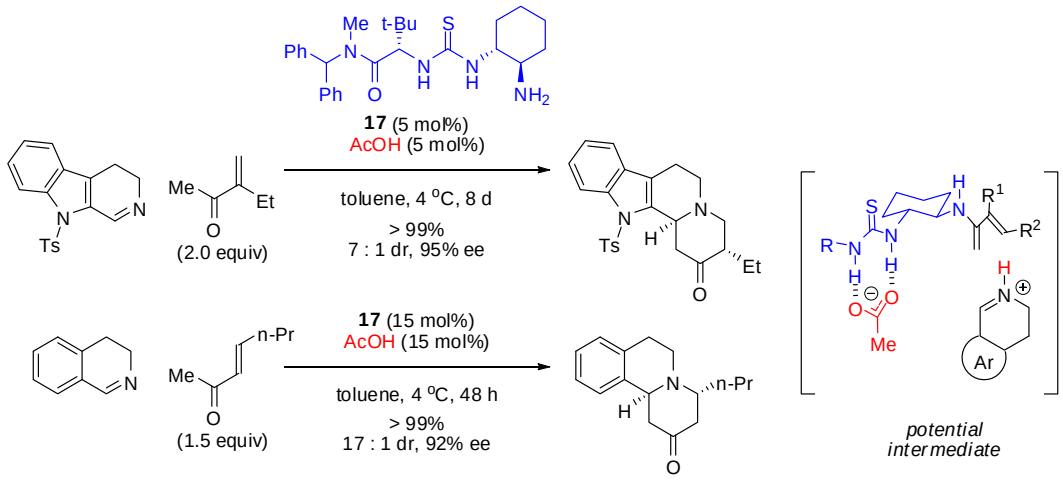

Scheme 2.5. Enantioselective Primary Aminothiourea-Catalyzed FADA Reactions of Enones and Cyclic Imines

[10] a) Lalonde, M. P.; McGowan, M. A.; Rajapaksa, N. S.; Jacobsen, E. N. *J. Am. Chem. Soc.* **2013**, *135*, 1891. b) For further details regarding the developing and scope of this transformation, see: Lalonde, M. P. Ph.D. Dissertation, Harvard University, **2008**.

Meredeth devised an alternative approach to the reserpine framework that proposed a catalyst-controlled diastereoselective FADA reaction between two components of comparable size, imine **18** and chiral enone **19** (Scheme 2.6).[11] Her progress is summarized in this section.

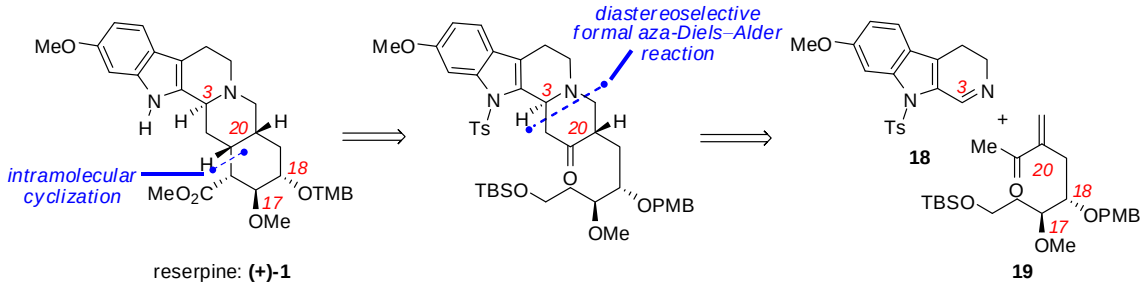

Scheme 2.6. Retrosynthetic Analysis of Reserpine

The synthetic efforts toward requisite enone component **19** began with a highly selective alcoholic kinetic resolution of racemic terminal epoxide **20**. Differentially protected 4-carbon triol **21** was obtained in 96% ee through the use of oligomeric cobalt salen catalyst **23**,[12] employing benzyl alcohol as the nucleophile (Scheme 2.7). Elaboration of protected alcohol **21** to aldehyde **22** was accomplished in a 3-step sequence consisting of methylation of the secondary alcohol, subsequent hydrogenolysis of the benzyl ether, and Swern oxidation of the resulting primary alcohol. The α-methoxy group of aldehyde **22** then served to direct a chelation-controlled diastereoselective allylation, thereby installing the adjacent C18 stereogenic center and providing vinyl bromide **24** as a single diastereomer.[13] Following protection of the C18 alcohol, lithium-

[11] Meredeth McGowan also applied an enantioselective FADA reaction of dihydroisoquinone and enone fragments to an asymmetric total synthesis of (–)-tubulosine. See reference 3a.

[12] White, D. E.; Jacobsen, E.N. *Tetrahedron: Asymmetry* **2003**, *14*, 3633.

[13] The sequence of allylsilane addition and subsequent PMB protection was adapted from: Evans, D. A.; Rajapakse, H. A.; Stenkemp, D. *Angew. Chem., Int. Ed.* **2002**, *41*, 4569.

halogen exchange and subsequent addition to acetaldehyde afforded an inconsequential mixture of diastereomeric alcohols (**25**/**26**) which was oxidized with the Dess–Martin periodinane to afford enone **19**. Efforts to directly access enone **19** through addition of the vinyllithium species derived from **24** to *N*-methoxy-*N*-methylacetamide proved less efficient due to competitive formation of the terminal olefin via protonolysis.

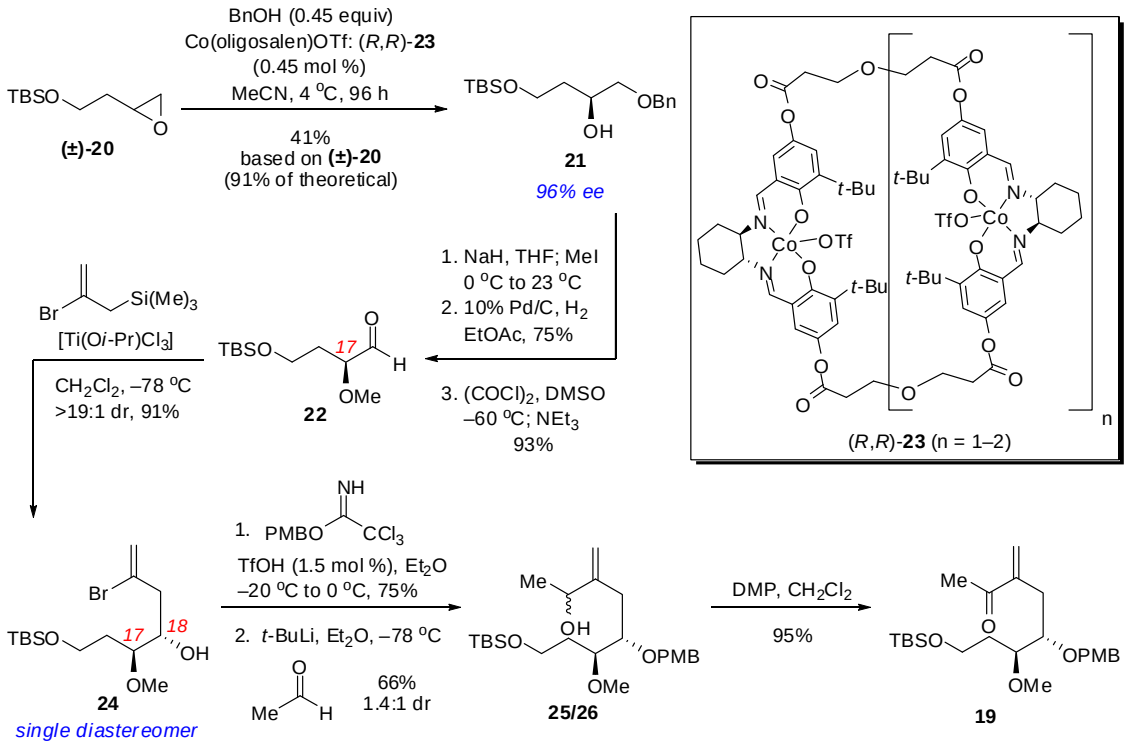

Scheme 2.7. Synthesis of Enantioenriched Enone **19**

The key coupling of enone **19** and 6-methoxytryptamine-derived dihydro-β-carboline **18**[14] to generate the D-ring of reserpine was then examined under a series of conditions (Scheme 2.8). The FADA reaction employing just a slight excess of complex enone **19** (1.2 equivalents) relative to imine **18** was only successful under the influence

[14] Imine **18** was synthesized from 6-methoxy-tryptamine through a formylation, Bischler–Napieralski cyclization, and tosylation with TsF. See refs. 10a,b for details.

of primary amine catalysts, consistent with previous observations employing simple, hindered enone derivatives and with the mechanistic hypothesis of enamine formation.[15] The degree of intrinsic substrate-induced diastereocontrol was evaluated using achiral amine promoters. With stoichiometric *n*-hexylamine,[16] ketones **27** and **28**, which contain a *trans*-relationship between the newly formed C3 and C20 stereocenters, were generated in a 1:1 diastereomeric ratio (entry 1). In contrast, high levels of chiral catalyst-controlled diastereoselectivity were observed in the presence of 20 mol% aminothiourea **17**, providing the desired diastereomer **27** in 76% isolated yield. Notably, the enantiomeric primary aminothiourea *ent*-**17** induced a reversal of diastereoselectivity in the FADA reaction to afford ketone **28** selectively (entry 3).

[15] No catalysis was observed with proline or related secondary amine catalysts. The proline-catalyzed formal aza-Diels–Alder reaction between dihydro-β-carboline and enones has been shown to require a large excess of enone (30 equivalents) relative to imine in those cases where catalysis is observed, see: Itoh, T.; Yokoya, M.; Miyauchi, K.; Nagata, K.; Ohsawa, A. *Org. Lett.* **2006**, *8*, 1533.

[16] Very low conversions (< 10% after 6 d) were obtained using 20 mol% *n*-hexylamine and 20 mol% acetic acid.

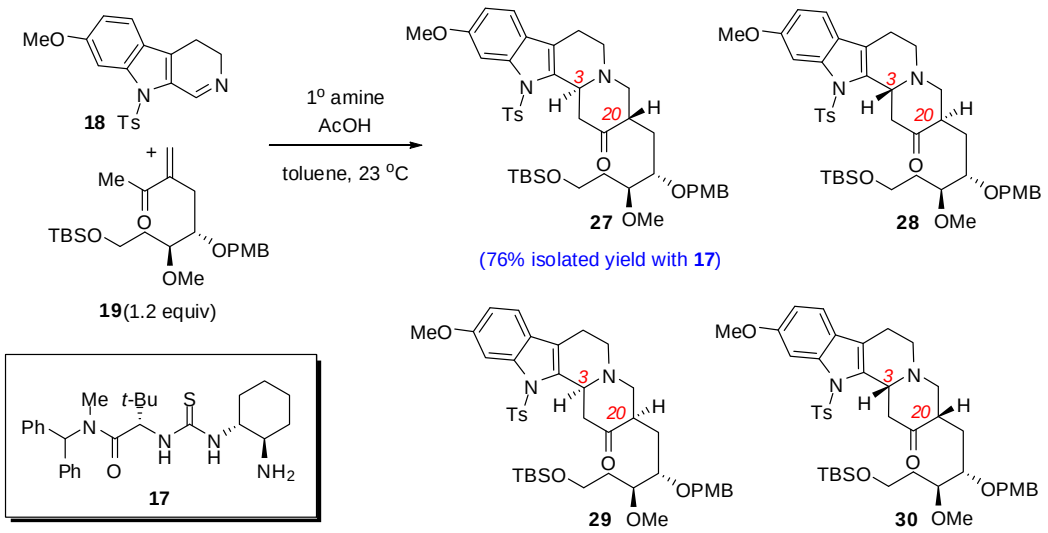

entry	amine (mol %)	AcOH (mol %)	time (d)	conv (%)	dr (**27**:**28**:**29**:**30**)
1	*n*-hexylamine (100)	100	9	90	1.0:1.0:0:0
2	**17** (20)	20	6	>99	11.5:1.0:1.8:0
3	*ent*-**17** (20)	20	6	>99	1.0:11.9:0:2.1

Scheme 2.8. Diastereoselective FADA Reactions of Imine **18** and Enone **19**

Closure of the E-ring to complete the carbon skeleton of reserpine could be accomplished by an intramolecular aldol reaction of keto-aldehyde **31** (Scheme 2.9). Intermediate **31** was obtained in two steps from FADA adduct **27** through cleavage of the primary TBS ether with pyridine-buffered HF and oxidation of the resulting primary alcohol with the Dess–Martin periodinane. Treatment of crude aldehyde **31** with piperidine and catalytic TsOH resulted in an intramolecular enamine aldol reaction to afford C15 tertiary alcohol **32** as a single diastereomer that contains *trans*-fused D- and E-rings.

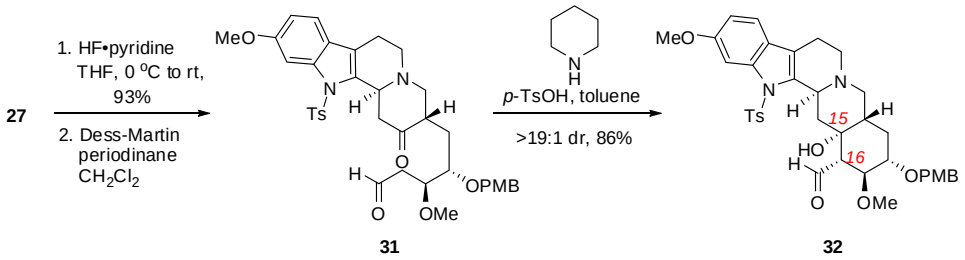

Scheme 2.9. Elaboration of the FADA Adduct to a Pentacyclic Framework Through an Aldol Cyclization

The most fruitful strategy evaluated for obtaining the correct oxidation state at C15 was an elimination-hydrogenation sequence (Scheme 2.10). Upon treatment of alcohol **32** with mesyl chloride and triethylamine, an *in situ* regioselective, albeit low-yielding, elimination took place to afford conjugated enal **33**. The C15-C16 olefin could be hydrogenated with PtO_2 in the presence of a mesyl chloride-derived additive.[17] Ultimately, however, compound **34** was not obtained in sufficient quantities to determine the stereochemical outcome of the hydrogenation.

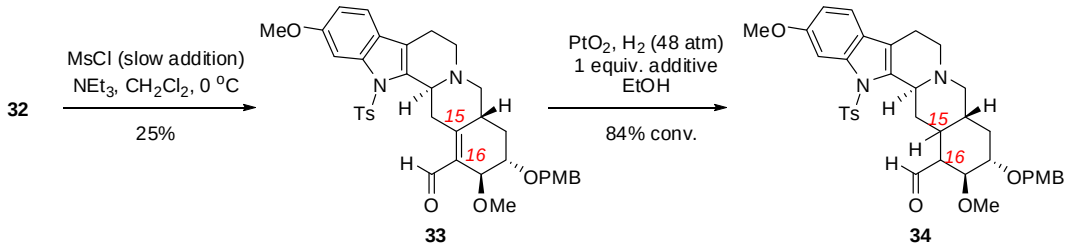

Scheme 2.10. Deoxygenation of **32** via an Elimination-Hydrogenation Sequence

2.4. Remaining Challenges

The previous synthetic work on this project established a route for generating four of the six stereocenters present in reserpine. The desired C18 and C17 stereocenters were installed by means of an enantioselective epoxide-opening reaction and a chelation-

[17] The beneficial additive was generated during the mesylation/elimination, and its identity was not conclusively determined. In the absence of the additive, enal decomposition was observed, and with excess (3 equiv) of the additive, lower conversion was obtained.

controlled allylation. Additionally, the primary aminothiourea-catalyzed FADA reaction of enone **19** and imine **18** introduced the desired stereochemistry at C3 and C20 to provide ketone **27** with a high degree of catalyst-induced diastereoselectivity. The primary goal of the work described herein was to develop a successful route for elaborating this key tetracyclic intermediate to (+)-reserpine. The remaining challenges included formation of the E-ring of the molecule and installation of the final two stereocenters at C15 and C16. As our overall synthetic strategy is a clear departure from previously published routes to reserpine, we anticipated completion of the synthesis would require developing an understanding of factors that influence the diastereoselectivity of transformations performed in such a complex setting. Additionally, while generating material to explore strategies to complete the synthesis, a secondary goal was to improve upon the synthesis of enone **19**. In particular, we investigated the direct conversion of vinyl bromide **24** to enone **19**.

2.5. Improved Synthesis of Enone 19[18]

As previously mentioned, attempts to form enone **19** directly from bromide **24** through a lithium-halogen exchange and subsequent addition to *N*-methoxy-*N*-methylacetamide (**35a)** [19] were unsatisfactory. This reaction formed a roughly 1:1 mixture of the desired enone and terminal olefin byproduct **36**, which is generated via protonolysis of the vinyllithium species (Table 2.1). This outcome contrasts with the analogous addition into acetaldehyde, which generates a diastereomeric mixture of secondary alcohols (**25**/**26**) in good yield and without formation of **36** (Scheme 2.7).

[18] This work was done in collaboration with Matthew Rienzo.

[19] Nahm, S.; Weinreb, S. M. *Tetrahedron Lett.* **1981**, *22*, 3815.

Table 2.1. Optimization of the Synthesis of Enone **19**

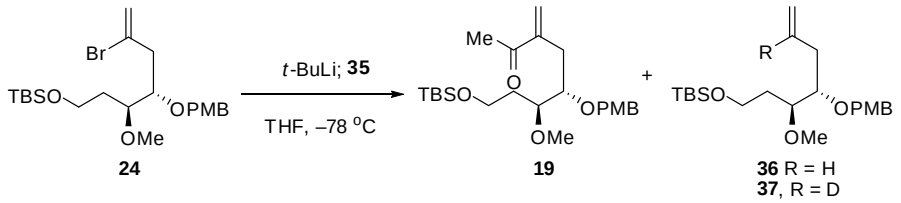

entry	electrophile	solvent	[**24**] (M)	**19** : **36** : **37**
1	**35a**	THF	0.1	1 : 1.0–1.4 : 0
2	**35a**	THF + D_2O quench	0.1	1 : 1.2 : 0
3	**35a**	THF	0.05	2.9 : 1 : 0
4	**35b**	THF	0.05	1.7 : 1 : 0
5	**35c**	THF	0.05	2.3 : 1 : 0
6	**35a**	Et_2O	0.05	5.3 : 1 : 0
7	**35a**	THF/toluene (1:1)	0.05	3.7 : 1 : 0
8	**35a**	Et_2O/pentane (1:1)	0.05	3.2 : 1 : 0

electrophiles:

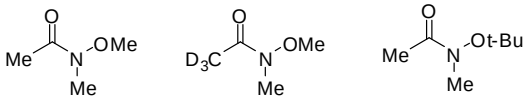

We speculated that formation of **36** directly involved electrophile **35a**, since efforts to rigorously exclude water did not suppress terminal olefin formation. We considered two possible scenarios for the formation of **36**: 1) incomplete consumption of the vinyllithium during the reaction, perhaps due to the formation of aggregates,[20] or 2) protonation of the vinyllithium species by amide **35a**. We ruled out the former possibility by quenching the reaction with D_2O (entry 2). The absence of deuterated olefin **37** and the observation that protonated olefin **36** was still formed indicated that the vinyllithium species was completely consumed during the reaction. Evidence against the latter possibility was provided through analogous reactions performed with deuterated

[20] In a related addition of an alkynyllithium species to a Weinreb amide, Collum and coworkers identified 1:1 aggregates that form between the tetrahedral adduct and unreacted organolithium reagent: Qu, B.; Collum, D. B. *J. Org. Chem.* **2006**, *71*, 7117.

amide **35b** and *N*-*tert*-butoxy-*N*-methylacetamide **35c**. Both reactions still afforded terminal olefin **36**, and without formation of **37**. These results suggested that electrophile **35a** was not undergoing deprotonation at the acetyl or alkoxy positions.[21] Although the proton source could not be determined, byproduct formation was suppressed through optimization of the reaction solvent (Table 2.1, entries 1, 6–8) and vinyl bromide concentration (entries 1 vs. 3). The reaction conducted in ether and at an initial vinyl bromide concentration of 0.05 M formed the enone in a ratio of 5.3:1 with olefin **36**. When the addition was performed on a preparative scale, the ratio improved to 6.7:1 and enone **19** was isolated in 76% yield. With this procedure, the synthesis of FADA coupling partner **19** could be accomplished in seven steps and in 33% overall yield from racemic epoxide **20** (Scheme 2.7).

2.6. Strategies for the Completion of the Reserpine Synthesis

We evaluated alternative strategies to an aldol cyclization for advancing FADA adduct **27** to the pentacyclic core of reserpine. Although the aldol cyclization was efficient and diastereoselective, the poor efficiency of the mesyl chloride-induced elimination and the capricious nature of the enal hydrogenation prompted us to consider an alternative intramolecular enamine-alkylation route.

2.6.1. Attempted Closure of the E-Ring Via Enamine Alkylation[22]

An alkylation strategy was particularly attractive as cyclization of an appropriately functionalized aldehyde (**38**) would afford a pentacycle with the C15 center

[21] Similar Weinreb amide deprotonation pathways have been identified: a) Mentzel, M.; Hoffman, H. M. R. *J. Prakt. Chem.* **1997**, *339*, 517. b) Sibi, M. P. *Org. Prep. Proced. Int.* **1993**, *25*, 15.

[22] This work was done in collaboration with Meredeth McGowan.

at the desired oxidation state (Scheme 2.11). Additionally, the stereospecificity of the transformation ensures that the C15 center would be formed with the desired stereochemistry.

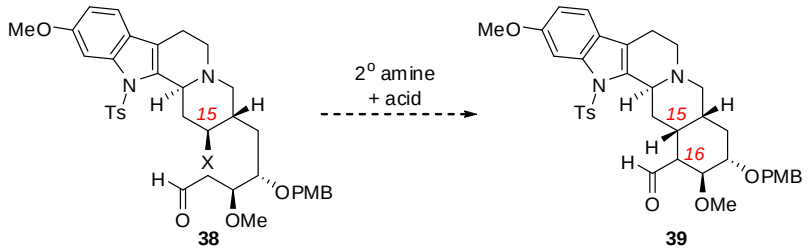

Scheme 2.11. Intramolecular Alkylation Strategy to Effect E-Ring Formation

Secondary mesylate **40** was synthesized from FADA adduct **27** through reduction of the ketone to afford a separable 3.4:1 mixture of alcohol diastereomers favoring the desired equatorial alcohol, and a subsequent mesylation. The proposed alkylation precursor **41** was obtained by removal of the silyl protecting group with TBAF, and oxidation of the resultant primary alcohol with the Dess–Martin Periodinane. However, treatment of aldehyde **41** with a variety of secondary amines only resulted in elimination of the C17 methoxy group to form (*E*)-olefin **43**, which still contains the C15 mesylate (Scheme 2.12).

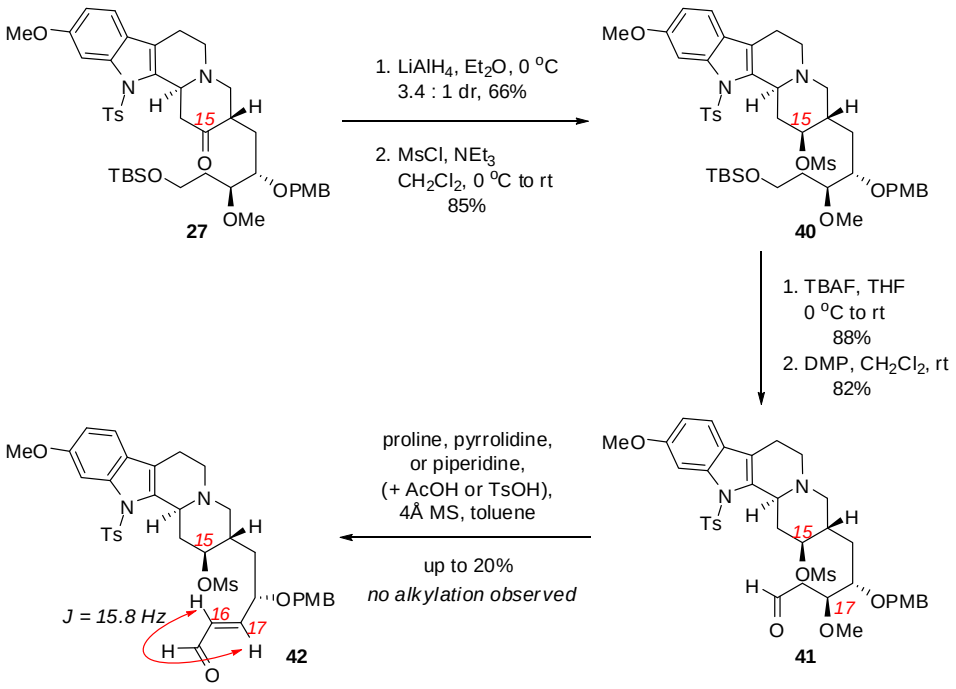

Scheme 2.12. Synthesis of Mesylate **41** and Attempted Enamine Alkylation

Although aldol precursor **31** and aldehyde **41** presumably access similar enamine intermediates upon exposure to a secondary amine and acid, the reaction outcomes are very different. Whereas the aldol cyclization afforded pentacycle **32** in high yield, the attempted alkylation did not afford any of the desired cyclization product (**39**, Scheme 2.13A).

An analysis of these results provided information about the reactivity of these intermediates and helped inform future routes. Aldol cyclization of keto-aldehyde **31** afforded *trans*-fused **32** as a single diastereomer, and without any elimination of the C17 methoxy group. This outcome corresponded to nucleophilic attack of the enamine occurring exclusively from the top face of the C15 ketone.[23] In contrast, the proposed

[23] The enamine aldol reaction installs the C16 center of **32** via protonation of an enamine intermediate, also from the top face. ^{1}H NMR and NOESY analysis of this intermediate (see the experimental section and ref. 3b) indicates that the E-ring is in a chair conformation, with all substituents in equatorial positions.

alkylation route would require the enamine derived from **41** to displace the C15 mesylate from the bottom face of the intermediate. Additionally, the enamine intermediate would need to access an unfavorable conformation (corresponding to **43b**) that places the C15 mesylate in an axial orientation. Unfavorable steric interactions between the C-ring and the C15 substituent may have rendered this pathway energetically inaccessible. Without a productive cyclization pathway available, the intermediate underwent an elimination of the C17 methoxy group to provide the only observed product, **42**. Together, these data strongly suggest that the top face of these tetracyclic intermediates is more accessible for nucleophilic attack. Based on this analysis, we moved forward with the aldol product **32** and investigated radical-based methods of obtaining the desired C15 oxidation state, since this same strong facial preference might render the mechanistically unselective radical pathway highly selective.

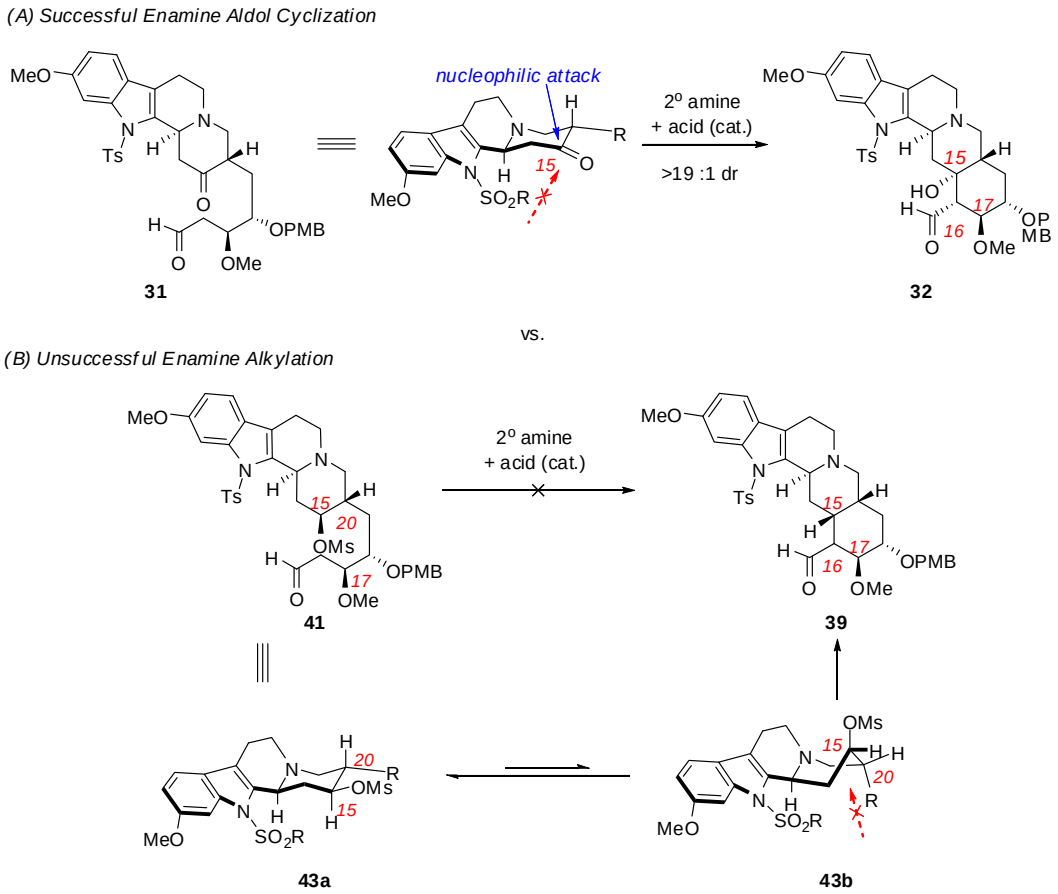

Scheme 2.13. Comparison of Aldol and Alkylation Routes

2.6.2. Radical Deoxygenation Attempts for Installing the C15 Stereocenter

The insight that these polycyclic intermediates may selectively undergo reactions on the top face encouraged us to pursue a radical deoxygenation approach to install the C15 center from aldol adduct **32**. In particular, we envisioned that if a C15 tertiary radical could be generated, it would likely react with a hydrogen radical from the top face of the intermediate, thereby affording the corresponding product that contains the correct oxidation state and configuration at C15. Because previous attempts to derivatize the C15 alcohol of **32** were met with limited success, an intramolecular activation strategy was employed (Scheme 2.14). Cyclic thiocarbonate **45** was identified as an appropriate

radical precursor, and literature precedent suggested that deoxygenation should occur via the more stable C15 tertiary radical instead of the C22 primary radical.[24, 25] Thiocarbonate **45** was obtained in two steps from aldehyde **32** through a sodium borohydride reduction and cyclization of the resultant diol with thiocarbonyl diimidazole.

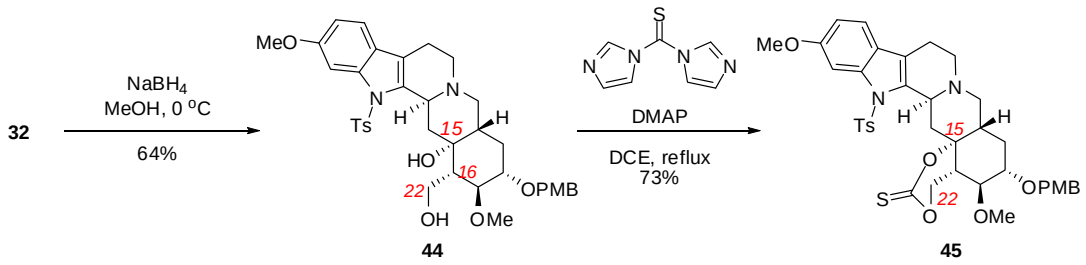

Scheme 2.14. Synthesis of Cyclic Thiocarbonate **45**

However, upon subjecting **45** to radical deoxygenation conditions (AIBN and tributyltin hydride) and then hydrolysis conditions, C15 tertiary alcohol **46** was obtained exclusively. We reasoned that the radical process may be under Curtin–Hammett control (Scheme 2.15), wherein **48**, the less-hindered of the two equilibrating radical species preferentially reacts with a hydrogen radical.[26]

[24] For a review of thiocarbonyl radical chemistry, see: Crich, D.; Quintero, L. *Chem. Rev.* **1989**, *89*, 1413.

[25] Radical deoxygenation of cyclic thiocarbonyl derivatives typically occurs through the more stable of the two possible radicals. For relevant examples, see: a) Barton, D. H. R.; Subramanian, R. *J. Chem. Soc. Perkin I*, **1977**, 1718. b) Liang, D.; Paula, H. W.; Fraser-Reid, B. *J. Chem. Soc.; Chem. Commun.* **1984**, 1123. c) Kangani, C. O.; Brückner, A. N.; Curran, D. P. *Org. Lett.* **2005**, *7*, 379.

[26] A similar radical equilibration mechanism was proposed to account for the significant selectivity for radical deoxygenation at the secondary center from a cyclic thiocarbamate derived from a secondary/ tertiary diol: Redlich, H.; Sudau, W.; Paulsen, H. *Tetrahedron* **1985**, *41*, 4253.

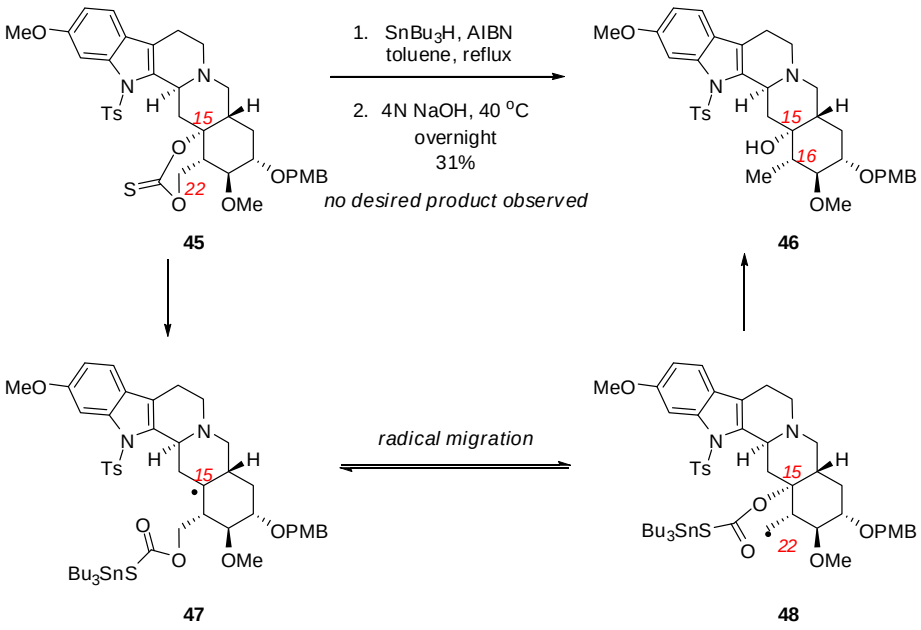

Scheme 2.15. Possible Curtin–Hammett Control in Radical Deoxygenation of **45**

Fortunately, we were successful in obtaining the C15 trifluoroacetate **49** as another possible precursor for radical deoxygenation (Scheme 2.16).[27] Trifluoroacetic anhydride, in contrast to several other derivatizing reagents, cleanly and quantitatively reacted with aldol adduct **32**. However, attempted purification of intermediate **49** revealed that it readily underwent hydrolysis back to alcohol **32** and elimination to yield conjugated enal **33**. This fortuitous discovery along with the prediction that enal **33** should selectively undergo reactions from the top face of the intermediate encouraged us to re-visit the hydrogenation strategy for setting the C15 and C16 stereocenters of reserpine.

[27] a) Kim, J.-G.; Cho, D. H.; Jang, D. O. *Tetrahedron Lett.* **2004**, *45*, 3031. b) Jang, D. O.; Kim, J.; Cho, D. H.; Chung, C.-M. *Tetrahedron Lett.* **2001**, *42*, 1073. c) Flyer, A. N.; Si, C.; Myers, A. G. *Nat. Chem.* **2010**, *2*, 886.

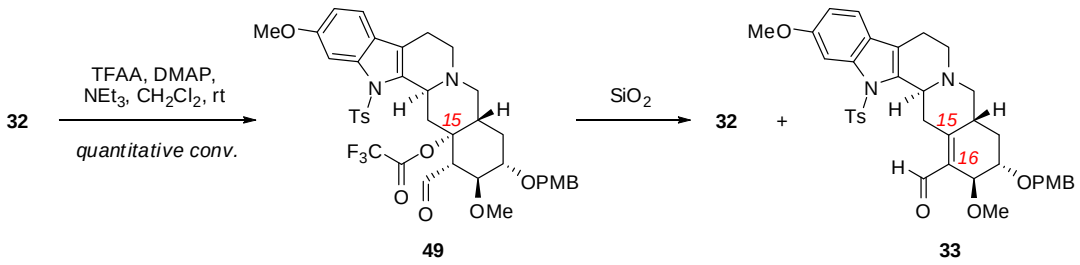

Scheme 2.16. Synthesis of C15 Trifluoroacetate and a SiO_2-Promoted Elimination

2.6.3. Re-evaluation of an Enal Hydrogenation

Through optimization studies, it was found that treatment of crude C15 trifluoroacetate **49** with diisopropylamine induced a regioselective elimination to afford enal **33** in 63% yield from aldol adduct **32** (Scheme 2.17).[28]

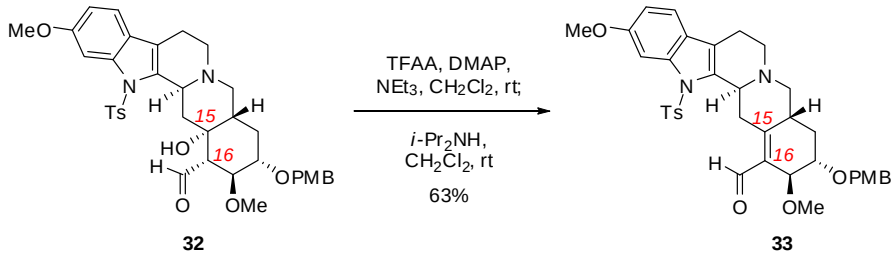

Scheme 2.17. Optimized Synthesis of Conjugated Enal **33**

Hydrogenation of enal **33** with PtO_2 occurred only at high hydrogen pressures (14-48 atm) and afforded products **34** and **50**–**52**, corresponding to reduction of the C15-C16 olefin, the carbonyl group, and the aromatic ring of the PMB ether (Scheme 2.18). After subjecting the crude hydrogenation product mixture to Dess–Martin oxidation

[28] The elimination of the C15 trifluoroacetate **49** was faster with secondary amines than with tertiary amine bases, suggesting that enamine intermediates may be involved. Based on this possibility, we attempted a cascade aldol-elimination sequence from keto-aldehyde **31**. However, enal **33** was formed as a minor product and in a 1:14 ratio with the aldol adduct **32**, so we moved forward with the two-step sequence.

conditions, saturated aldehyde **34** was obtained as a single diastereomer and in 40% yield over the two steps.[29]

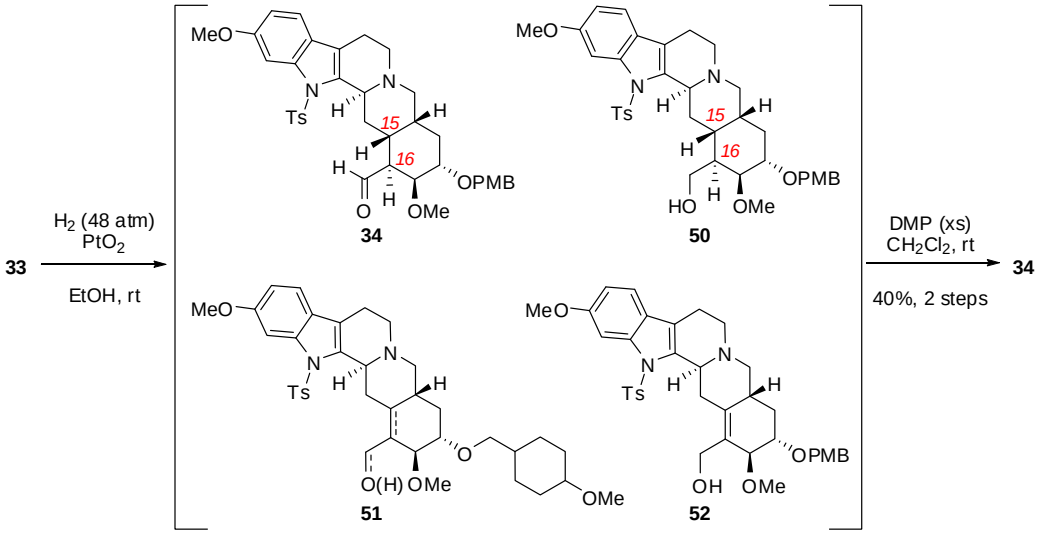

Scheme 2.18. PtO_2-Catalyzed Hydrogenation of Conjugated Enal **33**

The stereochemical outcome of olefin hydrogenation was determined by analysis of the corresponding methyl ester (**53**), obtained by subjecting aldehyde **34** to Pinnick oxidation conditions followed by treatment of the crude acid with diazomethane (Scheme 2.19). NMR studies performed on this intermediate led to the determination that it had the desired C15 configuration but the incorrect C16 configuration. The relevant nOe data from the proton at C16 of methyl ester **53** are summarized in Scheme 2.19. PMB- and Ts-protecting group removals were carried out with DDQ and magnesium in MeOH, respectively, to access 16-*epi*-methyl reserpate (**54**).

[29] Hydrogenation product **34** was equivalent to the one Meredeth McGowan had previously obtained (Scheme 2.10).

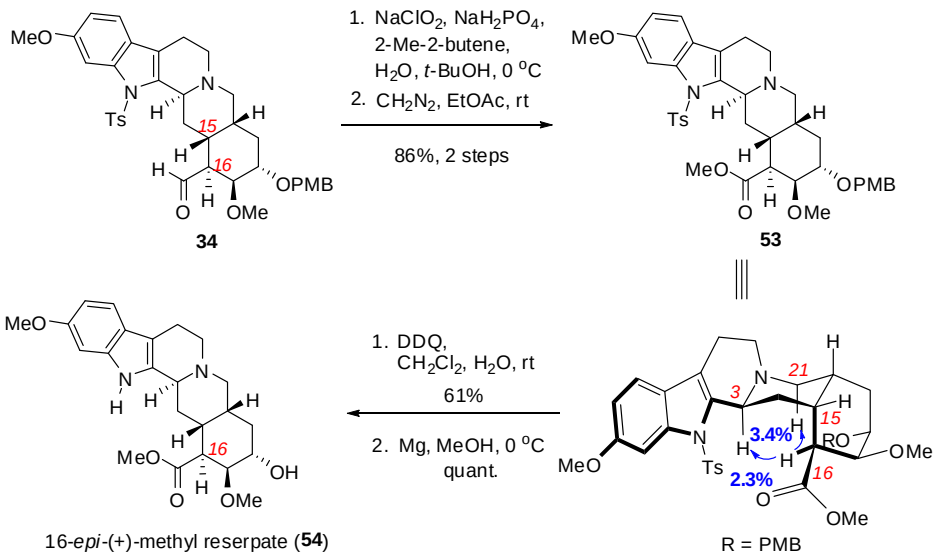

Scheme 2.19. Stereochemical Determination of the Enal Hydrogenation

A plausible explanation for this outcome is that hydrogen delivery occurred from the top face of the olefin, as predicted, to generate saturated aldehyde **55** but that unfavorable steric interactions between the C16 substituent and the tosyl protecting group drove epimerization at C16 (Scheme 2.20).

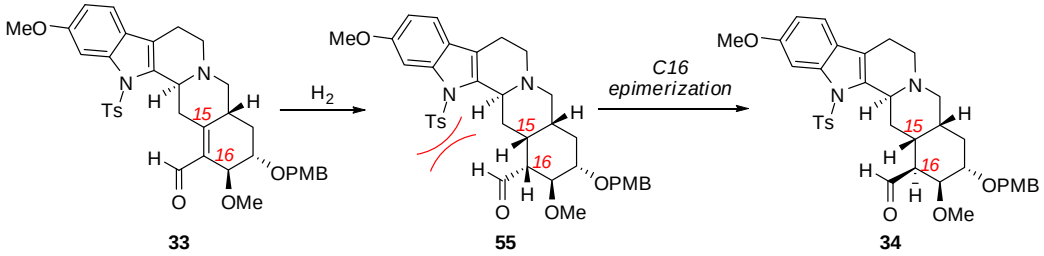

Scheme 2.20 Potential Explanation for the Hydrogenation Outcome

Based on this hypothesis, we proposed two strategies to prevent epimerization during hydrogenation of a C15-C16 olefin (Scheme 2.21). The first strategy involved the removal of the tosyl protecting group. It was proposed that if unfavorable steric interactions between the tosyl group and the C16 aldehyde substituent were responsible

for epimerization, then hydrogenation of the free indole substrate may proceed without epimerization (Scheme 2.22A). The second strategy involved modification of the C16 substituent to either an ester or primary alcohol, such that hydrogenation would generate a product that was less prone to epimerization at C16.

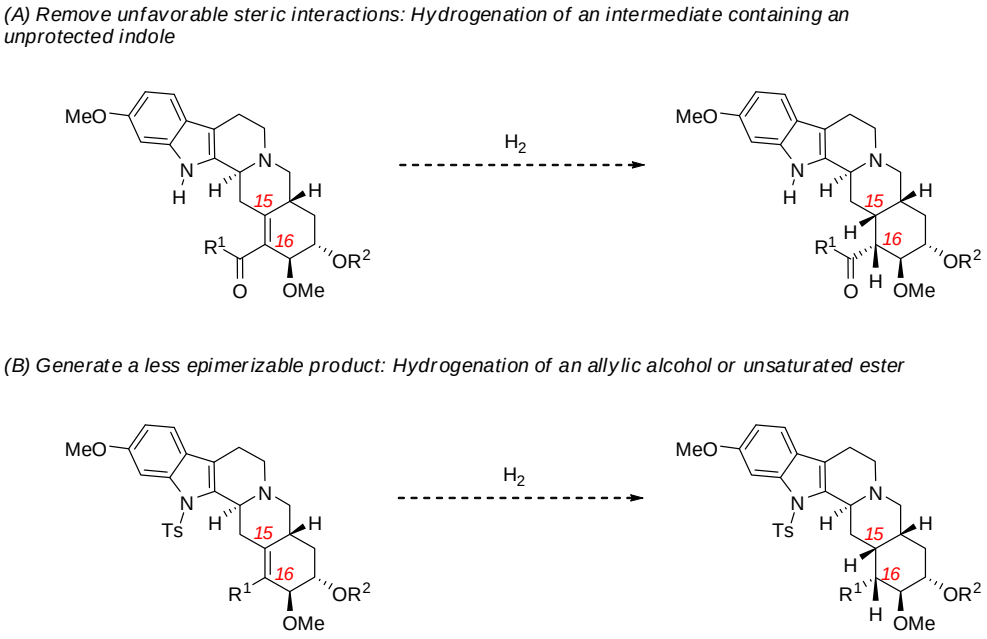

Scheme 2.21. Strategies for Preventing C16 Epimerization

2.6.4. Hydrogenation of an Unprotected Indole Intermediate

Through experimentation, we found that the unprotected methoxy indole of related intermediates was unstable to even mildly oxidative conditions. This observation suggested that oxidative manipulations, such as installation of the C16 ester and removal of the PMB protecting group should take place prior to removal of the tosyl group. Thus, we targeted unsaturated ester **58** as a hydrogenation substrate to evaluate our first strategy. Pinnick oxidation of aldehyde **32** to the corresponding carboxylic acid, followed by esterification with diazomethane provided methyl ester **56** (Scheme 2.22). The C15

alcohol of intermediate **56** proved very resistant to derivatization, and as with aldol adduct **32**, trifluoroacetylation was found to be the most effective strategy. Derivatization of **56** to a C15 tertiary trifluoroacetate was accomplished with *n*-BuLi and trifluoroacetic anhydride, and the crude product was subjected to DBU in refluxing toluene to effect a regioselective elimination forming enoate **57**.[30] The PMB protecting group was cleaved using DDQ, and the tosyl protecting group was removed using a 5% sodium/mercury amalgam to provide the free indole **58**.

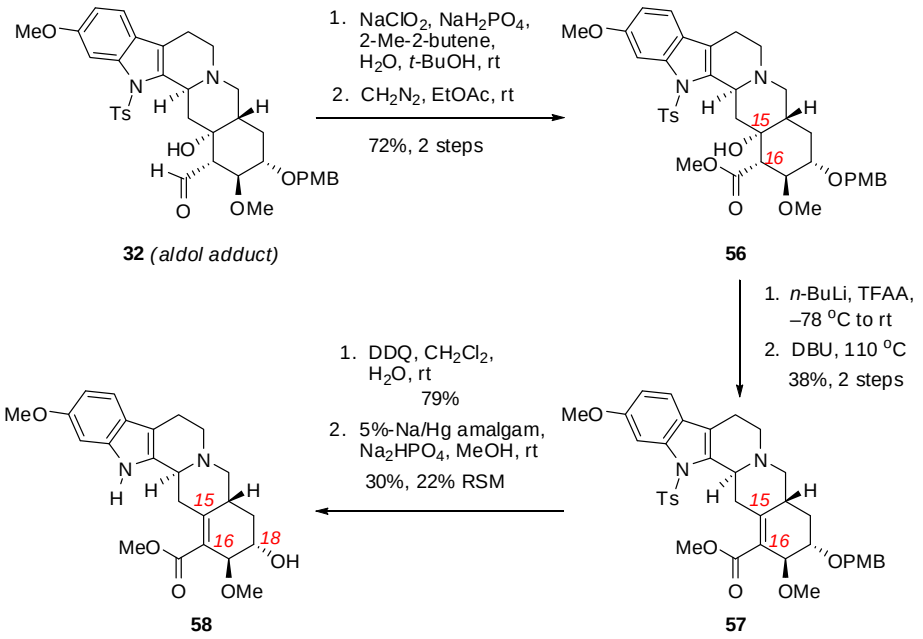

Scheme 2.22. Synthesis of Enoate **58**

C15-C16 olefin **58** underwent hydrogenation with PtO_2 at 1 atm of hydrogen pressure to afford saturated ester **59** (Scheme 2.23).[31] The stereochemical outcome of the hydrogenation was determined through NMR analysis of free indole **59**, and by comparing its spectrum to those of saturated ester **54** (obtained through the enal

[30] Attempted radical deoxygenation of the tertiary trifluoroacetate under conditions reported by Jang (Refs.25a,b) or Myers (Ref.25c) resulted in decomposition, hydrolysis, and elimination products.

[31] Although a diastereomeric ratio was not measured on the crude hydrogenation product, the high yield of hydrogenation product indicates that the dr must at least be 4:1 in favor of the observed product **59**.

hydrogenation, Scheme 2.19), and methyl reserpate (**10**), obtained through saponification of a commercially available sample of (–)-reserpine. Through this analysis we determined that hydrogenation occurred with undesired selectivity from the bottom face of intermediate **58**, providing the incorrect configurations at both C15 and C16.

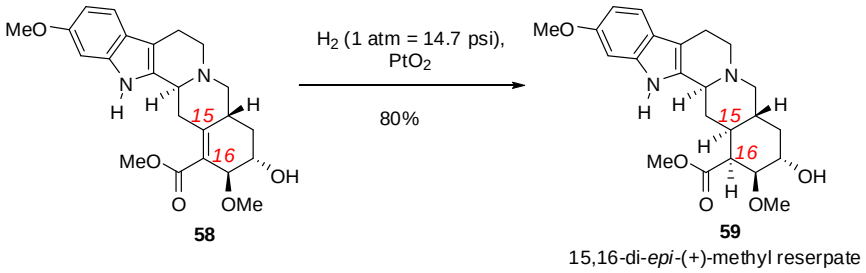

Scheme 2.23. Hydrogenation of **58** Occurs with Undesired Facial Selectivity

In comparing the two hydrogenation approaches and the outcomes, we determined that the facial selectivity of hydrogen delivery was influenced by the conformation of the intermediate, and this in turn was dependent on the presence or absence of an indole protecting group (Scheme 2.24). Substrate **33** containing a protected indole underwent hydrogenation exclusively from its top face, as the bottom face appears to be shielded by the bulky tosyl protecting group. In contrast, unprotected substrate **58**, which lacks this directing effect, underwent hydrogenation primarily from the bottom face of the olefin. These observations are in agreement with a series of hydrogenation studies done by Lounasmaa on tetracyclic indole-containing substrates.[32] Taking these results into consideration, we decided to move on to our second proposed endgame strategy and to carry out a hydrogenation in the presence of an indole protecting group and a C16 substituent that is unlikely to be susceptible to epimerization (Scheme 2.21B).

[32] a) Lounasmaa, M. *Tetrahedron* **1995**, *51*, 11892. b) Lounasmaa, M.; Jokela, R. *Tetrahedron* **1990**, *46*, 615.

We predicted that this strategy would allow for hydrogenation to occur with the desired facial selectivity and without C16 epimerization.

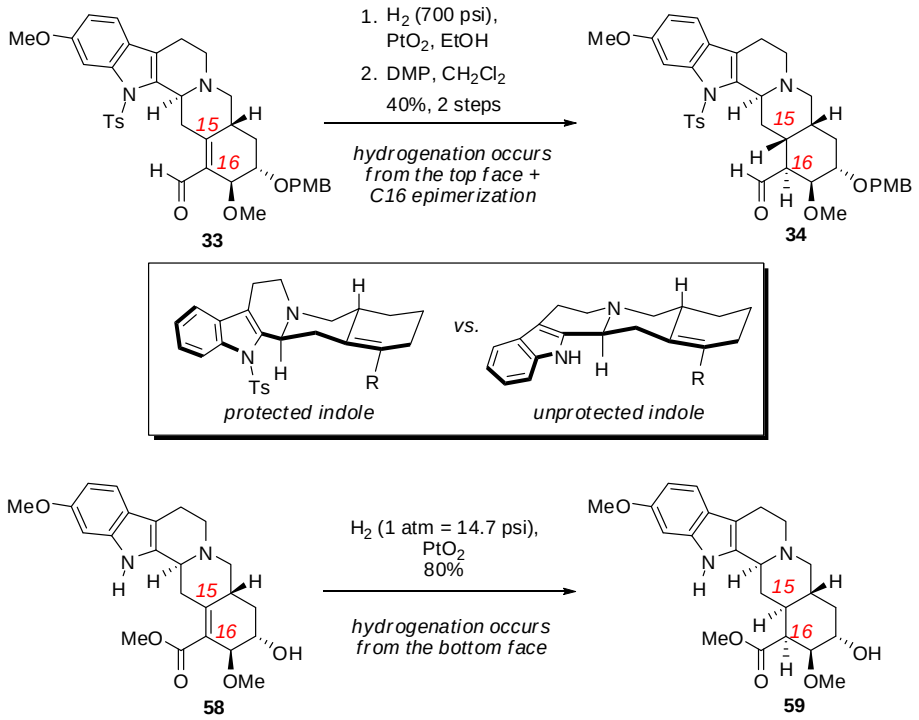

Scheme 2.24. Protecting-Group Dependent Hydrogenation Facial Selectivities

2.7. Completion of the Synthesis of (+)-Reserpine

We anticipated that allylic alcohol **52**, obtained through reduction of enal **33**, might be capable of coordinating to a homogeneous hydrogenation catalyst and thereby enable hydrogenation of the hindered C15-C16 olefin. Unfortunately, an evaluation of both homogeneous and heterogeneous hydrogenation catalysts was unfruitful, either returning unreacted alcohol **52** or resulting in reduction of the aromatic ring of the PMB ether (Scheme 2.25).

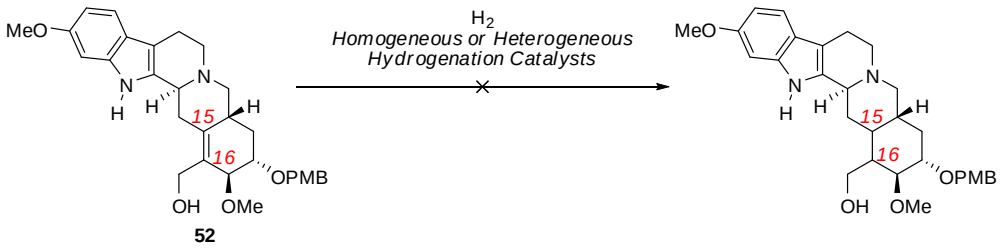

Scheme 2.25. Unsuccessful Attempts at Reducing Allylic Alcohol **52**

We therefore instead focused on hydrogenation of unsaturated ester **57**, obtained via elimination of a tertiary trifluoroacetate (Scheme 2.23), which maintains the PMB and Ts protecting groups. This olefin proved to be a particularly challenging hydrogenation substrate as it is hindered, tetrasubstituted, and electron-deficient. After an extensive evaluation of both homogeneous and heterogeneous catalytic systems under a range of conditions, cationic iridium complex **64**, bearing the noncoordinating BArF counteranion, was identified as uniquely effective in the reduction of the C15-C16 olefin of enoate **57** (Table 2.2).[33]

[33] a) Vazquez-Serrano, L. D.; Owens, B. T.; Buriak, J. M. *Inorg. Chim. Acta* **2006**, *359*, 2786. b) Wüstenberg, B.; Pfaltz, A. *Adv. Synth. Catal.* **2008**, *350*, 174.#

Table 2.2. Catalyst Screen for Hydrogenation of Enoate **57**

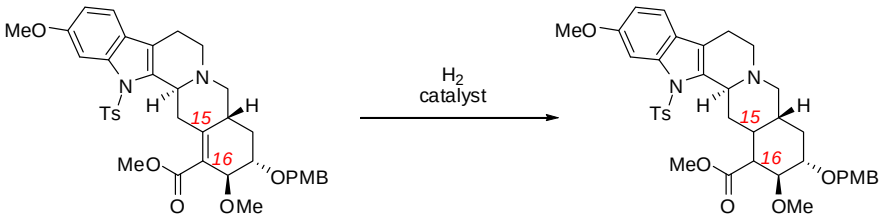

57 **60**

entry	catalyst	results
1	PtO_2	recovered starting material
2	Pd/C	recovered starting material
3	Raney Ni	recovered starting material
4	[Rh(DuPHOS)(COD)]BF_4 (**62**)	hydrogenation of the PMB ring
5	[Ir(PCy_3)(COD)]PF_6 (**63**)	recovered starting material
6	[Ir(PCy3)(COD)]BArF (**64**)	trace hydrogenation

Variation of the stoichiometry of enoate **57** to iridium complex **64** indicated that the catalytic use of **64** provided low amounts of conversion to the reduction product (Scheme Table 2.3, entries 1–2). However, hydrogenation with one full equivalent of complex **64** resulted in 54% conversion of **57** and proceeded with a significant degree of facial selectivity (6:1 dr), ultimately affording saturated ester **60** in 44% isolated yield (81% based on recovered olefin **57**) (entry 3).[34] The use of super stoichiometric amounts of iridium complex **64** offered a slight increase in yield but at the expense of recovered enoate (entry 4). The stereochemical outcome of the hydrogenation was determined by ^{1}H NMR analysis and indicated that the C15 and C16 stereogenic centers had been obtained in the correct configuration. The identity of saturated ester **60** was further confirmed by X-ray crystallographic analysis (Figure 2.2).

[34] Although improvements in the turnover of iridium hydrogenation catalysts have been accomplished through the formation of substrate amine salts or by the use of borate additives, these strategies were ineffective for the hydrogenation of **57** with **64**. For precedents, see: a) Trost, B. M.; Rudd, M. T. *Org. Lett.* **2003**, *5*, 1467. b) Maimone, T. J.; Shi, J.; Ashida, S. Baran, P. S. *J. Am. Chem. Soc.* **2009**, *131*, 17066.

Table 2.3. Loading Studies of Complex **64**

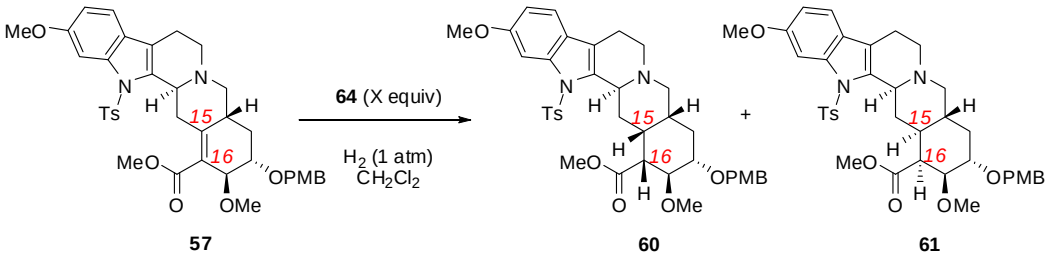

57 **60** *desired* **61**

Entry	X	Yield **A**	RSM	Yield **A** (brsm)	Yield **B**
1	0.01	<2	75	<5	<2
2	0.2	6	81	32	ND
3	1.0	44	46	81	4
4	2.0	51	31	74	ND

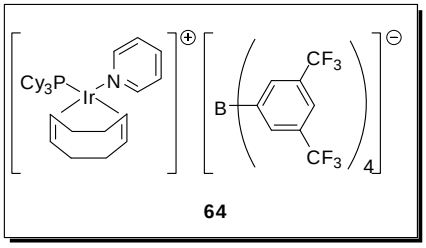

64

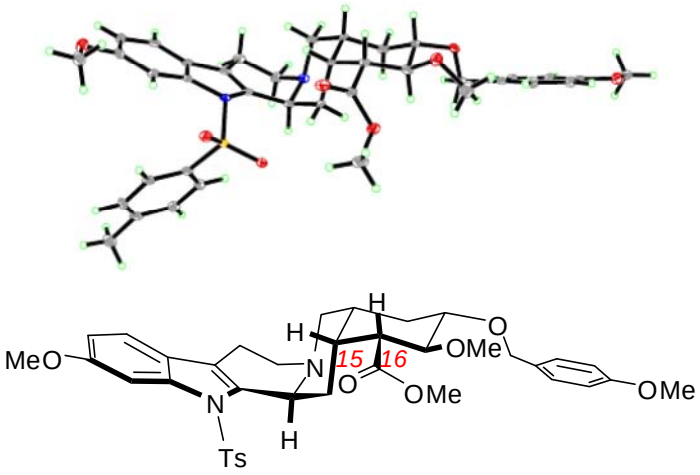

Figure 2.2. ORTEP Diagram of **60** Showing 50% Probability Displacement

With the fully elaborated pentacycle in hand, completion of the synthesis required only a global deprotection and installation of the trimethoxybenzoyl ester on the E-ring. Thus, treatment of **60** sequentially with TfOH and sodium/mercury amalgam resulted in cleavage of the PMB ether and tosyl protecting groups, respectively (Scheme 2.26).

Resulting C18 secondary alcohol **10** was esterified using conditions reported by Stork to deliver reserpine ((+)-**1**).[5q]

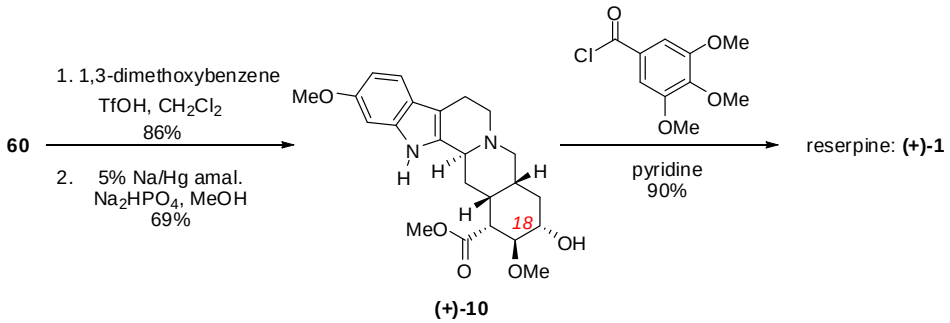

Scheme 2.26. Completion of the Synthesis of (+)-Reserpine

2.8. Conclusions

The enantioselective total synthesis of reserpine was accomplished in 19 steps in the longest linear sequence from racemic epoxide **20** (Scheme 2.27). The convergent approach relied on chiral catalysis to provide access to coupling component **19** and to address the historically problematic installation of the C3 stereogenic center. The insights we gained about substrate-controlled diastereoselectivity in reactions performed on highly functionalized tetracyclic and pentacyclic intermediates guided us to pursue a diastereoselective hydrogenation that enabled completion of the synthesis. Furthermore, through this process, we were able to identify synthetic routes to access intermediates corresponding to two unnatural diastereomers of (+)-methyl reserpate: 16-*epi*-(+)-methyl reserpate (**54**) and 15,16-di-*epi*-(+)-methyl reserpate (**59**).

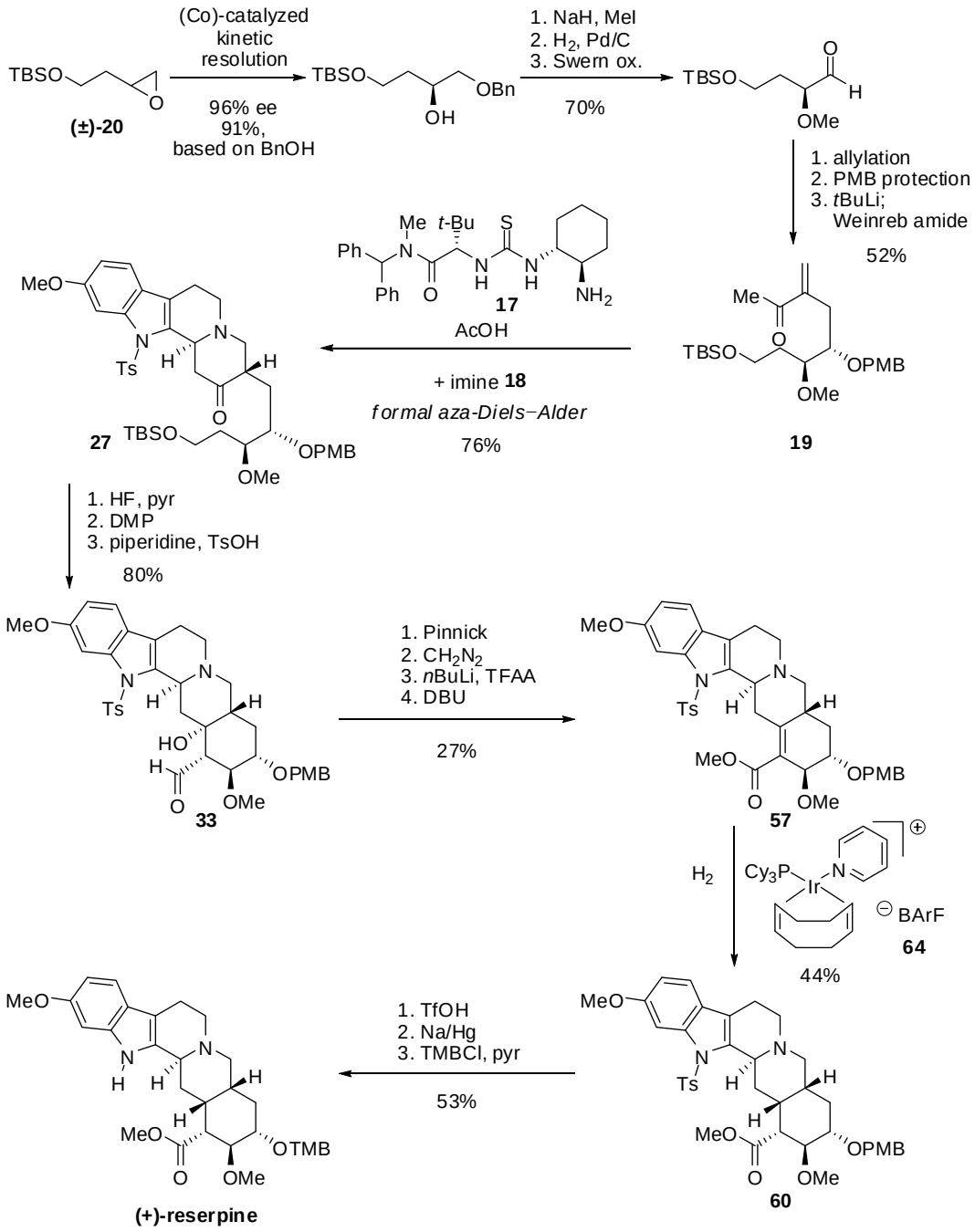

Scheme 2.27. Synthetic Route to (+)-Reserpine

2.9. Experimental Section

A. General Information.

Unless otherwise noted, all reactions were performed under a positive pressure of anhydrous nitrogen or argon in flame- or oven-dried glassware. Moisture- and air-sensitive reagents were dispensed using oven-dried stainless steel syringes or cannulae and were introduced to reaction flasks through rubber septa. Reactions conducted below ambient temperature were cooled by external baths (dry ice/acetone for –78 ^{o}C and ice/water for 0 ^{o}C). Reactions conducted above ambient temperature were heated by a silicone oil bath.

Analytical thin layer chromatography (TLC) was performed on glass plates pre-coated with silica 60 F_{254} plates, 0.25 mm). Visualization was carried out by exposure to a UV-lamp (short wave 254 nm, long wave 365 nm), and by heating after staining the plate with a ceric ammonium molybdate or a potassium permanganate solution. Extraction and chromatography solvents were reagent or HPLC grade and were used without further purification. Flash chromatography was carried out over silica gel (60 Å, 230–400 mesh) from EM Science or Davisil^{TM}. Where indicated, chromatography was conducted on a Biotage Isolera automated chromatography system.

Materials. Commercial reagents and solvents were used with the following exceptions: tetrahydrofuran, diethyl ether, toluene, dichloromethane, acetonitrile, and methanol employed as reaction solvents were dried by passage through columns of activated alumina. Pyridine and triethylamine were distilled from calcium hydride at 760 torr prior

to use. The Dess–Martin Periodinane was prepared according to known procedures.[35] Diazomethane was prepared as a 0.5 M solution in ether according to the known procedure.[36] 2-bromoallyltrimethylsilane was prepared according to the reported procedure.[37] Epoxide **(±)-20** was prepared according to the reported procedure and was distilled from calcium hydride prior to use.[38] Oligomeric cobalt salen catalyst (*R*, *R*)-**23** was prepared according to the reported procedure and stored over calcium sulfate in a –78 ^{o}C freezer.[12] Imine **18**, catalyst **17**, and catalyst *ent*-**17**, were prepared according to the reported procedures.[10a] Chloroform-d was dried over 3Å MS prior to use. Iridium complex **64** was prepared according to the reported procedure and was stored in a glove box under a N_2 atmosphere.[33a]

Instrumentation. Proton nuclear magnetic resonance (^{1}H NMR) spectra and carbon nuclear magnetic resonance (^{13}C NMR) spectra were recorded on a Varian Mercury-400 (400MHz), Inova-500 (500MHz), or an Inova-600 (600MHz) spectrometer at 23 ^{o}C. Chemical shifts for protons are reported in parts per million (ppm, δ scale) downfield from tetramethylsilane and are referenced to residual protium in the NMR solvent ($CHCl_3$: 7.26 ppm; C_6H_6: 7.16 ppm). Chemical shifts for carbons are reported in parts per million (ppm, δ scale) downfield from tetramethylsilane and are referenced to the NMR solvent ($CDCl_3$: 77.16 ppm). Data are represented as follows: chemical shift, multiplicity (s = singlet, d = doublet, t = triplet, q = quartet, m = multiplet, br = broad,

[35] Boeckman, R. K., Jr.; Shao, P.; Mullins, J. J. *Org. Synth.* **2000**, *77*, 141.

[36] Sigma Aldrich, 2003, "AL-180: Diazald, MNNG and Diazomethane Generators." http://www.sigmaaldrich.com/aldrich/bulletin/AL-180.pdf

[37] Trost, B. M.; Grese, T. A.; Chan, D. M. T. *J. Am. Chem. Soc.* **1991**, *113*, 7350.

[38] Ficini, J.; Barbara, C.; Desmaële, D.; Ourfelli, O. *Heterocycles* **1987**, *25*, 329.

app = apparent), integration, and coupling constant (*J*) in Hertz (Hz). Infrared (IR) spectroscopy was performed on the neat compounds on a Brucker Tensor 27 FT-IR Spectrometer using OPUS software. Data are represented as follows: frequency of absorption (cm^{-1}), intensity of absorption (s = strong, m = medium, w = weak). Mass spectra were obtained on an Agilent 1200 series 6120 Quadrupole LC/MS. Optical rotation data were collected using either a 2-mL cell with a 1 dm path length or a 1-mL cell using a 0.5 dm path length on a Jasco P-2000 polarimeter and are reported as $[\alpha]_D^{23}$ (concentration in grams/100 mL solvent). Reported rotations are the average of 3–5 measurements per sample.

B. Experimental procedures and characterization data.

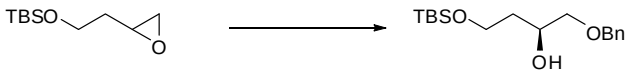

(±)-20 **21**

96% ee

(*S*)-1-(benzyloxy)-4-(*tert*-butyldimethylsilyloxy)butan-2-ol (**21**)

A 50-mL round-bottom flask was charged with a stir bar, epoxide (±)-**20** (10.0 g, 49.7 mmol, 1 equiv.), CH_3CN (2.4 mL), and anhydrous BnOH (2.32 mL, 22.4 mmol, 0.45 equiv.). The flask was cooled to 0 ºC, and (*R*,*R*)-**23** (185 mg, 0.227 mmol, 0.45 mol % based on Co) was added in one portion. The flask was sealed with a plastic cap and allowed to stir at 4 ºC for 96 h, at which point pyridinium *para*-toluenesulfonate (PPTS) (60 mg, 0.240 mmol) was added in one portion. The reaction mixture was filtered through a silica gel plug, eluting with Et_2O (400 mL). The filtrate was concentrated in vacuo to provide a dark orange oil which was purified immediately via flash

chromatography (silica gel, Biotage, 10% Et_2O in hexanes) to provide the desired secondary alcohol **21** as a clear oil (6.28 g, 20.2 mmol, 41% yield). R*f* = 0.44 (25% EtOAc in hexanes); ^{1}H NMR (500 MHz, $CDCl_3$) δ: 7.24 – 7.42 (m, 5 H) 4.58 (d, *J*=12.4 Hz, 1 H) 4.55 (d, *J*=11.9 Hz, 1 H) 4.03 (ddd, *J*=11.40, 6.90, 4.60 Hz, 1 H) 3.86 (m, 1 H) 3.79 (m, 1 H) 3.48 (dd, *J*=9.77, 4.39 Hz, 1 H) 3.43 (dd, *J*=8.79, 6.84 Hz, 1 H) 3.17 (br. s., 1 H) 1.70 (m, 2 H) 0.90 (s, 9 H) 0.06 (s, 6 H); ^{13}C NMR (126 MHz, $CDCl_3$) δ: 138.13, 128.36 (2C), 127.69 (2C), 127.64, 74.36, 73.32, 69.63, 61.32, 35.42, 25.85 (3C), 18.14, –5.52, –5.55; FTIR (neat, cm^{-1}); 3400(br m), 2953(m), 2928(m), 2857(m), 1497(w), 1471(w), 1463(w), 1389(w), 1362(w), 1253(m), 1205(w), 1090(s), 1005(m), 908(m), 833(s), 775(s), 733(s), 697(s), 663(m); LRMS (APCI) 311.2 $[M + H]^+$; $[\alpha]^{23}_D$ –1.2 (*c* 1.77, $CHCl_3$).

To assess the enantiomeric purity, the epoxide-opened product was elaborated to the corresponding diol in the following manner: Silyl ether **21** (22.7 mg, 0.073 mmol, 1 equiv.) was dissolved in THF (0.47 mL) and TBAF (1 M in THF, 0.152 mL, 2.1 equiv.) was added at 0 ºC. The solution was allowed to come to rt and stir 1 h. The reaction was then diluted with CH_2Cl_2 (5 mL) and the organic layer was washed with H_2O (3 x 5 mL), dried over Na_2SO_4, filtered, and concentrated in vacuo. The residue was purified by flash chromatography to provide the diol as a clear oil. The enantiomeric excess was determined to be 96% by chiral SFC analysis (OD-H, 5% MeOH, 4.0 ml/min) t_R(minor) = 6.88 min, t_R(major) = 7.52 min.

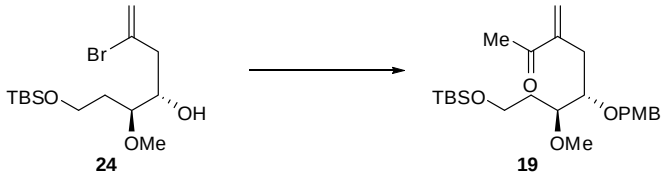

(5*S*,6*S*)-8-(*tert*-butyldimethylsilyloxy)-6-methoxy-5-(4-methoxybenzyloxy)-3-methyleneoctan-2-one (**19**)

Vinyl bromide **24** (286 mg, 0.60 mmol, 1 equiv.) was azeotroped from benzene twice and placed on high vacuum 2 h in a 50-mL round-bottomed flask. Et_2O (12 mL) was then added under N_2, and the flask was cooled to –78 ºC. *Tert*-butyllithium (741 µL of a 1.7 M solution in pentane, 1.26 mmol, 2.1 equiv.) was added dropwise over 5 min. The yellow solution was stirred for 30 min, after which *N*-methoxy-*N*-methylacetamide (138 µL, 0.90 mmol, 1.5 equiv.) was added. The reaction was stirred for an additional 1.5 h at –78 ºC, and was then quenched by addition of H_2O (5 mL) and immediately warmed to rt. The reaction mixture was diluted with H_2O (10 mL), and the aqueous layer was extracted with EtOAc (2 x 15 mL). The combined organics were dried over Na_2SO_4, filtered, and concentrated in vacuo. The resultant oil was purified by flash chromatography (silica gel, 0 to 15% EtOAc in hexanes) to provide **19** as a clear oil (199 mg, 0.46 mmol, 76% yield). R*f* = 0.19 (15% EtOAc in hexanes); ^{1}H NMR (600 MHz, $CDCl_3$) δ: 7.21 (d, *J*=8.49 Hz, 2 H) 6.84 (d, *J*=8.49 Hz, 2 H) 6.03 (s, 1 H) 5.87 (s, 1 H) 4.48 (d, *J*=11.42 Hz, 1 H) 4.40 (d, *J*=11.42 Hz, 1 H) 3.79 (s, 3 H) 3.52 – 3.69 (m, 3 H) 3.43 (dt, *J*=8.42, 4.14 Hz, 1 H) 3.39 (s, 3 H) 2.64 (ddd, *J*=13.55, 4.61, 0.88 Hz, 1 H) 2.37 (dd, *J*=13.62, 8.35 Hz, 1 H) 2.28 (s, 3 H) 1.78 (dddd, *J*=14.06, 8.20, 5.86, 4.10 Hz, 1 H) 1.61 (ddt, *J*=13.79, 8.67, 5.13, 5.13 Hz, 1 H) 0.85 – 0.90 (m, 9 H) 0.03 (s, 3 H) 0.02 (s, 3 H); ^{13}C NMR (126 MHz, $CDCl_3$) δ: 199.65, 159.10, 146.09, 130.72, 129.71 (2C) 127.52, 113.59 (2C) 77.89, 76.81, 71.90, 59.46, 58.17, 55.22, 32.66, 31.89, 25.91 (3C), 25.85,

18.21, –5.35, –5.41; IR 2949(m), 2929(s), 2856(m), 1678(s), 1613(m), 1586(w), 1464(m), 1441(w), 1362(m), 1324(w), 1032(w), 1247(s), 1090(s), 1036(m), 938(m), 833(s), 775(s), 662(m); LRMS (ESI) 459.2 $[M + Na]^+$; $[\alpha]^{23}_D$ –16.1 (*c* 3.03, $CHCl_3$).

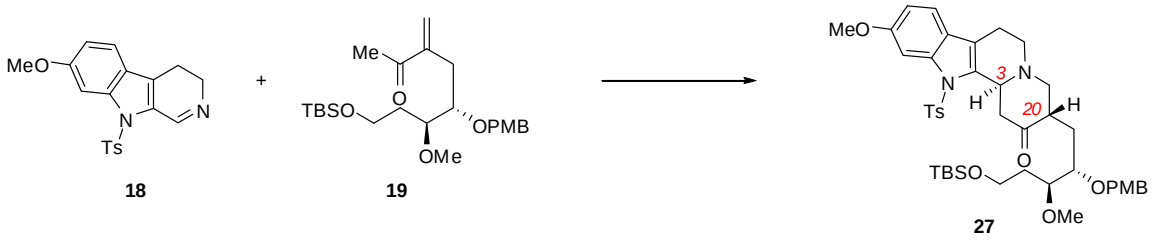

(3*S*,12b*S*)-3-((2*S*,3*S*)-5-(*tert*-butyldimethylsilyloxy)-3-methoxy-2-(4-methoxybenzyloxy)pentyl)-10-methoxy-12-tosyl-1,3,4,6,7,12b-hexahydroindolo[2,3-a]quinolizin-2(12H)-one (**27**)

An oven-dried 25-mL round-bottom flask with stir-bar was charged with enone **19** (788 mg, 1.80 mmol, 1.2 equiv.), imine **18** (533 mg, 1.50 mmol, 1 equiv.), and aminothiourea **17** (140 mg, 0.30 mmol, 20 mol %). The flask was placed under N_2 and toluene (4.5 mL) was added, followed by AcOH (17.2 µl, 0.30 mmol, 20 mol %) in one portion. The reaction was allowed to stir at rt 4.5 d, and then at 45 ^oC for 2 h. Analysis of the crude reaction mixture by ^1H NMR (comparison of a combination of C3 and PMB Bn signals) showed a 11.5:1.0:1.8:0 diastereomeric ratio of **27**:**28**:**29**:**30**. The crude reaction mixture was directly purified by flash chromatography (silica gel, Biotage, 0 – 50% EtOAc in hexanes gradient) to provide the desired diastereomer as a pale yellow solid (909 mg, 1.15 mmol, 76% yield). R*f* = 0.19 (50% EtOAc in hexanes); ^1H NMR (399 MHz, $CDCl_3$) δ 7.65 (d, *J*=2.20 Hz, 1 H, C12) 7.47 (d, *J*=8.42 Hz, 2 H, Ts) 7.17 – 7.25 (m, 3 H, PMB, C10) 7.10 (d, *J*=7.68 Hz, 2 H, Ts) 6.77 – 6.91 (m, 3 H, PMB, C9) 4.61 (d, *J*=11.34 Hz, 1 H, PMB Bn) 4.51 (dd, *J*=11.34, 2.20 Hz, 1 H, C3) 4.31 (d, *J*=11.34 Hz, 1 H, PMB Bn)

3.87 (s, 3 H, PMB OMe) 3.85 (ddd, *J*=10.61, 4.76, 2.56 Hz, 1 H, C18) 3.75 (dd, *J*=7.87, 4.57 Hz, 2 H, C**H**$_2$OTBS) 3.70 (s, 3 H, **Me**O) 3.54 (ddd, *J*=9.51, 4.57, 2.38 Hz, 1 H, C17) 3.50 (s, 3 H, C17 **Me**O) 3.31 (dd, *J*=13.17, 5.86 Hz, 1 H, C21) 3.10 – 3.20 (m, 2 H, C14, C5) 2.94 (t, *J*=12.44 Hz, 1 H, C21) 2.78 – 2.86 (m, 1 H, C5) 2.68 – 2.78 (m, 3 H, C6(2), C20) 2.39 (t, *J*=12.26 Hz, 1 H, C14) 2.28 (s, 3 H, Ts) 2.05 (ddd, *J*=13.80, 9.15, 2.38 Hz, 1 H, C19) 1.85 (dtd, *J*=14.00, 7.70, 7.70, 2.60 Hz, 1 H, C16) 1.58 (ddt, *J*=14.00, 9.38, 4.62, 4.62 Hz, 1 H, C16) 1.04 (ddd, *J*=13.80, 10.30, 3.40 Hz, 1 H, C19) 0.90 - 0.93 (m, 9 H, TBS) 0.08 (s, 3 H, TBS) 0.08 (s, 3 H, TBS); ^{13}C NMR (100 MHz, $CDCl_3$) δ 208.55, 159.21, 158.02, 144.63, 138.37, 134.52, 134.41, 130.76, 129.83 (2C), 129.61 (2C), 126.29 (2C), 123.97, 118.92, 118.81, 113.78 (2C), 112.73, 100.33, 78.22, 76.77, 72.43, 61.10, 59.59, 58.95, 58.37, 55.79, 55.17, 45.17, 44.56, 43.00, 32.82, 26.86, 25.94 (3C), 22.25, 21.49, 18.25, –5.29, –5.37; IR 2592(m), 2927(m), 2856(m), 1706(s), 1612(m), 1582(w), 1513(m), 1493(m), 1463(m), 1440(w), 1364(s), 1304(w), 1248(s), 1172(s), 1145(m), 1088(s), 1035(m), 975(m), 834(s), 775(m), 674(s), 626(m); LRMS (APCI) 791.4 $[M + H]^+$; $[\alpha]^{24}_D$ +65.8 º (*c* 1.11, $CHCl_3$).

The 1-D NOESY spectrum (500 MHz, $CDCl_3$) displayed the following nOe transfers:

Irradiation of C14 (δ 2.39): 0.3% C3 (δ 4.51),

1.2% C20 (δ 2.75)

Irradiation of C3 (δ 4.51): 0.9% Ts (δ 7.47), 1.7% C14 (δ 3.15),

1.9% C21 (δ 2.94)

Irradiation of C21 (δ 2.94): 1.2% C3 (δ 4.51)

Irradiation of C21 (δ 3.31): 2.6% C5 (δ 2.81), 4.5% C20 (δ 2.74)

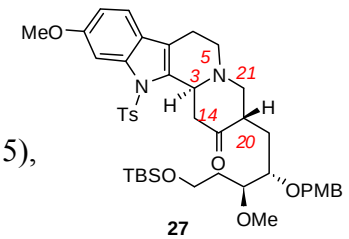

27

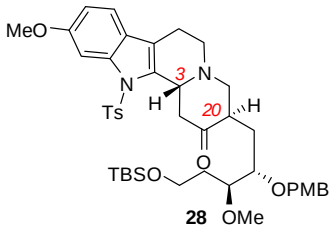

28

(3*R*,12b*R*)-3-((2*S*,3*S*)-5-(*tert*-butyldimethylsilyloxy)-3-methoxy-2-(4-methoxybenzyloxy)pentyl)-10-methoxy-12-tosyl-1,3,4,6,7,12b-hexahydroindolo[2,3-a]quinolizin-2(12H)-one (**28**)

R*f* = 0.28 (50% EtOAc in hexanes); ^{1}H NMR (500 MHz, $CDCl_3$) δ: 7.65 (d, *J*=2.29 Hz, 1 H) 7.48 (d, *J*=8.24 Hz, 2 H) 7.30 (d, *J*=8.24 Hz, 2 H) 7.20 (d, *J*=8.24 Hz, 1 H) 7.10 (d, *J*=8.24 Hz, 2 H) 6.88 (d, *J*=8.24 Hz, 2 H) 6.85 (dd, *J*=8.47, 2.06 Hz, 1 H) 4.63 (d, *J*=11.90 Hz, 1 H) 4.49 (m, 2 H) 3.87 (s, 3 H) 3.80 (s, 3 H) 3.69 (td, *J*=9.27, 5.27 Hz, 1 H) 3.62 – 3.66 (m, 1 H) 3.60 (dt, *J*=8.59, 4.64 Hz, 1H) 3.54 (dt, *J*=8.47, 4.01 Hz, 1 H) 3.39 (s, 3 H) 3.21 – 3.34 (m, 2 H) 3.06 – 3.16 (m, 1 H) 2.89 (t, *J*=12.36 Hz, 1 H) 2.65 – 2.83 (m, 4 H) 2.46 – 2.58 (dd, *J*=12.4, 11.8 Hz, 1 H) 2.29 (s, 3 H) 2.17 (ddd, *J*=14.19, 8.70, 5.04 Hz, 1 H) 1.74 – 1.88 (m, 1 H) 1.55 – 1.69 (m, 1 H) 1.32 – 1.46 (m, 1 H) 0.90 (s, 9 H) 0.05 (s, 3 H) 0.04 (s, 3 H); ^{13}C NMR (126 MHz, $CDCl_3$) δ ppm 208.31, 159.39, 158.22, 144.78, 138.68, 134.81, 134.53, 130.98, 129.95 (2C), 129.75 (2C), 126.53 (2C), 124.21, 119.37, 119.08, 113.92 (2C), 112.98, 100.62, 78.22, 74.89, 71.33, 60.14, 59.61, 59.00, 58.55, 56.00, 55.41, 45.45, 45.25, 43.22, 32.95, 26.31, 26.10 (3C), 22.49, 21.68, 18.41, –5.15, –5.21; IR 3008 (w), 2928 (m), 2856 (m), 1708 (m), 1613 (m), 1513 (m), 1494 (w), 1367 (s), 1250 (s), 1216 (w), 1173 (s), 1147 (m), 1090 (s), 1037 (m), 836 (s), 759 (s); LRMS (APCI) 791.4 $[M + H]^+$; $[\alpha]^{24}_D$ +16.9 º (*c* 0.29, $CHCl_3$).

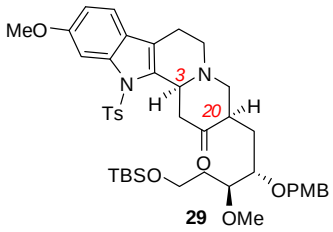

(3*R*,12b*S*)-3-((2*S*,3*S*)-5-(*tert*-butyldimethylsilyloxy)-3-methoxy-2-(4-methoxybenzyloxy)pentyl)-10-methoxy-12-tosyl-1,3,4,6,7,12b-hexahydroindolo[2,3-a]quinolizin-2(12H)-one (**29**)

R*f* = 0.36 (50% EtOAc in hexanes); ^{1}H NMR (600 MHz, $CDCl_3$) δ:7.60 (d, *J*=2.20 Hz, 1 H, C12) 7.44 (d, *J*=8.49 Hz, 2 H, Ts) 7.25 (d, *J*=8.49 Hz, 2 H, PMB) 7.12 (d, *J*=8.49 Hz, 1 H, C10) 7.08 (d, *J*=8.35 Hz, 2 H, Ts) 6.86 (d, *J*=8.64 Hz, 2 H, PMB) 6.81 (dd, *J*=8.49, 2.34 Hz, 1 H, C9) 4.43 (d, *J*=10.84 Hz, 1 H, PMB Bn) 4.32 (d, *J*=10.69 Hz, 1 H, PMB Bn) 4.04 (dd, *J*=11.10, 2.40 Hz, 1 H, C3) 3.86 (s, 3 H, PMB **Me**O) 3.78 (s, 3 H, **Me**O) 3.62 – 3.73 (m, 2 H, C18, C**H**HOTBS) 3.51 – 3.59 (m, 2 H, CH**H**OTBS, C17) 3.40 (s, 3 H, C17 **Me**O) 3.36 (ddd, *J*=14.57, 2.78, 1.40 Hz, 1 H, C14) 2.98 (m, 2 H, C5, C21) 2.91 (dd, *J*=11.57, 2.78 Hz, 1 H, C5) 2.75 (m, 1 H, C6) 2.54 – 2.64 (m, 3 H, C14, C20, C21) 2.47 (dd, *J*=15.96, 2.30 Hz, 1 H, C6) 2.28 (s, 3 H, Ts) 2.07 (dt, *J*=14.31, 8.80 Hz, 1 H, C19) 1.76 – 1.85 (m, 2 H, C16, C19) 1.56 – 1.44 (m, 1 H, C16) 0.87 – 0.91 (m, 9 H, TBS) 0.04 (s, 3 H, TBS) 0.04 (s, 3 H, TBS); ^{13}C NMR (126 MHz, $CDCl_3$) δ: 210.75, 159.13, 157.97, 144.48, 139.42, 134.90, 133.39, 130.48, 129.97 (2C) 129.23 (2C) 126.59 (2C) 124.57, 122.59, 118.83, 113.69 (2C) 112.92, 101.18, 77.17, 75.89, 71.30, 59.53, 59.33, 58.54, 58.32, 55.81, 55.24, 49.90, 48.26, 46.43, 32.51, 32.03, 25.93 (3C) 22.90, 21.52, 18.25, –5.31, –5.41; IR 2929 (m), 2857 (m), 1709 (m), 1613 (m), 1514 (m), 1368 (s), 1305 (w), 1249 (s), 1216 (s), 1090 (s), 1038 (m), 971 (w), 836 (m), 759 (s); LRMS (APCI) 791.4 $[M + H]^+$; $[\alpha]^{24}_D$ +38.6 º (*c* 1.72, $CHCl_3$).

The 1-D NOESY spectrum (500 MHz, $CDCl_3$) displayed the following nOe transfers:

Irradiation of C19 (δ 2.07): 3.0% C14 (δ 2.57),

2.3% C17 (δ 2.57)

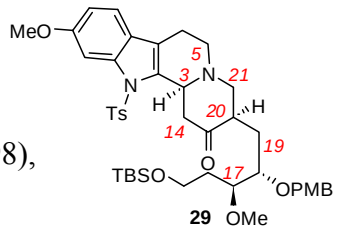

Irradiation of C3 (δ 4.04): 3.7% C14 (δ 3.36), 4.7% C5 (δ 2.98),

5.4% C21 (δ 2.58)

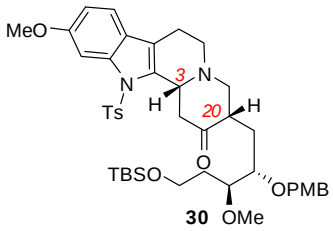

(3*S*,12b*R*)-3-((2*S*,3*S*)-5-(*tert*-butyldimethylsilyloxy)-3-methoxy-2-(4-methoxybenzyloxy)pentyl)-10-methoxy-12-tosyl-1,3,4,6,7,12b-hexahydroindolo[2,3-a]quinolizin-2(12H)-one (**30**)

R*f* = 0.61 (50% EtOAc in hexanes); ^{1}H NMR (600 MHz, $CDCl_3$) δ 7.63 (d, *J*=2.05 Hz, 1 H) 7.45 (d, *J*=8.49 Hz, 2 H) 7.32 (d, *J*=8.79 Hz, 2 H) 7.14 (d, *J*=8.49 Hz, 1 H) 7.08 (d, *J*=8.20 Hz, 2 H) 6.89 (d, *J*=8.49 Hz, 2 H) 6.82 (dd, *J*=8.35, 2.20 Hz, 1 H) 4.58 (d, *J*=10.84 Hz, 1 H) 4.48 (d, *J*=10.54 Hz, 1 H) 4.14 (dd, *J*=10.69, 2.49 Hz, 1 H) 3.87 (s, 3 H) 3.80 (s, 3 H) 3.69 (dd, *J*=7.76, 4.54 Hz, 2 H) 3.60 (ddd, *J*=10.40, 4.25, 2.34 Hz, 1 H) 3.48 – 3.52 (m, 1 H) 3.42 (dd, *J*=15.08, 3.08 Hz, 1 H) 3.33 (s, 3 H) 3.17 (dd, *J*=11.42, 5.86 Hz, 1 H) 3.02 (ddd, *J*=11.00, 4.69, 2.05 Hz, 1 H) 2.96 (dd, *J*=11.42, 3.22 Hz, 1 H) 2.74 – 2.85 (m, 2 H) 2.60 (td, *J*=10.54, 3.51 Hz, 1 H) 2.46 – 2.53 (m, 2 H) 2.29 (s, 3 H) 2.12 – 2.18 (m, 1 H) 1.79 – 1.84 (m, 1 H) 1.47 – 1.58 (m, 2H) 0.90 (s, 9 H) 0.05 (s, 3 H) 0.05 (s, 3 H); ^{13}C NMR (126 MHz, $CDCl_3$) δ: 210.99, 159.42, 158.24, 144.72, 139.62,

135.01, 133.61, 130.87, 130.04 (2C) 129.44 (2C) 126.75 (2C) 124.75, 122.80, 119.08, 114.00 (2C) 113.18, 101.40, 77.51, 76.45, 72.61, 59.76, 59.54, 59.00, 58.47, 56.01, 55.44, 49.97, 46.52, 32.71, 32.13, 29.86, 26.12, 22.95, 21.69, 18.44, –5.13, –5.22; IR 2929 (m), 2856 (m), 1711 (m), 1613 (m), 1514 (m), 1465 (w), 1369 (m), 1249 (s), 1173 (s), 1144 (m), 1090 (s), 1036 (m), 970 (w), 836 (s), 760 (s). LRMS (APCI) 791.4 $[M + H]^+$; $[\alpha]^{23}_D$ –2.46 º (*c* 0.69, $CHCl_3$).

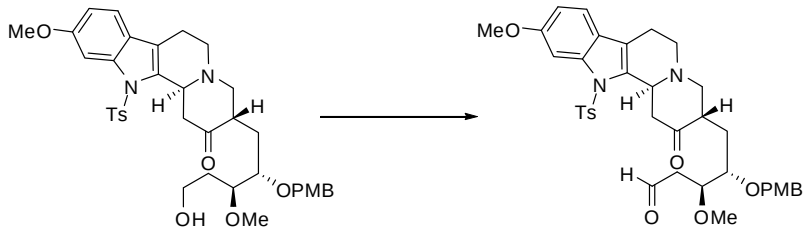

(3*S*,4*S*)-3-methoxy-5-((3*S*,12b*S*)-10-methoxy-2-oxo-12-tosyl-1,2,3,4,6,7,12,12b-octahydroindolo[2,3-a]quinolizin-3-yl)-4-(4-methoxybenzyloxy)pentanal (**31**)

Alcohol **S1** (442 mg, 0.653 mmol, 1 equiv.) was dissolved in CH_2Cl_2 (65 mL) in a 300-mL round-bottom flask at rt. To this was added the Dess–Martin periodinane (305 mg, 0.72 mmol, 1.1 equiv.) in one portion, and the solution was stirred 1 h, after which the reaction solution was diluted with Et_2O (60 mL). The reaction mixture was poured into a 500-mL Erlenmeyer flask containing 120 mL of a 1:1 aqueous solution of sat. $NaHCO_3$:10% $Na_2S_2O_3$. The biphasic mixture was stirred vigorously 1 h, after which additional CH_2Cl_2 was added (50 mL) and the layers were separated. The aqueous was extracted with CH_2Cl_2 (2 x 50 mL), and the combined organics were dried over Na_2SO_4, filtered and concentrated in vacuo to provide the crude aldehyde (**31**), which was carried forward without further purification. ^{1}H NMR (500 MHz, $CDCl_3$) δ: 9.81 (t, *J*=1.71 Hz, 1

H) 7.65 (d, *J*=1.95 Hz, 1 H) 7.47 (d, *J*=8.30 Hz, 2 H) 7.16 – 7.23 (m, 3 H) 7.10 (d, *J*=7.81 Hz, 2 H) 6.80 – 6.89 (m, 3 H) 4.54 (d, *J*=11.23 Hz, 1 H) 4.50 (dd, *J*=11.23, 2.44 Hz, 1 H) 4.31 (d, *J*=11.23 Hz, 1 H) 3.90 – 3.98 (m, 2 H) 3.87 (s, 3 H) 3.70 (s, 3 H) 3.48 – 3.50 (m, 3 H) 3.29 (dd, *J*=13.18, 6.35 Hz, 1 H) 3.15 (m, 2 H) 2.94 (t, *J*=12.45 Hz, 1 H) 2.83 (dt, *J*=10.74, 4.64 Hz, 1 H) 2.64 – 2.77 (m, 4 H) 2.59 (ddd, *J*=16.60, 7.81, 1.95 Hz, 1 H) 2.37 (t, *J*=12.20 Hz, 1 H) 2.28 (s, 3 H) 2.04 (ddd, *J*=14.16, 9.28, 2.20 Hz, 1 H) 1.01 (ddd, *J*=13.18, 9.77, 2.93 Hz, 1 H); ^{13}C NMR (126 MHz, $CDCl_3$) δ: 208.50, 201.11, 159.38, 158.04, 144.68, 138.37, 134.36, 134.31, 129.95 (2C), 129.62 (2C), 126.28 (2C), 123.94, 118.94, 118.87, 113.87 (2C), 112.75, 100.31, 76.45, 75.92, 72.59, 60.94, 58.93, 57.99, 55.80, 55.18, 45.18, 44.62, 43.92, 42.77, 29.66, 26.64, 22.24, 21.50; LRMS (APCI) 675.3 $[M + H]^+$

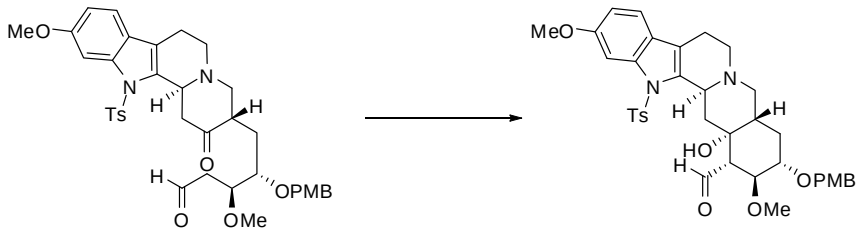

31 **32**

Pentacyclic aldehyde (**32**)

A flame-dried, 100-mL round-bottom flask was charged with crude aldehyde **31** (0.653 mmol, 1 equiv.), which was azeotroped twice from benzene and placed on high vacuum 30 min. A stir bar was then added under a positive pressure of nitrogen, followed by toluene (21 mL). To a separate 10-mL flask was charged with toluene (2 mL), piperidine (129 μL) and *p*-toluenesulfonic acid (24.8 mg), and 1 mL of this solution was transferred to the first flask (piperidine addition: 65.7 μL, 0.65 mmol, 1 equiv). The reaction was

allowed to stir overnight, after which it was quenched by the addition of saturated aqueous $NaHCO_3$ (10 mL). The reaction mixture was extracted with CH_2Cl_2 (3 x 15 mL), and the combined organics were dried over Na_2SO_4, filtered, and concentrated in vacuo.[39] The residue was azeotroped twice from benzene to aid in the removal of residual piperidine, after which the residue was dissolved in a 1:1 solution of hexanes:EtOAc. The solution was filtered to remove any precipitate, and the filtrate was concentrated in vacuo to provide **32** as a single diastereomer (382 mg, 0.56 mmol, 86% yield). ^{1}H NMR (600 MHz, C_6D_6) δ: 9.83 (d, *J*=2.44 Hz, 1 H) 8.16 (d, *J*=2.44 Hz, 1 H) 7.59 (d, *J*=8.30 Hz, 2 H) 7.33 (d, *J*=8.80 Hz, 2 H) 6.99 (d, *J*=8.30 Hz, 1 H) 6.88 (d, *J*=8.80 Hz, 1 H) 6.88 (d, *J*=8.30 Hz, 2 H) 6.38 (d, *J*=7.81, 2 H) 4.83 (dd, *J*=11.5, 1.5 Hz, 1 H) 4.59 (d, *J*=11.72 Hz, 1 H) 4.51 (d, *J*=11.72 Hz, 1 H) 4.07 (dd, *J*=10.99, 9.03 Hz, 1 H) 3.45 (s, 3H) 3.45 (s, 3 H) 3.38 – 3.51 (m, 1 H) 3.33 (s, 3 H) 3.25 (t, *J*=11.96, 1 H) 3.12 (br. s, 1 H), 2.91 (dd, *J*=13.18, 1.95 Hz, 1 H) 2.69 – 2.81 (m, 1 H) 2.41 – 2.57 (m, 2 H) 2.34 – 2.41 (m, 1 H) 2.29 (dd, *J*=10.99, 2.20, 1 H) 1.83 (ddd, *J*=12.30, 12.30, 12.30, 1 H) 1.53 (s, 3 H) 1.47 – 1.52 (m, 1 H) 1.42 (dd, *J*=13.18, 11.23 Hz, 1 H) 1.33 (m, 1 H); ^{13}C NMR (126 MHz, $CDCl_3$) δ: 206.34, 159.39, 158.08, 144.80, 139.10, 135.86, 134.26, 130.97, 129.71 (2C), 129.44 (2C), 126.70 (2C), 124.83, 120.42, 118.89, 114.05 (2C), 112.94, 101.09, 82.33, 82.13, 72.51, 71.67, 62.61, 61.21, 56.08, 55.52, 55.39, 53.68, 46.76, 40.03, 38.24, 28.99, 22.68, 21.76; IR 3500 (br m), 2956(m), 2926(s), 2853(m), 1721(m), 1612(m), 1583(w), 1513(m), 1492(m), 1462(m), 1441(w), 1363(s), 1278(m), 1247(s), 1170(s), 1144(m), 1102(s), 1087(s), 1033(s), 973(m), 909(w), 846(w), 810(s),

[39] The product can be chromatographed on Davisil™, but small amounts of decomposition are observed, and thus the reported workup procedure was devised to provide the pure product without need for flash chromatography.

731(m), 703(w), 657(m), 627(w); LRMS (APCI) 675.3 $[M + H]^+$; $[\alpha]^{24}_D$ +70.8º (*c* 1.00, $CHCl_3$).

The 1-D NOESY spectra (600 MHz, C_6D_6) displayed the following nOe transfers:

Irradiation of C17 (δ 4.07): 1.79% 19α (δ 1.83)

Irradiation of C16 (δ 2.29): 1.69% CHO (δ 9.83),

3.34% C20 (δ 1.33)

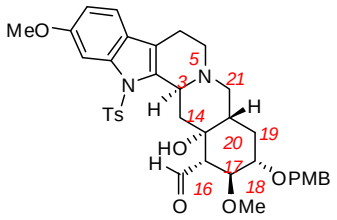

32

Irradiation of C3 (δ 4.83): 3.31% *o*-CH(Ts) (δ 7.59),

3.63% C21α (δ 3.25), 2.55% C14α (δ 2.91)

Irradiation of C20 (δ 1.33): 2.00% C18 (δ 3.41),

0.75% C5β (δ 2.72). 1.94% C21β (δ 2.44)

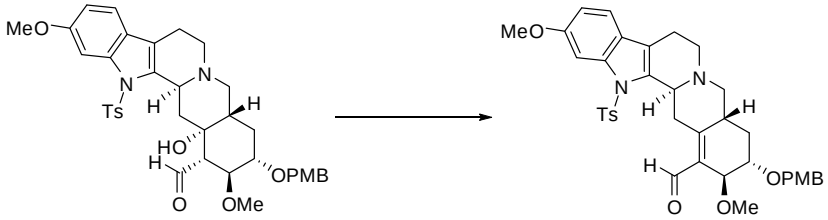

32 **33**

Enal (**33**)

A flame-dried 50-mL round-bottom flask was charged with aldol adduct **32** (208 mg, 0.31 mmol, 1 equiv) and azeotroped twice with benzene and placed on high vacuum for 15 min. A stir bar and and CH_2Cl_2 (7 mL) were added and the flask was cooled to 0 °C. To the stirred solution under nitrogen at 0 °C was added 7 mL of the following stock solution: (39 mg DMAP, 520 µL NEt_3, and 14 mL CH_2Cl_2). The amounts added were: DMAP (19.5 mg, 0.16 mmol, 0.5 equiv) and NEt_3 (260 µL, 3.5 mmol, 11.4 equiv).

TFAA was added to the cooled solution, neat via microliter syringe (236 μL, 0.75 mmol, 2.4 equiv) which caused an immediate color change from pale yellow to dark orange-red. After addition was complete, the ice bath was removed and the reaction was stirred at rt for 30 m. The stir bar was removed and the contents of the flask were concentrated in vacuo. The flask containing the crude product was charged with CH_2Cl_2 (20 mL) and diisopropyl amine (135 μL, 1.85 mmol, 6.0 equiv), and the contents were stirred at room temperature overnight. The contents were washed twice with DI H_2O (10 mL), and the aqueous layer was re-extracted twice with CH_2Cl_2 (2 x 10 mL). The combined organics were dried over Na2SO4, filtered, and concentrated. The residue was purified by flash chromatography (Biotage, 20-50% EtOAc/hexanes) to afford enal 33 as an orange solid (131 mg, 0.19 mmol, 63% yield). R*f* = 0.54 (100% EtOAc); ^{1}H NMR (600 MHz, $CDCl_3$) δ: 10.46 (s, 1 H, C**H**O) 7.67 (d, *J*=2.34 Hz, 1 H, C12) 7.46 (d, *J*=8.49 Hz, 2 H, Ts) 7.26 (d, *J*=8.79 Hz, 2 H, PMB) 7.19 (d, *J*=8.49 Hz, 1 H, C10) 7.08 (d, *J*=8.49 Hz, 2 H, Ts) 6.86 - 6.89 (m, 2 H, PMB) 6.85 (dd, *J*=8.49, 2.34 Hz, 1 H, C9) 4.53 (sk d, *J*=11.42 Hz, 1 H, PMB Bn) 4.51 (sk d, *J*=11.72 Hz, 1 H, PMB Bn) 4.39 (dd, *J*=3.22, 0.88 Hz, 1 H, C17) 4.36 (br. d, *J*=10.54 Hz, 1 H, C3) 4.23 (dd, *J*=12.89, 2.34 Hz, 1 H, C14) 3.87 (s, 3 H, PMB) 3.84 (q, *J*=3.22 Hz, 1 H, C18) 3.78 (s, 3 H, **Me**OAr) 3.43 - 3.51 (m, 1 H, C21) 3.45 (s, 3 H, C17 O**Me**) 3.27 (ddd, *J*=11.50, 8.57, 5.42 Hz, 1 H, C5) 3.14 (dd, *J*=12.89, 4.98 Hz, 1 H, C21) 2.84 (ddd, *J*=11.42, 5.56, 3.80 Hz, 1 H, C5) 2.65 - 2.75 (m, 3 H, C6(2), C20) 2.32 (dd, *J*=12.89, 10.84 Hz, 1 H, C14) 2.28 (s, 3 H, Ts) 2.14 (ddd, *J*=14.64, 7.61, 2.93 Hz, 1 H, C19) 1.57 - 1.60 (m, 1 H, C19). ^{13}C NMR (126 MHz, $CDCl_3$) δ: 190.23, 161.72, 159.01, 158.03, 144.64, 138.32, 134.58, 134.29, 130.53, 130.50, 129.63 (2C), 128.96 (2C), 126.27 (2C), 123.97, 119.15, 118.91, 113.73 (2C), 112.70, 100.33,

72.27, 70.38, 70.29, 62.87, 59.67, 58.38, 55.79, 55.17, 44.81, 33.95, 32.24, 25.39, 22.23, 21.45; FTIR (neat, cm^{-1}) 2924 (m), 2874(m), 2835(m), 1726(w), 1663(s), 1612(s), 1581(w), 1512(m), 1493(m), 1453(m), 1440(m), 1361(s), 1304(w), 1245(s), 1170(s), 1103(s), 1080(s), 1034(s), 983(m), 946(w), 924(m), 845(w), 811(m), 731(m), 674(s), 657(s), 617(w); LRMS (APCI) 657.3 $[M + H]^+$; $[\alpha]^{23}_D$ 224.8º (*c* 0.83, $CHCl_3$).

33 **34**

Saturated Aldehyde (**34**)

A 20-mL vial equipped with a stir bar was charged sequentially with enal **33** (10 mg, 0.015 mmol, 1 equiv), EtOH (2.5 mL), and PtO_2 (9 mg, 0.040 mmol, 2.6 equiv). The uncapped vial was placed in a Paar hydrogenation bomb over a stir place, and the bomb was charged with H_2 gas (48 atm). The solution was stirred at room temperature at this pressure for 65 h, after which point the bomb was carefully vented. The contents of the vial were filtered through a short plug of Celite® into a 10-mL round-bottom flask and concentrated in vacuo to afford an orange solid that was carried on to the next step without purification. [The ^{1}H NMR spectrum of one of the products, saturated alcohol **50**, is: ^{1}H NMR (600 MHz, $CDCl_3$) δ ppm 7.58 (d, *J*=2.34 Hz, 1 H) 7.46 (d, *J*=8.20 Hz, 2 H) 7.30 (d, *J*=8.49 Hz, 2 H) 7.12 (d, *J*=8.49 Hz, 1 H) 7.07 (d, *J*=7.91 Hz, 2 H) 6.87 - 6.94 (m, 2 H) 6.79 (dd, *J*=8.49, 2.05 Hz, 1 H) 4.58 (d, *J*=11.42 Hz, 1 H, PMB Bn) 4.44 (d, *J*=11.72 Hz, 1 H, PMB Bn) 4.35 (d, *J*=11.42 Hz, 1 H, C3) 4.30 (br. s., 1 H, CH**H**OH)

4.03 (d, *J*=10.54 Hz, 1 H, C**H**HOH) 3.84 (s, 3 H, MeO) 3.82 (s, 3 H, MeO) 3.78 (t, *J*=13.03 Hz, 1 H, C21) 3.72 - 3.75 (m, 1 H, C18) 3.71 (br. s., 1 H, C17) 3.39 (s, 3 H, MeO) 3.23 - 3.30 (m, 1 H) 2.81 (dd, *J*=13.18, 3.81 Hz, 1 H) 2.57 - 2.77 (m, 4 H) 2.53 (d, *J*=14.35 Hz, 1 H, C14) 2.40 - 2.47 (m, 1 H, C16) 2.33 - 2.40 (m, 1 H, C15) 2.21 - 2.30 (m, 1 H, C20) 2.27 (s, 3 H, Ts) 1.86 (ddd, *J*=14.86, 6.08, 3.37 Hz, 1 H, C19) 1.76 (ddd, *J*=14.13, 11.79, 4.83 Hz, 1 H, C14) 1.68 (d, *J*=14.94 Hz, 1 H, C19)].

The flask containing the crude hydrogenation product was charged with a stir bar and CH_2Cl_2 (3 mL) and cooled to 0 ^oC. To this solution was added the Dess–Martin periodinane (19.3 mg, 0.046 mmol, 3.0 equiv). The reaction mixture was stirred for 2 h, at which point it was first diluted with Et_2O (3 mL) and then quenched by pouring the solution into 6 mL of a 1:1 mixture of saturated aqueous $NaHCO_3$ and 10% aqueous sodium thiosulfate. The contents were stirred vigorously for 1 h and extracted with CH_2Cl_2 (3 x 5mL). The organics were dried over Na_2SO_4, filtered, and concentrated. The crude residue was purified by flash chromatography (Davisil^{TM}, 20-50% EtOAc/hexanes) to afford saturated aldehyde **34** (4.0 mg, 0.0061 mmol, 40 % yield).

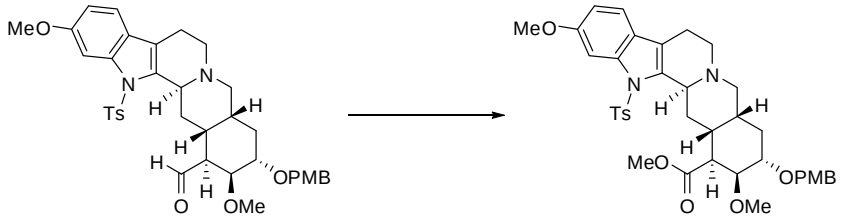

34 **53**

Saturated Ester (**53**)

A 1-dram vial containing aldehyde **34** (4.0 mg, 0.0061 mmol, 1 equiv) was charged with a stir bar, *t*-BuOH (300 µL), H_2O (200 µL) and 2-methyl-2-butene (91 µL, 0.86 mmol,

140 equiv). To this mixture, cooled to 0 °C, were added NaH_2PO_4 (3.8 mg, 0.027 mmol, 4.5 equiv) followed by $NaClO_2$ (80% technical grade, 3.1 mg, 0.027 mmol, 4.5 equiv) as solids. After 2 h, the reaction was determined to be complete (based on consumption of starting material by LC/MS). The reaction was diluted with DI H_2O and extracted with CH_2Cl_2 (4 x 1 mL). The combined organics were dried over Na_2SO_4, filtered, and concentrated in vacuo to afford the crude carboxylic acid as a pale yellow solid. The crude product, in an uncapped vial, was dissolved in EtOAc (~3 mL) and treated with a solution of CH_2N_2 (1 M in Et_2O) dropwise (8 drops) until a bright yellow color persisted. The solution was stirred for 2 min, after which excess CH_2N_2 and the solvent were removed by a positive pressure of N_2. The resultant residue was purified by flash column chromatography (DavisilTM, 20-50% EtOAc/hexanes) to afford saturated ester **53** as a yellow-orange solid (3.6 mg, 0.005 mmol, 86% yield). ^{1}H NMR (500 MHz, $CDCl_3$) δ ppm 7.58 (d, *J*=1.95 Hz, 1 H, C12) 7.45 (d, *J*=8.79 Hz, 2 H) 7.31 (d, *J*=8.30 Hz, 2 H) 7.12 (d, *J*=8.30 Hz, 1 H, C9) 7.07 (d, *J*=8.30 Hz, 2 H) 6.86 - 6.96 (m, 2 H) 6.79 (dd, *J*=8.55, 2.20 Hz, 1 H, C10) 4.56 (d, *J*=11.72 Hz, 1 H, PMB Bn) 4.50 (d, *J*=11.72 Hz, 1 H, PMB Bn) 4.14 (d, *J*=11.23 Hz, 1 H, C3) 3.84 (s, 3 H, MeO) 3.83 (s, 3 H, MeO) 3.80 (s, 3 H, MeO) 3.78 - 3.80 (m, 1 H, C17) 3.72 (d, *J*=2.90 Hz, 1 H, C18) 3.63 (t, *J*=12.94 Hz, 1 H, C21) 3.40 (dd, *J*=12.70, 2.93 Hz, 1 H, **C16**) 3.30 (s, 3 H, MeO) 3.14 - 3.23 (m, 1 H, C5) 2.76 (dd, *J*=13.43, 4.15 Hz, 1 H, C21) 2.63 - 2.72 (m, 2 H, C6, C5) 2.50 - 2.63 (m, 3 H, C6, C15, C14) 2.20 - 2.31 (m, 1 H, C20) 2.27 (s, 3 H, Ts-Me) 1.84 - 1.94 (m, 1 H, C19) 1.73 - 1.84 (m, 1 H, C14) 1.64 (d, *J*=15.14 Hz, 1 H, C19).

The 1-D NOESY spectra (500 MHz, $CDCl_3$) displayed the following nOe transfers:

Irradiation of C21 (δ 3.63): 5.2% C3 (δ 4.14),

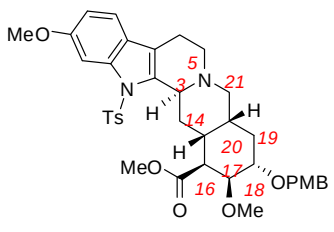

0.94% C16 (δ 2.25)

Irradiation of C3 (δ 4.50): 2.1% C16 (δ 2.25),

1.4% *o*-CHTs (δ 7.45)

Irradiation of C16 (δ 3.40): 2.3% C3 (4.14), 3.4% C21α (3.63), 3.0% C17 (3.80)

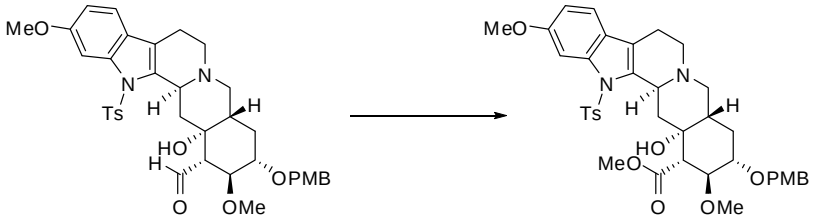

32 **56**

Pentacyclic methyl ester (**56**)

Aldol adduct **32** (100 mg, 0.148 mmol, 1 equiv.) was dissolved in *t*-BuOH (2.5 mL), H_2O (2.5 mL) and acetone (1.4 mL) in a 25-mL round-bottom flask. 2-methyl-2-butene (58 μL, 0.55 mmol, 3.7 equiv.) was then added via microliter syringe, followed by NaH_2PO_4 (92 mg, 0.67 mmol, 4.5 equiv.) and $NaClO_2$ (80% technical grade, 75 mg, 0.67 mmol, 4.5 equiv.) as solids. The biphasic reaction was stirred vigorously 1.5 h, after which saturated aqueous NH_4Cl (5 mL) was added. The reaction mixture was extracted with CH_2Cl_2 (3 x 10 mL) and the combined organics were dried over Na_2SO_4, filtered, and concentrated in vacuo. The resultant yellow solid was suspended in EtOAc (10 mL), to which EtOH was added dropwise until the reaction mixture was homogenous (~ 4 mL). To this was added a solution of CH_2N_2 (1 M in Et_2O) dropwise until a bright yellow color persisted (~200 μL). Excess CH_2N_2 and solvent were removed by evaporation under a steady stream of nitrogen, followed by high vacuum (~5 min). The residue was purified by flash chromatography (silica gel, 20 – 100% EtOAc in hexanes) to provide the ester **56** (74.9

mg, 0.11 mmol, 72% yield). R*f* = 0.44 (100% EtOAc); ^{1}H NMR (500 MHz, $CDCl_3$) δ 7.66 (d, *J*=2.29 Hz, 1 H) 7.48 (d, *J*=8.24 Hz, 2 H) 7.29 (d, *J*=8.70 Hz, 2 H) 7.12 (d, *J*=8.24 Hz, 1 H) 7.08 (d, *J*=8.24 Hz, 2 H) 6.88 (d, *J*=8.70 Hz, 2 H) 6.81 (dd, *J*=8.70, 2.29 Hz, 1 H) 4.63 (d, *J*=11 Hz, 1 H) 4.60 (d, *J*=11.45 Hz, 1 H) 4.54 (d, *J*=10.53 Hz, 1 H) 3.84 – 3.89 (m, 1 H), 3.85 (s, 3 H), 3.81 (s, 3 H) 3.80 (s, 3 H) 3.54 (s, 3 H) 3.39 – 3.48 (m, 1 H) 3.22 (s, 1 H) 3.16 (t, *J*=11.68 Hz, 1 H) 3.02 – 3.11 (m, 1 H) 2.62 – 2.75 (m, 3 H) 2.52 – 2.62 (m, 1 H) 2.37 (dd, *J*=12.36, 1.83 Hz, 1 H) 2.34 (d, *J*=10.99 Hz, 1 H) 2.27 (s, 3 H) 1.61 - 1.76 (m, 3 H) 1.57 (dd, *J*=13.05, 11.22 Hz, 1 H); ^{13}C NMR (126 MHz, $CDCl_3$) δ: 174.09, 159.23, 157.91, 144.66, 138.86, 134.30, 130.98, 129.63 (2C), 129.32 (2C), 126.57 (2C), 124.71, 119.92, 118.75, 113.91 (2C), 112.77, 100.89, 83.52, 81.57, 71.72, 70.98, 61.12, 57.76, 55.95, 55.41, 55.35, 53.54, 52.34, 46.30, 39.62, 37.76, 31.71, 29.23, 22.54, 21.65; IR 3004 (w), 2929 (m), 1717 (m), 1613 (m), 1514 (m), 1493 (m), 1439 (m), 1365 (s), 1280 (m), 1211 (m), 1172 (s), 1147 (m), 1108 (m), 1036 (m), 992 (w), 848 (m), 757 (s), 667 (s) LRMS (APCI) 705.3 $[M + H]^+$; $[\alpha]^{23}_D$ +142.7º (*c* 1.04, $CHCl_3$).

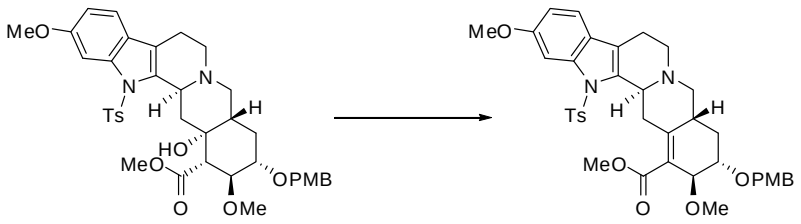

56 **57**

Unsaturated methyl ester (**57**)

A 25-mL round-bottom flask with stir bar was charged with tertiary alcohol **56** (50.9 mg, 0.072 mmol, 1 equiv.), which had been azeotroped from benzene twice and placed under high vacuum for 30 min. The alcohol was dissolved in THF (3.6 mL), and the flask was

cooled to –78 °C under a positive pressure of argon. A 1.3 M *n*-butyllithium solution in hexanes (110 μL, 0.144 mmol, 2 equiv.) was added dropwise, and the solution was stirred 10 min, after which trifluoroacetic anhydride (50.9 μL, 0.36 mmol, 5 equiv.) was added. The reaction mixture was allowed to come to rt over 3 h and was then quenched at 0 °C by slow addition of H_2O. The crude reaction mixture was extracted with CH_2Cl_2 (3 x 5 mL), and the combined organics were washed with a saturated aqueous $NaHCO_3$ solution (1 x 5 mL), dried over Na_2SO_4, filtered, and concentrated in vacuo to afford 60.4 mg of an orange solid. This material consisted of a 3:1 mixture of the tertiary trifluoroacetate to alcohol starting material and was carried forward without further purification. The crude trifluoroacetate, which was azeotroped twice from benzene and placed under high vacuum for 30 min, was transferred to a 25-mL sealed tube and dissolved in 11.5 mL toluene. To this solution was added a stir bar and freshly distilled DBU (86 μL, 10 equiv.) at rt. The flask was then sealed and immersed in a 110 °C oil bath, and the solution was stirred at this temperature for 15 h. The reaction was removed from the oil bath and the solution was concentrated in vacuo. The residue was purified by flash chromatography (silica gel, 1% EtOH/CH_2Cl_2) to provide the unsaturated methyl ester **57** as a pale yellow solid (18.0 mg, 0.026 mmol, 36% yield). ^{1}H NMR (400 MHz, $CDCl_3$) δ 7.64 (d, *J*=1.83 Hz, 1 H) 7.47 (d, *J*=8.42 Hz, 2 H) 7.31 (d, *J*=8.42 Hz, 2 H) 7.16 (d, *J*=8.78 Hz, 1 H) 7.07 (d, *J*=8.05 Hz, 2 H) 6.88 (d, *J*=8.78 Hz, 2 H) 6.82 (dd, *J*=8.42, 2.20 Hz, 1 H) 4.61 (s, 2 H) 4.27 (d, *J*=6.59 Hz, 1 H) 4.08 (d, *J*=11.34 Hz, 1 H) 3.88 (s, 3 H) 3.86 (s, 3 H) 3.80 (s, 3 H) 3.63 – 3.75 (m, 2 H) 3.54 (s, 3 H) 3.06 – 3.25 (m, 1 H) 3.12 (dd, *J*=12.81, 5.12 Hz, 1 H) 2.88 (t, *J*=12.08 Hz, 1 H) 2.67 – 2.79 (m, 2 H) 2.54 – 2.67 (m, 2 H) 2.27 (s, 3 H) 2.16 – 2.25 (m, 1 H) 1.94 – 2.07 (m, 1 H) 1.27 – 1.41 (m, 1 H); ^{13}C NMR

(126 MHz, $CDCl_3$) δ 168.60, 159.12, 157.87, 144.43, 143.76, 138.52, 135.39, 134.38, 130.71, 129.47, 129.24, 126.60, 126.43, 124.24, 119.22, 118.79, 113.79, 112.59, 100.54, 80.01, 71.10, 61.99, 59.89, 58.96, 55.82, 55.25, 51.72, 45.59, 34.25, 33.71, 29.68, 29.12, 22.31, 21.49; IR 2925(m), 1720 (m), 1613 (w), 1513 (m), 1366 (m), 1248 (m), 1172 (m), 1115 (m), 911 (s), 813 (m), 734 (s), 669 (m); LRMS (APCI) 687.4 $[M + H]^+$; $[\alpha]^{24}_D$ +162.4 (*c* 1.01, $CHCl_3$).

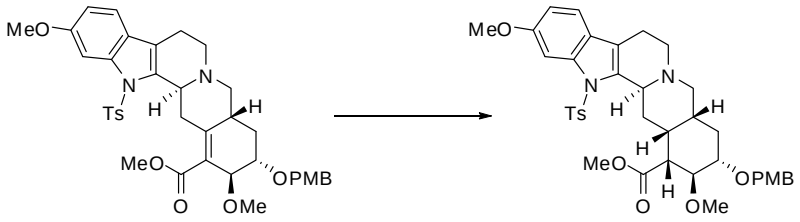

57 **60**

<u>*N*-tosyl, 18-(4-methoxybenzyloxy)-methyl reserpate (**60**)</u>

A 2-mL Biotage microwave vial was brought into a glove box and charged with a stir bar and unsaturated ester **57** (5.0 mg, 7.3 μmol, 1 equiv.) which had been azeotroped from benzene (3x) and placed under high vacuum for 30 min. Iridium complex **64** (11.0 mg, 7.3 μmol, 1 equiv.) was added to the vial followed by CH_2Cl_2 (360 μL), which had been degassed through three freeze-pump-thaw cycles. The vial was sealed with a Teflon-lined pressure seal cap and transferred out of the glove box. The vial was evacuated and back-filled with H_2 (4x), after which it was stirred 16 h at rt under a balloon of H_2. The reaction mixture was then concentrated in vacuo. Analysis of the crude reaction mixture by ^1H NMR (comparison of the PMB Bn signals) showed a 6:1 diastereomeric ratio of olefin hydrogenation products. The mixture was purified by preparatory thin layer chromatography to provide recovered unsaturated ester **57** (2.3 mg, 3.3 μmol, 46%

recovered starting material) and the desired saturated ester **60** as a white solid (2.2 mg, 3.2 μmol, 44% yield, 81% based on recovered starting material). R*f* = 0.51 (EtOAc); ^{1}H NMR (500 MHz, $CDCl_3$) δ: 7.61 (d, *J*=2.29 Hz, 1 H) 7.32 (d, *J*=8.24 Hz, 2 H), 7.32 (m, 2 H), 7.05 (d, *J*=8.70 Hz, 1 H) 7.02 (d, *J*=8.24 Hz, 2 H) 6.90 (d, *J*=8.70 Hz, 2 H) 6.80 (dd, *J*=8.24, 2.29 Hz, 1 H) 4.64 (d, *J*=10.99 Hz, 1 H) 4.58 (d, *J*=10.99 Hz, 1 H) 4.40 (dd, *J*=5.27, 2.52 Hz, 1 H) 3.89 (s, 3 H) 3.88 (s, 3 H) 3.83 (s, 3 H) 3.72 (dd, *J*=10.99, 9.16 Hz, 1 H) 3.67 (s, 3 H) 3.33 – 3.42 (m, 1 H) 3.12 (dd, *J*=13.28, 5.49 Hz, 1 H) 2.93 – 3.03 (m, 1 H) 2.79 (dd, *J*=11.45, 4.58 Hz, 1 H) 2.85 (ddt, *J*=17.06, 5.72, 2.80, 2.80 Hz, 1 H) 2.64 (dt, *J*=14.54, 3.03 Hz, 1 H) 2.52 (dd, *J*=10.99, 5.04 Hz, 1 H) 2.34 (dd, *J*=11.68, 1.60 Hz, 1 H) 2.27 (s, 3 H) 2.15 – 2.26 (m, 2 H) 2.09 (td, *J*=13.28, 11.90 Hz, 1 H) 1.92 – 2.01 (m, 1 H) 1.87 (dt, *J*=13.16, 3.95 Hz, 1 H) 1.72 (d, *J*=12.36 Hz, 1 H); ^{13}C NMR (126 MHz, $CDCl_3$) δ: 172.51, 159.01, 157.97, 144.23, 140.33, 135.72, 132.38, 131.12, 129.12 (2C), 128.82 (2C), 126.74, 125.65, 123.95, 118.49, 113.72, 113.06, 102.50, 82.88, 79.37, 71.19, 61.13, 56.27, 55.89, 55.26, 52.06, 51.89, 50.66, 50.08, 33.63, 32.33, 30.36, 26.27, 21.49, 18.15.; FTIR (neat, cm^{-1}); 2930 (br m), 1737 (m), 1614 (m), 1514 (m), 1364 (m), 1278 (m), 1171 (s), 1093 (m), 911 (w), 814 (w), 735 (s); LRMS (APCI) 689.3 $[M + H]^+$; $[\alpha]^{23}_D$ + 166.0 (*c* 1.35, $CHCl_3$).

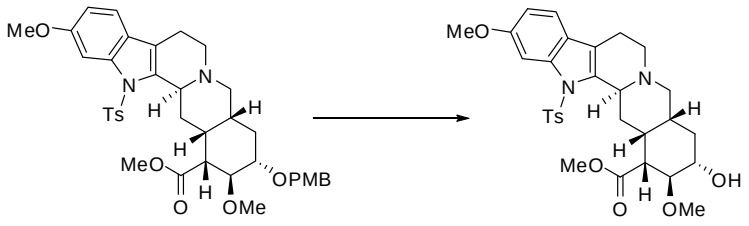

60 **S2**

<u>*N*-tosyl-methyl reserpate (**S2**)</u>

A 2-dram vial with a septum cap and stir bar was charged with PMB ether **60** (11.4 mg, 16.5 μmol, 1 equiv.), followed by CH_2Cl_2 (1.1 mL) and 1,3-dimethoxybenzene (6.5 μL, 49.5 μmol, 3 equiv.). The vial was cooled to 0 ^oC, and a TfOH solution in CH_2Cl_2 (44 μL of a 50 μL TfOH/1 mL CH_2Cl_2, 24.7 μmol, 1.5 equiv.) was added dropwise via microliter syringe. Consumption of the starting material was monitored using LC/MS (APCI). Upon completion (~30 min after addition of TfOH), the reaction was quenched with a half-saturated aqueous solution of $NaHCO_3$ (1 mL) and diluted with CH_2Cl_2 (0.5 mL). The layers were separated and the aqueous layer was extracted with CH_2Cl_2 (3 x 1 mL). The combined organic layers were dried over Na_2SO_4, filtered, and concentrated in vacuo. The resultant residue was purified (silica gel, 5-10% MeOH/CH_2Cl_2, followed by an eluent of 10:1:1:1 EtOAc: H_2O: MeOH: acetone), to afford alcohol **S2** as a pale yellow solid (8.1 mg, 14.2 μmol, 86% yield). R*f* = 0.28 (10:1:1:1 EtOAc: H_2O: MeOH: acetone); ^1H NMR (500 MHz, $CDCl_3$) δ: 7.60 (d, *J*=1.95 Hz, 1 H) 7.31 (d, *J*=8.30 Hz, 2 H) 7.04 (d, *J*=8.30 Hz, 1 H) 7.01 (d, *J*=7.81 Hz, 2 H) 6.78 (dd, *J*=8.30, 2.44 Hz, 1 H) 4.39 (br. s., 1 H) 3.88 (s, 3 H) 3.87 (s, 3 H) 3.65 (s, 3 H) 3.58 (td, *J*=10.74, 8.79 Hz, 1 H) 3.52 (m, 1 H) 3.11 (dd, *J*=12.94, 5.62 Hz, 1 H) 2.96 (td, *J*=12.33, 4.64 Hz, 1 H) 2.76 – 2.87 (m, 1 H) 2.79 (dd, *J*=11.23, 4.88 Hz, 1 H) 2.64 (dt, *J*=14.41, 3.30 Hz, 1 H) 2.50 (dd, *J*=10.74, 4.88 Hz, 1 H) 2.35 (d, *J*=11.72 Hz, 1 H) 2.26 (s, 3 H) 2.07 – 2.23 (m, 3 H) 1.93 - 2.03 (m, 1 H) 1.71 – 1.84 (m, 2 H); ^{13}C NMR (126 MHz, $CDCl_3$) δ: 172.57, 157.99, 144.29, 140.33, 135.65, 132.38, 128.86 (2C), 126.74 (2C), 125.64, 123.97, 118.54, 113.07, 102.51, 81.35, 75.30, 61.18, 56.27, 55.90, 51.98, 51.44, 50.65, 50.05, 33.79, 32.79, 32.52, 26.43, 21.50, 18.21; FTIR (neat, cm^{-1}); 1737 (m), 1614 (m), 1493 (w), 1365 (m), 1278 (w), 1254 (w),

1172 (s), 1089 (m), 909 (m), 812 (w), 735 (s); LRMS (APCI) 569.2 $[M + H]^+$; $[\alpha]^{23}_D$ + 211.3 (*c* 0.81, $CHCl_3$).

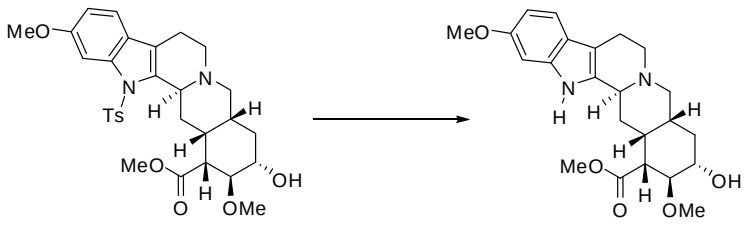

S2 **(+)-10**

(+)-Methyl reserpate (**10**)

A 20-mL vial was charged with a stir bar, **S2** (10.0 mg, 0.018 mmol, 1 equiv.), and MeOH (3.2 mL) under a positive pressure of N_2. To this was added Na_2HPO_4 (75.1 mg, 0.51 mmol, 30 equiv.) as a solid in one portion, followed by 5%-sodium/mercury amalgam (32 mg, 0.070 mmol, 4 equiv.). The heterogeneous mixture was stirred vigorously at rt and consumption of the **S2** was monitored using LC/MS (APCI). After 4 h, a second portion of Na_2HPO_4 (38 mg, 0.26 mmol, 15 equiv.) was added, followed by 5%-sodium/mercury amalgam (20 mg, 0.043 mmol, 2.7 equiv.). Upon completion (1 h after second addition of reagents), the reaction mixture was transferred away from the bead of mercury that had formed, using CH_2Cl_2 (10 mL) to complete the transfer. The solution was washed with H_2O (2 x 5 mL) and brine (5 mL), dried over Na_2SO_4, filtered, and concentrated in vacuo. The resultant residue was purified by flash chromatography (10% MeOH/CH_2Cl_2) to afford, as a white solid, **10** (5.0 mg, 0.012 mmol, 69%). R*f* = 0.19 (10:1:1:1 EtOAc:H_2O:MeOH:acetone); ^{1}H NMR data were in agreement with literature values.[40] ^{13}C NMR (126 MHz, $CDCl_3$) δ: 173.17, 156.38, 136.78, 128.84,

[40] Lounasmaa, M.; Tolvanen, A.; Kan, S.-K. *Heterocycles* **1985**, *23*, 371–375.

121.63, 118.51, 109.31, 107.13, 95.24, 80.95, 75.00, 60.93, 55.79, 54.20, 51.97, 51.15, 51.04, 49.00, 33.97, 32.40, 32.12, 23.97, 16.48; FTIR (neat, cm^{-1}); 3372 (m), 2929 (m), 2852 (w), 1723 (m), 1629 (w), 1463 (m), 1279 (w), 910 (s), 732 (s); LRMS (APCI) 415.1 $[M + H]^+$; $[\alpha]^{22}_D$ +96.8 (*c* 0.23, $CHCl_3$).

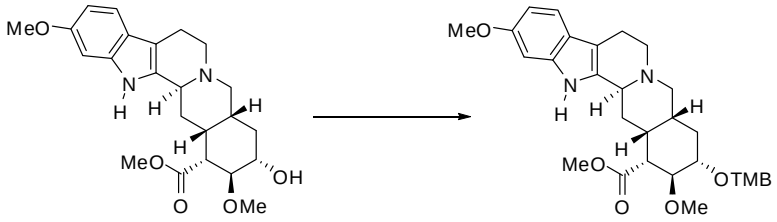

10 reserpine: **(+)-1**

Reserpine (+)-(**1**)[41]

A 1-dram vial with a screw-top septum cap was charged with a stir bar, secondary alcohol **(+)-10** (5.0 mg, 0.012 mmol, 1 equiv.) and 3,4,5-trimethoxybenzoyl chloride (16.7 mg, 0.072 mmol, 5 equiv). Freshly distilled pyridine (300 μL) was added under argon, the vial was wrapped in aluminum foil, and the reaction mixture was allowed to stir at rt 4 d under argon. Upon completion of the reaction, the pyridine was removed in vacuo. The crude residue was cooled to 0 ^oC, dissolved in CH_2Cl_2 (2 mL) and treated dropwise with a saturated aqueous solution of Na_2CO_3 (2 mL). The layers were separated, and the aqueous layer was extracted twice with CH_2Cl_2. The combined organics were washed once with deionized water, dried over Na_2SO_4, filtered, and concentrated in vacuo. The resultant solid was purified by flash chromatography (silica gel, 70% EtOAc in hexanes) to provide (+)-reserpine (6.6 mg, 0.011 mmol, 90% yield) as an off-white solid. The synthetic sample of (+)-reserpine gave identical TLC R*f*, ^1H

[41] This procedure was adapted the Stork synthesis of reserpine: See ref. 5q

NMR, and ^{13}C NMR data to a commercial sample of (–)-reserpine from Aldrich, and were in agreement with literature values (^{1}H NMR, ^{13}C NMR).[40,42] R*f* = 0.21 (EtOAc) ^{1}H NMR (600 MHz, $CDCl_3$) δ: 7.48 (br. s, 1 H) 7.34 (d, *J*=8.79 Hz, 1 H) 7.32 (s, 2 H) 6.85 (d, *J*=2.05 Hz, 1 H) 6.78 (dd, *J*=8.64, 2.20 Hz, 1 H) 5.06 (ddd, *J*=11.64, 9.45, 4.98 Hz, 1 H) 4.48 (br. s., 1 H) 3.92 (s, 9 H) 3.91 (m, 1 H) 3.85 (s, 3 H) 3.82 (m, 3 H) 3.51 (s, 3 H) 3.12 – 3.25 (m, 2 H) 3.06 (dd, *J*=12.15, 2.78 Hz, 1 H) 2.96 (m, 1 H) 2.70 (dd, *J*=11.13, 4.69 Hz, 1 H) 2.44 – 2.54 (m, 2 H) 2.28 – 2.41 (m, 2 H) 2.04 – 2.12 (m, 1 H) 2.00 (ddd, *J*=12.67, 4.17, 0.73 Hz, 1 H) 1.92 (d, *J*=11.72 Hz, 1 H) 1.80 (d, *J*=14.64 Hz, 1 H); ^{13}C NMR (126 MHz, $CDCl_3$) δ: 172.79, 165.39, 156.28, 152.98, 142.28, 136.31, 130.36, 125.39, 122.20, 118.59, 109.09, 108.23, 106.78, 95.19, 77.98, 77.82, 60.93, 60.77, 56.27, 55.83, 53.72, 51.84, 51.77, 51.23, 49.06, 34.04, 32.31, 29.75, 24.35, 16.81; IR 3433 (w), 2987 (w), 1730 (m), 1711 (m), 1587 (m), 1499 (m), 1456 (m), 1412 (m), 1331 (s), 1273 (s), 1249 (m), 1225 (s), 1186 (w), 1120 (s), 1062 (m), 1002 (m), 976 (m), 763 (m). LRMS (APCI) 609.2 $[M + H]^+$; $[\alpha]^{22}_D$ +114.6 (*c* 0.20, $CHCl_3$).

[42] Martin, S. F.; Rüeger, H.; Williamson, S. A.; Grzejszczak, S. *J. Am. Chem. Soc.* **1987**, *109*, 6124.

2.10. Spectroscopic Comparisons of Synthetic (+)- and Commercial (-)-Reserpine

^{1}H NMR Spectra ($CDCl_3$, 600 MHz)

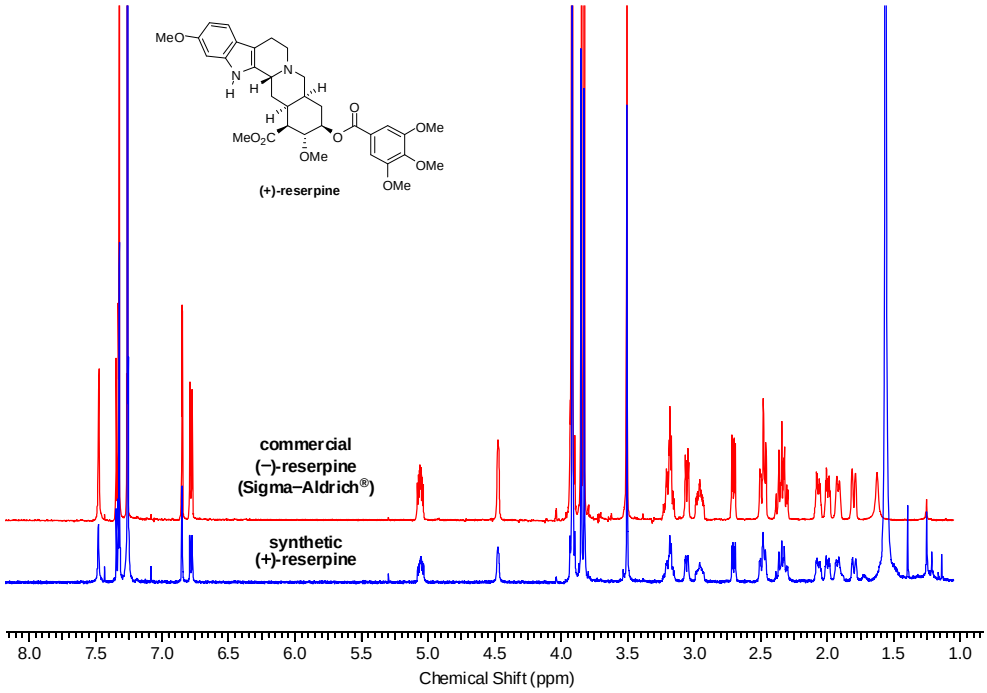

^{13}C NMR Spectra ($CDCl_3$, 126 MHz)

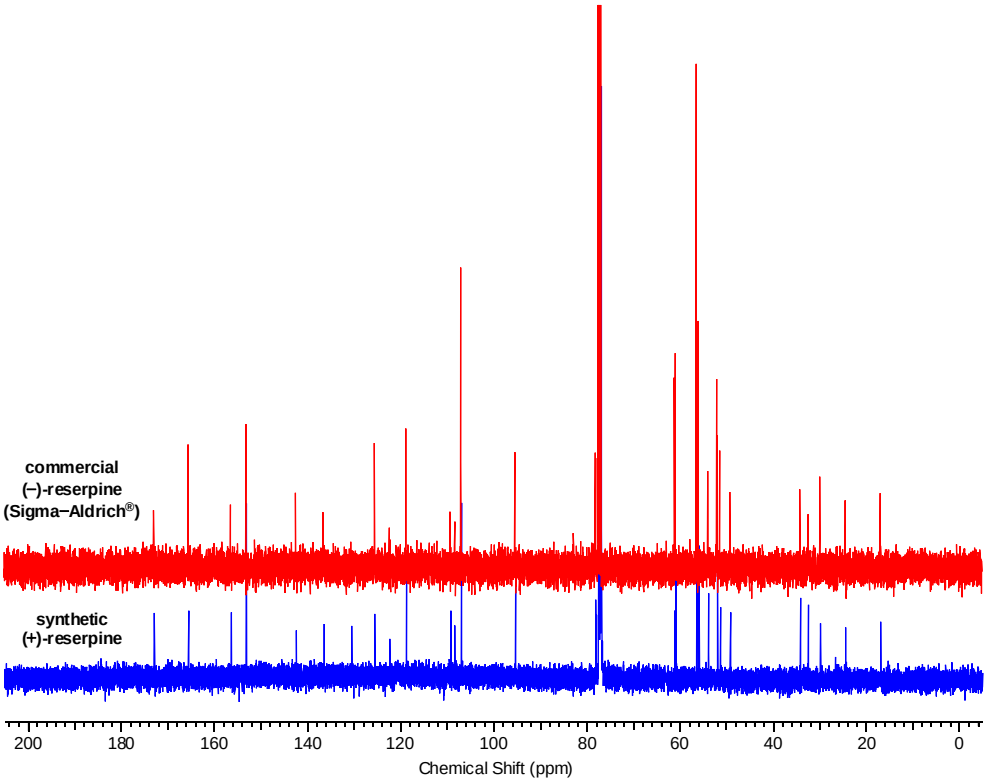

Circular Dichroism Spectra (CH_2Cl_2)

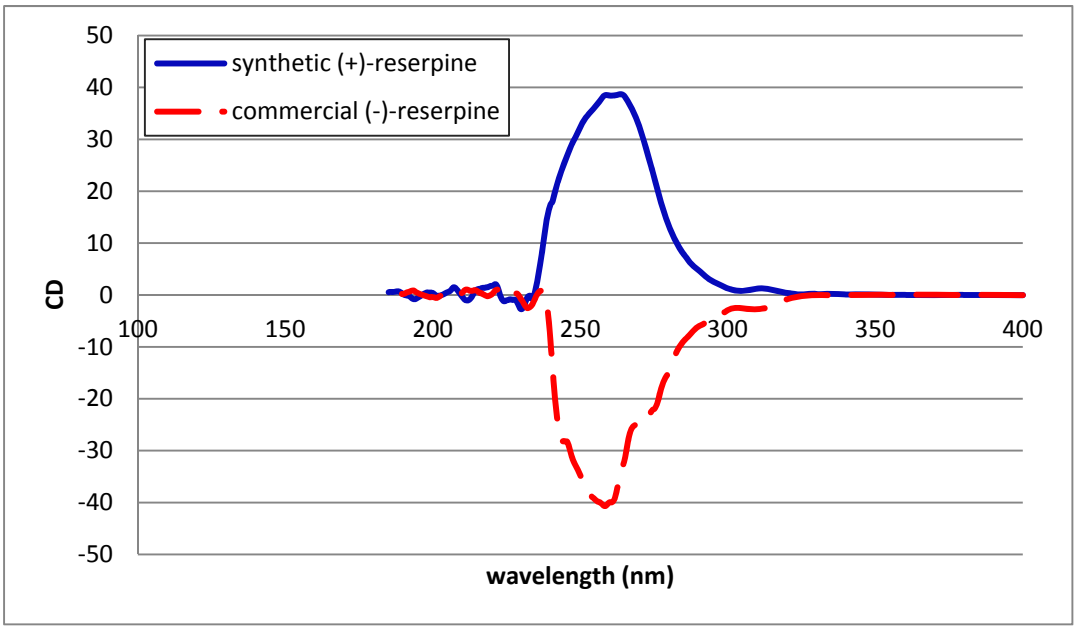

2.11. X-Ray Crystallographic Analysis of 60

Acknowledgment

We thank Dr. Shao-Liang Zheng at the Center for Crystallographic Studies at Harvard University for X-ray data collection and structure determination. We thank Dr. Yu-Sheng Chen at ChemMatCARS, APS, for his assistance with single-crystal data. ChemMatCARS Sector 15 is principally supported by the National Science Foundation/Department of Energy under grant number NSF/CHE-0822838. Use of the Advanced Photon Source was supported by the U. S. Department of Energy, Office of Science, Office of Basic Energy Sciences, under Contract No. DE-AC02-06CH11357." (See: http://cars9.uchicago.edu/chemmat/pages/acknowledge.html)

Procedure

A crystal mounted on a diffractometer was collected data at 100 K. The intensities of the reflections were collected by means of a Bruker APEX II CCD along with the D8 Diffractometer (30 KeV, λ = 0.413280 Å), and equipped with an Oxford Cryosystems

nitrogen open flow apparatus. The collection method involved 0.5° scans in Phi at -5° in 2θ. Data integration down to 0.82 Å resolution was carried out using SAINT V7.46 A (Bruker diffractometer, 2009) with reflection spot size optimisation. Absorption corrections were made with the program SADABS (Bruker diffractometer, 2009). The structure was solved by the direct methods procedure and refined by least-squares methods again F^2 using SHELXS-97 and SHELXL-97 (Sheldrick, 2008). Non-hydrogen atoms were refined anisotropically, and hydrogen atoms were allowed to ride on the respective atoms. Crystal data as well as details of data collection and refinement are summarized in Table 1, while geometric parameters are shown in Tables 2. The Ortep plots produced with SHELXL-97 program, and the other drawings were produced with Accelrys DS Visualizer 2.0 (Accelrys, 2007).

Table 2.4. Experimental details

	naomi1101_APS
Crystal data	
Chemical formula	$C_{38}H_{44}N_2O_8S$
M_r	688.81
Crystal system, space group	Triclinic, *P*1
Temperature (K)	15
a, *b*, *c* (Å)	10.5400 (9), 13.2962 (12), 13.7619 (13)
α, β, γ (°)	71.577 (2), 89.697 (2), 69.957 (2)
V (Å^3)	1707.4 (3)
Z	2
Radiation type	Synchrotron, λ = 0.41328 Å
μ (mm^{-1})	0.09
Crystal size (mm)	0.02 × 0.01 × 0.01
Data collection	
Diffractometer	Bruker D8 goniometer with CCD area detector diffractometer
Absorption correction	Multi-scan *SADABS*
T_{min}, T_{max}	0.998, 0.999

Table 2.4. (Continued).

No. of measured, independent and observed [$I > 2\sigma(I)$] reflections	35992, 11719, 10083
R_{int}	0.075
Refinement	
$R[F^2 > 2\sigma(F^2)]$, $wR(F^2)$, S	0.045, 0.102, 1.02
No. of reflections	11719
No. of parameters	887
No. of restraints	3
H-atom treatment	H-atom parameters constrained
$\Delta\rho_{max}$, $\Delta\rho_{min}$ (e Å^{-3})	0.28, -0.34
Absolute structure	Flack H D (1983), Acta Cryst. A39, 876-881
Flack parameter	-0.28 (16)

Computer programs: *APEX2* v2009.3.0 (Bruker-AXS, 2009), *SAINT* 7.46A (Bruker-AXS, 2009), *SHELXS97* (Sheldrick, 2008), *SHELXL97* (Sheldrick, 2008), Bruker *SHELXTL*.

Table 2.5. Geometric parameters (Å, º)

S1—O1	1.424 (2)	S2—O12	1.424 (2)
S1—O2	1.429 (2)	S2—O11	1.426 (2)
S1—N1	1.679 (2)	S2—N3	1.694 (3)
S1—C20	1.757 (3)	S2—C60	1.766 (3)
O3—C13	1.433 (4)	O13—C43	1.376 (4)
O3—C28	1.433 (4)	O13—C67	1.432 (4)
O4—C32	1.360 (4)	O14—C68	1.415 (4)
O4—C35	1.435 (4)	O14—C53	1.438 (4)
O5—C36	1.409 (4)	O15—C72	1.371 (4)
O5—C14	1.441 (4)	O15—C75	1.433 (4)
O6—C37	1.354 (4)	O16—C76	1.402 (4)
O6—C38	1.450 (4)	O16—C54	1.429 (4)
O7—C37	1.193 (4)	O17—C77	1.349 (4)

Table 2.5. (Continued).

O8—C3	1.365 (4)	O17—C78	1.438 (3)
O8—C27	1.414 (4)	O18—C77	1.202 (4)
N1—C1	1.438 (4)	N3—C41	1.431 (4)
N1—C19	1.446 (4)	N3—C59	1.447 (4)
N2—C9	1.465 (4)	N4—C49	1.463 (4)
N2—C10	1.474 (4)	N4—C50	1.480 (4)
N2—C18	1.479 (4)	N4—C58	1.483 (4)
C1—C6	1.388 (4)	C41—C42	1.390 (4)
C1—C2	1.394 (4)	C41—C46	1.394 (4)
C2—C3	1.396 (4)	C42—C43	1.385 (4)
C2—H2	0.9500	C42—H42	0.9500
C3—C4	1.390 (5)	C43—C44	1.403 (4)
C4—C5	1.377 (5)	C44—C45	1.387 (4)
C4—H4	0.9500	C44—H44	0.9500
C5—C6	1.398 (4)	C45—C46	1.396 (4)
C5—H5	0.9500	C45—H45	0.9500
C6—C7	1.448 (4)	C46—C47	1.440 (4)
C7—C19	1.349 (4)	C47—C59	1.346 (4)
C7—C8	1.498 (4)	C47—C48	1.496 (4)
C8—C9	1.539 (4)	C48—C49	1.534 (4)
C8—H8A	0.9900	C48—H48A	0.9900
C8—H8B	0.9900	C48—H48B	0.9900
C9—H9A	0.9900	C49—H49A	0.9900
C9—H9B	0.9900	C49—H49B	0.9900
C10—C11	1.518 (4)	C50—C51	1.516 (4)
C10—H10A	0.9900	C50—H50A	0.9900
C10—H10B	0.9900	C50—H50B	0.9900
C11—C16	1.526 (4)	C51—C52	1.520 (4)
C11—C12	1.527 (4)	C51—C56	1.540 (4)
C11—H11	1.0000	C51—H51	1.0000
C12—C13	1.525 (4)	C52—C53	1.515 (4)

Table 2.5. (Continued).

C12—H12A	0.9900	C52—H52A	0.9900
C12—H12B	0.9900	C52—H52B	0.9900
C13—C14	1.518 (4)	C53—C54	1.533 (4)
C13—H13	1.0000	C53—H53	1.0000
C14—C15	1.523 (4)	C54—C55	1.524 (4)
C14—H14	1.0000	C54—H54	1.0000
C15—C37	1.514 (4)	C55—C77	1.521 (4)
C15—C16	1.535 (4)	C55—C56	1.545 (4)
C15—H15	1.0000	C55—H55	1.0000
C16—C17	1.537 (4)	C56—C57	1.535 (4)
C16—H16	1.0000	C56—H56	1.0000
C17—C18	1.522 (4)	C57—C58	1.529 (4)
C17—H17A	0.9900	C57—H57A	0.9900
C17—H17B	0.9900	C57—H57B	0.9900
C18—C19	1.518 (4)	C58—C59	1.517 (4)
C18—H18	1.0000	C58—H58	1.0000
C20—C21	1.389 (4)	C60—C65	1.388 (4)
C20—C25	1.396 (4)	C60—C61	1.391 (4)
C21—C22	1.394 (4)	C61—C62	1.384 (4)
C21—H21	0.9500	C61—H61	0.9500
C22—C23	1.384 (5)	C62—C63	1.392 (4)
C22—H22	0.9500	C62—H62	0.9500
C23—C24	1.391 (5)	C63—C64	1.390 (4)
C23—C26	1.514 (4)	C63—C66	1.509 (4)
C24—C25	1.383 (4)	C64—C65	1.397 (4)
C24—H24	0.9500	C64—H64	0.9500
C25—H25	0.9500	C65—H65	0.9500
C26—H26A	0.9800	C66—H66A	0.9800
C26—H26B	0.9800	C66—H66B	0.9800
C26—H26C	0.9800	C66—H66C	0.9800
C27—H27A	0.9800	C67—H67A	0.9800

Table 2.5. (Continued).

C27—H27B	0.9800	C67—H67B	0.9800
C27—H27C	0.9800	C67—H67C	0.9800
C28—C29	1.505 (4)	C68—C69	1.511 (4)
C28—H28A	0.9900	C68—H68A	0.9900
C28—H28B	0.9900	C68—H68B	0.9900
C29—C30	1.377 (5)	C69—C70	1.382 (5)
C29—C34	1.396 (4)	C69—C74	1.388 (4)
C30—C31	1.394 (4)	C70—C71	1.379 (5)
C30—H30	0.9500	C70—H70	0.9500
C31—C32	1.383 (4)	C71—C72	1.393 (4)
C31—H31	0.9500	C71—H71	0.9500
C32—C33	1.395 (4)	C72—C73	1.401 (4)
C33—C34	1.365 (4)	C73—C74	1.382 (5)
C33—H33	0.9500	C73—H73	0.9500
C34—H34	0.9500	C74—H74	0.9500
C35—H35A	0.9800	C75—H75A	0.9800
C35—H35B	0.9800	C75—H75B	0.9800
C35—H35C	0.9800	C75—H75C	0.9800
C36—H36A	0.9800	C76—H76A	0.9800
C36—H36B	0.9800	C76—H76B	0.9800
C36—H36C	0.9800	C76—H76C	0.9800
C38—H38A	0.9800	C78—H78A	0.9800
C38—H38B	0.9800	C78—H78B	0.9800
C38—H38C	0.9800	C78—H78C	0.9800
O1—S1—O2	120.14 (13)	O12—S2—O11	119.84 (13)
O1—S1—N1	105.64 (13)	O12—S2—N3	106.48 (12)
O2—S1—N1	107.84 (12)	O11—S2—N3	106.65 (12)
O1—S1—C20	108.92 (14)	O12—S2—C60	109.36 (13)
O2—S1—C20	107.56 (14)	O11—S2—C60	108.82 (14)
N1—S1—C20	105.88 (13)	N3—S2—C60	104.61 (13)
C13—O3—C28	116.6 (2)	C43—O13—C67	116.4 (3)

Table 2.5. (Continued).

C32—O4—C35	118.1 (2)	C68—O14—C53	113.9 (2)
C36—O5—C14	115.5 (3)	C72—O15—C75	116.5 (2)
C37—O6—C38	115.2 (2)	C76—O16—C54	114.8 (2)
C3—O8—C27	117.4 (3)	C77—O17—C78	115.9 (2)
C1—N1—C19	106.1 (2)	C41—N3—C59	105.1 (2)
C1—N1—S1	114.53 (19)	C41—N3—S2	113.43 (19)
C19—N1—S1	122.8 (2)	C59—N3—S2	116.58 (19)
C9—N2—C10	109.9 (2)	C49—N4—C50	109.3 (2)
C9—N2—C18	111.1 (2)	C49—N4—C58	109.9 (2)
C10—N2—C18	113.0 (2)	C50—N4—C58	112.9 (2)
C6—C1—C2	122.9 (3)	C42—C41—C46	123.1 (3)
C6—C1—N1	108.4 (3)	C42—C41—N3	128.2 (3)
C2—C1—N1	128.7 (3)	C46—C41—N3	108.6 (3)
C1—C2—C3	116.3 (3)	C43—C42—C41	116.9 (3)
C1—C2—H2	121.8	C43—C42—H42	121.6
C3—C2—H2	121.8	C41—C42—H42	121.6
O8—C3—C4	115.9 (3)	O13—C43—C42	123.2 (3)
O8—C3—C2	122.9 (3)	O13—C43—C44	115.2 (3)
C4—C3—C2	121.2 (3)	C42—C43—C44	121.6 (3)
C5—C4—C3	121.7 (3)	C45—C44—C43	120.1 (3)
C5—C4—H4	119.2	C45—C44—H44	119.9
C3—C4—H4	119.2	C43—C44—H44	119.9
C4—C5—C6	118.2 (3)	C44—C45—C46	119.5 (3)
C4—C5—H5	120.9	C44—C45—H45	120.2
C6—C5—H5	120.9	C46—C45—H45	120.2
C1—C6—C5	119.6 (3)	C41—C46—C45	118.7 (3)
C1—C6—C7	107.4 (3)	C41—C46—C47	107.9 (3)
C5—C6—C7	133.0 (3)	C45—C46—C47	133.4 (3)
C19—C7—C6	109.1 (3)	C59—C47—C46	108.0 (3)
C19—C7—C8	123.7 (3)	C59—C47—C48	123.0 (3)
C6—C7—C8	127.2 (3)	C46—C47—C48	128.9 (3)

Table 2.5. (Continued).

C7—C8—C9	108.8 (3)	C47—C48—C49	108.7 (2)
C7—C8—H8A	109.9	C47—C48—H48A	109.9
C9—C8—H8A	109.9	C49—C48—H48A	109.9
C7—C8—H8B	109.9	C47—C48—H48B	109.9
C9—C8—H8B	109.9	C49—C48—H48B	109.9
H8A—C8—H8B	108.3	H48A—C48—H48B	108.3
N2—C9—C8	113.3 (3)	N4—C49—C48	114.6 (3)
N2—C9—H9A	108.9	N4—C49—H49A	108.6
C8—C9—H9A	108.9	C48—C49—H49A	108.6
N2—C9—H9B	108.9	N4—C49—H49B	108.6
C8—C9—H9B	108.9	C48—C49—H49B	108.6
H9A—C9—H9B	107.7	H49A—C49—H49B	107.6
N2—C10—C11	112.7 (2)	N4—C50—C51	114.1 (2)
N2—C10—H10A	109.1	N4—C50—H50A	108.7
C11—C10—H10A	109.1	C51—C50—H50A	108.7
N2—C10—H10B	109.1	N4—C50—H50B	108.7
C11—C10—H10B	109.1	C51—C50—H50B	108.7
H10A—C10—H10B	107.8	H50A—C50—H50B	107.6
C10—C11—C16	109.9 (2)	C50—C51—C52	114.0 (3)
C10—C11—C12	113.2 (3)	C50—C51—C56	109.0 (2)
C16—C11—C12	111.3 (2)	C52—C51—C56	111.7 (3)
C10—C11—H11	107.4	C50—C51—H51	107.3
C16—C11—H11	107.4	C52—C51—H51	107.3
C12—C11—H11	107.4	C56—C51—H51	107.3
C13—C12—C11	110.1 (3)	C53—C52—C51	109.9 (2)
C13—C12—H12A	109.6	C53—C52—H52A	109.7
C11—C12—H12A	109.6	C51—C52—H52A	109.7
C13—C12—H12B	109.6	C53—C52—H52B	109.7
C11—C12—H12B	109.6	C51—C52—H52B	109.7
H12A—C12—H12B	108.2	H52A—C52—H52B	108.2
O3—C13—C14	113.1 (2)	O14—C53—C52	114.6 (2)

Table 2.5. (Continued).

O3—C13—C12	113.8 (3)	O14—C53—C54	111.6 (3)
C14—C13—C12	111.1 (2)	C52—C53—C54	111.0 (2)
O3—C13—H13	106.0	O14—C53—H53	106.3
C14—C13—H13	106.0	C52—C53—H53	106.3
C12—C13—H13	106.0	C54—C53—H53	106.3
O5—C14—C13	109.1 (2)	O16—C54—C55	105.7 (2)
O5—C14—C15	106.1 (3)	O16—C54—C53	110.8 (2)
C13—C14—C15	111.5 (2)	C55—C54—C53	111.2 (3)
O5—C14—H14	110.0	O16—C54—H54	109.7
C13—C14—H14	110.0	C55—C54—H54	109.7
C15—C14—H14	110.0	C53—C54—H54	109.7
C37—C15—C14	114.4 (3)	C77—C55—C54	110.3 (3)
C37—C15—C16	108.6 (2)	C77—C55—C56	109.3 (2)
C14—C15—C16	115.3 (3)	C54—C55—C56	114.5 (2)
C37—C15—H15	105.9	C77—C55—H55	107.5
C14—C15—H15	105.9	C54—C55—H55	107.5
C16—C15—H15	105.9	C56—C55—H55	107.5
C11—C16—C15	111.6 (2)	C57—C56—C51	110.6 (2)
C11—C16—C17	109.7 (2)	C57—C56—C55	112.7 (2)
C15—C16—C17	112.6 (2)	C51—C56—C55	110.9 (2)
C11—C16—H16	107.6	C57—C56—H56	107.5
C15—C16—H16	107.6	C51—C56—H56	107.5
C17—C16—H16	107.6	C55—C56—H56	107.5
C18—C17—C16	113.3 (2)	C58—C57—C56	111.7 (2)
C18—C17—H17A	108.9	C58—C57—H57A	109.3
C16—C17—H17A	108.9	C56—C57—H57A	109.3
C18—C17—H17B	108.9	C58—C57—H57B	109.3
C16—C17—H17B	108.9	C56—C57—H57B	109.3
H17A—C17—H17B	107.7	H57A—C57—H57B	107.9
N2—C18—C19	109.0 (2)	N4—C58—C59	109.1 (2)
N2—C18—C17	108.0 (2)	N4—C58—C57	109.5 (2)

Table 2.5. (Continued).

C19—C18—C17	118.9 (3)	C59—C58—C57	116.0 (2)
N2—C18—H18	106.8	N4—C58—H58	107.3
C19—C18—H18	106.8	C59—C58—H58	107.3
C17—C18—H18	106.8	C57—C58—H58	107.3
C7—C19—N1	109.0 (3)	C47—C59—N3	110.3 (3)
C7—C19—C18	123.5 (3)	C47—C59—C58	124.2 (3)
N1—C19—C18	127.3 (3)	N3—C59—C58	125.1 (3)
C21—C20—C25	121.4 (3)	C65—C60—C61	121.3 (3)
C21—C20—S1	119.9 (2)	C65—C60—S2	119.4 (2)
C25—C20—S1	118.6 (2)	C61—C60—S2	119.3 (2)
C20—C21—C22	118.7 (3)	C62—C61—C60	118.2 (3)
C20—C21—H21	120.6	C62—C61—H61	120.9
C22—C21—H21	120.6	C60—C61—H61	120.9
C23—C22—C21	120.9 (3)	C61—C62—C63	122.3 (3)
C23—C22—H22	119.5	C61—C62—H62	118.8
C21—C22—H22	119.5	C63—C62—H62	118.8
C22—C23—C24	119.0 (3)	C64—C63—C62	118.2 (3)
C22—C23—C26	120.4 (3)	C64—C63—C66	121.5 (3)
C24—C23—C26	120.6 (3)	C62—C63—C66	120.2 (3)
C25—C24—C23	121.5 (3)	C63—C64—C65	120.9 (3)
C25—C24—H24	119.2	C63—C64—H64	119.6
C23—C24—H24	119.2	C65—C64—H64	119.6
C24—C25—C20	118.4 (3)	C60—C65—C64	119.0 (3)
C24—C25—H25	120.8	C60—C65—H65	120.5
C20—C25—H25	120.8	C64—C65—H65	120.5
C23—C26—H26A	109.5	C63—C66—H66A	109.5
C23—C26—H26B	109.5	C63—C66—H66B	109.5
H26A—C26—H26B	109.5	H66A—C66—H66B	109.5
C23—C26—H26C	109.5	C63—C66—H66C	109.5
H26A—C26—H26C	109.5	H66A—C66—H66C	109.5
H26B—C26—H26C	109.5	H66B—C66—H66C	109.5

Table 2.5. (Continued).

O8—C27—H27A	109.5	O13—C67—H67A	109.5
O8—C27—H27B	109.5	O13—C67—H67B	109.5
H27A—C27—H27B	109.5	H67A—C67—H67B	109.5
O8—C27—H27C	109.5	O13—C67—H67C	109.5
H27A—C27—H27C	109.5	H67A—C67—H67C	109.5
H27B—C27—H27C	109.5	H67B—C67—H67C	109.5
O3—C28—C29	107.0 (2)	O14—C68—C69	110.3 (3)
O3—C28—H28A	110.3	O14—C68—H68A	109.6
C29—C28—H28A	110.3	C69—C68—H68A	109.6
O3—C28—H28B	110.3	O14—C68—H68B	109.6
C29—C28—H28B	110.3	C69—C68—H68B	109.6
H28A—C28—H28B	108.6	H68A—C68—H68B	108.1
C30—C29—C34	117.4 (3)	C70—C69—C74	117.9 (3)
C30—C29—C28	122.2 (3)	C70—C69—C68	118.4 (3)
C34—C29—C28	120.4 (3)	C74—C69—C68	123.6 (3)
C29—C30—C31	122.0 (3)	C71—C70—C69	122.2 (3)
C29—C30—H30	119.0	C71—C70—H70	118.9
C31—C30—H30	119.0	C69—C70—H70	118.9
C32—C31—C30	119.7 (3)	C70—C71—C72	119.7 (3)
C32—C31—H31	120.2	C70—C71—H71	120.2
C30—C31—H31	120.2	C72—C71—H71	120.2
O4—C32—C31	125.3 (3)	O15—C72—C71	124.3 (3)
O4—C32—C33	116.1 (3)	O15—C72—C73	116.8 (3)
C31—C32—C33	118.6 (3)	C71—C72—C73	118.9 (3)
C34—C33—C32	121.0 (3)	C74—C73—C72	120.0 (3)
C34—C33—H33	119.5	C74—C73—H73	120.0
C32—C33—H33	119.5	C72—C73—H73	120.0
C33—C34—C29	121.4 (3)	C73—C74—C69	121.3 (3)
C33—C34—H34	119.3	C73—C74—H74	119.3
C29—C34—H34	119.3	C69—C74—H74	119.3
O4—C35—H35A	109.5	O15—C75—H75A	109.5

Table 2.5. (Continued).

O4—C35—H35B	109.5	O15—C75—H75B	109.5
H35A—C35—H35B	109.5	H75A—C75—H75B	109.5
O4—C35—H35C	109.5	O15—C75—H75C	109.5
H35A—C35—H35C	109.5	H75A—C75—H75C	109.5
H35B—C35—H35C	109.5	H75B—C75—H75C	109.5
O5—C36—H36A	109.5	O16—C76—H76A	109.5
O5—C36—H36B	109.5	O16—C76—H76B	109.5
H36A—C36—H36B	109.5	H76A—C76—H76B	109.5
O5—C36—H36C	109.5	O16—C76—H76C	109.5
H36A—C36—H36C	109.5	H76A—C76—H76C	109.5
H36B—C36—H36C	109.5	H76B—C76—H76C	109.5
O7—C37—O6	123.6 (3)	O18—C77—O17	123.6 (3)
O7—C37—C15	124.6 (3)	O18—C77—C55	127.2 (3)
O6—C37—C15	111.7 (3)	O17—C77—C55	109.2 (3)
O6—C38—H38A	109.5	O17—C78—H78A	109.5
O6—C38—H38B	109.5	O17—C78—H78B	109.5
H38A—C38—H38B	109.5	H78A—C78—H78B	109.5
O6—C38—H38C	109.5	O17—C78—H78C	109.5
H38A—C38—H38C	109.5	H78A—C78—H78C	109.5
H38B—C38—H38C	109.5	H78B—C78—H78C	109.5
O1—S1—N1—C1	-62.8 (2)	O12—S2—N3—C41	-58.6 (2)
O2—S1—N1—C1	167.6 (2)	O11—S2—N3—C41	172.4 (2)
C20—S1—N1—C1	52.7 (2)	C60—S2—N3—C41	57.2 (2)
O1—S1—N1—C19	166.1 (2)	O12—S2—N3—C59	179.1 (2)
O2—S1—N1—C19	36.5 (3)	O11—S2—N3—C59	50.0 (2)
C20—S1—N1—C19	-78.4 (2)	C60—S2—N3—C59	-65.2 (2)
C19—N1—C1—C6	0.8 (3)	C59—N3—C41—C42	-175.2 (3)
S1—N1—C1—C6	-137.9 (2)	S2—N3—C41—C42	56.4 (4)
C19—N1—C1—C2	-178.0 (3)	C59—N3—C41—C46	2.7 (3)
S1—N1—C1—C2	43.3 (4)	S2—N3—C41—C46	-125.8 (2)
C6—C1—C2—C3	1.2 (5)	C46—C41—C42—C43	0.8 (4)

Table 2.5. (Continued).

N1—C1—C2—C3	179.8 (3)	N3—C41—C42—C43	178.4 (3)
C27—O8—C3—C4	-176.5 (3)	C67—O13—C43—C42	0.5 (4)
C27—O8—C3—C2	3.5 (4)	C67—O13—C43—C44	-179.2 (3)
C1—C2—C3—O8	-179.6 (3)	C41—C42—C43—O13	-179.5 (3)
C1—C2—C3—C4	0.3 (5)	C41—C42—C43—C44	0.1 (4)
O8—C3—C4—C5	178.1 (3)	O13—C43—C44—C45	179.1 (3)
C2—C3—C4—C5	-1.9 (5)	C42—C43—C44—C45	-0.5 (5)
C3—C4—C5—C6	1.8 (5)	C43—C44—C45—C46	0.0 (4)
C2—C1—C6—C5	-1.2 (5)	C42—C41—C46—C45	-1.3 (4)
N1—C1—C6—C5	179.9 (3)	N3—C41—C46—C45	-179.3 (2)
C2—C1—C6—C7	177.5 (3)	C42—C41—C46—C47	176.4 (3)
N1—C1—C6—C7	-1.4 (3)	N3—C41—C46—C47	-1.6 (3)
C4—C5—C6—C1	-0.3 (5)	C44—C45—C46—C41	0.8 (4)
C4—C5—C6—C7	-178.6 (3)	C44—C45—C46—C47	-176.2 (3)
C1—C6—C7—C19	1.5 (4)	C41—C46—C47—C59	-0.3 (3)
C5—C6—C7—C19	179.9 (3)	C45—C46—C47—C59	177.0 (3)
C1—C6—C7—C8	-175.3 (3)	C41—C46—C47—C48	-177.6 (3)
C5—C6—C7—C8	3.1 (6)	C45—C46—C47—C48	-0.3 (5)
C19—C7—C8—C9	10.2 (4)	C59—C47—C48—C49	4.9 (4)
C6—C7—C8—C9	-173.4 (3)	C46—C47—C48—C49	-178.1 (3)
C10—N2—C9—C8	-59.8 (3)	C50—N4—C49—C48	-58.4 (3)
C18—N2—C9—C8	65.9 (3)	C58—N4—C49—C48	66.1 (3)
C7—C8—C9—N2	-42.4 (4)	C47—C48—C49—N4	-41.0 (3)
C9—N2—C10—C11	-176.7 (2)	C49—N4—C50—C51	178.6 (2)
C18—N2—C10—C11	58.6 (3)	C58—N4—C50—C51	55.9 (3)
N2—C10—C11—C16	-55.0 (3)	N4—C50—C51—C52	71.8 (3)
N2—C10—C11—C12	70.1 (3)	N4—C50—C51—C56	-53.8 (3)
C10—C11—C12—C13	176.5 (2)	C50—C51—C52—C53	176.3 (2)
C16—C11—C12—C13	-59.2 (3)	C56—C51—C52—C53	-59.5 (3)
C28—O3—C13—C14	78.6 (3)	C68—O14—C53—C52	-53.0 (3)
C28—O3—C13—C12	-49.5 (3)	C68—O14—C53—C54	74.4 (3)

Table 2.5. (Continued).

C11—C12—C13—O3	-170.6 (2)	C51—C52—C53—O14	-171.9 (3)
C11—C12—C13—C14	60.3 (3)	C51—C52—C53—C54	60.5 (3)
C36—O5—C14—C13	-110.9 (3)	C76—O16—C54—C55	146.1 (3)
C36—O5—C14—C15	128.9 (3)	C76—O16—C54—C53	-93.3 (3)
O3—C13—C14—O5	59.8 (3)	O14—C53—C54—O16	58.5 (3)
C12—C13—C14—O5	-170.8 (3)	C52—C53—C54—O16	-172.3 (2)
O3—C13—C14—C15	176.6 (3)	O14—C53—C54—C55	175.7 (2)
C12—C13—C14—C15	-53.9 (3)	C52—C53—C54—C55	-55.1 (3)
O5—C14—C15—C37	-66.5 (3)	O16—C54—C55—C77	-66.5 (3)
C13—C14—C15—C37	174.8 (3)	C53—C54—C55—C77	173.1 (2)
O5—C14—C15—C16	166.5 (2)	O16—C54—C55—C56	169.6 (2)
C13—C14—C15—C16	47.8 (4)	C53—C54—C55—C56	49.3 (3)
C10—C11—C16—C15	178.0 (3)	C50—C51—C56—C57	53.6 (3)
C12—C11—C16—C15	51.7 (3)	C52—C51—C56—C57	-73.3 (3)
C10—C11—C16—C17	52.5 (3)	C50—C51—C56—C55	179.4 (2)
C12—C11—C16—C17	-73.7 (3)	C52—C51—C56—C55	52.4 (3)
C37—C15—C16—C11	-176.7 (2)	C77—C55—C56—C57	-47.7 (3)
C14—C15—C16—C11	-46.8 (4)	C54—C55—C56—C57	76.7 (3)
C37—C15—C16—C17	-52.8 (3)	C77—C55—C56—C51	-172.2 (3)
C14—C15—C16—C17	77.1 (3)	C54—C55—C56—C51	-47.9 (3)
C11—C16—C17—C18	-55.5 (3)	C51—C56—C57—C58	-56.7 (3)
C15—C16—C17—C18	179.6 (2)	C55—C56—C57—C58	178.6 (2)
C9—N2—C18—C19	-50.6 (3)	C49—N4—C58—C59	-49.5 (3)
C10—N2—C18—C19	73.4 (3)	C50—N4—C58—C59	72.9 (3)
C9—N2—C18—C17	179.0 (3)	C49—N4—C58—C57	-177.4 (2)
C10—N2—C18—C17	-57.0 (3)	C50—N4—C58—C57	-55.0 (3)
C16—C17—C18—N2	56.3 (3)	C56—C57—C58—N4	56.2 (3)
C16—C17—C18—C19	-68.4 (3)	C56—C57—C58—C59	-67.9 (3)
C6—C7—C19—N1	-0.9 (3)	C46—C47—C59—N3	2.1 (3)
C8—C7—C19—N1	176.0 (3)	C48—C47—C59—N3	179.6 (3)
C6—C7—C19—C18	-176.5 (3)	C46—C47—C59—C58	-170.6 (3)

Table 2.5. (Continued).

C8—C7—C19—C18	0.5 (5)	C48—C47—C59—C58	6.9 (5)
C1—N1—C19—C7	0.1 (3)	C41—N3—C59—C47	-3.0 (3)
S1—N1—C19—C7	134.5 (2)	S2—N3—C59—C47	123.6 (2)
C1—N1—C19—C18	175.4 (3)	C41—N3—C59—C58	169.6 (3)
S1—N1—C19—C18	-50.2 (4)	S2—N3—C59—C58	-63.8 (3)
N2—C18—C19—C7	19.2 (4)	N4—C58—C59—C47	15.7 (4)
C17—C18—C19—C7	143.5 (3)	C57—C58—C59—C47	140.0 (3)
N2—C18—C19—N1	-155.4 (3)	N4—C58—C59—N3	-155.9 (2)
C17—C18—C19—N1	-31.2 (4)	C57—C58—C59—N3	-31.6 (4)
O1—S1—C20—C21	4.9 (3)	O12—S2—C60—C65	27.4 (3)
O2—S1—C20—C21	136.6 (2)	O11—S2—C60—C65	160.0 (2)
N1—S1—C20—C21	-108.3 (2)	N3—S2—C60—C65	-86.3 (3)
O1—S1—C20—C25	-171.7 (2)	O12—S2—C60—C61	-154.1 (2)
O2—S1—C20—C25	-40.0 (3)	O11—S2—C60—C61	-21.5 (3)
N1—S1—C20—C25	75.1 (3)	N3—S2—C60—C61	92.2 (3)
C25—C20—C21—C22	0.5 (4)	C65—C60—C61—C62	-0.8 (5)
S1—C20—C21—C22	-176.0 (2)	S2—C60—C61—C62	-179.2 (2)
C20—C21—C22—C23	-0.5 (5)	C60—C61—C62—C63	0.9 (5)
C21—C22—C23—C24	0.1 (5)	C61—C62—C63—C64	0.2 (5)
C21—C22—C23—C26	179.1 (3)	C61—C62—C63—C66	-178.2 (3)
C22—C23—C24—C25	0.5 (5)	C62—C63—C64—C65	-1.4 (5)
C26—C23—C24—C25	-178.6 (3)	C66—C63—C64—C65	177.0 (3)
C23—C24—C25—C20	-0.5 (5)	C61—C60—C65—C64	-0.4 (5)
C21—C20—C25—C24	0.0 (4)	S2—C60—C65—C64	178.0 (2)
S1—C20—C25—C24	176.6 (2)	C63—C64—C65—C60	1.5 (5)
C13—O3—C28—C29	-175.4 (2)	C53—O14—C68—C69	-163.1 (2)
O3—C28—C29—C30	-119.7 (3)	O14—C68—C69—C70	166.7 (3)
O3—C28—C29—C34	59.5 (4)	O14—C68—C69—C74	-17.5 (4)
C34—C29—C30—C31	-0.4 (5)	C74—C69—C70—C71	-2.1 (5)
C28—C29—C30—C31	178.8 (3)	C68—C69—C70—C71	173.9 (3)
C29—C30—C31—C32	0.3 (5)	C69—C70—C71—C72	-0.3 (5)

Table 2.5. (Continued).

C35—O4—C32—C31	2.1 (4)	C75—O15—C72—C71	-1.7 (4)
C35—O4—C32—C33	-178.5 (3)	C75—O15—C72—C73	177.4 (3)
C30—C31—C32—O4	179.9 (3)	C70—C71—C72—O15	-179.1 (3)
C30—C31—C32—C33	0.6 (5)	C70—C71—C72—C73	1.9 (5)
O4—C32—C33—C34	179.2 (3)	O15—C72—C73—C74	179.9 (3)
C31—C32—C33—C34	-1.4 (5)	C71—C72—C73—C74	-1.0 (4)
C32—C33—C34—C29	1.3 (5)	C72—C73—C74—C69	-1.5 (5)
C30—C29—C34—C33	-0.4 (5)	C70—C69—C74—C73	3.0 (5)
C28—C29—C34—C33	-179.6 (3)	C68—C69—C74—C73	-172.8 (3)
C38—O6—C37—O7	1.6 (4)	C78—O17—C77—O18	-2.4 (4)
C38—O6—C37—C15	-174.3 (2)	C78—O17—C77—C55	174.3 (2)
C14—C15—C37—O7	159.7 (3)	C54—C55—C77—O18	-11.8 (4)
C16—C15—C37—O7	-69.9 (4)	C56—C55—C77—O18	115.0 (3)
C14—C15—C37—O6	-24.4 (4)	C54—C55—C77—O17	171.6 (2)
C16—C15—C37—O6	106.0 (3)	C56—C55—C77—O17	-61.6 (3)

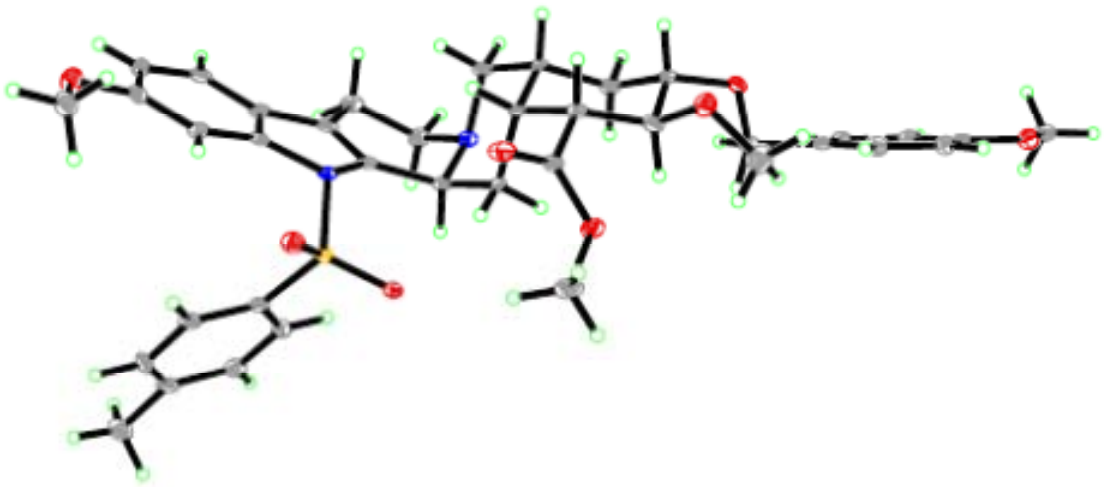

Figure 2.3. Perspective views showing 50% probability displacement.

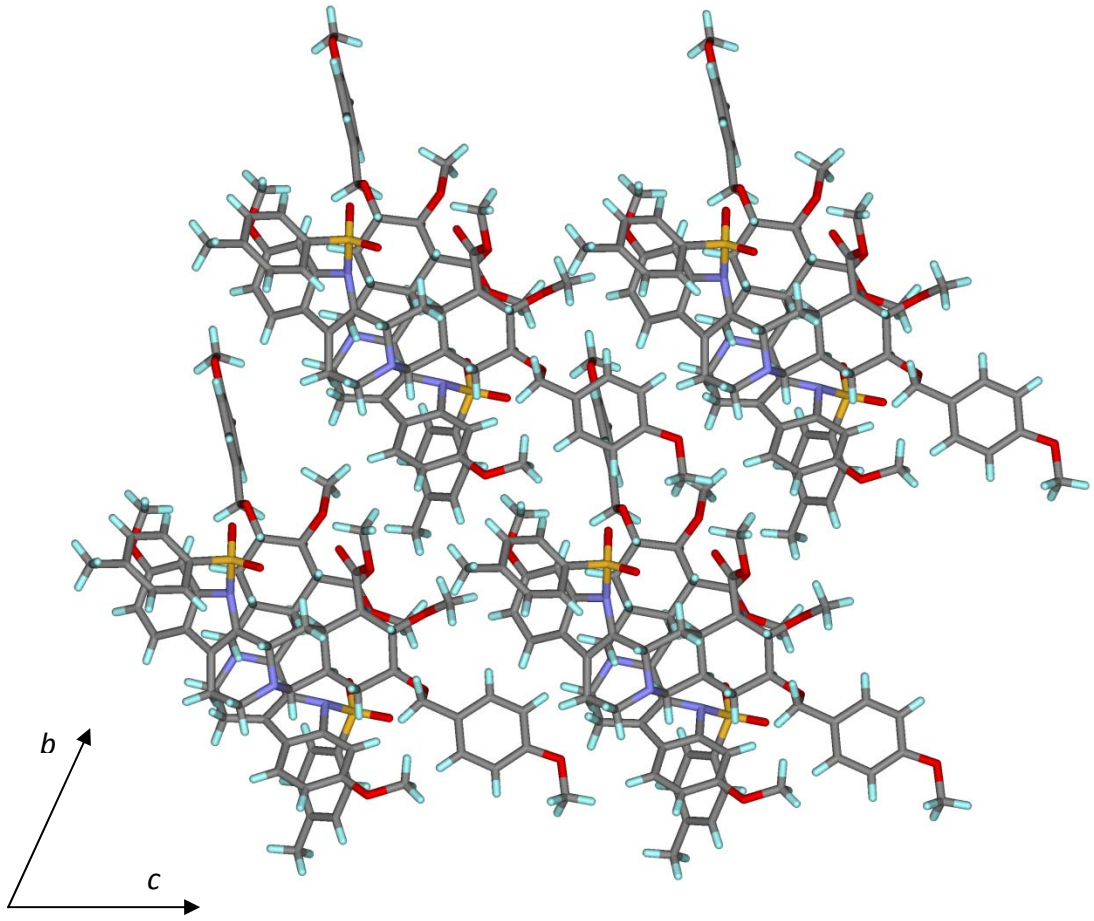

Figure 2.4. Three-dimensional supramolecular architecture viewed along the *a*-axis direction.

Chapter 3

Synthesis of Chiral Bisthiourea Catalysts

3.1. Introduction

Recent mechanistic investigations of a thiourea-catalyzed asymmetric alkylation of α-chloroethers with silyl ketene acetals have led to the hypothesis that two molecules of catalyst are involved in both productive electrophile activation and in nonproductive ground state aggregation. This chapter describes our efforts to synthesize chiral bisthioureas that can activate electrophiles but cannot self-aggregate. Ongoing efforts are presented and future directions are suggested.

3.2. Hydrogen Bond Donor-Assisted Anion-Abstraction

Chiral dual hydrogen bond donors have been shown to catalyze a number of enantioselective transformations of cationic electrophiles through mechanisms involving catalyst-bound ion pairs.[1,2] A particularly effective strategy for generating such electrophiles is through hydrogen bond donor-assisted abstraction of anions from neutral precursors. This mechanism was first investigated in the context of a thiourea-catalyzed Pictet–Spengler-type reaction of *in situ* generated α-chlorolactams (Scheme 3.1A),[3] and since then has been used as a guiding principle to develop asymmetric transformations involving carbenium ions (Scheme 3.1B)[4] and oxocarbenium ions (Scheme 3.1C).[5]

---

[1] a) Doyle, A. G.; Jacobsen, E. N. *Chem. Rev.* **2007**, *107*, 5713. b) Brak, K.; Jacobsen, E. N. *Angew. Chem., Int. Ed.* **2013**, *52*, 534. c) Mahlau, M.; List, B. *Angew. Chem., Int. Ed.* **2013**, *52*, 518. d) Phipps, R. J.; Hamilton, G. L.; Toste, F. D. *Nat. Chem.* **2012**, *4*, 603.

[2] For a review on catalysis via thiourea-bound ion pairs, see: Zhang, Z.; Schreiner, P. R. *Chem. Soc. Rev.* **2009**, *38*, 1187.

[3] Raheem, I. T.; Thiara, P. S.; Peterson, E. A.; Jacobsen, E. N. *J. Am. Chem. Soc.* **2007**, *129*, 13404 .

[4] Brown, A. R.; Kuo, W.-H.; Jacobsen, E. N. *J. Am. Chem. Soc.* **2010**, *132*, 9286.

[5] Reisman, S. E.; Doyle, A. G.; Jacobsen, E. N.; *J. Am. Chem. Soc.* **2008**, *130*, 7198.

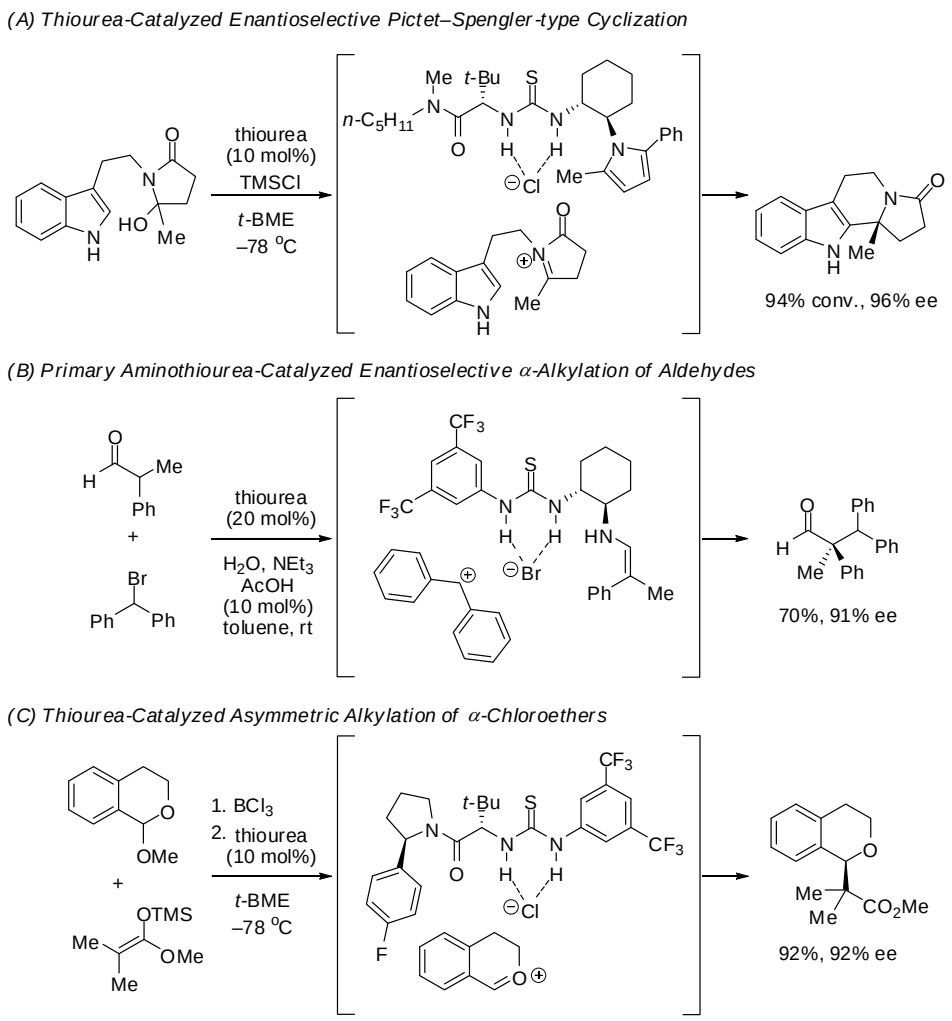

Scheme 3.1. Anion-Abstraction in Thiourea-Catalyzed Transformations

With the goal of gaining insight into the anion-abstraction process, David Ford and Dr. Dan Lehnherr, current Jacobsen group members, have undertaken mechanistic studies on the enantioselective thiourea-catalyzed addition of silyl ketene acetal **1** to pre-formed α-chloroether **2** (Scheme 3.2).[6] This transformation is conducted with 10 mol% of arylpyrrolidino-thiourea **3** and provides isochroman **4** in 85% ee.

[6] Ford, D. D.; Lehnherr, D.; Jacobsen, E. N. *Manuscript in preparation.*

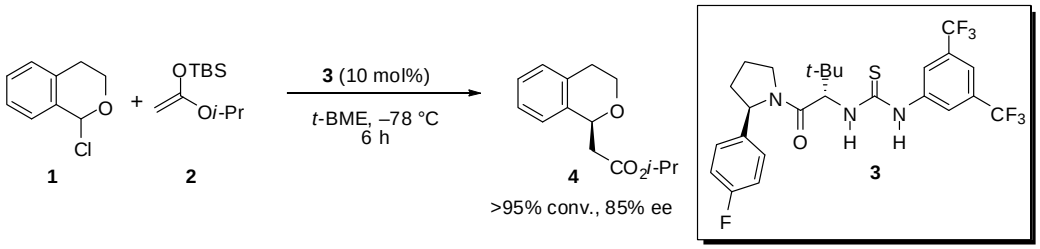

Scheme 3.2. Model Reaction for Mechanistic Investigations

3.3. Proposed Mechanistic Scenario

Through these investigations it was determined that the reaction has a first order kinetic dependence on thiourea at high catalyst concentrations and a second order kinetic dependence at low concentrations. These results are consistent with the involvement of two thiourea molecules in the rate-determining transition state along with a dimeric catalyst resting state at high concentrations and a monomeric catalyst resting state at low concentrations. X-ray crystallographic data, in combination with NMR data, have been used to characterize the dimeric resting state (**5**) in which the hydrogen bond donor functionality of each thiourea is bound to the amide of the other (Figure 3.1). A second thiourea dimerization mode became apparent through analysis of an X-ray crystal structure of the thiourea co-crystallized with tetramethylammonium chloride in a 2:1 stoichiometry (**6**) (Figure 3.2).

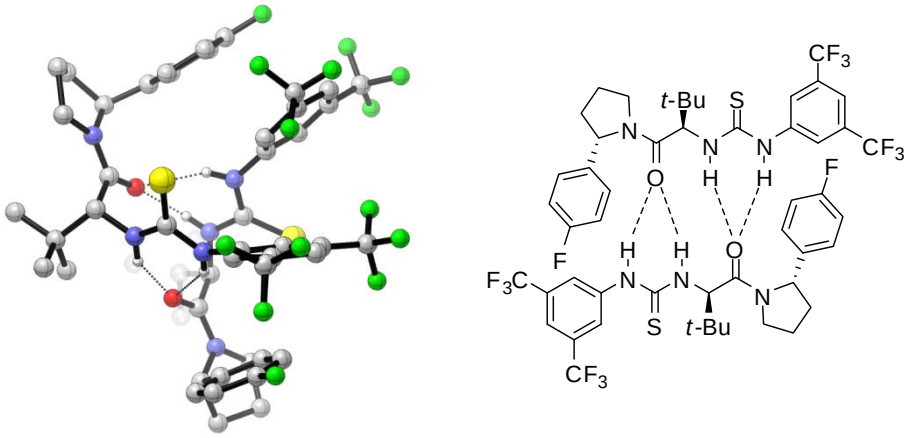

inactive dimer (**5**),
consisting of two molecules of ***ent*-3**

Figure 3.1. Crystal Structure Depicting the Dimeric Resting State of ***ent*-3**

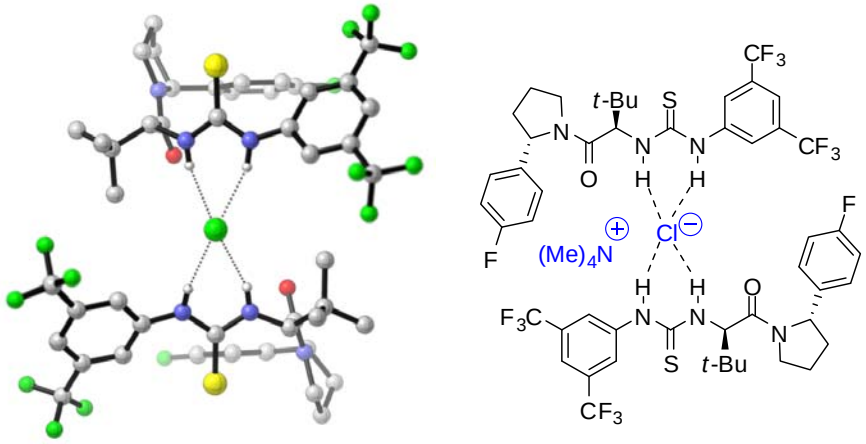

2:1 complex of ***ent*-3**:NMe_4Cl (**6**)

Figure 3.2. Crystal Structure of a 2:1 ***ent*-3**:NMe_4Cl Complex
($[NMe_4]^+$ has been omitted from the left structure for clarity)

Together, these data suggest that the ground state dimer must dissociate and recombine in a productive geometry to allow for dual electrophile activation of α-chloroether substrates via anion-abstraction (Scheme 3.3). Furthermore, this mechanistic scenario raised the possibility that covalently linking two thiourea moieties could prevent inactive dimer formation while allowing for cooperative electrophile activation. Such a

dimer would effectively increase the concentration of active catalyst, potentially allowing for the use of a lower catalyst loading and more efficient catalysis.

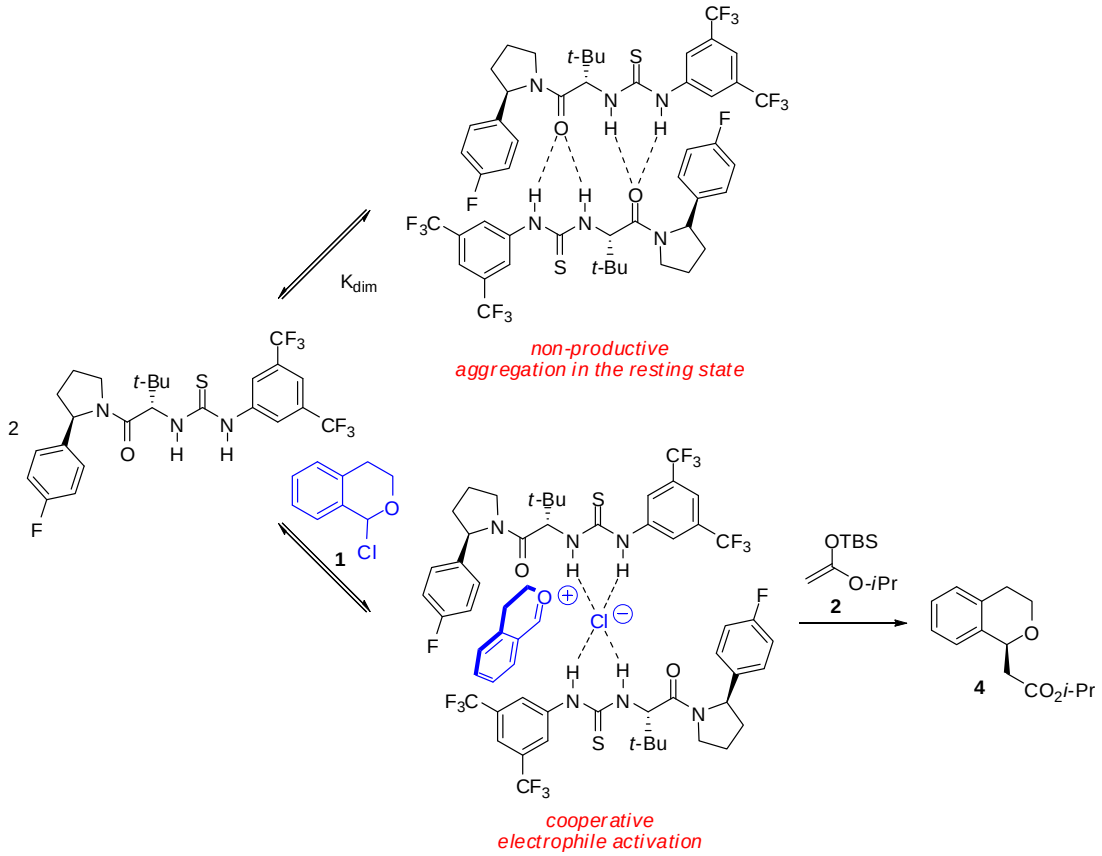

Scheme 3.3. Proposed Mechanistic Scenario for the Thiourea-Catalyzed Addition to Oxocarbenium Ions

With this goal in mind, Dan Lehnherr has investigated various symmetrical tethering strategies (represented as S1–S3, Figure 3.3) and has identified dimeric catalysts that afford higher reactivity than monomer **3** while maintaining comparable selectivity. An examination of crystal structures **5** and **6** suggests that an unsymmetrical linking strategy may better accomplish the goal of selectively disfavoring thiourea-thiourea interactions while enhancing cooperative electrophile activation. The proximity of the amino acid *t*-Bu group of one molecule of catalyst to the aniline-derived portion of

the second catalyst in crystal structure **6**, and the relatively far distance between them in the unproductive aggregate **5**, led to the proposal that tethering these two portions would be beneficial (Figure 3.4). We targeted the synthesis of bisthioureas **7** and **8**.[7] The ester functionality was introduced to aid in the synthetic accessibility of the bisthioureas while maintaining the electron-deficient nature of the parent 3,5-bis(trifluoromethyl)phenyl group. Computational modeling studies using DFT calculations indicated that a 1–2 atom linker (n = 1–2, Figure 3.4) would be optimal to achieve cooperative electrophile activation and conformationally restrict access to the geometry of the unproductive aggregate. For the remainder of the chapter, the top portion of the bisthioureas, as drawn in Figure 3.4, will be referred to as "thiourea A" and the bottom as "thiourea B".

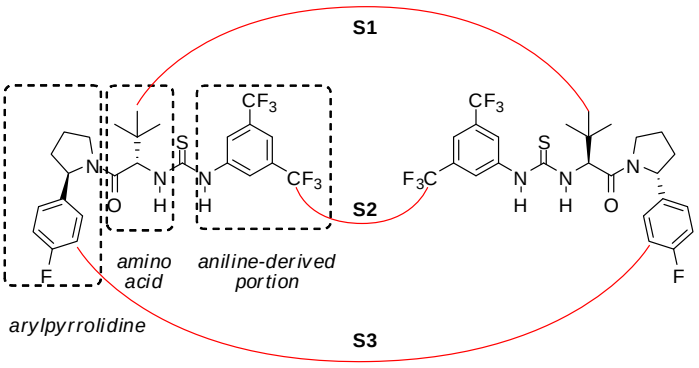

Figure 3.3. Symmetrical Linking Strategies Evaluated

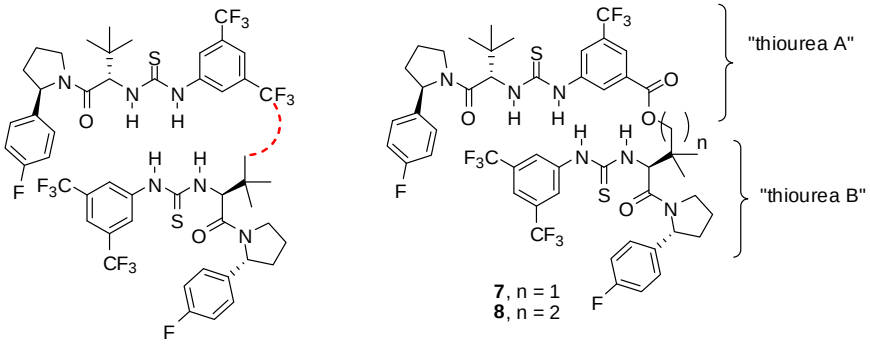

Figure 3.4. Proposed Tethering Strategy and Target Bisthioureas

[7] Bisthioureas **7** and **8** were proposed by Dan Lehnherr.

3.4. Synthetic Strategies

Three potential synthetic routes to access **7** were identified: (1) esterification of two monomeric thioureas, (2) late-stage installation of thiourea B, and (3) late-stage installation of thiourea A (Figure 3.5). Ultimately, the third strategy proved successful. In this section, the problems encountered with the first two routes are described and a successful final route is presented.

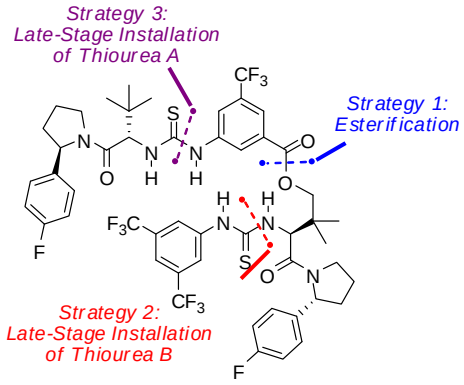

Figure 3.5. Retrosynthetic Analysis of Bisthiourea **7**

3.4.1. Strategy 1: Esterification of Two Functionalized Thiourea Monomers

The most attractive strategy in terms of convergency is an esterification of two functionalized analogs of **3**, carboxylic acid **9** and neopentyl alcohol **10** (Scheme 3.4).[8]

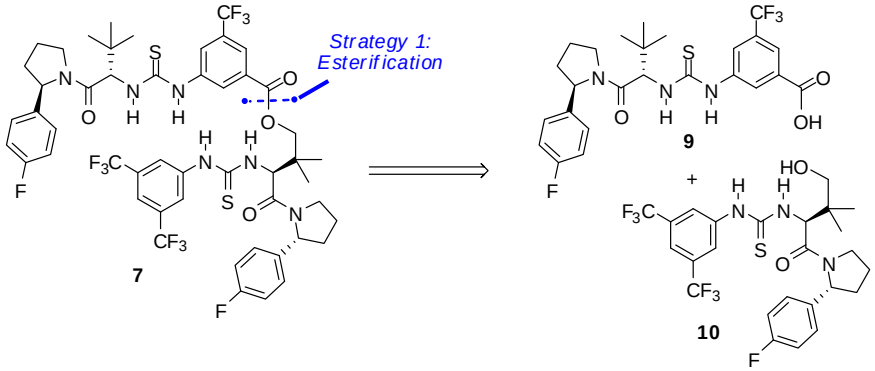

Scheme 3.4. Proposed Esterification Route to Bisthiourea **7**

[8] Another possible coupling strategy is a Mitsunobu reaction of **9** and **10**; however, the conditions would likely result in cyclization of thiourea **10**: Lee, G.-J.; Kim, J. N.; Kim, T. H. *Bull Korean Chem. Soc.* **2002**, *23*, 19.

Carboxylic acid **9** was readily obtained through saponification of methyl ester **11** with LiOH (Scheme 3.5);[9] however, alcohol **10** proved more challenging to access. Dan Lehnherr identified a route to the required amide fragment **14** from (*R*)-pantolactone (**12**) that employs a trimethylaluminum-mediated lactone opening with arylpyrrolidine **13** (Scheme 3.6).[10,11,12] Attempted elaboration of Boc-protected amine **14** to **10** under conditions used for synthesis of monomer **3** furnished undesired thioureas **18** and **19**. Lactone **18** was obtained in 70% yield and was characterized by ^{1}H NMR and LRMS. The outcome indicates that amine deprotection using acidic conditions also effected amide bond cleavage to afford **16** and **17**, which subsequently react with isothiocyanate **15**. These results were unexpected because acidic conditions have been used to effect the deprotection of Boc-amines on related primary alcohol intermediates without amide hydrolysis.[13,14]

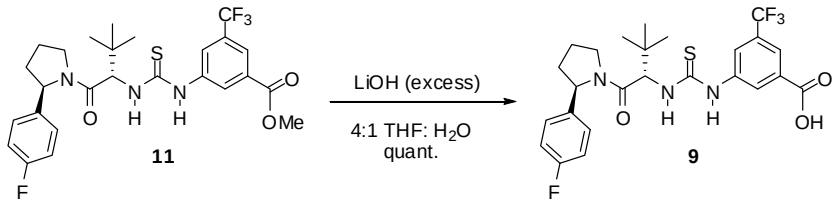

Scheme 3.5. Synthesis of Carboxylic Acid **9**

[9] Hydrolysis of symmetrical thiourea dimers linked through the aniline-derived portion also provided a route to carboxylic acid **9**. The analogous hydrolysis of dimers linked through the hydroxy-*tert*-leucine amino acid residues did not afford alcohol **10**.

[10] Freskos, J. N. *Synth. Commun.* **1994**, *24*, 557.

[11] Marshall, J. A.; Piettre, A.; Paige, M. A.; Valeriote, F. *J. Org. Chem.* **2003**, *68*, 1771.

[12] Arylpyrrolidine **13** was synthesized according to the reported procedure: Reddy, L. R.; Das, S. G.; Liu, Y.; Prashad, M. *J. Org. Chem.* **2010**, *75*, 2236.

[13] Augeri, D. J. et al. *J. Med. Chem.* **2005**, *48*, 5025.

[14] We also attempted a ring-opening of lactone **18** with arylpyrrolidine **13** in the presence of $AlMe_3$; however, the desired amide was not formed.

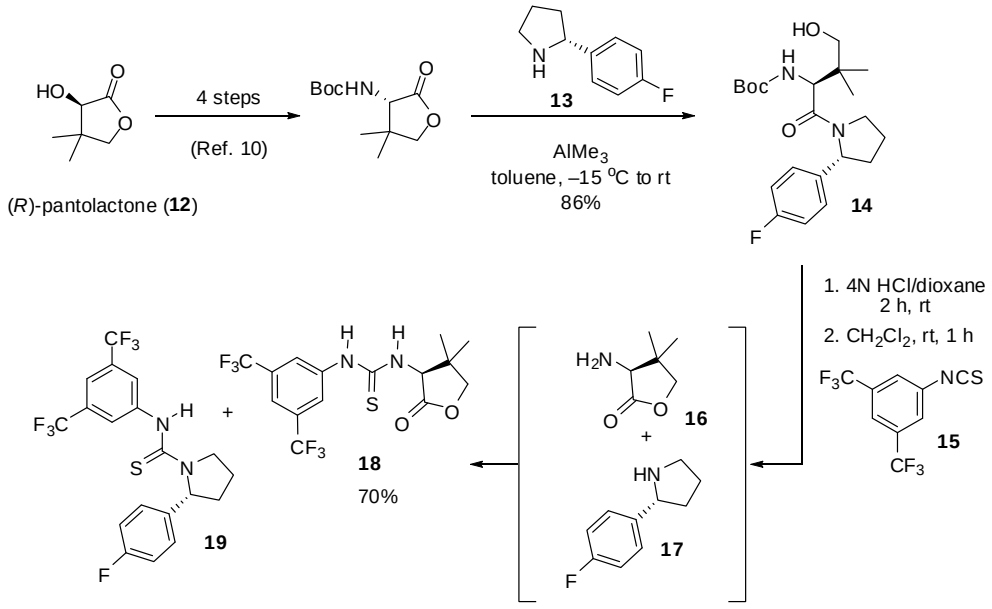

Scheme 3.6. Amide Bond Cleavage During Amine Deprotection

Based on these results, we protected primary alcohol **14** as the corresponding benzyl ether **20** to access thiourea **21** (Scheme 3.7). However, attempted hydrogenolysis of the benzyl ether to obtain primary alcohol **10** was unsuccessful.[15] Because we were encountering problems obtaining alcohol **10**, we chose to focus on two alternative routes to bisthiourea **7**: a late-stage installation of thiourea B and a late-stage installation of thiourea A.

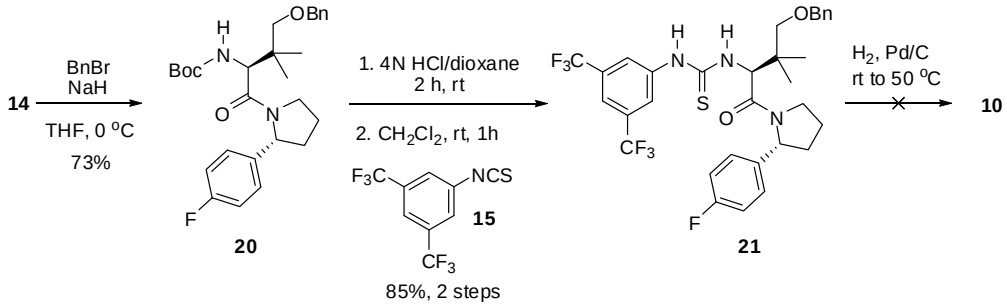

Scheme 3.7. Synthesis of Benzyl Ether **21**

[15] Recent results obtained by Dr. Kaid Harper, a postdoctoral fellow in the group, indicate that cleavage of a silyl ether related to **21** is also problematic.

3.4.2. Strategy 2: Late-Stage Installation of Thiourea B

Our second strategy, late-stage installation of thiourea B (Scheme 3.8), also presented a problematic amine deprotection.

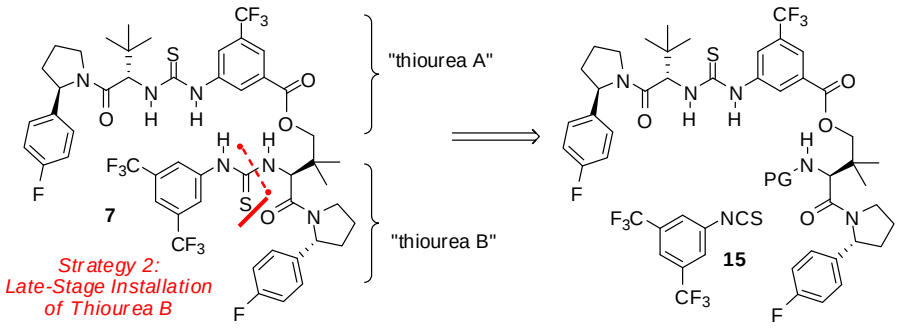

Scheme 3.8. Proposed Late-Stage Installation of Thiourea B

Alcohol **14** was elaborated to isothiocyanate **24** through a three-step sequence consisting of esterification, transfer hydrogenation of the aromatic nitro group, and a subsequent reaction with thiophosgene (Scheme 3.9). The crude isothiocyanate **24** was treated with amine **25** to complete installation of thiourea A. Unfortunately, deprotection of intermediate **26** was accompanied by undesired reactions, resulting in a complex mixture of products (Scheme 3.10). Although the byproducts were not rigorously characterized, mass spectrometric analysis of the crude reaction mixture indicated that loss of an arylpyrrolidine fragment occurred during removal of the Boc group.[16] We did not determine which of the two amide bonds of **26** was cleaved, but based on literature precedent we hypothesize that it was the amide of thiourea A.[17] In analogy to the outcome of the attempted deprotection of Boc-amine **14** in the presence of a free primary

[16] When the reaction was monitored by LC/MS, the peaks corresponding to the masses of [**26** – Boc]$^+$, [**26** – arylpyrrolidine]$^+$, and [**26** – Boc – arylpyrrolidine]$^+$ were all present, suggesting that amide bond cleavage occurs competitively with removal of the Boc group.

[17] Analogous acid-promoted cyclizations have been reported: a) Lehmann, J.; Linden, A.; Heimgartner, H. *Tetrahedron* **1998**, *54*, 8721. b) Breitenmoser, R. A.; Linden, A.; Heimgartner, H. *Helv. Chim. Acta* **2002,** *85*, 990.

alcohol (Scheme 3.6), it is likely that the thiourea functionality serves as an internal nucleophile under the deprotection conditions to generate 5-membered cyclic product **28** (or a related tautomeric structure). With a different protecting group choice, this route may be viable. Ultimately, with the success of the third route, we did not investigate this strategy any further.

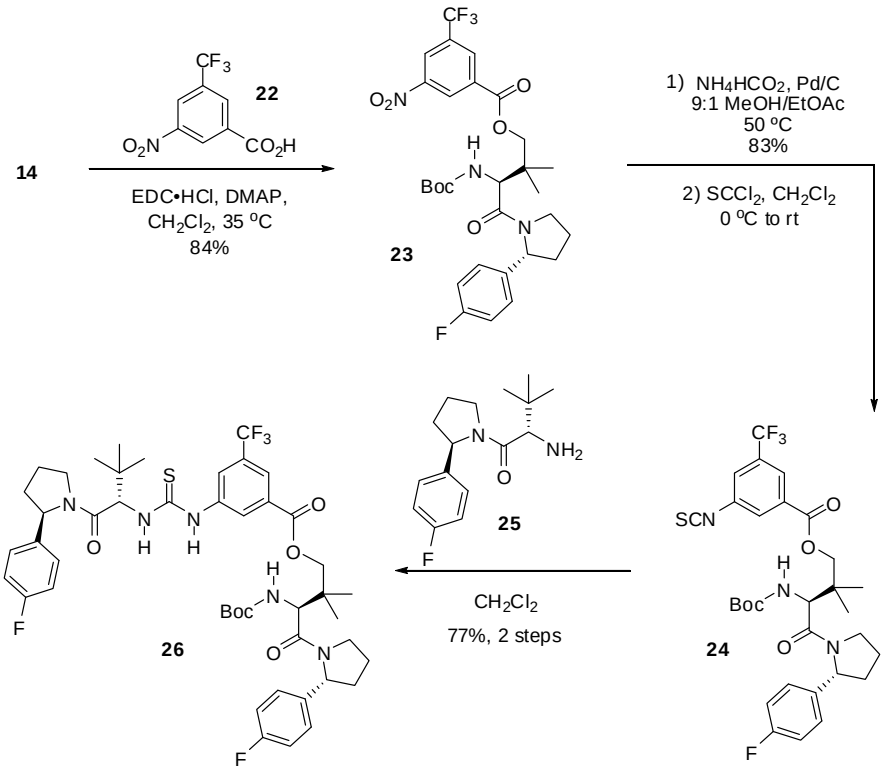

Scheme 3.9. Synthesis of Intermediate **26**

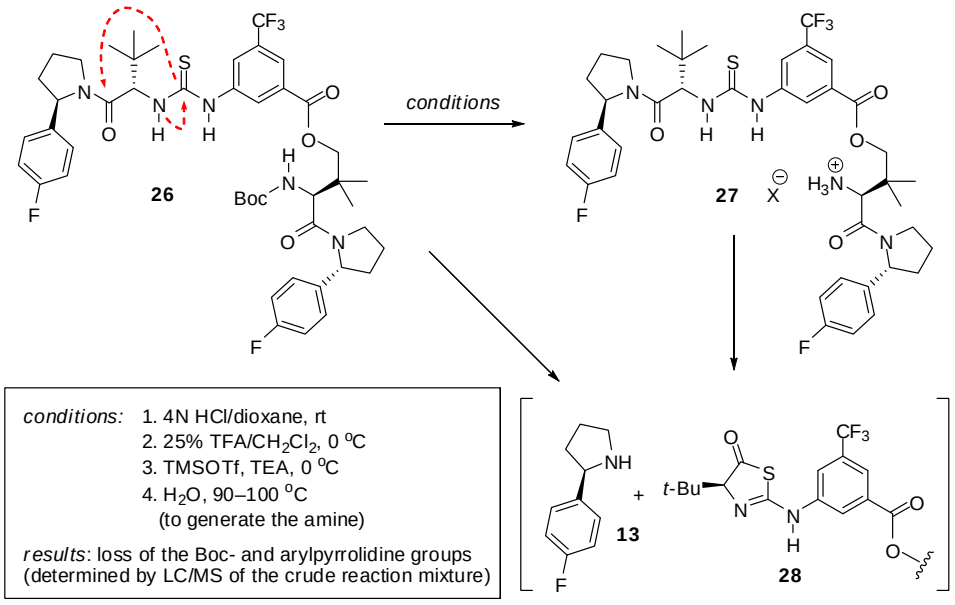

Scheme 3.10. Potential Rearrangement during the Deprotection of Intermediate **26**

3.4.3. Strategy 3: Late-Stage Installation of Thiourea A

The route that proved to be most fruitful was a late-stage installation of thiourea A (Scheme 3.11).

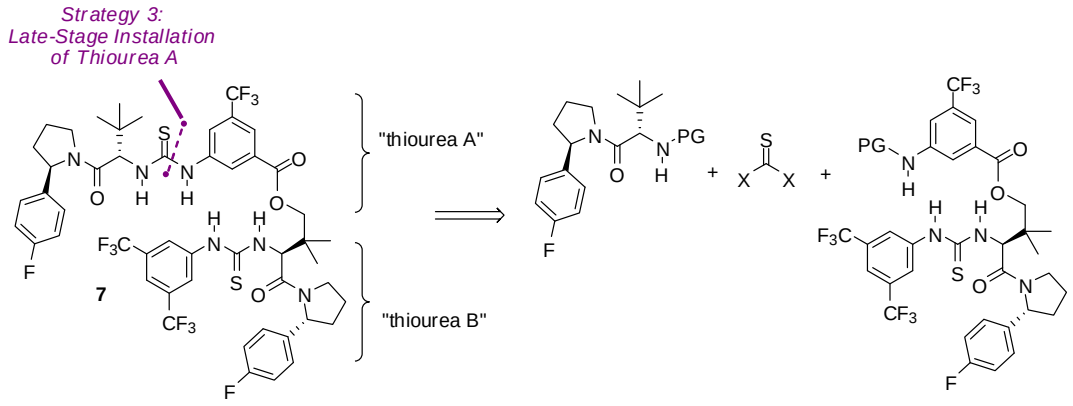

Scheme 3.11. Proposed Late-Stage Installation of Thiourea A

From intermediate **23**, removal of the Boc group followed by a subsequent reaction with isothiocyanate **15** installed thiourea B (Scheme 3.12). The success of the amine deprotection in this context lends support to the hypothesis that amide bond

cleavage only occurs under acidic conditions when the intermediate contains an internal nucleophile. Hydrogenation of the nitro group of **29** could be accomplished with palladium on carbon at 50 °C. [18] Aniline **30** was treated with 1,1'-thiocarbonyldiimidazole to access an isothiocyanate that was reacted with amine **25** to furnish desired bisthiourea **7**.

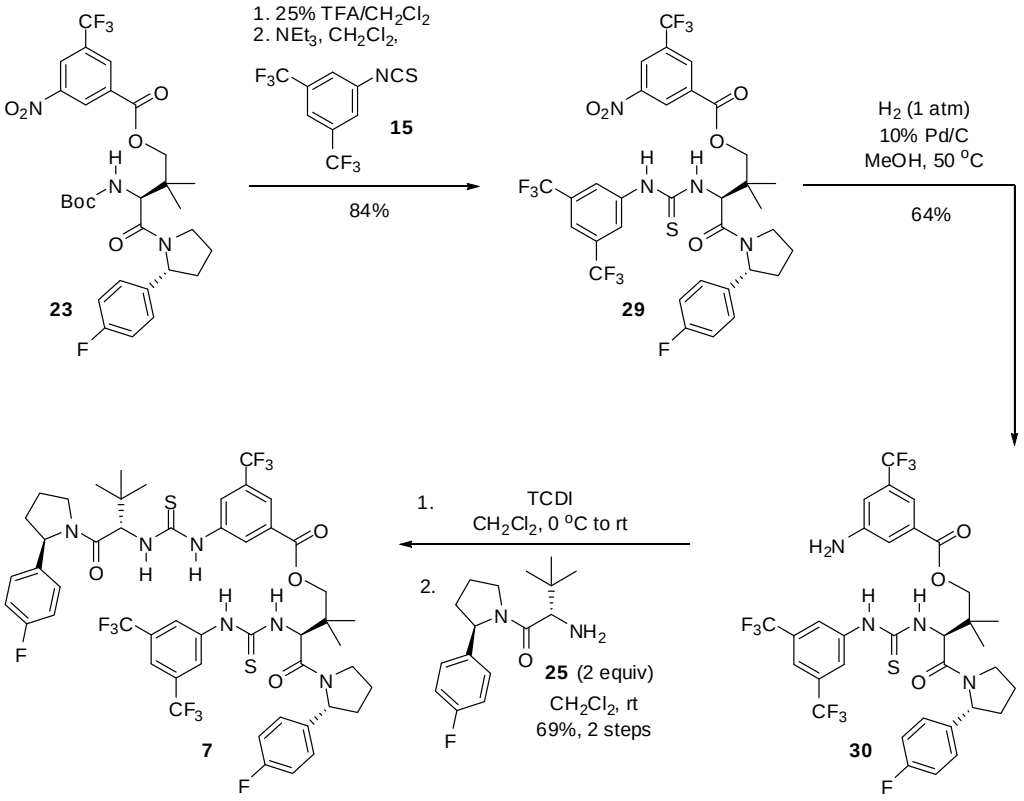

Scheme 3.12. Synthetic Route to Bisthiourea **7**

*3.4.4. Synthesis of Bisthiourea **8***

We used the same strategy to access bisthiourea **8**, which contains a 2-carbon linker between the two thiourea moieties. We obtained the necessary primary alcohol **35**

[18] Hydrogenation of **29** with Pd/C at room temperature and 20 atm H_2 resulted in over reduction to the corresponding cyclohexylamine. Other reductions evaluated (e.g. NH_2HCO_2 transfer hydrogenation, $SnCl_2$, room temperature hydrogenation) stalled at the hydroxylamine stage (determined by LRMS). The difficulty of this reduction is in contrast to the straightforward reduction of **23** (Scheme 3.9) and suggests that thiourea B may be poisoning the reagents or interacting with the nitro group.

through the sequence presented in Scheme 3.13. Amino acid **32** was obtained in 93% ee and was synthesized according to the procedure reported by Rossi.[19] This route uses an Ireland-Claisen rearrangement of Boc-glycine ester **31** and a classical resolution of the resultant racemic amino acid with (*S*)-phenylglycinol **33**. Amide **34** was formed using EDC and HOBt, and a subsequent hydroboration-oxidation sequence afforded primary alcohol **35**. The completion of the synthesis of bisthiourea **8** is shown in Scheme 3.14.

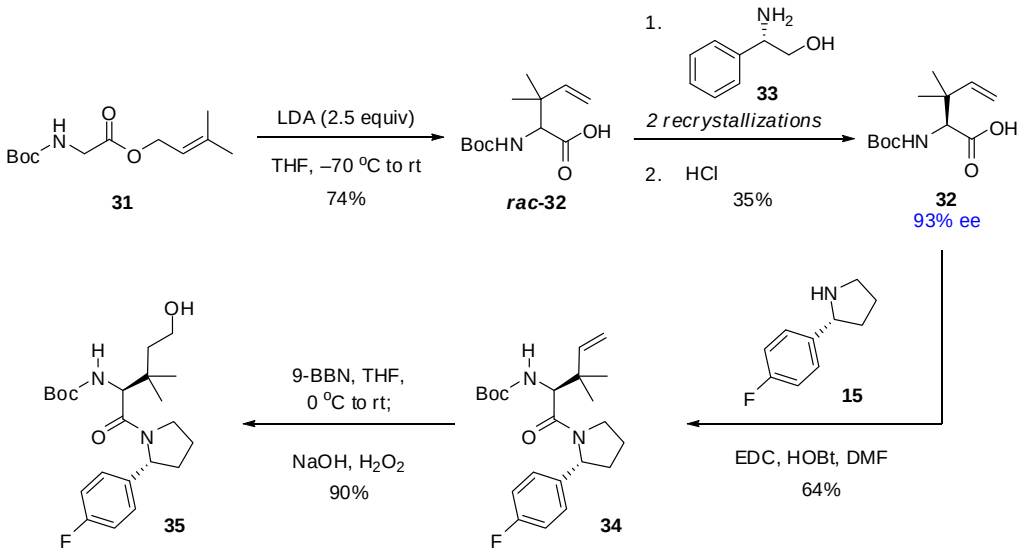

Scheme 3.13. Synthesis of arylpyrrolidino-amide fragment **35**

[19] Rossi, F. et al. *Org. Process Res. Dev.* **2008**, *12*, 322.

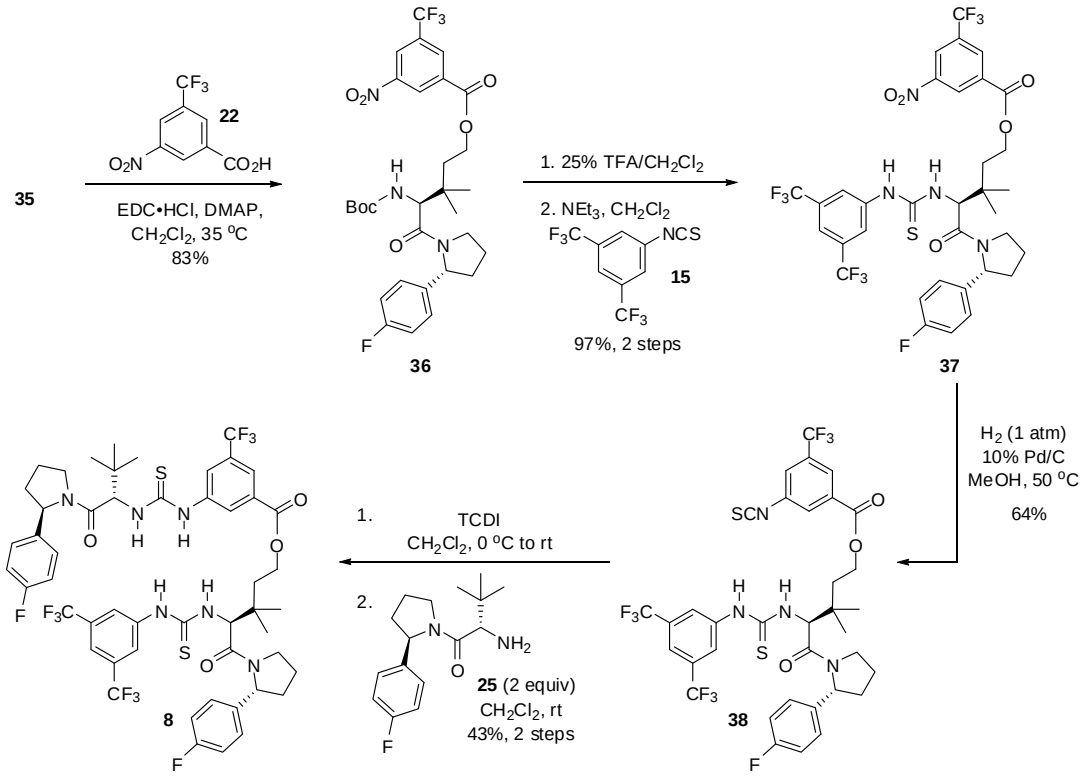

Scheme 3.14. Synthesis of Bisthiourea **8**

This sequence was first used to generate approximately 90 mg of bisthiourea **8**. After we obtained encouraging preliminary data on the reactivity of this catalyst (see Section 3.4), Dr. Masayuki Wasa, a postdoctoral fellow in the group, investigated the scalability of this route. Through this effort, he was able to synthesize 1.3 g of bisthiourea **8**, and he also used isothiocyanate **39** as a diversification point to prepare bisthioureas **40** and **41** (Scheme 3.15).

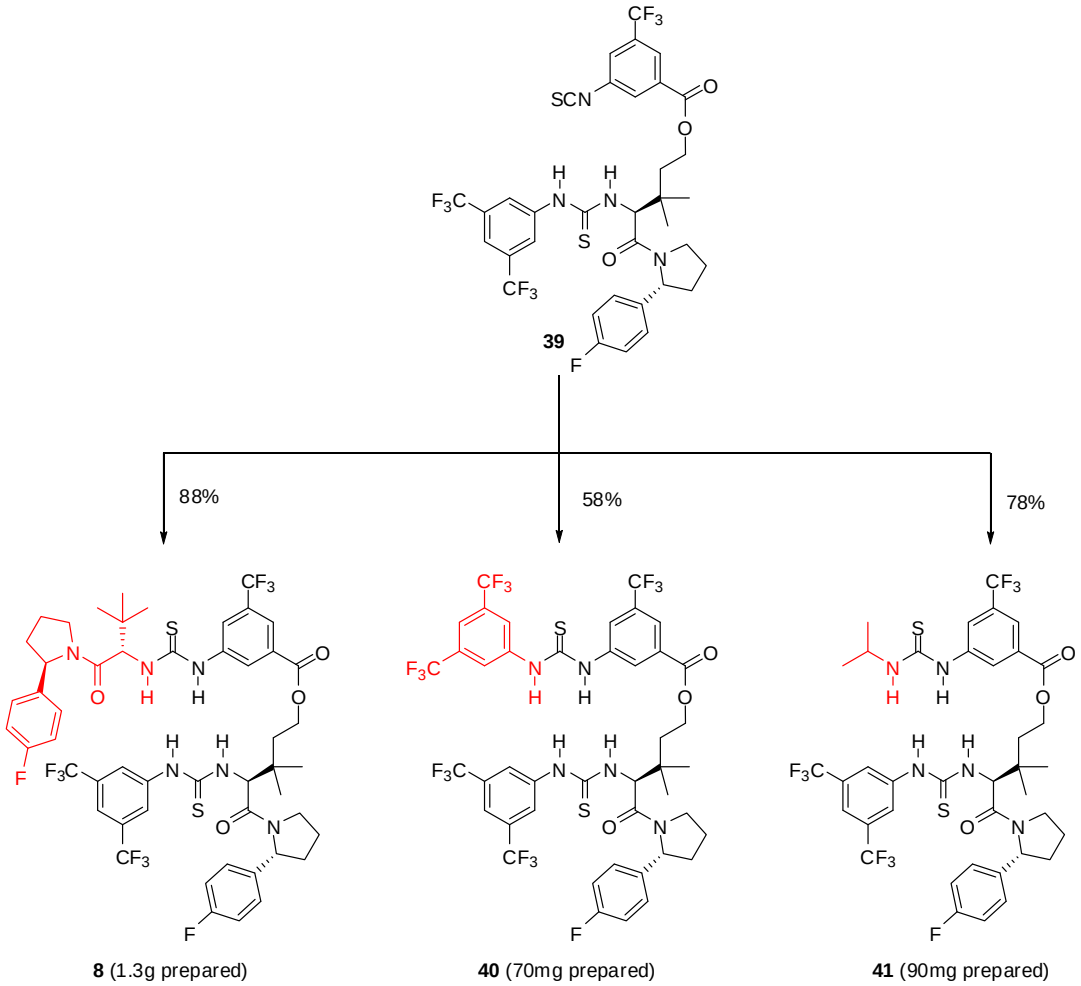

Scheme 3.15. Gram-scale Preparation of Bisthiourea **8**

3.5. Comparison of Bisthioureas 7 and 8 with Monomer 3

The thiourea-catalyzed asymmetric alkylation of α-chloroether **1** with silyl ketene acetal **2** was evaluated with the standard monomeric catalyst (**3**) and bisthioureas **7** and **8** (Scheme 3.16).[20] In order to determine the relative reactivity of the three thioureas, a low catalyst loading (1 mol%, based on thiourea moiety) and a short reaction time (1 hour) were used in this assay. Under these conditions, thiourea **3** afforded isochroman **4** in 6% yield and 81% ee. Bisthioureas **7** and **8** afforded significantly higher conversions, albeit

[20] These results were obtained by Dan Lehnherr.

with slightly diminished selectivity. Bisthiourea **8**, with a 2-atom linker, was more reactive and marginally more selective than **7**, providing 95% conversion and 77% ee.

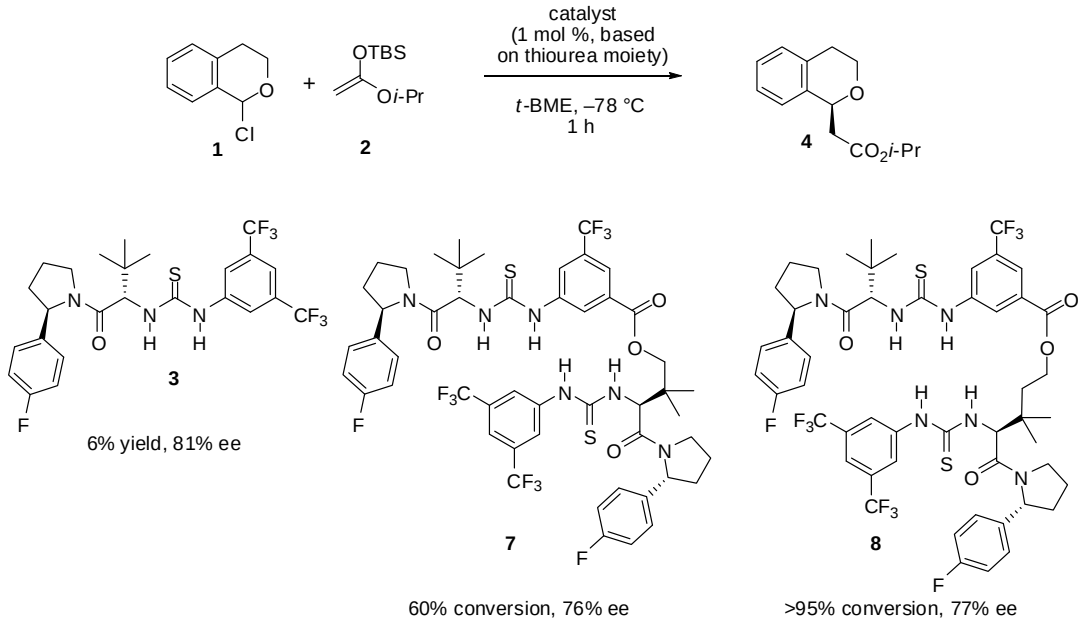

Scheme 3.16. Comparison of monomer **3** and bisthioureas **7** and **8**

3.6. Conclusions and Outlook

The syntheses of bisthioureas **7** and **8** were accomplished through sequential installations of thiourea B and thiourea A. The final route is scalable and has been used to access 1.3 grams of bisthiourea **8**. Most importantly, these covalently tethered thioureas demonstrate substantially higher reactivity than analogous monomeric thioureas in the asymmetric alkylation of α-chloroethers. Current efforts in the Jacobsen group are focused on probing the generality of these observations. Dr. Kaid Harper, a postdoctoral fellow in the group, has recently made a comparison of monomer **3** and bisthiourea **8** in a catalyst-controlled diastereoselective glycosylation of propargyl alcohol with α-chloroether **42** (Scheme 3.17). The background reaction of chloroether **42** (9:1 α:β) with

propargyl alcohol provides the corresponding product **43** in a 3:1 diastereomeric ratio in favor of the α-anomer. The product ratio is unchanged in the presence of monomeric thiourea **3**, but it is reversed to 1:5.7 in the presence of bisthiourea **8**. Although the basis for this reversal of diastereoselectivity is not well understood at this time, it is clear that there is a benefit to using bisthiourea **8**.

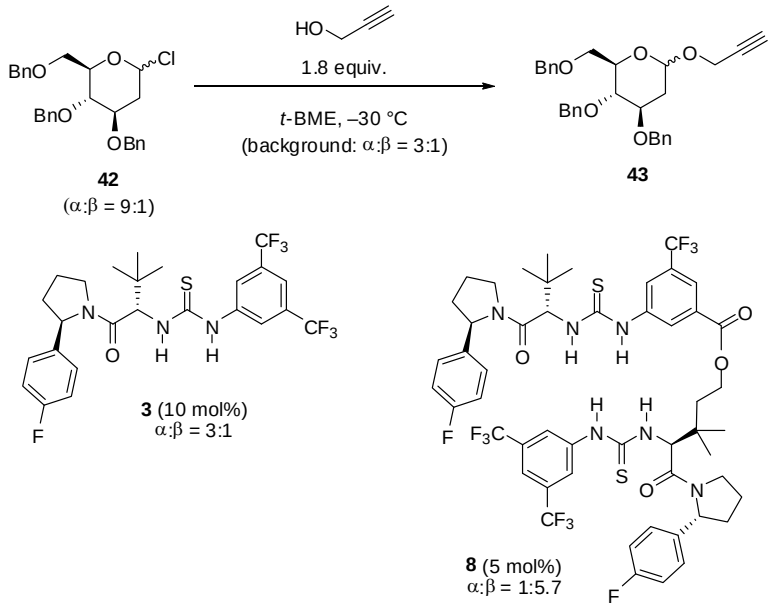

Scheme 3.17. Preliminary Results in a Thiourea-Catalyzed Glycosylation

Ongoing work in the group involves the modification of various portions of bisthiourea **8** to enhance reactivity and selectivity. Because an esterification of two thiourea monomers (Strategy 1, section 3.3.1) is potentially the most convergent route to bisthioureas, this strategy should be revisited. It is possible that the problems encountered in the synthesis of **7** will be alleviated with the longer tether length of **8**.

Additionally, the symmetrical orientation of the two monomeric catalysts in the 2:1 complex with tetramethylammonium chloride (**6**, Figure 3.2) suggests that a cyclic dimer scaffold may provide an optimal geometry for productive electrophile activation

(Scheme 3.18). Although macrocyclization to obtain large cyclic structures is often challenging, we envision that chloride-binding properties of thioureas can be exploited in a templated macrolactonization to provide access to 22-membered cyclic dimer **44**.[21,22]

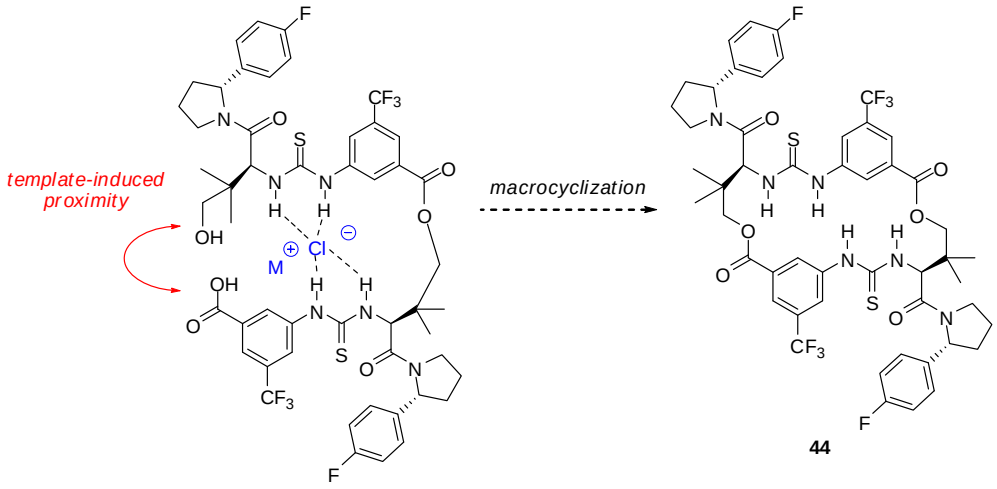

Scheme 3.18. Proposed Template-Induced Macrolactonization

Our progress towards this dimer, a cyclic analog of bisthiourea **7**, is summarized in Scheme 3.19. Isothiocyanate **47** was prepared from ester **23** according to the developed route. The remaining steps, installation of thiourea A and macrocyclization, will likely be challenging and may require protecting group manipulations. As such, it will be best to pursue a cyclic dimerization once an optimal bisthiourea is identified.

[21] For a general review of templated macrocylizations, see: Laughrey, Z. R.; Gibb, B. C. in *Top. Curr. Chem.* Vol. 249 (Eds. Schalley, C. A.; Vögtle, F.; Dötz, K. H.) Springer-Verlag, Heidelberg, **2005**, 67.

[22] For a recent example of a chloride-templated macrolactamization, see: Kataev, E. A.; Kolesinkov, G. V.; Arnold, R.; Lavrov, H. V.; Khrustalev, V. N. *Chem. Eur. J.* **2013**, *19*, 3710.

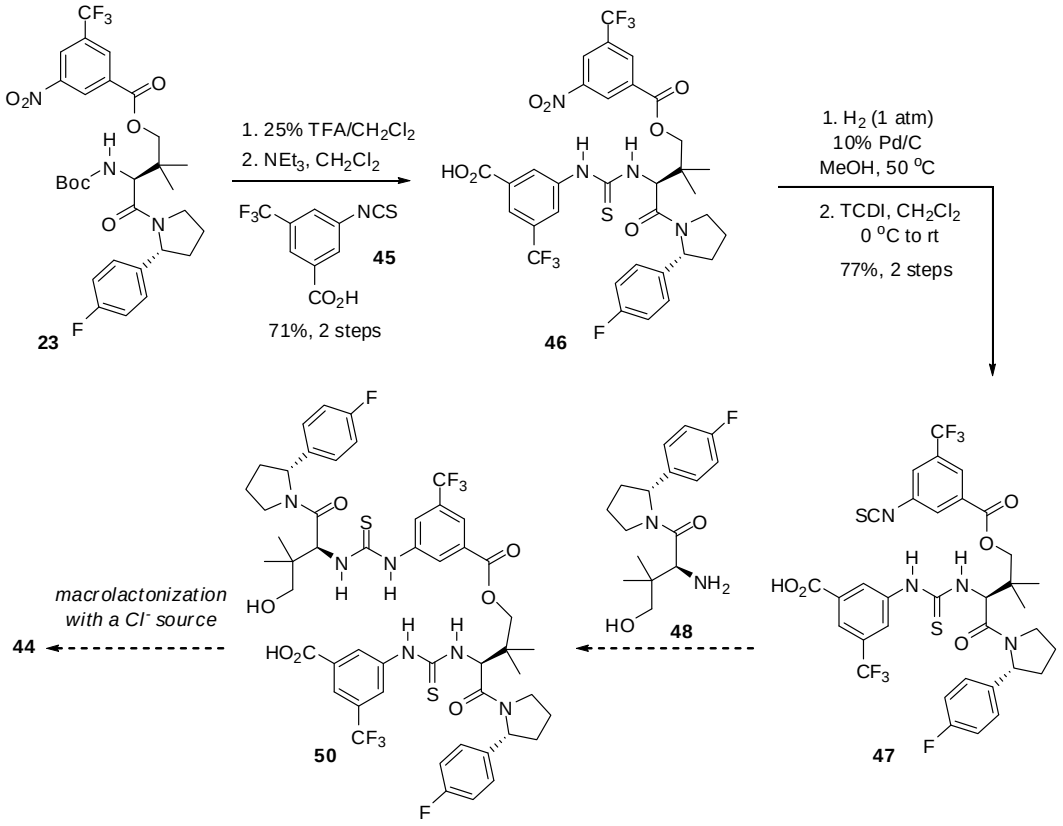

Scheme 3.19. Progress towards Cyclic Dimer **44**

3.7. Experimental Section

A. General Information.

Unless otherwise noted, all reactions were performed under a positive pressure of anhydrous nitrogen or argon in flame- or oven-dried glassware. Moisture- and air-sensitive reagents were dispensed using oven-dried stainless steel syringes or cannulae and were introduced to reaction flasks through rubber septa. Reactions conducted below ambient temperature were cooled by external baths (dry ice/acetone for –78 ^{o}C and ice/water for 0 ^{o}C). Reactions conducted above ambient temperature were heated by an oil bath.

Analytical thin layer chromatography (TLC) was performed on glass plates pre-coated with silica 60 F_{254} plates, 0.25 mm). Visualization was carried out by exposure to a UV-lamp (short wave 254 nm, long wave 365 nm), and by heating after staining the plate with a ceric ammonium molybdate or a potassium permanganate solution. Extraction and chromatography solvents were reagent or HPLC grade and were used without further purification. Flash chromatography was carried out over silica gel (60 Å, 230–400 mesh) from EM Science. Where indicated, chromatography was conducted on a Biotage Isolera automated chromatography system.

Materials. Commercial reagents and solvents were used with the following exceptions: tetrahydrofuran, dichloromethane, and 1,4-dioxane employed as reaction solvents were dried by passage through columns of activated alumina. Triethylamine was distilled from calcium hydride at 760 torr prior to use. Chloroform-d was dried over 3Å MS prior to use.

Instrumentation. Proton nuclear magnetic resonance (^{1}H NMR) spectra and carbon nuclear magnetic resonance (^{13}C NMR) spectra were recorded on a Varian Mercury-400 (400MHz), Inova-500 (500MHz), or an Inova-600 (600MHz) spectrometer at 23 ^{o}C. Chemical shifts for protons are reported in parts per million (ppm, δ scale) downfield from tetramethylsilane and are referenced to residual protium in the NMR solvent ($CHCl_3$: 7.26 ppm).

B. Preparation and Characterization of Selected Intermediates

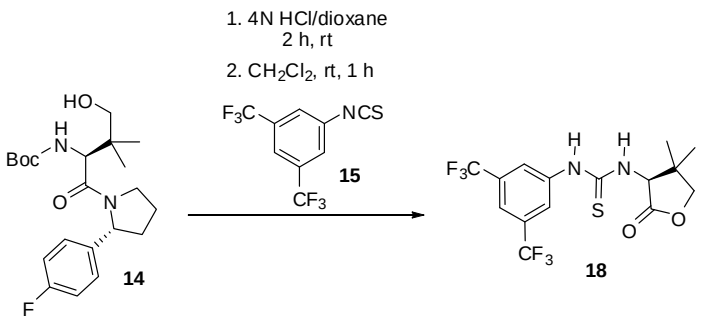

(S)-1-(3,5-bis(trifluoromethyl)phenyl)-3-(4,4-dimethyl-2-oxotetrahydrofuran-3-yl)thiourea (**18**)

A flame-dried 10-mL round-bottom flask was charged with alcohol **14** (50 mg, 0.127 mmol, 1.0 equiv) and dioxane (1.27 mL). The flask was cooled to 0 ^{o}C and a solution of HCl in dioxane (127 μL, 0.508 mmol, 4.0 equiv) was added dropwise under an atmosphere of N_2. The reaction mixture was allowed to gradually warm to room temperature over a period of 2 h. At this point, the reaction mixture was concentrated in vacuo to provide a sticky oil. The crude product was dissolved in CH_2Cl_2 (650 μL). NEt_3 (53 μL, 3.0 equiv) and isothiocyanate **15** (26 μL, 0.143 mmol, 1.1 equiv) were added sequentially and the reaction mixture was stirred at room temperature overnight. The

contents were concentrated in vacuo and purified via flash column chromatography (Biotage, SiO_2, 0-50% EtOAc/hexanes) to afford **18** as a pale yellow solid (35.2 mg, 0.088 mmol, 70% yield). R*f*=0.47 (50% EtOAc/hexanes). ^{1}H NMR (500 MHz, $CDCl_3$) δ ppm 7.76 - 7.98 (m, 5 H) 4.24 (s, 1 H) 3.73 (d, *J*=10.74 Hz, 1 H) 3.56 (d, *J*=10.74 Hz, 1 H) 1.18 (s, 3 H) 1.11 - 1.14 (m, 3 H).

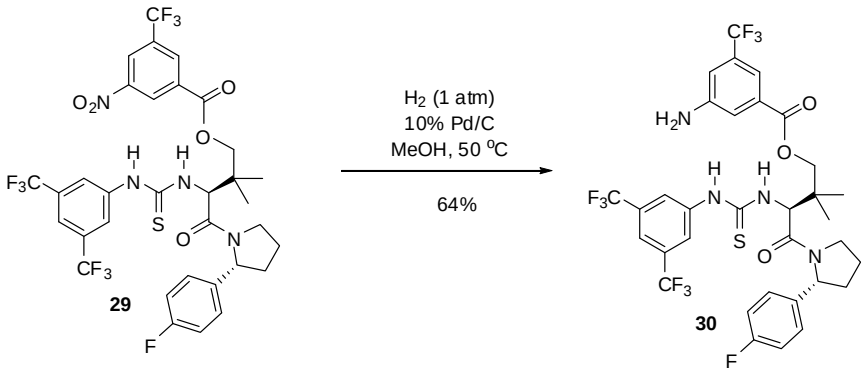

Aniline (**30**)

A flame-dried 50-mL round-bottom flask was charged with a stir bar and 10% Pd/C (44 mg, 0.4 equiv). The flask was fitted with a septum, evacuated, and refilled with argon. MeOH (4.0 mL) was added to the flask under an atmosphere of argon, followed by a solution of nitro aromatic **29** (152 mg, 0.19 mmol, 1 equiv) in MeOH (4.1 mL). The flask was evacuated and refilled with H_2 gas (3x) and then maintained under an atmosphere of H_2. The flask was immersed in an oil bath set at 50 °C and stirred at this temperature overnight. The hydrogen balloon was removed and the contents of the flask were filtered through a short pad of Celite®. The filtrate was concentrated in vacuo to provide a dark brown product, which was carried forward without further purification. In $CDCl_3$ the compound exists as a 1.7:1 mixture of rotamers. One of the resonances in the ^{1}H NMR spectrum corresponding to a proton of the minor rotamer was integrated to 1, and all other integration data are reported relative to it. ^{1}H NMR (500 MHz, $CDCl_3$ δ

ppm 9.24 (s, 1.4 H) 8.92 (br. s., 2.1 H) 7.94 (s, 2 H) 7.80 (s, 3.7 H) 7.51 - 7.70 (m, 9.7 H) 7.42 (m, 1.1 H) 7.23 (m, 1.8 H) 7.05 (s, 1.7 H) 6.92 - 7.01 (m, 6 H) 6.66 - 6.74 (m, 3.6 H) 5.93 (d, *J*=9.62 Hz, 1.7 H) 5.89 (d, *J*=7.78 Hz, 1 H) 5.61 (d, *J*=10.07 Hz, 1 H) 5.05 - 5.10 (m, 1.9 H) 4.47 - 4.55 (m, 2 H) 4.28 - 4.33 (m, 1.8 H) 4.22 - 4.28 (m, 1.9 H) 4.07 (s, 3.1 H) 3.98 - 4.03 (m, 1.7 H) 3.79 - 3.89 (m, 2.9 H) 3.51 - 3.66 (m, 2.4 H) 2.26 - 2.38 (m, 1.6 H) 2.14 - 2.24 (m, 2.4 H) 1.91 - 2.01 (m, 4.0 H) 1.75 - 1.89 (m, 5 H) 1.28 (s, 4.3 H) 1.26 (s, 4.3 H) 0.96 - 1.00 (m, 3 H) 0.70 (s, 3 H).

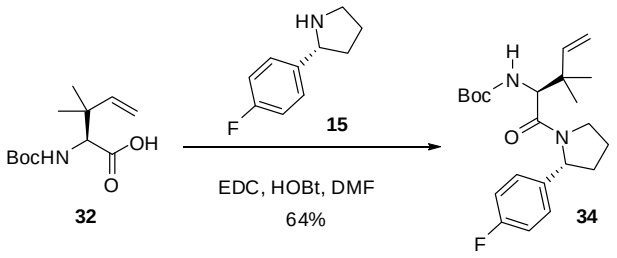

tert-butyl (*S*)-1-((*R*)-2-(4-fluorophenyl)pyrrolidin-1-yl)-3,3-dimethyl-1-oxopent-4-en-2-ylcarbamate (**34**)

A flame-dried 100-mL round-bottom flask was charged with arylpyrrolidine **15** (3.46 mmol, 1.0 equiv), amino acid **32** (884 mg, 3.63 mmol, 1.05 equiv), HOBt (583 mg, 3.80 mmol, 1.1 equiv), and EDC (728 mg, 3.80 mmol, 1.1 equiv) and DMF (17.3 mL). The reaction mixture was stirred overnight, after which it was diluted with DI H_2O (20 mL) and extracted with EtOAc (3x). The combined organics were washed with saturated aqueous NH_4Cl (1x) and brine (1x), dried over Na_2SO_4, filtered, and concentrated in vacuo. The crude residue was purified by flash chromatography (Biotage®, 0-50% EtOAc/hexanes) to afford amide **34** as a white solid (859 mg, 2.20 mmol, 64% yield). In $CDCl_3$ the compound exists as a 4.0:1 mixture of rotamers. One of the resonances in the ^1H NMR spectrum corresponding to a proton of the minor rotamer ($C(Me)_2C\mathbf{H}CH_2$) was integrated to 1, and all other integration data are reported relative to it. ^1H NMR (600

MHz, $CDCl_3$) δ ppm 7.28 - 7.35 (m, 3 H) 7.04 - 7.16 (m, 11 H) 6.95 (t, *J*=8.79 Hz, 8 H) 6.08 (dd, *J*=17.28, 10.84 Hz, 4 H) 5.89 (dd, *J*=17.57, 10.84 Hz, 1 H) 5.48 (dd, *J*=8.05, 2.20 Hz, 1 H) 5.19 (dd, *J*=7.91, 2.34 Hz, 5 H) 5.08 - 5.15 (m, 13 H) 5.05 (s, 1 H) 4.98 (dd, *J*=10.84, 1.17 Hz, 1 H) 4.89 (dd, *J*=17.57, 1.17 Hz, 1 H) 4.39 (d, *J*=9.96 Hz, 4 H) 4.20 - 4.27 (m, 4 H) 4.12 - 4.20 (m, 1 H) 3.64 - 3.83 (m, 7 H) 2.37 (s, 1 H) 2.21 - 2.32 (m, 4 H) 1.90 - 2.06 (m, 13 H) 1.79 - 1.90 (m, 5 H) 1.45 - 1.55 (m, 52 H) 1.14 - 1.21 (m, 27 H) 0.81 (s, 3 H) 0.67 (s, 3 H).

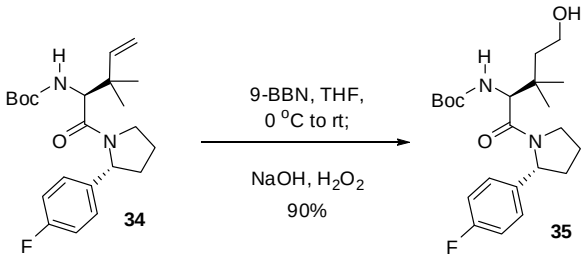

tert-butyl (S)-1-((R)-2-(4-fluorophenyl)pyrrolidin-1-yl)-5-hydroxy-3,3-dimethyl-1-oxopentan-2-ylcarbamate (**35**)

An oven-dried 200-mL round-bottom flask was charged with alkene 34 (802 mg, 2.05 mmol, 1 equiv) and THF (20.5 mL). The flask was cooled to 0 oC and stirred at that temperature for 5 min, after which 9-BBN (0.4M hexanes, 15.4 mL, 6.16 mmol, 3.0 equiv) was added dropwise over 10 min. The reaction was allowed to warm to room temperature overnight. The flask was returned to 0 oC and 2N NaOH (4 drops) was cautiously added, resulting in vigorous bubbling. Another 9.25 mL 2N NaOH were slowly added followed by 30% H_2O_2 (8.2 mL). The ice bath was removed and the contents were stirred rapidly at room temperature for 4 h. The contents were diluted with H_2O and extracted with EtOAc (3x). The combined organics were washed sequentially with DI H_2O, 10% aqueous sodium thiosulfate, and brine, dried over Na_2SO_4, filtered,

and concentrated. The crude residue was purified by flash chromatography (Biotage®, SiO_2, 20-80% EtOAc/hexanes) to afford primary alcohol **35** as a white foamy solid (757 mg, 90% yield). R*f*=0.19 (50% EtOAc/hexanes, CAM). In $CDCl_3$ the compound exists as a 2.3:1 mixture of rotamers. One of the resonances in the ^1H NMR spectrum corresponding to a proton of the minor rotamer was integrated to 1, and all other integration data are reported relative to it. ^1H NMR (500 MHz, $CDCl_3$) δ ppm 7.29 (m, 1.9 H) 7.00 - 7.14 (m, 5.6 H) 6.93 (t, *J*=8.47 Hz, 4.3 H) 6.34 - 6.50 (m, 3.2 H) 5.47 (d, *J*=7.33 Hz, 1 H) 5.19 (d, *J*=7.33 Hz, 2.3 H) 4.53 (d, *J*=10.07 Hz, 2.3 H) 4.25 - 4.35 (m, 2.3 H) 4.22 (d, *J*=10.53 Hz, 1.1 H) 4.04 (br s., 2.3 H) 3.70 - 3.80 (m, 4.9 H) 3.58 - 3.70 (m, 3.8 H) 3.45 - 3.58 (m, 1.5 H) 2.29 - 2.40 (m, 1.3 H) 2.29 (s, 2.6 H) 1.76 - 2.01 (m, 10.8 H) 1.44 - 1.51 (m, 21.9 H) 1.1 (s, 4.9 H) 1.08 (s, 4.9 H) 0.68 (s, 2.2 H) 0.49 (s, 2.2 H); ^{13}C NMR (126 MHz, $CDCl_3$) All observed resonances are reported: δ ppm 172.7, 171.4, 171.2, 163.1, 162.6, 161.2, 160.7, 156.8, 156.1, 139.8 (d, *J*=3.66 Hz), 138.1 (d, *J*=3.66 Hz), 128.3 (d, *J*=8.24 Hz), 126.8 (d, *J*=7.32 Hz) 115.6 (d, *J*=22.0 Hz), 115.3 (d, *J*=21.1 Hz), 79.62, 79.57, 61.0, 60.4, 60.1, 58.6, 58.5, 58.3, 57.3, 48.3, 47.3, 41.64, 41.60, 36.2, 36.1, 35.8, 34.3, 28.43, 28.40, 26.9, 26.6, 25.0, 24.6, 23.1, 21.7, 21.0, 14.2.

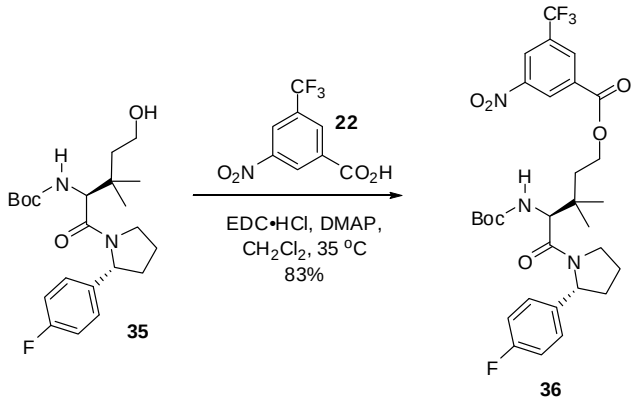

(*S*)-4-(tert-butoxycarbonylamino)-5-((*R*)-2-(4-fluorophenyl)pyrrolidin-1-yl)-3,3-dimethyl-5-oxopentyl 3-nitro-5-(trifluoromethyl)benzoate (**36**)

An oven-dried 2-dram vial was charged with a stir bar, alcohol **35** (195mg, 0.478 mmol, 1.0 equiv), and acid **22** (135 mg, 0.573 mmol, 1.2 equiv). CH2Cl2 (1.5 mL) and DMF (1 mL) were added, followed by EDC (275 mg, 1.4 mmol, 3.0 equiv) and DMAP (175 mg, 1.4 mmol, 3.0 equiv). The reaction mixture was stirred at room temperature overnight. It was then diluted with DI H_2O and extracted with EtOAc (3x). The combined organics were dried over Na_2SO_4, filtered, and concentrated in vacuo. The crude product was purified by flash chromatography to afford ester **36** as a white foamy solid (248 mg, 83% yield). In $CDCl_3$ the compound exists as a 1.7:1 mixture of rotamers. One of the resonances in the ^1H NMR spectrum corresponding to a proton of the minor rotamer was integrated to 1, and all other integration data are reported relative to it. ^1H NMR (500 MHz, $CDCl_3$) δ ppm 9.01 (d, *J*=1.83 Hz, 1.7 H) 8.88 - 8.96 (m, 1 H) 8.66 (d, *J*=1.83 Hz, 2.3 H) 8.60 (s, 1.6 H) 8.53 (s, 1.1 H) 7.26 - 7.36 (m, 2 H) 6.96 - 7.08 (m, 4.5 H) 6.91 (t, *J*=8.70 Hz, 3.2 H) 5.34 (d, *J*=5.95 Hz, 1 H) 5.06 - 5.20 (m, 3.9 H) 4.53 (t, *J*=7.33 Hz, 3 H) 4.49 (br. s., 1.7 H) 4.15 - 4.30 (m, 3.6 H) 3.60 - 3.81 (m, 3.6 H) 2.20 - 2.44 (m, 3 H) 1.77 - 2.10 (m, 11.5 H) 1.50 - 1.60 (m, 2 H) 1.40 - 1.50 (m, 17.4 H) 1.09 - 1.18 (m, 7.8 H) 0.88 (s, 2 H) 0.68 (s, 2 H). ^{13}C NMR (126 MHz, $CDCl_3$) All observed resonances are reported: δ ppm 171.6, 171.2, 170.2, 163.3, 163.0, 162.7, 161.2, 160.7, 156.4, 155.8, 148.6, 140.10, 140.08, 138.51, 138.48, 133.6, 133.5, 133.1, 132.8, 131.99, 131.96, 131.9, 128.5, 128.4, 127.6, 127.5, 126.8, 126.7, 124.54, 124.51, 123.61, 115.8, 115.6, 115.4, 115.2, 80.16, 63.6, 63.4, 61.1, 60.5, 60.4, 58.2, 56.8, 48.5, 47.2, 37.1, 37.0, 36.7, 36.5, 36.0, 34.3, 28.40, 28.37, 23.8, 23.4, 23.3, 23.2, 22.1, 21.1, 14.3.

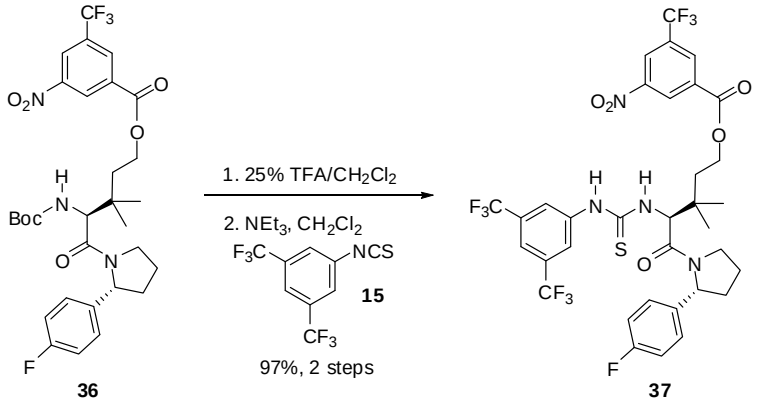

Thiourea (**37**)

A 50-mL round-bottom flask was charged with Boc-protected amine **36** (248 mg, 0.40 mmol, 1.0 equiv) and CH_2Cl_2 (10 mL). The flask was cooled to 0 ^oC and TFA (3.3 mL) was added dropwise under an atmosphere of N_2. The reaction mixture was stirred at this temperature for 2 h, at which point the contents were concentrated in vacuo. The crude amine salt was dissolved in CH_2Cl_2 (4 mL), and 1.3 mL of this solution was removed (for use in a different reaction). The solution was cooled to 0 ^oC, and NEt_3 (110 μL, 3.0 equiv) and isothiocyanate 15 (97 μL, 2.0 equiv) were sequentially added to the flask dropwise. The reaction mixture was stirred and allowed to warm to room temperature over a period of 4h, at which point the contents were concentrated in vacuo. The crude reside was purified by flash chromatography (Biotage®, 15-70% EtOAc/hexanes) to afford thiourea 37 as a white foam (204 mg, 97%, 2 steps). In $CDCl_3$ the compound exists as a 1.3:1 mixture of rotamers. One of the resonances in the ^1H NMR spectrum corresponding to a proton of the minor rotamer was integrated to 1, and all other integration data are reported relative to it. ^1H NMR (500 MHz, $CDCl_3$) δ ppm 9.51 (br. s., 1 H) 9.42 (br. s., 1.3 H) 8.94 - 9.08 (m, 1.4 H) 8.88 - 8.94 (m, 1 H) 8.65 - 8.74 (m, 1.97 H) 8.61 (s, 1.3 H)

8.52 (s, 1.1 H) 8.06 (s, 1.87 H) 7.92 (s, 2.3 H) 7.69 (s, 0.9 H) 7.64 (s, 1.3 H) 7.42 - 7.58 (m, 2.2 H) 7.31 - 7.40 (m, 1.8 H) 7.04 (t, *J*=8.70 Hz, 1.9 H) 6.89 (dd, *J*=8.01, 5.27 Hz, 2.3 H) 6.70 (t, *J*=8.47 Hz, 2.4 H) 5.84 (d, *J*=7.78 Hz, 1 H) 5.69 (d, *J*=9.62 Hz, 1.3 H) 5.47 (d, *J*=9.62 Hz, 1 H) 5.09 (d, *J*=6.87 Hz, 1.3 H) 4.58 - 4.70 (m, 2.3 H) 4.47 - 4.58 (m, 1.4 H) 4.35 (ddd, *J*=11.22, 8.01, 5.95 Hz, 1.3 H) 3.78 - 3.91 (m, 1.4 H) 3.50 - 3.66 (m, 2 H) 2.20 - 2.47 (m, 2.7 H) 2.09 - 2.18 (m, 1 H) 1.73 - 2.02 (m, 6.3 H) 1.57 - 1.71 (m, 1.5 H) 1.34 - 1.49 (m, 1.5 H) 1.28 (d, *J*=2.29 Hz, 6 H) 1.00 - 1.10 (m, 2.4 H) 0.68 (s, 2.3 H). ^{13}C NMR (126 MHz, $CDCl_3$) All observed resonances are reported: δ ppm 182.0, 181.6, 172.3, 171.5, 170.3, 163.3, 163.0, 162.5, 160.5, 148.62, 148.59, 140.4, 139.8, 139.15, 139.13, 137.07, 137.05, 133.4, 133.3, 133.2, 132.9, 132.4, 132.2, 132.15, 132.0, 131.95, 131.9, 131.87, 128.5, 128.4, 127.5, 127.4, 124.7, 124.6, 124.1, 124.0, 122.1, 122.0, 121.4, 118.9, 118.8, 116.1, 115.9, 115.2, 115.0, 63.3, 62.2, 62.0, 60.9, 60.6, 60.4, 49.1, 48.0, 38.1, 37.8, 37.7, 37.4, 35.4, 34.3, 24.4, 24.2, 24.1, 23.5, 23.1, 21.6, 21.2, 14.3.